Master's thesis

NTNU
Norwegian University of Science and Technology
Faculty of Engineering
Department of Geoscience and Petroleum

Vetle Arild Mathisen

Blowout and Kill Simulator

Calibrated for Exploration Wells on the Norwegian Continental Shelf

Master's thesis in Petroleum Geoscience and Engineering
Supervisor: Sigbjørn Sangesland
May 2020

NTNU
Kunnskap for en bedre verden

Vetle Arild Mathisen

Blowout and Kill Simulator

Calibrated for Exploration Wells on the Norwegian Continental Shelf

Master's thesis in Petroleum Geoscience and Engineering
Supervisor: Sigbjørn Sangesland
May 2020

Norwegian University of Science and Technology
Faculty of Engineering
Department of Geoscience and Petroleum

Preface

This thesis is written as a part of the degree ”Master of science” within the field of ”Petroleum technology with specialization in drilling technologies” for the Department of Geoscience and Petroleum (IGP) in the Norwegian University of Science and Technology (NTNU) during the spring of 2020.

The content of this thesis is based on the preliminary work conducted in a project thesis during the autumn of 2019. The preliminary work conducted in the project thesis included the main idea on how to create the blowout and kill simulator, but only a small fraction of the conducted work remains unaltered.

This thesis was written during the spring of 2020 with the unfortunate global pandemic caused by the Corona virus and the resulting disease Covid-19. The pandemic caused the university campus to be closed for most parts of the spring and the author was not allowed to be present on the campus. During these special times I would like to thank my supervisor, Sigbjørn Sangesland, for motivation and professional guidance. Harald Asheim must also be thanked due to his insight of multiphase flow and our discussions throughout the spring. I would also hand out a thank you to all my co-students, friends and family for their support during my time as a student. Lastly, I want to give a big thank you to the company Aker BP and their Trondheim's office for professional guidance throughout the autumn of 2019 and the first months of 2020, as well as allowing me to use some of their data related to the subject of blowout and kill. This master thesis was not written together with the company, but solely with the Department of Geoscience and Petroleum at NTNU.

Summary

Introduction
A blowout is the worst-case scenario that can happen in the petroleum industry. When a blowout occurs, it is a huge risk to the involved rig personnel. The oil spills from a blowout is disastrous to the environment and require a lot of remedial work to come back to nature's normal. One of the most recent blowout accidents is the Macondo blowout in the Gulf of Mexico in 2010. In the accident 11 people lost their lives and 17 more were injured, the estimated volume of oil spill was 780 000 Sm^3. One common way to regain control and kill the blowout is to drill a relief well that intersect the blowing well and kill fluid is pumped into the wellbore.

Background
Most governmental regulations, such as NORSOK, demand that a blowout and kill simulation is conducted and shows that it is possible to kill the well and regain control if the worst-case scenario of a blowout happens. The blowout and kill simulation should be based on realistic reservoir properties and the planned well design. Today several companies are specialized in the simulation of blowout and kill, and upon request from the operators they simulate the planned well. It may take several weeks before the operator receives the conducted simulation, and if the results shows that the well cannot be killed, a new well design and a new simulation must be conducted. This may result in a long alternating process between the simulation company and the operator. The solution is a blowout and kill simulator the operator themselves can use.

Theory
This thesis discusses the most commons reasons of why uncontrolled influx, a kick, to the wellbore occurs and how a kick is developed into a full blowout. Several ways to regain control and avoid the blowout is discussed, together with different methods to kill the well when the blowout has occurred. These methods include well capping, natural bridging and relief well drilling. The theory behind the calculation of the blowout rate and the required kill rate are presented.

Simulator
The main work in this thesis is about the creation of a blowout simulator in Matlab and Excel. A blowout and kill simulator was created that calculates the blowout rate and the kill rate for several scenarios for a well. The created simulator is intuitive and easy to use. The user of the simulator requires no skills in the programming software Matlab, all data inputs happens in Microsoft Excel and the results from the simulator are presented in an automatically generated PDF report. The simulator gives the opportunity to choose between two multiphase pressure correlations (Olgjenka and Orkiszewski) and two PVT-correlations (Glasø and Standing). The thesis presents the workflow of the simulator and go through a detailed calculation example for one of the wells.

Simulated blowout rates
The results from the created simulator is compared against the results from the specialized companies in the industry, who commonly uses the commercially available blowout and kill simulator "Olga-Well-Kill". In total 17 wells were simulated in the created simulator and compared with the professional simulations.

In total 68 blowout simulations were simulated for the 17 wells for a blowout to both seabed and surface through both open/cased hole and annulus. The created simulator gave promising results, and the average error for the two multiphase pressure correlations with the Standing PVT correlation were -7.5% and -11.0% for Olgjenka and Orkiszewski, respectively.

Simulated kill rates
Kill simulations were conducted for 11 different wells and compared against the professional simulations. The simulations included 7 wells with a surface release point and 7 wells with a seabed release point. In total 36 different kill simulations were conducted, based on the kill fluid density. The average error for the two multiphase correlations were -33.1% and -15.6% for Olgjenka and Orkiszewski, respectively.

Calibration of the kill rates
Four calibration formulas for the kill rate were created with a non-linear regression, based on the input data and the difference between the calculated rates and the professional rates. The average calibrated errors were -2.95% and 1.65% for Olgjenka and Orkiszewski, when the outlier wells were excluded. The absolute average errors were 12.7% and 20.0% in the same order. The two outlier wells were unsuccessfully calibrated, and the kill rate errors increased after the calibration.

Sammendrag

Introduksjon
En ukontrollert utblåsning er en alvorlig hendelse. Når en utblåsning oppstår, er det en stor risiko for det involverte riggpersonalet. Oljeutslippet fra en utblåsning er alvorlig for miljøet og krever mye restaureringsarbeid for at naturen skal bli som normalt igjen. En av de seneste utblåsningsulykkene er Macondo-utblåsningen i Mexicogulfen i 2010. Ulykken krevde 11 menneskeliv og 17 til ble skadet, det estimerte volumet av oljeutslipp var 780 000 Sm^3. En vanlig måte for å gjenvinne kontrollen på er ved å drepe utblåsningen med en avlastningsbrønn. Dette skjer ved å bore en avlastningsbrønn som krysser den blåsende brønnen, deretter blir drepe væske pumpet inn i brønnen.

Bakgrunn
De fleste statlige forskrifter, for eksempel NORSOK, krever at det utføres en utblåsnings- og drepesimulering som viser at det er mulig å drepe brønnen og gjenvinne kontrollen dersom en utblåsning oppstår. Utblåsnings- og drepesimuleringen skal være basert på realistiske reservoaregenskaper og den planlagte brønnkonstruksjonen. I dag er flere selskaper spesialisert i simuleringen av utblåsning og dreping, og på forespørsel fra operatøren simulerer de den planlagte brønnen. Det kan ta flere uker før operatøren mottar den gjennomførte simuleringen, og hvis resultatene viser at brønnen ikke kan drepes, må brønnkonstruksjonen endres og en ny simulering må utføres. Dette kan resultere i en lang prosess mellom simuleringsselskapet og operatøren. Løsningen er en utblåsnings- og drepesimulator operatøren selv kan bruke.

Teori
I denne masteroppgaven diskuteres de vanligste årsakene til at ukontrollert innstrømning, et spark, til borehullet oppstår og hvordan et spark utvikles til en full utblåsning. Flere måter å gjenvinne kontrollen og forhindre utblåsningen blir diskutert, samt ulike måter å drepe utblåsningen når den har oppstått. Ulike drepe teknikker inkluderer brønnavdekking, naturlig stenging/ reservoar kollaps og boring av en avlastningsbrønn. Teorien bak utregningen av utblåsningsraten og nødvendig dreperate er presentert.

Simulator
Hovedarbeidet i denne oppgaven handler om å utvikle en utblåsing og drepesimulator i Matlab og Excel. Det ble utviklet en utblåsnings- og drepesimulator som beregner utblåsningsraten og injeksjonsraten av drepe-fluid for flere scenarier for en brønn. Den utviklede simulatoren er intuitiv og enkel å bruke. Brukeren av simulatoren krever ingen ferdigheter i programmeringsprogramvaren Matlab, utfylling av nødvendige parametere skjer i Microsoft Excel og resultatene fra simulatoren presenteres i en automatisk generert PDF-rapport. Simulatoren gir muligheten til å velge mellom to flerfasetrykk korrelasjoner (Olgjenka og Orkiszewski) og to PVT-korrelasjoner (Glasø og Standing). Masteroppgaven presenterer de ulike stegene i simulatoren og hvordan de ulike ratene utregnes med et eksempel.

Simulerte utblåsningsrater
Resultatene fra den utviklede simulatoren ble sammenlignet med resultater fra de spesialiserte selskapene i bransjen. I bransjen brukes ofte den kommersielle tilgjengelige utblåsnings- og drepesimulatoren "Olga-Well-Kill".

Totalt ble 17 brønner simulert i den utviklede simulatoren, og resultatene ble sammenlignet med profesjonelle simuleringer. Totalt ble det simulert 68 utblåsningssimuleringer for de 17 brønnene med fire ulike strømningsveier. Strømningsveiene inkluderer utblåsning til både havbunn og overflate gjennom åpent hull/foringsrør og ringrom. Den opprettede simulatoren ga lovende resultater, og gjennomsnittlig feil for utblåsningsraten for de to flerfasetrykk korrelasjoner var henholdsvis -7.5 % og -11.0 % for Olgjenka og Orkiszewski.

Simulerte dreperater
Simuleringer av brønndreping ble utført for 11 forskjellige brønner og sammenlignet med de profesjonelle simuleringene. Det var totalt 7 brønner med utslippspunkt til overflaten og 7 brønner med utslippspunkt til havbunnen. Totalt ble 36 ulike drepesimuleringer utført. Den gjennomsnittlige feilen for de to flerfasekorrelasjonene var henholdsvis -33.1 % og -15.6 % for Olgjenka og Orkiszewski.

Kalibrering av dreperater
Fire kalibreringsformler for dreperaten ble opprettet gjennom ikke-linear regresjon, basert på inngangsdataen og forskjellen mellom de beregnede dreperatene og de profesjonelle dreperatene. Gjennomsnittlig feil for de kalibrerte ratene var -2,95 % og 1,65 % for Olgjenka og Orkiszewski, når en brønn ble ekskludert for hver av utslippspunktene. De absolutte gjennomsnittlige feilene var 12.7 % og 20.0 % i samme rekkefølge. For to av brønnene var kalibreringen mislykket og den gjennomsnittlige feilen økte.

Table of Contents

List of Tables

List of Figures

Nomenclature

Abbreviations

AC	=	Alternating current
AOF	=	Absolute open flow potential
BHA	=	Bottom hole assembly
BOP	=	Blowout preventer
DP	=	Drill pipe
FBHP	=	Flowing bottom hole pressure
HWDP	=	Heavy weight drill pipe
ID	=	Innter diameter
IP	=	Interception point
IPR	=	Inflow performance relationship
IPR	=	Inflow performance relationship
LPM	=	Liters per minute
MAASP	=	Maximum allowable annular surface pressure
MD	=	Measured depth
MSL	=	Mean sea level
MWD	=	Measurements while drilling
NCS	=	Norwegian continental shelf
OBM	=	Oil-based mud
OD	=	Outer diameter
OH	=	Open hole
PI	=	Productivity index
PPFG	=	Pore pressure and fracture gradient
PVT	=	Pressure volume temperature
RKB	=	Rotary kelly bushing
ROP	=	Rate of penetration
ROV	=	Remotely operated vehicles
RW	=	Relief well
STB	=	Stock tank barrel
TVD	=	True vertical depth
VBA	=	Visual Basics
VLP	=	Vertical lift performance
WBM	=	Water-based mud
XLOT	=	Extended leak off test

Symbols and letters

B	=	Formation volume factor
C_dp	=	Kill rate calibration factor
cp	=	Centipoise
d_h	=	Hydraulic diameter
f	=	Friction factor
h	=	Reservoir height
H_l	=	Liquid holdup
J	=	Productivity index
p_b	=	Bubble point pressure
q	=	Flow rate
R	=	Gas-Oil-ratio
R_s	=	Solution Gas-Oil-ratio
R_t	=	Total Gas-Oil-ratio
S	=	Skin factor
T	=	Temperature
U	=	Thermal conductivity
v	=	Velocity

Greek symbols

β	=	Permeability anisotropy factor
ϵ	=	wall roughness or error
Γ	=	Liquid distribution coefficient
γ	=	Specific gravity
γ_{API}	=	Api density
μ	=	Viscosity
ρ	=	Density
σ	=	Interfacial tension
θ	=	Inclination

Subscripts

a	=	Acceleration
b	=	Bubble
c	=	Coefficient
g	=	Gas or gravity
f	=	Friction
L	=	Liquid
m	=	Mixture
o	=	Oil
t	=	Total
tp	=	Two-phase

Chapter 1

Previous work

Some preliminary work was conducted before the start of this thesis, a project thesis written by the author, (Mathisen, 2019), was based on the same subject. Only a small fraction of the work conducted in the project thesis is used in the presented master thesis. Some chapters from the project thesis is included in the master thesis to give the reader a full understanding of the subject, these chapters are not altered or only slightly altered. The chapters from a previous work are presented in table 1.1. Most of the work conducted in this thesis is related the coding of the simulator. Based on the different scripts used in the simulator it is assumed that about 5-10% of the code originate from the project thesis.

Table 1.1: Previous work based on the project thesis by (Mathisen, 2019)

Chapter/section	Location	Partly changed	Not changed
Introduction	Chapter 2	Yes	
Secondary well control	Chapter 3		Yes
Tertiary well control	Chapter 4	Yes	
Productivity index	Appendix A.1		Yes
Inflow performance relationship	Appendix A.2		Yes
Multiphase flow correlation	Appendix A.5.1	Yes	
Orkiszewski correlation	Appendix A.5.2		Yes
Glasø correlation	Appendix A.6.2	Yes	

At least two master theses is previously written with the ”Department of Geoscience and Petroleum” at NTNU on the subject of blowout and kill simulation. These two theses are (Evensen, 2013) and (Solgren, 2014). Both simulators used the multiphase pressure correlation created by (Beggs and Brill, 1973). These theses were read and some of the methodology regarding how the simulators were build was used to create the blowout and kill simulator in this thesis. Only the Matlab script from (Evensen, 2013) was found, none of the previous coding is a part of the created simulator.

Chapter 2

Introduction

Well control is the most important aspect of all drilling related activities. If well control is not maintained most, if not all, governmental regulations forbid any further drilling until well control is regained. When the primary well control is lost, i.e. the mud is no longer in overbalance in a permeable formation, pore fluid will flow into the well and a kick situation occurs. If the kick is not properly handled it can evolve into an uncontrolled blowout.

Background
During the planning phase of a well one, important part is to show that it is possible to kill the well in the unlikely situation of a worst-case blowout. The common practice today is that the operator is responsible for the well planning, where the casing program is mainly based on the PPFG-curve (pore pressure and fracture gradient), while a specialized company conducts the blowout and kill simulation for the planned casing program. The simulation shows whether the well is killable or not. It may take several weeks before the specialized company has finished the simulation, leaving the operator with two choices: first keep going on with the well planning with the given casing program and assume that it is possible to kill the well, or secondly cease most of the planning until the simulation results are back. If the simulations show that the well is not killable, given the standard limitations of a modern drilling unit, the entire casing program must be altered and a new blowout and kill simulation must be conducted. This may lead to a long and costly iterative process, going back and forth with the casing sizes and setting depths with the blowout and kill simulation.

Solution
A solution to this problem is to allow the operator to conduct the blowout and kill simulation on their own, by using an easy to use blowout and kill simulator. This will not only remove the iterative process between the operator and the simulation company, but also allow the operator to have a better understanding of the sensitivity of the input data used in the blowout and kill simulation.

This thesis will shortly describe different well control scenarios, but the main part is about the development of a blowout and kill simulator in Matlab.

The company Oliasoft launched their blowout and kill simulator in April 2018 (Oliasoft, 2018). This simulator allows the operator companies to conduct blowout and kill simulations themselves. One of the multiphase correlations, Orkiszewski correlation by (Orkiszewski, 1967), used in the Oliasoft simulator is also used in the created simulator. The Olgjenka correlation by (Asheim, 2020) is new and have not been tested out in a blowout and kill simulator before. Only the stationary part of the Olgjenka correlation is used.

Chapter 3

Secondary Well Control

3.1 Causes of taking a kick

There are several reasons for taking a kick, but in short terms all incidents are related to a lower wellbore pressure than the formation pressure. This allows the pore fluid to flow into the wellbore and a kick is initiated. The material written by (Grace, 2017) presents four main causes for taking a kick:

1. Failure to keep overbalance in the wellbore due to too low mud weight.
2. Failure to refill the mud level when tripping out.
3. Too high swab pressures while tripping out.
4. Losing the mud column due to lost circulation.

Failure to keep overbalance
The primary source of well control is always to be in overbalance, i.e. the pressure in the well is higher than the formation pressure. This will prevent any formation fluid to flow into the wellbore. In many occasions overbalance is not maintained, which can be caused by too low mud weight, i.e. the density of the mud will cause too low hydrostatic pressure. The mud weight is based on the pore pressure curve and it will be too low if the assumed pore pressure curve is under predicted. The pore pressure curve is created by the subsurface team and are based on data from offset wells and geological understanding of the area. A common reason for taking a kick is caused by unidentified abnormal pressured zones. These over pressured zones are more frequently encountered in exploration wells since the area is less explored and the closest offset wells may be far away. (Grace, 2017)

Failure to refill the mud level
When tripping out, several stands of drill pipe are removed from the well and the mud column is reduced due to less material in the borehole. When the mud column is reduced

the hydrostatic pressure will decrease. If the pressure in any parts of the well becomes less than the formation pressure, influx will happen. Most of the mud inside the stands will flow back into the well, but some will be spilled as the connections are broken up. The main reason for a lower mud column is caused by the fact that a considerable steel volume is removed from the well. To show how considerable the steel volume is a reference is made to table 3.1, which show the capacities and displacements of two drill pipes. The table show how that the steel volume (open end displacement) of a normal drill pipe are almost half of the capacity. Considering the heavy weight drill pipe the steel volume are greater than the capacity. Refilling the wellbore is time consuming and for efficiently tripping refilling is only conducted a few times for each trip out. (Grace, 2017)

Pipe type and size	Closed End [l/m]	Open End [l/m]	Capacity [l/m]
5 7/8" DP	18.13	5.84	12.30
5 7/8" HWDP	18.58	10.43	8.15

Table 3.1: Capacities and displacements of 5 7/8 drill pipe

Too high swab pressure
When tripping out, the upwards pipe movement results in a decrease in the well pressure. The pressure decrease is proportional to the velocity of the pipe, i.e. the faster the tripping speed the higher the pressure decreases. The pressure decrease can be considerable high, leaving the well pressure lover than formation pressure which will result in influx of formation fluid. A normal procedure to avoid a too high pressure decrease while swabbing, is to provide the driller with a specification sheet with maximum tripping speed for a given depth interval, these velocities are calculated to avoid getting too high swab pressures.

Lost circulation
One of the most dangerous reasons for taking a kick is caused by lost circulation. A lost circulation incident can happen if the mud flow into the formation instead of up the annulus and out of the wellbore through the flow lines. Two common reasons are fracturing the formation or drilling into pre-fractured formations or cave systems. The mud level will be balanced so the hydrostatic pressure in the well and the formation equals. When the mud level top is no longer at surface no fluid will flow into the tripping pits and the primary kick detection method is lost. A serious situation may now occur, the well is no longer in overbalance allowing formation fluid to enter the wellbore and the primary method of kick detection is lost, the warning signs of kick detection will be described more in the detail in the next section. During a lost circulation situation a kick can go unnoticed for a long period of time due to the lack of flow control, as the kick fluid is migrating up the wellbore the distance to the BOP decreases and thus the time to react before disaster is a fact shortens. (Grace, 2017)

3.2 Early warning signs for taking a kick

When an influx happens, several observations can tell that a kick has occurred. In the list below item 1 and 2 are commonly the first signs observed. In the end of this section an industry example is presented, showing several of the warning signs for a kick. Some common observations prior to taking a kick are presented by (Grace, 2017).

1. A drilling break is observed, a sudden increase in the rate of penetration.
2. Increasing pit volume, more fluid flow out of the well than what the mud pumps are pumping in, e.g. $q_{out} > q_{in}$.
3. Reduced standpipe pressure.
4. Changes in hook load.
5. Reservoir fluid in the mud.

Drilling break
Impermeable and low porosity rocks are commonly stronger and harder to drill than permeable and porous formations. Going from a low ROP in either shale or cemented carbonates to a rapid increase in the ROP can suggest that a permeable formation is penetrated. If the pore pressure in this formation is under predicted a kick situation is frequently encountered. To reduce the potential kick volume, no more than 2-5 ft of the permeable formation should be penetrated without stopping the pumps and checking for influx. If this procedure was followed, several extremely costly blowouts would have been avoided, due to a smaller inflow area and easier handling of the well control situation (Grace, 2017). A drilling break is often a good indicator of a change of lithology, given that the parameters such as flow rate and weight on bit are kept constant. A formation change can also be penetrated without an increased ROP, this can be masked by the bit type and in some situations one can experience a negative drilling break when going from shale to sand. However, a drilling break cannot alone determine a kick situation.

Increasing pit volume
An increase in the pit volume is a strong indicator that more fluid is flowing out of the wellbore than what is pumped in. If influx into the wellbore is presumed a common procedure is to stop the mud pumps and check if the pit volume keeps increasing. An increase in the pit volume when the mud pumps are off does not automatically indicate a kick situation since the ballooning-effect can be of a significant magnitude.

The flow rate into the wellbore can either be high or low. How rapid the influx of formation fluid is determined by several factors such as the differential pressure between the permeable formation and the wellbore, the productivity index of the formation and the type of formation fluid. Having a minor influx of formation fluid over a long time can cause serious damage. If gas is the formation fluid, gas expansion due to lower pressure in the well will manifest itself rapidly. If an oil-based mud is used, gas will be dissolved into the mud and first go out of solution when the pressure is less than the bubble point pressure. This can mask the influx until the it is too little time to close the well or the gas is already located in the riser (Gomes et al., 2018).

As with drilling breaks there are several reasons that can cause masking of the pit volume increase. Movement caused by either waves or crane operations can hide minor influxes on a floater. If the driller redirect some of the flow from the tripping pits, such as filling the shaker pits at the moment the kick is initiated, considerable volumes may be masked.

Reduction in Standpipe Pressure
A kick is often determined by a drilling break and a pit volume increase, but a reduction in the standpipe pressure can also be a secondary indicator. When the formation is pumping fluid into the wellbore this fluid commonly has a lower density than the mud used, resulting in a lower hydrostatic pressure in the annulus. This will cause an u-tube or gravity pull effect since the heavier mud in the drill string will try to equal the hydrostatic pressure in the annulus. (Grace, 2017)

Changes in hook load
The hook load, i.e. the weight of the entire drill string lifted by the hook, mainly consist of the actual weight of the drill string minus the buoyancy forces exerting an upward force on the drill string. Drag factors also play a part in the total hook load. If an influx of reservoir fluid happens, this will replace some of the drilling mud in the wellbore. The reservoir fluid is in most cases lighter than the drilling mud which will result in a lower buoyancy force. The lower buoyancy force will result in a higher hook load.

Reservoir fluid in the mud
If significant amounts of reservoir fluid are spotted in the returning mud, it is also a clear indicator that influx into the wellbore has happened. Small amounts of reservoir fluid are caused by reservoir fluid in the pores of the penetrated formation and in the cuttings, which does not necessarily indicate a kick.

An industry example
An industry example from an onshore operation in the United States taking a kick is presented by (Grace, 2017). This example shows the first four early warning signs as listed above. The logs from this operation can be viewed in figure 3.1 and each of the first four warnings sign are easily determined in this example. The rig crew failed to see the clear signs that a kick was initiated just after three o clock, it took almost 30 minutes before the well was closed in. This long time before the well was shut-in resulted in a total gain of 118 barrels of reservoir fluid. It is a common practice in the united states to shut-in the well if a gain of more than 20 barrels is observed. The sudden spike in flow rate and the drilling break encountered between 03.01 and 03.04 together should be clear indications that a kick is initiated. (Grace, 2017)

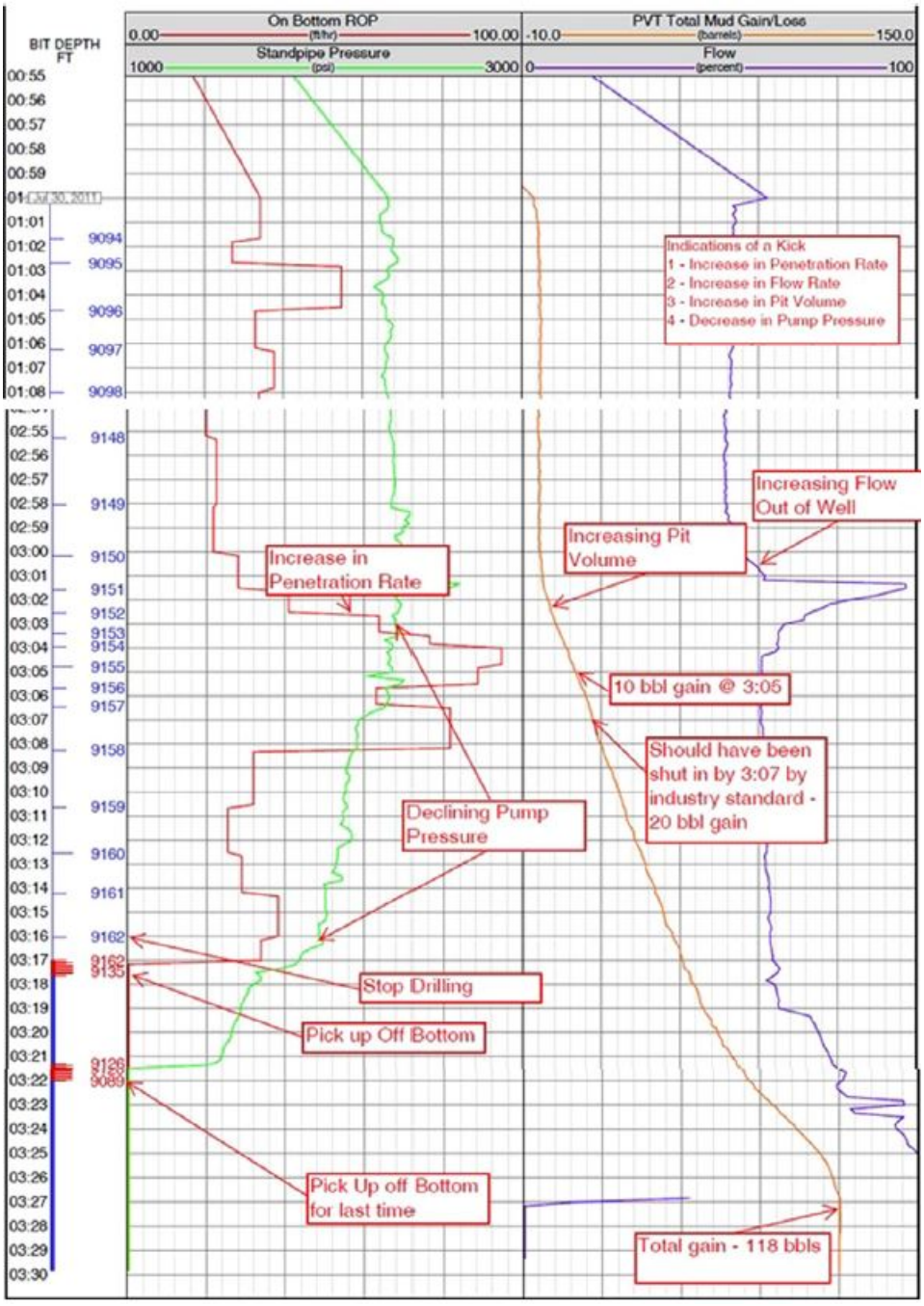

Figure 3.1: An industry example of early kick warning signs as presented by (Grace, 2017).

3.3 Shut-in procedure

When any of the warning sign described in section 3.2 is noticed and if a kick is the likely cause, a shut-in procedure must be started. The exact details of the procedure may differ from country to country and operator to operator, but a typical shut-in procedure as presented by (Grace, 2017) and recommended by the API RP 59 is as follows.

1. If a drilling break is observed, drill no more than 3 ft.
2. Pick the bit of bottom and space out so no tool joint is obstructing the BOP elements.
3. Turn of the mud pumps and check for flow.
4. If flow is observed, the well shall now be shut in. First open the choke lines, then close the pipe rams and last close the choke.
5. Take recordings of the drill pipe pressure, annulus pressure and the increase of pit volume.
6. Close the annular preventer, then open the pipe rams.
7. Determine kick displacing strategy and prepare for displacing the kick

A common difference in this procedure is whether the annular preventer or pipe rams are closed first, this is often a matter of time usage for closing the different elements. Another difference if the procedure uses a ”soft shut-in” or a ”hard shut-in”. A ”soft shut-in” is described in step 4 which is first open the choke lines, then close the BOP before the choke line is closed. A ”hard shut-in” is to close the BOP with already closed choke lines. When spacing out the drill string to avoid tool joint obstruction in the BOP the mud pumps should still be kept going. This is because it is preferred to have a distributed homogeneous flow of any kick fluid and not a sudden plug flow. In step 4 it is common to observe for flow in 15 minutes, but several factors affect the recommended time. If drilling with oil-based mud and if the kick fluid is gas, the gas will go into solution and mask itself. Longer wells should have a longer observation time than shorter wells. If no flow is observed, a common practice is to be on the safe side and circulate bottoms up before commencing drilling again. (Grace, 2017)

Several of the most expensive blowouts occurred have been a result of an underground blowout, commonly fracturing the formation beneath the surface casing. Underground blowouts can be avoided by not fracturing the weakest formation, which can be obtained by observing the surface pressure after the well is closed in and not allow it to exceed the maximum allowable annular surface pressure (MAASP), i.e. a surface pressure limit that will cause fracturing of the weakest formation or 80% of the burst pressure limit of the casing. To avoid the pressure exceeding the fracture pressure in the weakest formation a solution can be to open the choke to ventilate some of the pressure out. However, ventilating the pressure out through the choke lines may cause serious damage to the well control equipment and result in a surface blowout. Grace (2017); DrillingFormulas (2014)

Kick Tolerance
An important concept to be aware of when it comes to well control is kick tolerance. Kick tolerance is the volume of kick fluid that can be circulated out of the well without exceeding the fracture pressure of the weakest formation, commonly the formation beneath the last casing shoe. The kick tolerance is usually calculated as a part of the well planning of each section, but it is also updated as the well is drilled, allowing new information to be available such as fracture pressure from leak-off tests.

3.4 Circulating out the kick

When a kick is observed actions must be conducted to safely circulate out the kick fluid before drilling can continue. For all classic well control procedures, it is important to keep the shut-in bottom hole pressure constant to avoid additional influx of formation fluid and fracturing the formation. The two most used methods for secondary well control are the driller's method and wait and weight method:

3.4.1 Driller's Method

The driller's method is one of the most used methods to circulate out a kick. When the kick is noticed the first action is to close the BOP, then decide which of the circulation methods that shall be used. If it is decided to go through with the driller's method, the procedure is to circulate out the kick fluid in one go by using the same mud that was used for drilling. When circulating out the kick, it is crucial to keep a constant bottom hole pressure to avoid more pore fluid to flow into the well. A constant bottom hole pressure is maintained by manually controlling the choke on the kill- and choke line, e.g. reducing the choke will increase the bottom hole pressure due to lower friction loss as a result of less restriction in the flow area.

The driller commonly has two measurements to focus on during a kick circulation procedure, the choke pressure and standpipe pressure. When using the driller's method, the driller needs to first focus on keeping the standpipe pressure constant until the kick fluid is circulated out of the well, then only drilling mud is in the drill pipe and annulus. The next step is to use a new heavier kill mud to regain overbalance and the bottom hole pressure is kept constant by focusing on keeping a constant casing pressure. The correlation between the drill pipe pressure and casing pressure during the driller's method is illustrated in figure 3.2. A detailed procedure for the Driller's method is presented by (Grace, 2017) and will not be discussed any further in this thesis.

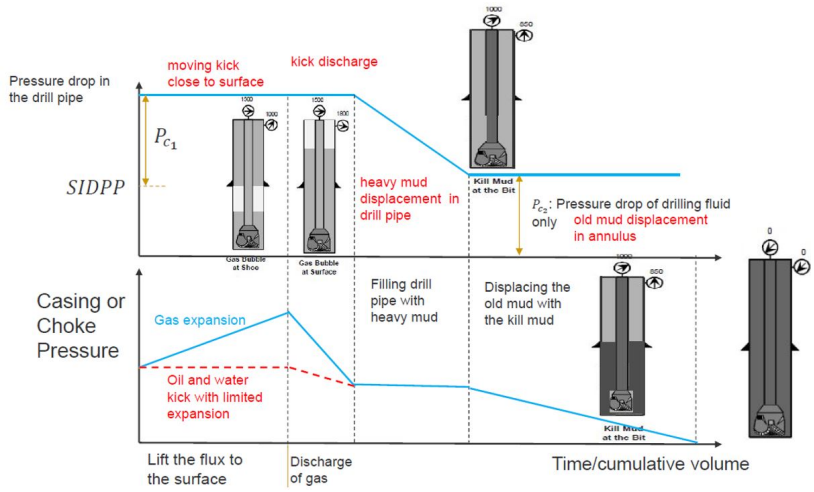

Figure 3.2: Pressure profile for the standpipe pressure and choke pressure during driller's method, courtesy of (Mostofi, 2019)

3.4.2 Wait and Weight

Another classic kick circulation method is the wait and weight method. This is a one circulation method, meaning that both the kick fluid and the old mud is replaced with a heavier kill mud and the well is killed in one circulation. As the name implies, there is a waiting period as the kill mud is being weighted up before the circulation process can start. In recent time the waiting period has been reduced significantly as a result of modern mud-mixing systems. (Grace, 2017)

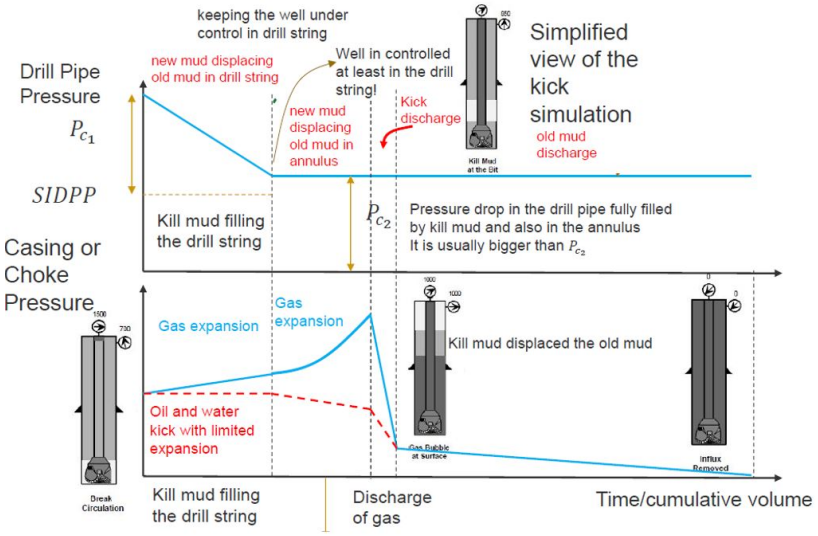

Figure 3.3: Pressure profile for the standpipe pressure and choke pressure during Wait and Weight method, courtesy of (Mostofi, 2019)

Chapter 4

Tertiary Well Control

When a worst-case blowout has occurred, killing the blowing well becomes the highest priority. Killing the well can be done in several ways, first the reservoir may collapse upon the well causing a natural bridging that kill the well. The well can be killed by human intervention, which is either well capping or killing the well by a relief well. Each of these different killing methods is discussed in the following chapter.

4.1 Relief Well

During the planning phase of each well it is necessary to create a plan for killing the well, commonly referred to as a ”Blowout Contingency Plan” or ”Relief Well plan”. When operating on the Norwegian continental shelf the governmental standard NORSOK applies, which states that every well should have two or more relief well spud locations, including anchoring assessment at these locations. Commonly only one relief well is necessary to kill the well, but by having two locations the optimum spud location can be selected based on the wind and current. When the relief well planning and blowout and kill simulations shows that two relief wells are required, one additional spud location is necessary. An illustration of relief wells that intersects a blowing well is shown in figure 4.1. During the planning of a relief well several factors must be accounted for. (Flores et al., 2014) lists five factors that must be considered during the planning of a relief well:

1. Surface location selection, including shallow gas hazard assessment, metocean considerations and rig logistics.
2. Selection of drilling, evaluation, ranging and interception tool.
3. Directional trajectory design utilizing a bottom-up approach.
4. Project execution (drilling operations).

5. Intercepting the well considering cased hole, open hole or the reservoir section of the blowout well.

Surface location
Before the optimal relief well spud location can be determined a site-survey must be conducted at the area, screening for shallow gas anomalies. The spud locations should be located where no shallow gas is expected and at least 500m from the blowing well, upwind and up current of the blowing well. Other considerations that must be taken into account are possible fracture orientations and hard rocks. A simplified relief well trajectory which intersect the blowing well must also be created, this is a requirement in the NORSOK standard.

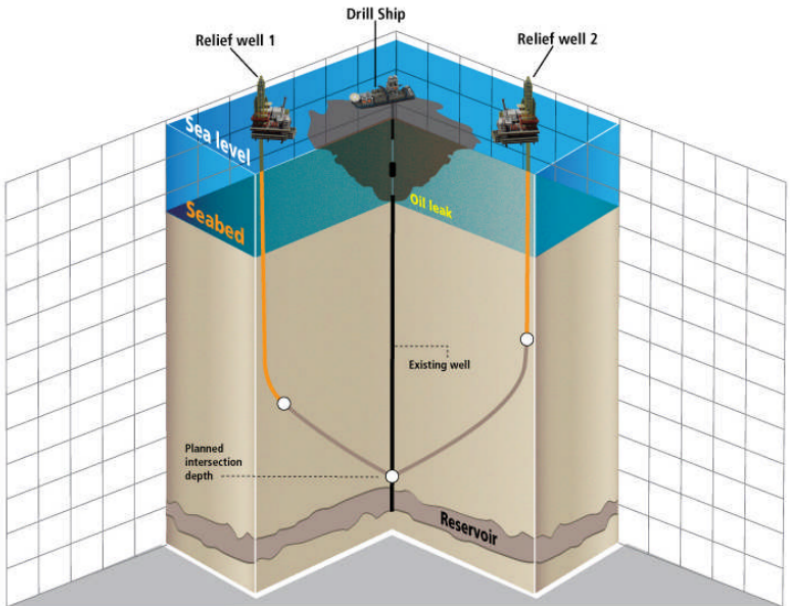

Figure 4.1: Relief well illustration, courtesy of (Flores et al., 2014)

There are two types of relief wells based on how they are used to kill the blowing well, these categories are direct intercept relief wells and geometric relief wells. The direct intercept relief well are as the name implies intercepting the blowing well, while the geometric relief well are drilled near enough the blowing well to establish communication between the two boreholes through the formation. In both methods deciding where the interception or communication point with the well will be is of high importance. Geometric relief wells were often used in the early days of the petroleum industry, but as more accurate ranging methods have been developed the intersecting relief well method has become the industry standard (Grace, 2017)

Well ranging

The ideal situation is to intervene the blowing well at the lowest possible depth, commonly just above the reservoir. This ensures maximum frictional force and hydrostatic head in the blowing well. To accurately intersect the blowing well just above the reservoir is dependent on having either casing or drill pipe in the wellbore at the given depth. The reason behind this is because the normal intervene technique is to use magnetic logging, which require steel in the wellbore. There are two methods of magnetic logging used, either passive magnetic ranging or active magnetic ranging. Another method to intersect the blowing well is to depend solely on the wellbore survey data, but this is not recommended due to the associated uncertainty.

The passive magnetic method uses sensitive magnetometers that measures and analyses the natural magnetic field and detect anomalies caused by the presence of the excessive steel, i.e. casing and/or the drill pipe. Today most of the passive magnetic measurements are included in different measurement while drilling (MWD) tools, but these tools must be within a distance of 30ft to detect anomalies in the earth's magnetic field caused by the presence of casing or drill pipe. (Grace, 2017) Pre-magnetizing of the casing shoe before it is run in the hole will increase the detection range.(AddEnergy, 2018)

The active magnetic method on the other hand consist of two main components which are separated by insulation. These components are a magnetic field-sensor and an electrode. The electrode emits an alternating current (AC) into the nearby formation. The current will short-circuit in contact with casing or drill pipe and travel up and down the tubular causing a fluctuating magnetic field around the steel in the target well, this is illustrated in figure 4.2. This magnetic field can be measured by the magnetic sensors in the relief well making it possible to calculate the direction and distance to the target well. The industry's standard active magnetic tool is the WellSpot tool, which commonly is run on wireline. This tool has an effective range of up to 40m or 130 ft and an accuracy of $\pm$ 20%. (AddEnergy, 2018)

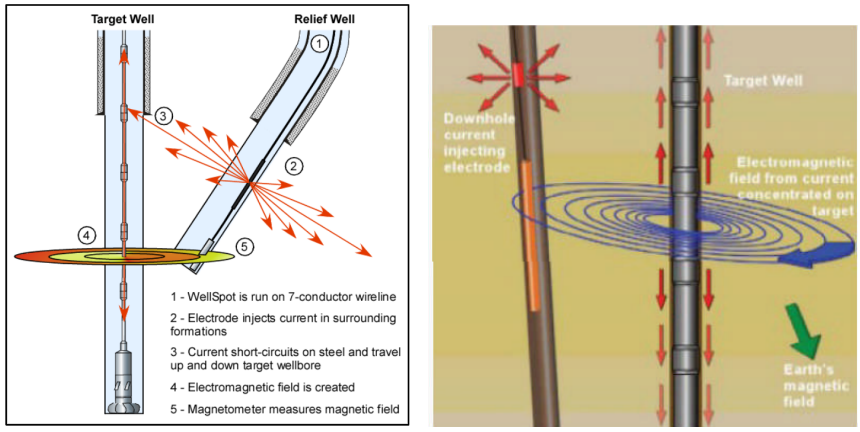

Figure 4.2: Wireline based magnetic ranging on drill pipe and casing, courtesy of (AddEnergy, 2018; Flores et al., 2014)

Killing procedure
When closing in on the target well a normal procedure is to place a casing just above the intersection point to be able to conduct a killing without damaging the relief well. The last distance to the intersection point is drilled with a mill tooth bit. When the relief well is ready to intersect the blowing well, a kill fluid is pumped through the annulus of the relief well and the drill pipe is used for pressure monitoring. The bottom hole pressure is kept between the formation pressure of the blowing well and the fracture pressure of the surrounding formation by adjusting the flow rate into the wellbore. As soon as the target well has been intersected a hydraulic kill process is ongoing.

The kill process is illustrated in figure 4.3. In figure a) the relief well is just about to intersect with the target well. In figure b) The drill bit is retrieved back into the casing shoe to avoid damaging it and kill fluid (blue) is being injected through the annulus into the blowing well. As more and more of the heavy kill fluid is filling the wellbore above the intersection point less formation fluid will flow due to the increased hydrostatic head and friction. In figure c) the blowing well has been killed and it is hydrostatic equilibrium between the kill mud and the reservoir fluid.(Flores et al., 2014; WildWellControl, 2019)

Between figure b) and c) the well is dynamically killed, i.e. the flowing bottom hole pressure (FBHP) exceeds the reservoir pressure and no hydrocarbon flow from the reservoir. The pumps must keep pumping since a part of the FBHP is caused by friction pressure due to flow. When the well is dynamically killed the pump rate is decreased to avoid fracturing the formation. A denser kill fluid is pumped into the wellbore to ensure that the hydrostatic pressure exceeds the reservoir pressure. When dynamically kill is reached the wellbore still contain some hydrocarbons and a common procedure is to circulate two times bottom-up. (Ranold, 2018)

(a) **(b)** **(c)**

Figure 4.3: Intersection and killing procedure, courtesy of (WildWellControl, 2019)

Limiting factors
The limiting factors when killing the well are typically the injection rate or the mud pump pressure, but the required mud volume may also be of a considerable volume. One of several companies that conduct a blowout and kill simulation are Ranold, and their typical kill requirements limitations for a 6th generation drilling unit are shown in table 4.1. However, most of these quantities are on the lower side of what most modern rigs can perform, one example is the mud volume where several of the modern rigs have a capacity between 1000-2000 m^3. In addition, several measures can be made to increase these quantities in a killing situations, such as the kill rate can be increased by using a "Relief well injection spool" which allow several vessels to inject kill fluid simultaneously, more details in Appendix A.7. The mud volume can easily be increased by installing temporary mud tanks on the drilling unit. (AddEnergy, 2018; Ranold, 2018)

Table 4.1: Kill requirements limits for a 6th generation drilling unit, courtesy of (Ranold, 2018)

Quantity	Kill requirement limit
Topside pressure	7500 psig (517 barg)
Horsepower required	8800 hp (4x2200 hp)
Maximum kill rate required	12500 LPM
Volume of kill mud to stop the influx	500 m^3

4.2 Well Capping

A capping stack is an equipment which is placed upon the top end of a blowout preventer (BOP) and seals of the blowing well. The capping stack will be used in the unlikely scenario that a blowout occurs, and the BOP is not capable of shutting the well in. Figure 4.4 shows a capping stack besides a blowout preventer. During the installation of the capping stack upon the top end of the BOP, the stack can either be open allowing formation fluid to flow through the equipment or closed. Having the valves open will reduce the forces acting on the stack, but the installation process will take longer. When the capping stack is properly connected to the BOP, valves are slowly closed until the well is completely shut-in.

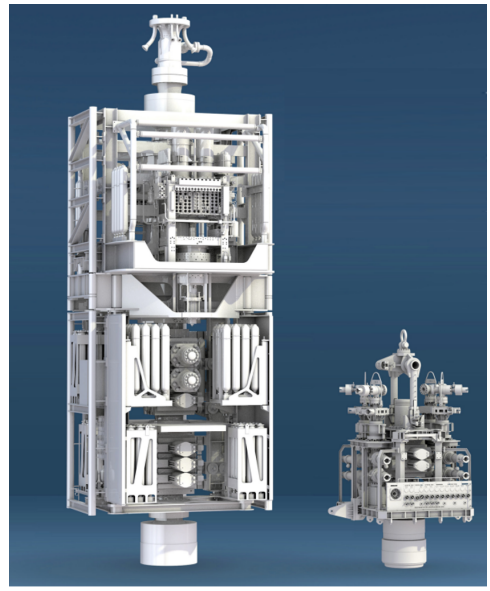

Figure 4.4: A blowout preventer on the left side and a capping stack on the right side, courtesy of (Equinor, 2019)

(Sadenwater, 2014) differentiate between two categories of capping stacks, where the main different depends on if the wellbore have full pressure integrity during a shut-in or not. If the wellbore has sufficient pressure integrity it will be safe to completely shut-in the well, if not a capping stack with the possibility to divert and choke the flow must be used. The flow can be redirected through flexible pipes up to the surface vessels. When the well is securely shut-in, the process with killing the well by injecting kill mud can begin. The capping stack has one or more outlets for pumping kill fluid into the wellbore. (Equinor, 2019; Madrid and Matson, 2014).

During the Macondo blowout in 2010 the first capping stack was designed and placed upon the blowing well with success. Today it is a common practice to have one or more capping stack ready for the operators in a certain basin. The closest capping stack available for the Norwegian continental shelf is located in Montrose Scotland. If the unlikely event of a blowout would happen, the capping stack will be loaded on a crane vessel and shipped out to the blowing well. At the location, the crane vessel will lower the capping stack down guided by ROVs. Before the stack arrives the ROVs have checked the well equipment, removed debris, cleaned and prepared the wellhead for installation. When the capping stack is installed chemicals can be injected through different injection ports, commonly injected chemicals are methanol and glycol to prevent the formation of hydrates. Figure 4.5 illustrates the installation process. (Madrid and Matson, 2014)

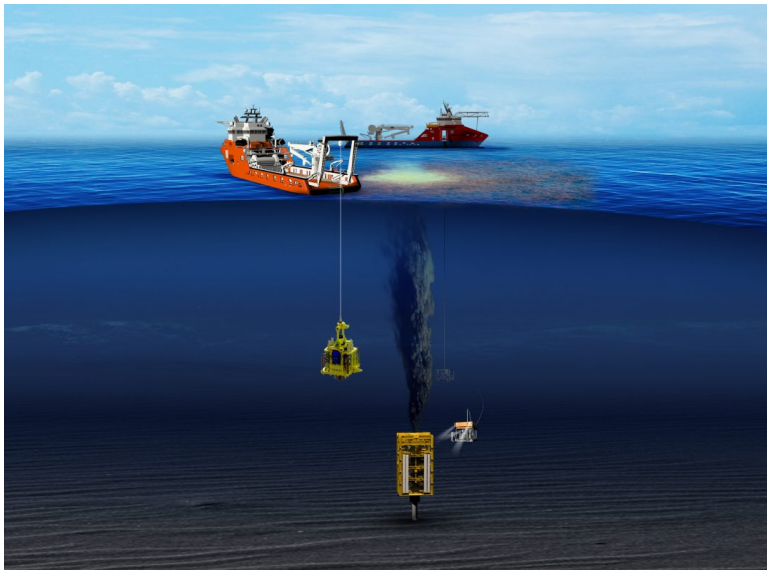

Figure 4.5: The installation process of a capping stack, courtesy of (LatamEnergy, 2019)

4.3 Natural Bridging

Natural bridging is when the blowouts end after a certain period, it is self-killing. The causes of natural bridging are that the borehole or sediments in the uncased part of the wellbore collapses and form a seal in the wellbore, restricting the formation fluid from flowing. The mechanism for this collapse are many, some examples given by (Willson et al., 2013) are: ”borehole collapse of soft shales, sand erosion leading to cavity collapse, gas depressurization and brine influx” If natural bridging occur it is most likely to happen within a short time period. In some cases, natural bridging occurs after just a couple of hours, but in most cases within a week. Two mechanism of natural bridging are shown in figure 4.6. (Danenberger, 1993)

If natural bridging will happen depends on several factors such as the strength of the formation, the blowout rate and how sudden the well goes from a normal state to a full blowout. A study conducted by (Willson et al., 2013) describes a method to determine if a well is likely to self-kill by natural bridging. This procedure has four main stages and is presented as following:

1. **Kick-development analysis:** this stage focuses on determining the time it takes for the kick to develop into a fully blowout, and how the wellbore pressure and velocities change with time
2. **Assessment of borehole collapse:** this stage takes into account the formation strength and the variation in wellbore pressure with respect to wellbore stability.
3. **Cavings volume and transport analysis:** this stage focuses on the development of cavings in the formation surrounding the wellbore and how the particle are transported out of the wellbore by fluid velocity.
4. **Cavings bridging analysis:** Based on the concentration of cavings or spalled material in the well an analysis is conducted telling if natural bridging is likely or not.

For a well to self-kill by natural bridging it is crucial that cavings, particles or any parts of the formation seal the borehole. The failure of the formation can happen in several ways. Failure can be caused by pressure related mechanism causing a borehole stability problem such as shear failure or tensile failure. These pressure related failure mechanisms can be calculated by using the Mohr-Coloumb method. The well may self-kill if the fluid velocity is below the slip-velocity, causing accumulation of cuttings. If erosion of the borehole wall causes a large part of cavings to fall out. The cutting concentration may approach a critical cutting concentration value where the viscosity goes to infinite, resulting in a reduced flow and cuttings accumulation killing the well. Several studies such as (Pabst, 2004; Senapati et al., 2009) discuss the effect suspended cuttings have on the viscosity and that a critical concentration exist where the viscosity skyrockets. This critical concentration is commonly in the range [0.50 - 0.64]. Erosion my lead to huge cavings beneath a more consolidated layer. This consolidated layer cannot support itself without support from beneath for a given length, when the cavings exceeds this threshold the consolidated layer is evident to collapse which may seal the wellbore and kill the well. (Willson et al., 2013)

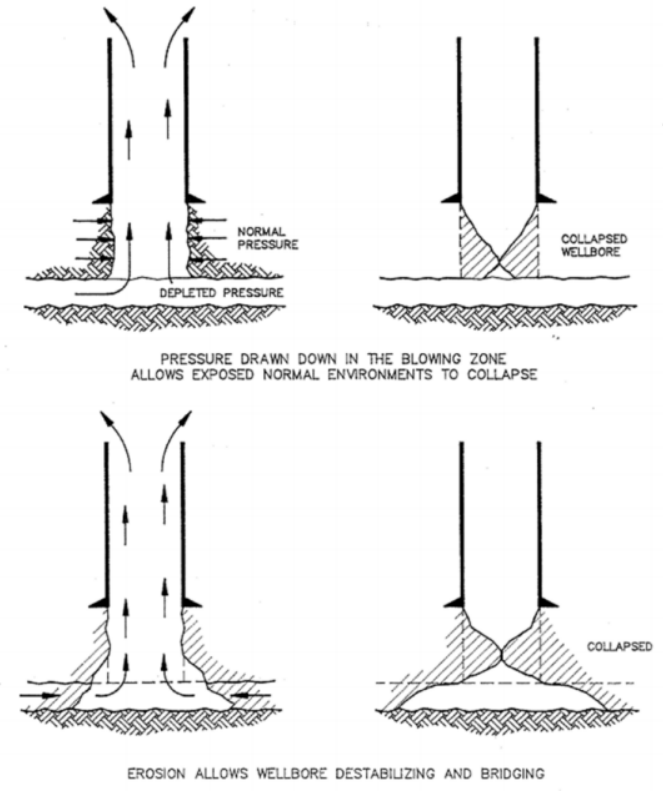

Figure 4.6: Borehole collapse causing natural bridging, courtesy of (Willson et al., 2013)

During the period between 1971 and 1991 a total of 87 blowouts occurred while drilling almost 21 500 wells in the Gulf of Mexico. Of all the wells drilled exploration wells accounts for 37.4%, but the number of blowouts that occurred during drilling of the exploration represents 55.4%. This leaves a higher statistical chance for facing a blowout during the drilling of an exploration well than productions or appraisal wells. The increased chance to encounter a blowout during the drilling of an exploration well is most likely caused by absence of geological information and drilling data. As most of the exploration wells will not find a producible hydrocarbon interval it is safe to conclude that most of these blowouts were caused by shallow gas. By taking the wellbore depth when facing the blowout into account it is shown that almost two thirds of both the exploration wells and development wells were caused by shallow gas. (Danenberger, 1993)

Of all the 87 wells were a blowout occurred most of the blowouts were of short duration. 20.7% stopped flowing after less than 1 hour, while more than half (57.5 %) stopped flowing after one day. In less than one week most of the wells ceased flowing, a cumulative amount of 83.9%. Figure 4.7a shows the distribution of how long it took for the blowouts to stop flowing. Most of these wells faced natural bridging, a total of 71%. Figure 4.7b shows

the distribution of how the blowouts were stopped. It is important to see that not all the wells in figure 4.7a were stopped as a result of natural bridging. However, most of the wells were naturally bridged and one can assume the distribution still is valid. (Danenberger, 1993)

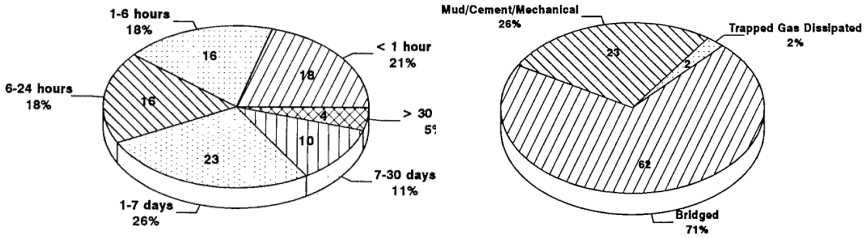

Figure 4.7: Blowout stoppage time and causes of stoppage, courtesy of (Danenberger, 1993)

Chapter 5

Blowout

Taking a blowout is a fatal consequence of having an improper well control, but not all blowouts are the same. The impact of the blowout can in many ways be determined by the magnitude of the uncontrolled blowout rate, commonly in the range of several thousand Sm^3/day, but some blowout rates may be low (less than 10 $Sm3/day$). How high the blowout rate becomes depends on several factors such as the reservoir productivity, the length of the well, the depth of the reservoir, the reservoir fluid and if the blowout is to surface or seabed. This chapter describes some of the different dynamics regarding the blowout behavior and some statistics from the latest years.

5.1 Different types of blowouts

There are several ways to classify the blowout type, one type of blowout classification is based on the blowout location. The blowout can be a blowout to surface, a blowout to seabed or an underground blowout. Other ways to classify the blowout is based on the reservoir fluid, which may be a gas blowout, an oil blowout, a water blowout or most commonly a combination of the different fluids. The blowout can also be classified based on the blowout rate. (Grace, 2017)

- **Surface blowout** - The hydrocarbons flow through the well and flow out to surface against the atmospheric pressure (1.013 Bar). This is commonly the blowout type with the highest blowout rate, due to the low back pressure. This type of blowout can cause huge damage on the drilling rig, equipment and personnel. (Krieg, 2018)
- **Seabed blowout** - The blowout happens at the seabed against the hydrostatic pressure from the water column above. This require an offshore well and that the riser is partly or fully disconnected. This kind of blowout can affect the buoyancy of a floating drilling unit, especially if the blowout fluid consists mainly of gas.

- **Underground blowout** - Somewhere along the wellbore the formation and/or casing have fractured, the reservoir is now injecting reservoir fluid into another less pressurized formation. If the formation consist of fractures and a connectivity to surface is present, a blowout to surface some distance away from the well location may occur.

An important factor for determining the blowout rate is how the reservoir fluid flow through the wellbore. Given that the wellbore and formation are intact, three different flow paths may happen: blowout through open/cased hole, blowout through annulus and blowout through the inside of the drill string. A smaller area available for flow will, i.e. the cross-section area, result in a higher friction pressure which will increase the flowing bottom hole pressure (FBHP). The blowout rate is a function of the flowing bottom hole pressure, i.e. a decrease in the cross-section area will result in a lower blowout rate. A worst case scenario will be a blowout through open/cased hole and the best case scenario a blowout through drillpipe. The different types of blowout paths are presented in figure 5.1 for a scenario of blowout to surface.

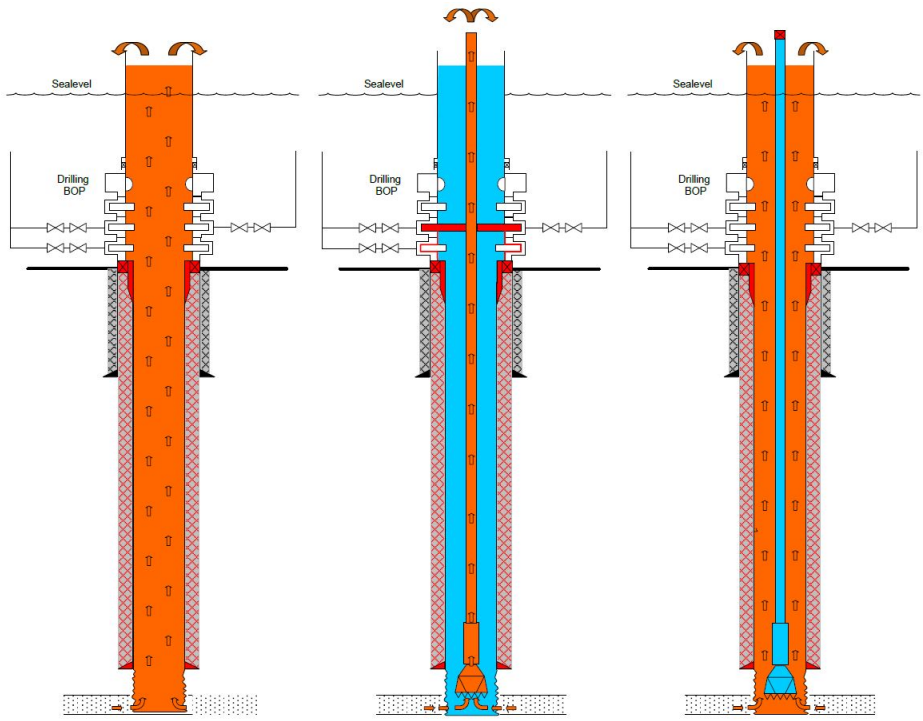

Figure 5.1: Possible blowout paths for a blowout to surface. From left: Open hole, drill string and annulus. The orange represents the reservoir fluid, while blue represents the drilling mud. Courtesy of (Ranold, 2018)

5.2 Blowout statistics

As discussed above there are several blowout paths and scenarios which will have an impact on the blowout rate. It is important to be aware of the statistical distributions of these blowout scenarios to be best prepared of taking a blowout. Some important statistics are presented below.

When using a floating drilling unit, the typical statistical distribution of blowout release point is presented in table 5.1. Where one can see that the probability of having a subsea blowout is twice as probable as a blowout to surface. These statistics are based on the ”Sintef Offshore Blowout database” (Sintef, 2020) and was presented by (Ranold, 2018), this database includes information from 642 offshore blowout worldwide. The data are not directly representative for the Norwegian continental shelf due to a different set of standards used in the world.

Table 5.1: Blowout statistics - Release point when using a floating drilling unit

Scenario	Probability
Blowout with a surface release point	32 %
Blowout with a seabed release point	68 %

Further on, the blowout path has a statistical distribution as presented in table 5.2, (Sintef, 2020; Ranold, 2018). Where one can see that a blowout through annulus has the highest probability by far.

Table 5.2: Blowout statistics - blowout flow paths

Scenario	Probability
Blowout through open/cased hole	16 %
Blowout through drill pipe	12 %
Blowout through annulus	72 %

During the drilling of the well a blowout preventer stack (BOP) is placed on the top of the wellhead. The BOP consists of a set of hydraulic operated valves that can either close around the tabular or cut and seal the wellbore. The BOP shall be able to stop a blowout, but in some cases it malfunction, is not properly activated or activated too late. Based on “OLF Guidelines for estimation of blowout potentials” (olje og gass) presented by (Ranold, 2018) uses the statistical representation of BOP failures as presented in table 5.3

Table 5.3: Blowout statistics - restrictions in flow area

Scenario	Probability
Restricted in flow area due to BOP	70 %
No restriction in flow area	30 %

How much of the reservoir that is penetrated when the well control is loss highly affect the total productivity of the reservoir and thus the blowout rate. Having a partly penetration will result in a lower blowout rate than a full reservoir penetration. A partly penetration of 5 m MD is the common value to assume. If a blowout has occurred the probabilities whether it is a fully or partly reservoir penetration are presented in table 5.4, which show that a blowout occurs with a partly reservoir penetration 3 / 5 times. If the blowout occurs with a partly reservoir penetration one can assume that the rig is currently drilling, i.e. drillpipe is still inside the wellbore. This will result a blowout path through either annulus with an 86% probability or through drillpipe with a 14% probability. (Ranold, 2018). More on how the partly reservoir penetration affects the productivity index is discussed in Appendix A.1.

Table 5.4: Blowout statistics - reservoir penetration

Scenario	Probability
Partly reservoir penetration	60 %
Full reservoir penetration	40 %

By combining all of the different scenarios described above one can calculate the total blowout risk for the possible combinations of blowout scenarios and paths. The total risk for the different blowout scenarios are visualized in figure 5.2.

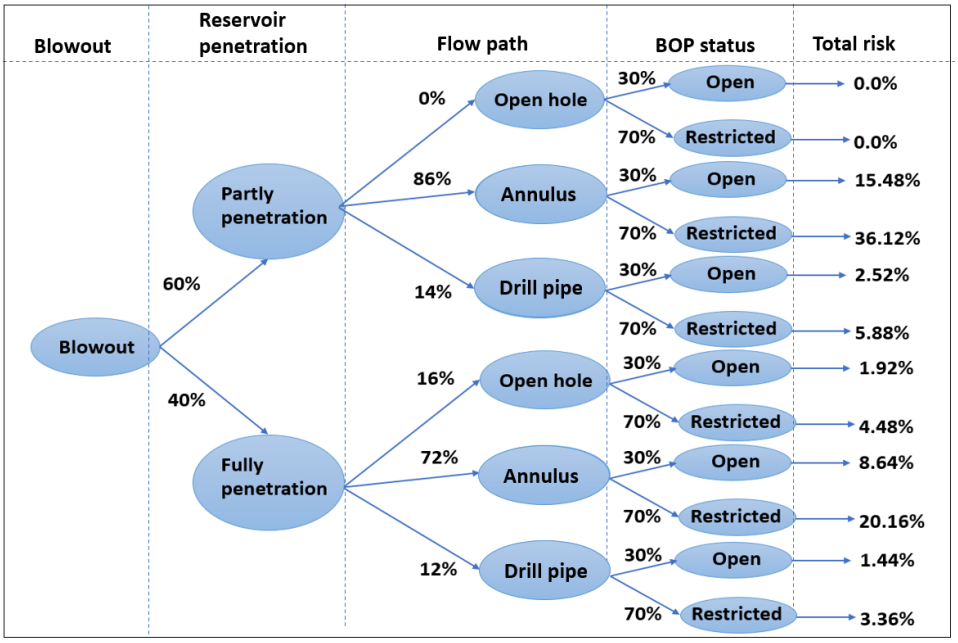

Figure 5.2: Different blowout scenario combinations and probability for each scenario, together with the total risk for a given combination

Chapter 6

The blowout and kill simulator

The predominance of the workload in this master thesis is connected to coding the blowout and kill simulator. By combining the theory described in section 3 to 5, as well as the theory described in Appendix A, a blowout and kill simulator can be created. In this chapter the main elements from the simulator will be discussed and references to the theory behind each section will be made.

6.1 User friendliness and input data

One important factor with all kinds of software, applications and in this case a simulator is user friendliness. An intuitive and simple user interface will make the simulator easy to use and more effective when it comes to running simulations for new cases. One of the key elements with this simulator is to have an easy user interface for input data, running the simulation and reviewing the results.

6.1.1 Input data

Since more or less everyone is used to ”Microsoft Excel”, it was chosen to be the platform of data input. An Excel file that include all the necessary input data was created, an example of this excel sheet is presented in figure 6.1. The excel sheet ask for information related to the rig, well design, reservoir, reservoir fluid and the relief well. Since the petroleum industry often uses a mixed set of units, two sets of units were added to the ”Simulator - input sheet”. Allowing the user to switch between ”Oil field units” and ”Semi SI-units”. The conversion from one unit to the next goes automatically through a piece of code created in Visual Basics (VBA), Excel’s programming language. A well schematic is also included in the ”Simulator - input sheet”, making it easier for the user to control that the well design is as desired. The user can choose from two multiphase pressure correlations, Olgjenka or Orkiszewski, and two sets of PVT correlations, Standing or Glasø. The multiphase pressure correlations are described in Appendix A.5, while the PVT correlations are described in Appendix A.6. All the input values in the excel file are read by the simulator and converted to the proper units before the simulation starts.

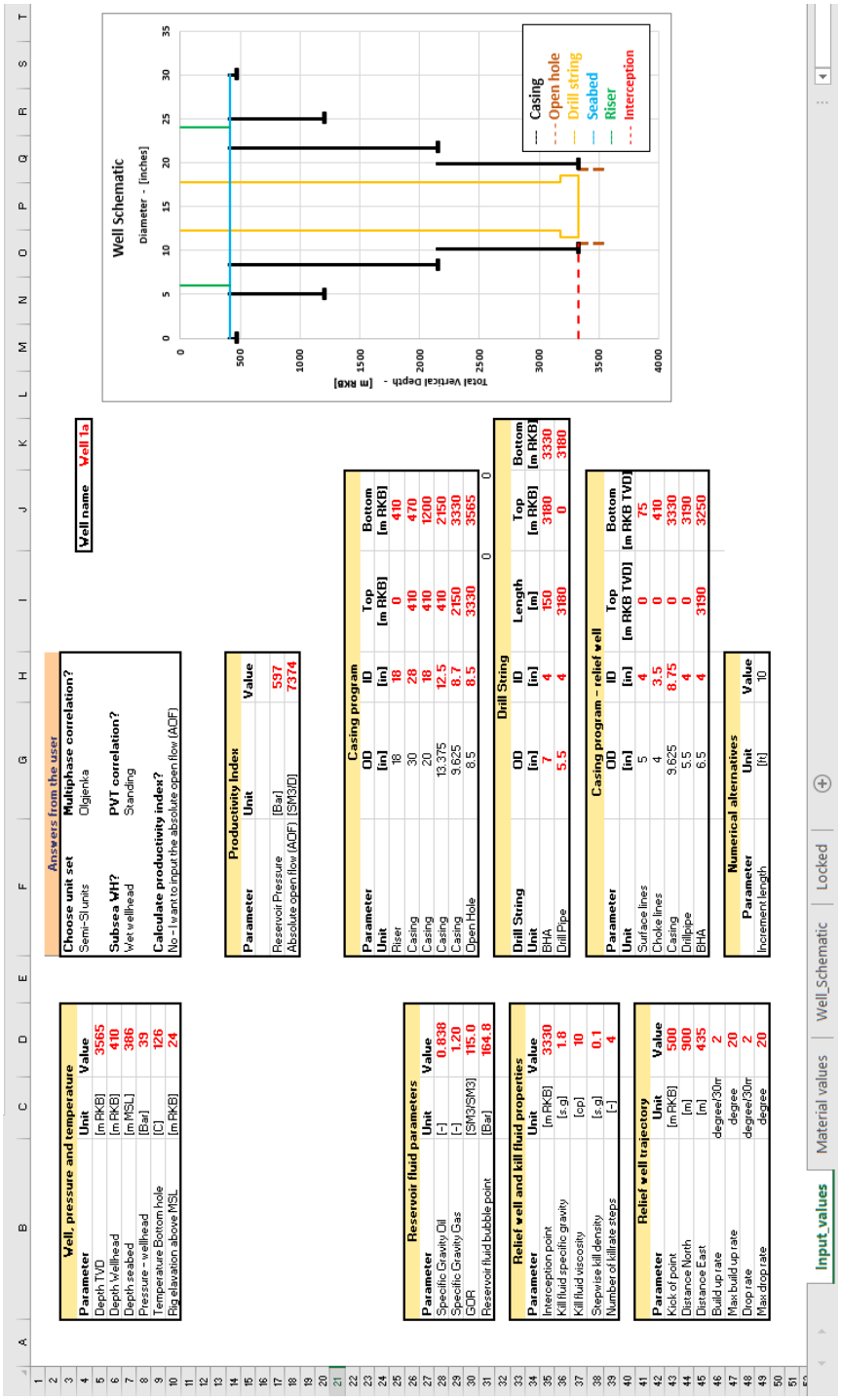

Figure 6.1: The simulator's Excel input file

6.1.2 Running the simulator

When all the necessary input parameters are filled out in the ”Simulator - input file” the simulations can begin. The only required action is to open the Matlab file ”The_Simulator”, click the green play symbol ”Run” in the software or F5 on the keyboard and the simulator will ask for the ”Simulator - input file”. When the excel file is located the simulator will calculate several scenarios based on the input values. The simulator calculates the blowout rate for a seabed and surface blowout for two flow paths, open/cased hole and annulus. Kill rates through an open/cased hole for both a surface and seabed release point are calculated. For both release points the simulator calculates four different kill rates: ”best prediction”, ”not adjusted”, ”higher rate” and ”lower rate”. The ”not adjusted” is an uncalibrated kill rate, while the other three are based on the calibration process described in section 7.4.3.

In total 4 blowout rates, 8 kill rates and 8 times the number of kill fluid density steps are calculated by the simulator. The simulator workflow is described in section 6.2 and a detailed example is gone through in section 6.3.

6.1.3 Automatically generated report

A report is automatically generated when all the different scenarios are calculated. The simulator shows the used input data and the different blowout rates, kill rates and required pumping capacities for each scenario. An example on the generated report is shown in Appendix B, the same well which is detailed explained in section 6.3. The simulator is written with the Matlab release - ”Matlab R2020a” and this release or a newer release may be required to run the automatically generated report.

6.2 The workflow of the simulator

The created blowout and kill simulator follows a complex work flow. The best way to describe the workflow is by a stepwise process for the different parts of the simulator. A flow chart is created to give an overview of the workflow in the simulator, this flow chart is presented in figure 6.2. A stepwise process which gives an overview of the workflow for the entire simulator is presented in section 6.2.1. A more detailed procedure is described for the blowout rate in section 6.2.2 and for the kill rate in section 6.2.3. The simulator goes through four iterative loops as listed below.

In total the simulator consists of 32 different scripts with almost 4000 lines of code, more details of the codes are presented in Appendix C.

- Scenario loop - Determine the blowout or kill scenario, blowout release point, the flow path, kill fluid density and kill rate calibration factor.
- Kill rate loop - Calculates the kill rate for the scenario.
- Blowout rate loop - Calculates the blowout rate.
- Well/increment loop - Calculates the Flowing bottom hole pressure (FBHP).

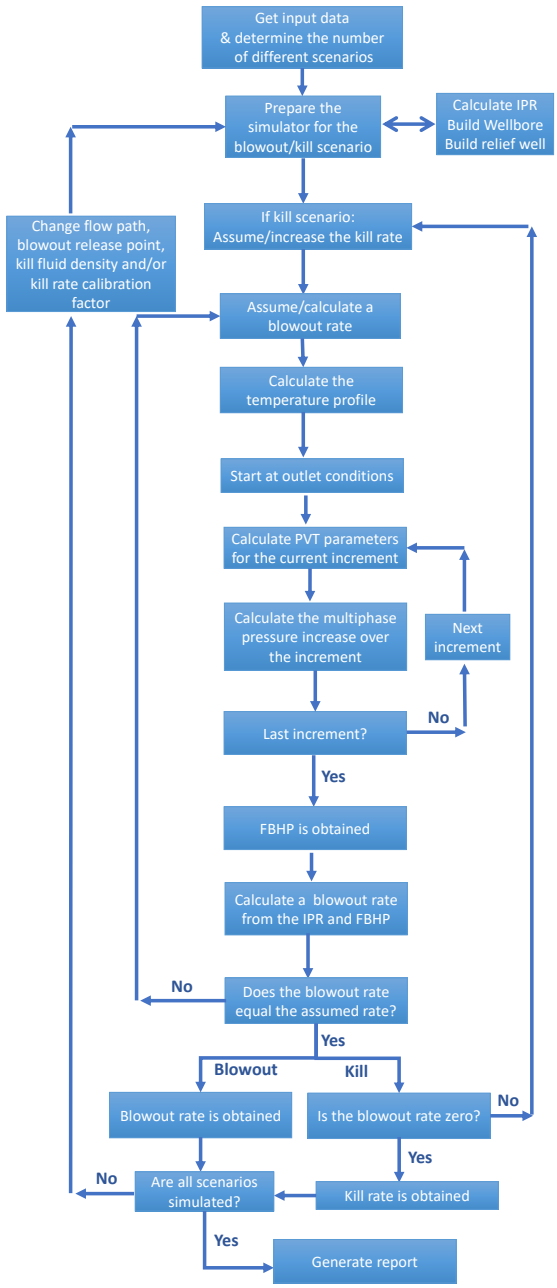

Figure 6.2: Flow chart over the blowout and kill simulator

6.2.1 The simulator's stepwise process - overview

1. The Matlab script reads the data input from the excel file and determine the number of scenarios to be simulated.
2. Based on the different options from the user the Excel file calculates certain parameters, such as the productivity index or the absolute open flow potential.
3. The inflow performance relationship (IPR) is calculated based on the input data, the theory is described in Appendix A.2.
4. Based on the well design, a sorted well is created taking only the innermost tubular into consideration, i.e. neglecting casings that are not in contact with the flowing fluid. This sorted well is used to calculate the flowing liquid velocity at different depths in the wellbore and play a vital part in the calculation of the friction pressure.
5. A relief well is built with a S-trajectory, a simple build, hold and drop well path. This gives the total length of the relief well which is used for pump pressure calculations and the kill fluid temperature profile.
6. The blowout rate is calculated. (See the blowout rate procedure - section 6.2.2)
7. The kill rate is calculated. (See the kill rate procedure - section 6.2.3)
8. A report is automatically created as a pdf file for the conducted simulation. The report contains most of the input data and the calculated results for all simulated scenarios.

6.2.2 The simulator's stepwise procedure - Blowout rate

1. Before the blowout simulation is started some information must be present: a) blowout release point, b) multiphase correlation, c) PVT correlation and d) flow path.
2. An initial blowout rate is calculated based on the inflow performance relationship and an assumed flowing bottom hole pressure that equals 80% of the reservoir pressure.
3. The well is divided into N numbers of increments with a predefined length, in the simulations run in this thesis this length equals 10 ft.
4. A temperature profile is calculated for each of the increments based on the reservoir temperature, the blowout rate, heat capacity of the reservoir fluid, the thermal conductivity of the casing or formation and the temperature in the surrounding formation.
5. The well/increment iterative loop is started, going through all the increments for the entire well. The iterative process starts either on:
   a) The drill floor with a back pressure of 1 atmosphere, given that the blowout release point chosen is to surface.

b) The seabed with a back pressure equals the hydrostatic pressure at the seafloor, given that the blowout release point is to seabed.

6. It is possible to choose between two different sets of PVT correlations. These are the Glasø-set (Appendix A.6.2) and Standing-set (Appendix A.6.1). The PVT parameters are calculated for the pressure and temperature for the current increment.
7. For each increment the pressure increase over the length of the increment is calculated. The simulator distinguishes between two different multiphase pressure correlations:
   a) The Orkiszewski's correlation - Appendix A.5.2
   b) The Olgjenka correlation - Appendix A.5.3
8. When the well/increment iterative loop (started in step 5) is finished, the flowing bottom hole pressure (FBHP) equals the pressure in the last length increment. This pressure is used with the IPR to calculate a new blowout rate.
9. If the calculated blowout rate does not equal the blowout rate calculated/assumed in step 2 within a predefined difference, the stepwise process repeats itself starting at step-2 with the new blowout rate.
   *Note some additional calculations for the new blowout rate is made to avoid an eternal loop with the Orkiszewski correlation, see Appendix A.9.
10. When the blowout rate calculated/assumed in step 2 equals the calculated blowout rate in step 8 within the predefined difference the blowout simulation is finished. The final blowout rate is calculated and the well-reservoir-system is in a stationary equilibrium, at least in a short time frame neglecting that the average reservoir pressure is reduced with time.

6.2.3 The simulator's stepwise procedure - Kill rate

The kill rate procedure is almost the same as the blowout procedure, but the kill rate loop is included as well which require some additional steps.

1. Before the kill simulation is started some information must be present: a) blowout release point, b) multiphase correlation, c) PVT correlations, d) flow path, e) kill fluid density and f) kill rate calibration factor.
2. The blowout rate is calculated based on the blowout rate procedure. This blowout rate remains as a starting point for each new kill rate. For each blowout iteration loop the calculated blowout rate is used.
3. A kill rate is calculated based on a predefined kill rate step size. In the simulations presented later in this master thesis, the kill rate step equals 250 LPM.
4. The well is divided into N numbers of increments with a predefined length, in the simulations run in this thesis this length equals 10 ft.
5. A temperature profile is calculated for each of the increments based on the reservoir temperature, the blowout rate, the kill rate, heat capacity of the reservoir fluid and

kill fluid, the thermal conductivity of the casing or formation and the temperature in the surrounding formation. Above the interception point, between the blowing well and the relief well the two fluids will mix and the temperature is equal the temperature of the mixture, see Appendix A.4.

6. The well/increment iterative loop is started, going through all the increments for the entire well. The iterative process starts either on:
   a) The drill floor with a back pressure of 1 atmosphere, given that the blowout release point chosen is to surface.
   b) The seabed with a back pressure equals the hydrostatic pressure at the seafloor, given that the blowout release point is to seabed.
7. The PVT parameters are calculated with one of the two PVT correlations for the pressure and temperature at the current increment. The density and viscosity of the liquid phase is adjusted to take into the account of both oil and kill fluid.
8. For each increment the pressure increase over the length of the increment is calculated. The simulator distinguishes between two different multiphase pressure correlations:
   a) The Orkiszewski's correlation - Appendix A.5.2
   b) The Olgjenka correlation - Appendix A.5.3
9. The pressure calculation uses the down hole flow rate of hydrocarbons and kill fluid for all the increments that are shallower than the interception point. It is assumed that only hydrocarbons are below the interception point, see Appendix A.8.1.
10. When the well/increment loop (started in step 6) is finished the flowing bottom hole pressure equals the pressure in the last increment. This pressure is used with the IPR to calculate a new blowout rate.
11. If the calculated blowout rate does not equal the blowout rate calculated/assumed used going into step 3 within a predefined difference, the stepwise process repeats itself starting at step 3 with the new blowout rate to be used together with the current kill rate.
    *Note some additional calculations for the new blowout rate is made to avoid an eternal loop with the Orkiszewski correlation.
12. When the blowout rate calculated in step 3 equals the calculated blowout rate in step 10 within the predefined difference, the kill simulation is finished for the current kill rate. The final blowout rate is calculated and the blowing well - relief well - reservoir-system is in a stationary equilibrium.
13. When the system is in stationary equilibrium and the blowout rate calculated in step 10 does not equal zero, a new kill rate is used and the blowout rate is set to the original blowout rate from the blowout procedure. The process repeats itself starting from step 3 with the new kill rate.
14. When the system is in stationary equilibrium and the blowout rate calculated in step 10 equals zero, the kill simulation for the given kill fluid density is finished and the kill rate required to kill the well is obtained.

6.3 Example - Well 1a

Several wells are simulated as a part of this master thesis, but in this section a detailed description of the stepwise blowout and kill simulation procedure is conducted for one scenario for Well 1a. The chosen scenario is a blowout through open/cased hole to surface and a surface kill with a kill fluid density of 1.8. s.g.

6.3.1 Step 1 - Input data

The Matlab scripts reads the input parameters from the "Simulator - input file" and convert the units. The input parameters for the example well is presented in table 6.1 to 6.7

Table 6.1: Example well 1a - Rig and well properties

Well	Total depth [m TVD RKB]	Water depth [m MSL]	Rig elevation [m MSL]
Well 1a	3565	386	24

Table 6.2: Casing program - well 1a

Parameter Unit	OD [in]	ID [in]	Top [m RKB]	Bottom [m RKB]
Riser	18	18	0	410
Casing	30	28	410	470
Casing	20	18	410	1200
Casing	13.375	12.5	410	2150
Casing	9.625	8.7	2150	3330
Open Hole	8.5	8.5	3330	3565

Table 6.3: Reservoir fluid - well 1a

Oil gravity [s.g.]	Gas gravity [s.g.]	GOR [Sm3/Sm3]	Saturation pressure [Bar]
0.838	1.200	115	165

Table 6.4: Reservoir productivity - well 1a

Productivity Index [Sm3/d/bar]	AOF [Sm3/d]	Reservoir temperature [Celsius]	Reservoir pressure [Bar]
-	7374	126	597

Table 6.5: Relief well casing program - Well 1a

Parameter Unit	OD [in]	ID [in]	Top [m RKB TVD]	Bottom [m RKB TVD]
Surface lines	5	4	0	75
Choke lines	4	3.5	0	410
Casing	9.625	8.75	0	3300
Drillpipe	5.5	4	0	3190
BHA	6.5	4	3190	3250

Table 6.6: Interception and kill fluid - well 1a

Parameter	Unit	Value
Interception point	[m RKB]	3330
Kill fluid specific gravity	[s.g]	1.8
Kill fluid viscosity	[cp]	10
Stepwise kill density	[s.g]	0.1
Number of kill rate steps	[-]	4

Table 6.7: Relief well trajectory - well 1a

Parameter	Unit	Value
Kick of point	[m RKB]	500
Distance North	[m]	900
Distance East	[m]	435
Build up rate	degree/30m	2
Max build up rate	degree	20
Drop rate	degree/30m	2
Max drop rate	degree	20

6.3.2 Step 2 and 3 - Parameter conversion and IPR calculations

Based on the answers given by the user different parameters must be calculated. One example is the reservoir productivity. The user can choose between:

- Calculate the well productivity based on reservoir parameters, see appendix A.1.
- Calculate the well productivity based on the absolute open flow potential (AOF).
- Calculate the well productivity based on the productivity index (PI).

For each of the above-mentioned choices the productivity index is used to calculate the inflow performance relationship (IPR). The theory behind the productivity index and reservoir parameters are presented in Appendix A.1. For well 1A the absolute open flow potential of 7374 $[Sm^3/D]$ is used as an input value which gives a productivity index equal

14.1 $[Sm^3/d/bar]$. The conversion from AOF to PI can be done using the equations presented in Appendix A.2. The inflow performance relationship is calculated and the IPR is presented in figure 6.3 for well 1a.

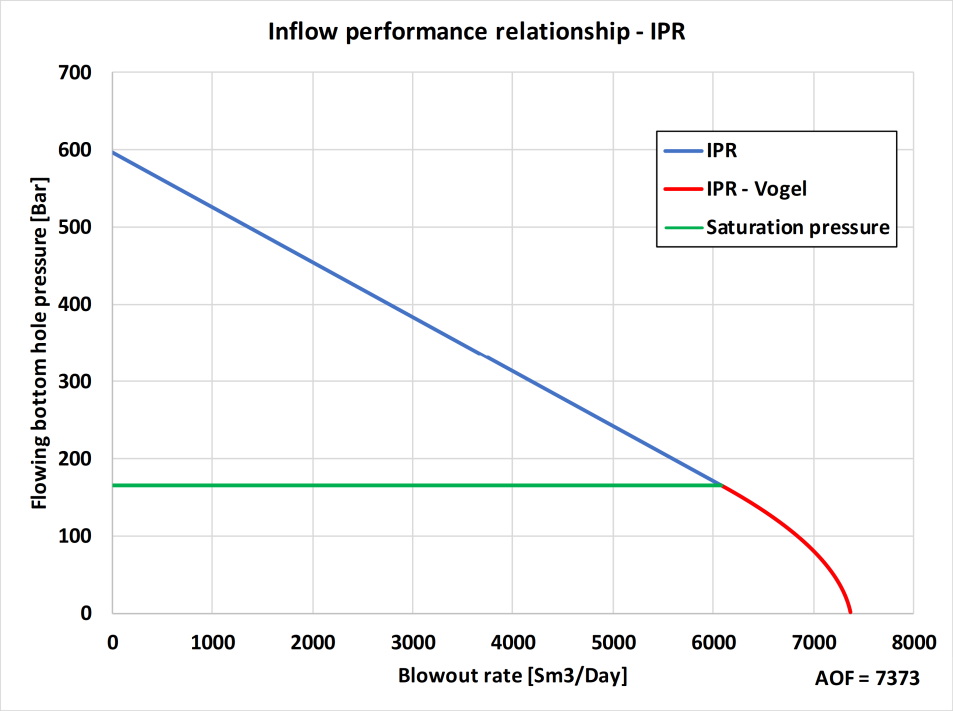

Figure 6.3: Well 1a - Inflow performance relationship

6.3.3 Step 4 - Well construction

Based on the casing design given in table 6.2 a matrix is created to account for the parts of the well that are in contact with the flowing fluid, i.e. a matrix consisting of a depth vector, an outer diameter vector and an inner diameter vector given that the drill string is inside the wellbore). Figure 6.4 is an illustration of the actual well versus the used well when no drill string is in the wellbore.

The length of the well is divided into N increments with an increment length of 10 ft or 3.05m. For the presented case this equal 1170 increments. The increment step size can be changed in the simulator, but a length of 10ft was chosen to avoid having too large gaps when going from one size of casing to the next. Another important factor when choosing the step size is to have both an acceptable accuracy and run time, i.e. a lower the step size might give a better accuracy on the cost of a longer simulation time.

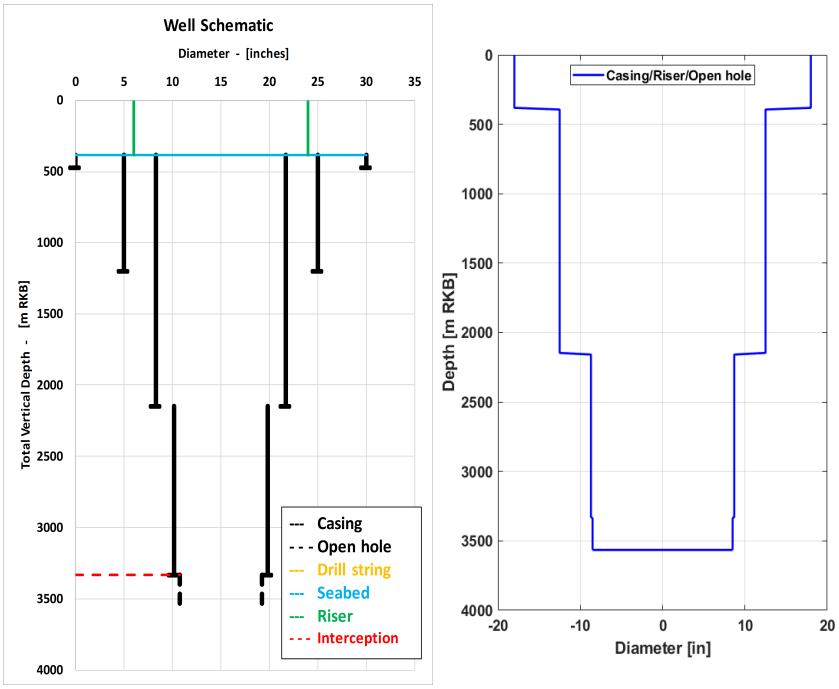

Figure 6.4: Well 1a open/cased hole to surface. From the left: The actual well design, on the right: The well design used in the simulator - the set of tubulars that are in contact with the flowing fluid

6.3.4 Step 5 - The relief well

The relief well is discussed in chapter 4. It is the connection between the mud pumps on the relief well rig and the blowing wellbore. The mud pumps inject kill fluid through the relief well into the blowing well, with the intent to increase the flowing bottom hole pressure so it exceeds the reservoir pressure and influx from the reservoir stops. It is also important that the formation along the wellbore does not fracture. In the simulation of the kill procedure the relief well is represented by a flow rate increase from the interception point to the blowout release location.

To be able to calculate both the kill fluid temperature at the interception point (IP) and the necessary mud pump topside pressure a relief well must be created. In the simulator, a relief well with a simple build-hold-drop trajectory (an S-well) is approximated. Since a relief well should be drilled as easy as possible this approximation should not be too bad, but often a relief well must be drilled through troublesome formation making a S-trajectory incorrect. In other occasions the reservoir depth or the lowest depth possible to magnetically range the blowing well might be too shallow to allow a S-trajectory, making a J-trajectory the preferred choice.

During the magnetic ranging from the relief well, different wireline tools are used, these tools often have an angle restriction of 60 degrees. As a part of the input data it is possible

the choose the build-up rate, the maximum build angle, the drop rate and the maximum drop angle to account for the restriction related to the wireline tools. Governmental regulations, such as NORSOK, often regulate the minimum distance the relief well spud location can have to be within a safe zone of poisonous fumes or oil spills from of the blowout. To be able to account for this distance in the simulator the distance in both Northing and Easting relative to the blowing well is an input option in the ”Simulator - input file”.

The theory related to the well trajectory is discussed in Appendix A.3, which is based on a constant azimuth and the radius of curvature. The relief well used in the simulation of case well 1a is shown in figure 6.5. Values such as the measured depth (MD), horizontal departure (H) and total vertical depth (TVD) are listed as text inside the figure, a plot showing the distance north, east and the azimuth (α) in the top right corner. The red lines show the build or drop radius with the angle included.

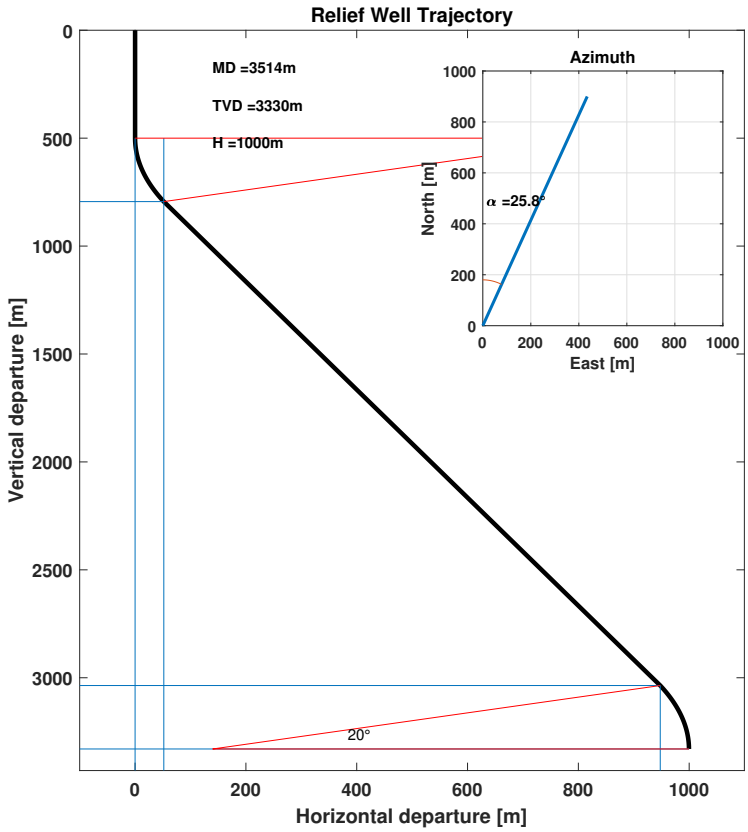

Figure 6.5: The relief well created during the simulation of well 1a, the bottom of the relief well intersects the blowing wellbore

6.3.5 Step 6 - Blowout rate procedure

The blowout rate procedure is started and follows the procedure described in section 6.2.2.

Step 1-2
In this example a blowout release point to surface is chosen. The multiphase correlation chosen is Olgjenka together with the Standing-set of PVT correlations. The initial blowout rate used for the step wise procedure is calculated based on the inflow performance relationship and 80% of the reservoir pressure. The calculated FBHP is 477.5 bar, which gives an initial blowout rate of 1681 Sm^3/day as a first guess in the blowout rate loop.

Step 3
The well is divided into N-number of intervals based on the blowout release point and the interval step size. For the example well 1a with a blowout to surface gives a total well length of 3565 m, using a step size of 10 ft gives 1170 intervals for the entire wellbore.

Step 4
A temperature profile for the fluid inside the wellbore is calculated based on the theory presented in Appendix A.4. The temperature is calculated based on the specific heat capacity of the fluids, the mass rate of the fluids, the thermal conductivity of the section and the diameter of the section. The temperature calculation uses a simplified wellbore-formation system which is more detailed described in Appendix A.4. Whenever a change is made related to the influx of either reservoir fluid or kill fluid a new temperature profile is calculated to account for the new flow rates.

The temperature profile for the surrounding formation is based on the reservoir temperature, the seabed temperature and the temperature of the sea surface. In the example the surrounding formation temperature is shown in figure 6.7. For a blowout rate of 1681 Sm^3/D the temperature profile inside the wellbore is shown in figure 6.6, where four different zones are present.

The first zone is the open hole section (3565 to 3330 m RKB) with a thermal conductivity of 3.06 W/(m-K). The second zone is the liner section (3330 - 2150 m RKB) with a thermal conductivity of 0.95 W/(m-K). The third is the cased interval (2150 to 410 m RKB) with the same thermal conductivity as zone 2, but a larger pipe diameter (12.5”). The fourth zone is the riser section (410 to 0 m RKB) which uses a thermal conductivity of 0.24 W/(m-K). More details on how the temperature profile is calculated and the parameters used is described in Appendix A.4. The temperature profile is assigned to a temperature vector with the same size as the length vector.

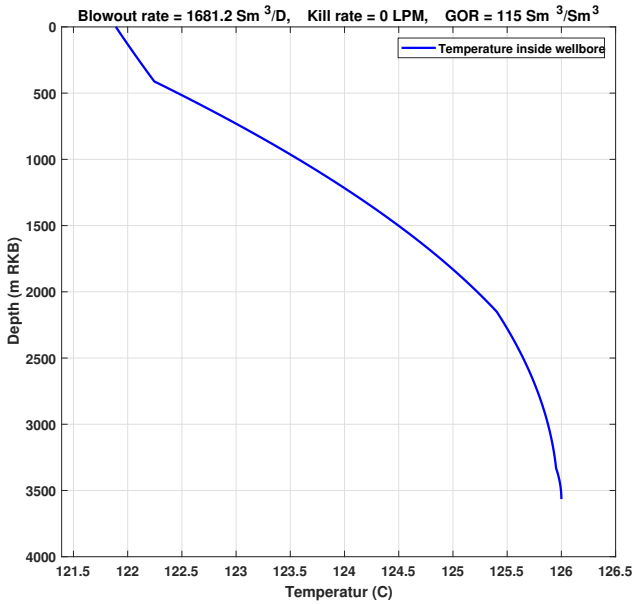

Figure 6.6: Well 1a - Temperature profile in the wellbore for a blowout rate of 1681 Sm^3/D

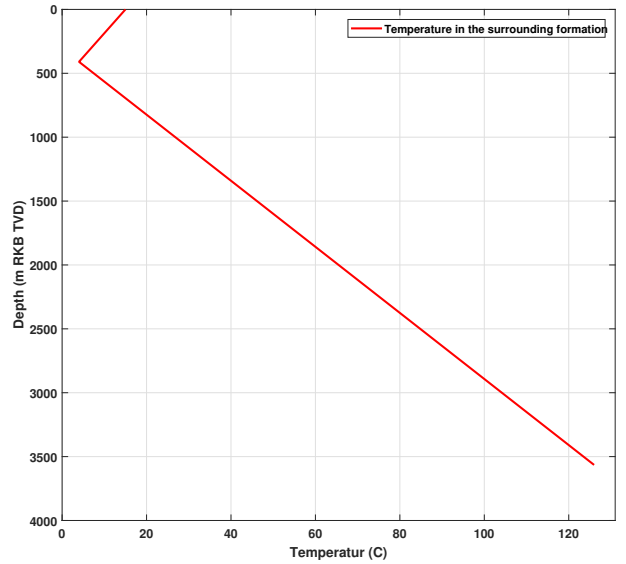

Figure 6.7: Well 1a - Temperature profile in the surrounding formation/water

Step 5 - 7
An iterative process is started where the pressure increase is calculated over all the 1170 length increments for well 1a. The first iteration starts with an initial pressure equal to the atmospheric pressure (blowout to surface). The Standing-PVT set is chosen to calculate the PVT parameters and the Olgjenka correlation is used to calculate the pressure increase over the length increments. The theory behind the two kinds of PVT-sets is discussed in Appendix A.6 and the theory behind the different multiphase correlations in Appendix A.5.

The first length increment ranges from the RKB and 3.05 m (10ft) downwards. Some of the key parameters used to calculate the pressure increase and the pressure increase is presented in table 6.8. The calculated pressure increase is 499 Pa or 0.005 Bar, the calculated pressure in the bottom of length increment 1 or top of increment 2 equals 1.0185 Bar, e.g. 1.0135 Bar + 0.005 Bar. The next length increment uses the calculated pressure from the previous increment and repeat the same process. This iterative process is repeated for all of the 1170 length increments in the example.

Table 6.8: Well 1a - Parameters used to calculate the pressure increase over the first length increment

Parameter	Unit	Value
Down hole oil rate	m3/s	0.0214
Down hole gas rate	m3/s	2.95
Two phase density	kg/m3	7.7
Oil density	kg/m3	762
Gas density	kg/m3	1.1
Oil FVF	m3/Sm3	1.1
Solution GOR	Sm3/Sm3	1.07
Oil viscosity	cp	0.85
Two phase friction factor	-	0.037
Friction pressure increase	Pa	264
Gravity pressure increase	Pa	235
Total pressure increase	Pa	499

Step 8
When the pressure increase is calculated over all the length increments the well/increment loop is finished and the pressure profile for the wellbore is obtained. The pressure profile and the pressure change in the wellbore are shown in figure 6.8 for a blowout rate of 1681 Sm^3/d. The calculated flowing bottom hole pressure is 37.8 Bar.

By examining figure 6.8b one can see that the gravitational pressure is the predominant source of the pressure increase. The accumulated pressure increase caused by gravity is 31.5 bar which represents 83.3% of the total pressure gain. By studying the frictional pressure curve, one can observe some areas (410m and 2150m) with large steps in the pressure change and some areas with smaller steps (904m and 3330m). The two large steps are caused by a decrease in the diameter with a resulting higher fluid velocity. The small step around 904m is caused by a transition from turbulent to laminar flow, thus a

change of the equation used to calculate the friction factor, the details around the friction factor are presented in Appendix A.5. The decreasing trend between each step is caused by a decrease in the total fluid velocity caused by free gas going into solution in the oil and reducing the flowing velocity.

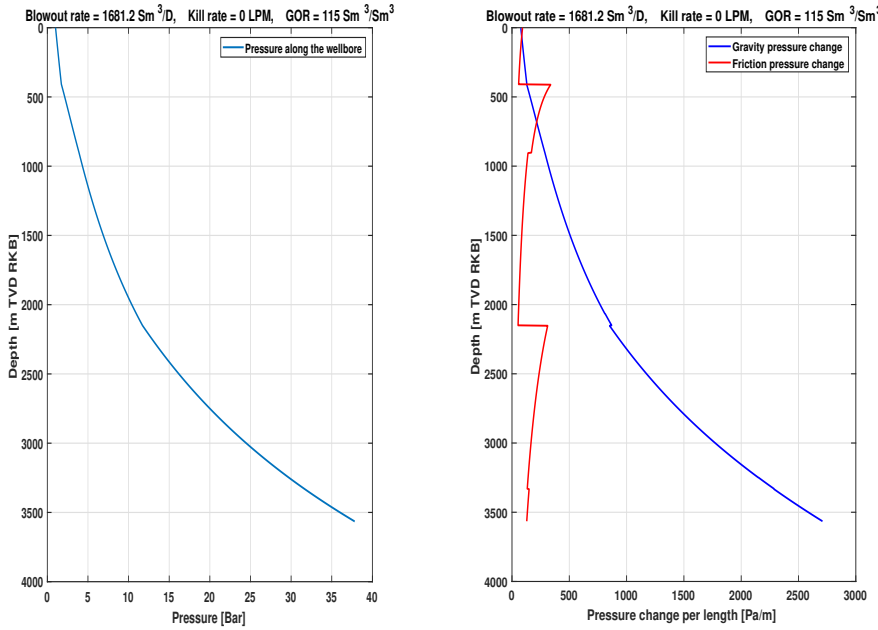

(a) **(b)**

Figure 6.8: Well 1a - first iteration a) Pressure profile, b) Pressure change along the wellbore

In step 2 an assumption was made that the flowing bottom hole pressure equalled 80% of the reservoir pressure, which gave a flowing bottom hole pressure of 477.5 Bar and a resulting blowout rate of 1681 Sm^3/d. By using this assumed blowout rate in step 4 to 7 a flowing bottom hole pressure of 37.8 bar was calculated. By using the inflow performance relationship, discussed in Appendix A.2, a new blowout rate for the given flowing bottom hole pressure is calculated. A flowing bottom hole pressure of 37.8 bar will result in a blowout rate of 7260.7 Sm^3/d with the used reservoir productivity.

Step 9

The calculated blowout rate of 7260.7 Sm^3/d is more than 4 times higher than the assumed blowout rate, which makes it evident that the calculation procedure must be repeated. Step 4 - 8 is repeated until the assumed blowout rate and the calculated blowout rate equal each other with a 1 $[Sm^3/d]$ difference. Figure 6.9 shows the pressure profiles for the next three repeated iterations for the blowout iteration loop (step 4-8), the pressure profile from iteration 1 is used as a reference. Table 6.9 shows the used blowout rate and the resulting calculated blowout rate and flowing bottom hole pressure for the en-

tire simulation process. The process is finished when an equilibrium between the vertical lift performance of the well and the inflow performance relationship from the reservoir is obtained.

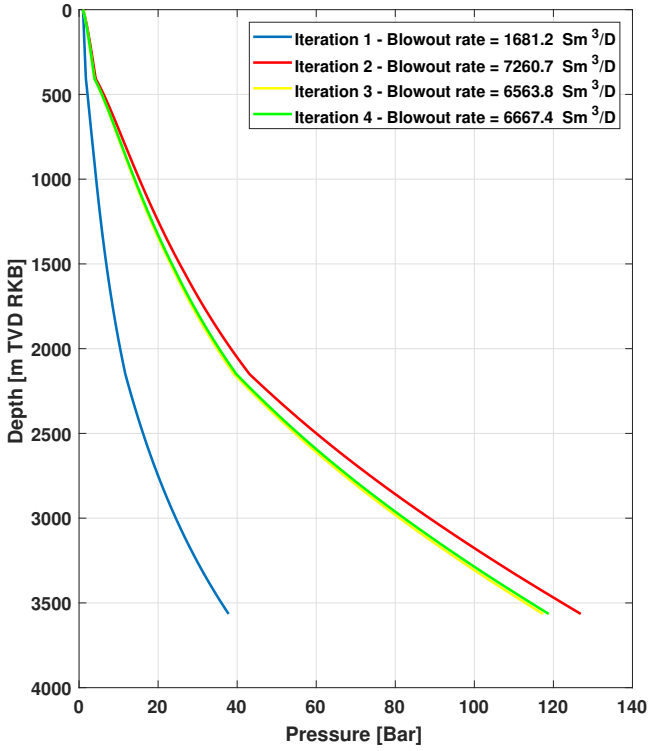

Figure 6.9: Well 1a - The first four pressure profile - blowout to surface

Table 6.9: Well 1a - Blowout to surface used and calculated blowout rates

Iteration	Blowout rate used	Calculated blowout rate	Flowing bottom hole pressure
-	[Sm3/D]	[Sm3/D]	[Bar]
1	1681.1	7260.7	37.8
2	7260.7	6563.8	126.9
3	6563.8	6667.3	117.4
4	6667.3	6652.2	118.8
5	6652.2	6654.5	118.6
6	6654.5	6654.2	118.6

By examining the results presented in table 6.9 and figure 6.9 one can see that the simulator is able to calculate the blowout rate that gives an equilibrium between influx and outflux of the well. It does not matter if the first assumed blowout rate is either under predicted or over predicted, the simulator is able to find the blowout rate that results in an equilibrium.

Step 10
In the last iteration the difference between the used blowout rate (6654.5 Sm^3/d) and the calculated blowout rate (6654.2 Sm^3/d) at the end of the iteration was less than the predefined stop criteria - 1 Sm^3/d. Since the stop criteria was fulfilled the blowout rate is in stationary equilibrium and the simulation is stopped. The blowout rate to surface is 6654.2 Sm^3/d.

To further specify the process in action. An equilibrium is met between what the reservoir is able to produce for a given flowing bottom hole pressure and what the well is able to lift out with the same flowing bottom hole pressure. This concept is known as inflow performance relationship (IPR)- vertical lift performance (VLP) matching. Figure 6.10 illustrates the concept of IPR-VLP-matching for the presented example.

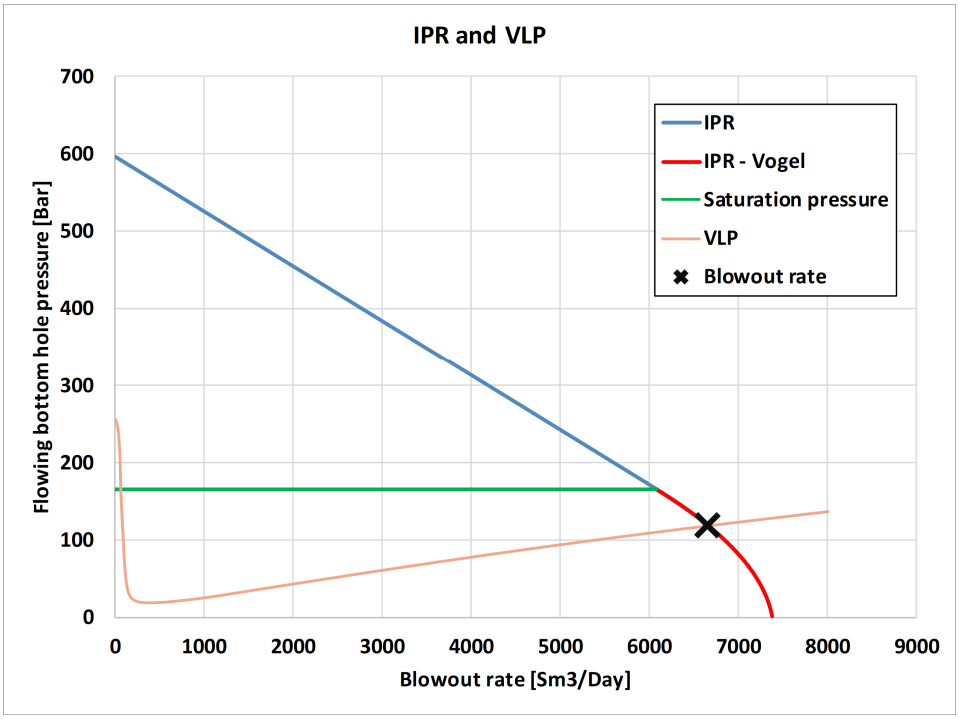

Figure 6.10: Well 1a - blowout to surface - IPR and VLP matching

The inflow performance relationship shows the calculated reservoir production for a given flowing bottom hole pressure. The vertical lift performance calculates the flowing bottom hole pressure for a given production rate, i.e. what pressure is required to lift the given production rate out of the wellbore. The interception point between the IPR and VLP curves is the equilibrium where the reservoir produce as much as the well is able to lift out for the given FBHP. This equilibrium rate is the blowout rate.

6.3.6 Kill procedure

The best way to explain the kill procedure is to continue the example from the blowout with the same input data.

Step 1 - 4
A surface blowout and kill are simulated with the Olgjenka multiphase pressure correlation and the Standing PVT-set. The blowout rate calculated in the blowout procedure, 6654.2 Sm^3/d, is used for the first kill iteration together with a kill rate of 250 LPM (360 Sm^3/d) and a kill fluid with a density of 1800 kg/m^3 and a viscosity of 10 cp. The well still consist of 1170 length increments from the reservoir to surface.

Step 5
A temperature profile is calculated both for the relief well and the blowing well. The temperature profile in the relief well uses the temperature of the mud pits as a starting point and calculates the temperature profile based on the relief well trajectory, i.e. the temperature calculation account for a non-vertical wellbore and uses the measured depth instead of the vertical depth.
The temperature profile for the relief well is shown in figure 6.11, where two sections are present. The kill and choke line section, where the temperature remains almost constant due to a high flow velocity and a low thermal conductivity of the pipe. The casing is the second section where the temperature starts to decrease caused by a higher temperature inside the relief well than the surrounding formation and a lower velocity. The temperature at the bottom of the relief well and the resulting interception point equal 22.6 $°C$, and is used to calculate the temperature of the hydrocarbon-kill fluid mixture.
The temperature profile in the blowing well is presented in figure 6.12. Just below the intersection point the temperature of the hydrocarbons is 125.98 $°C$ (a negligible reduction from the reservoir temperature), and the mixture temperature is 110.5 $°C$. The mixture temperature has decreased with 15.5 degrees, with a higher kill rate the temperature reduction would have been bigger. More on the theory and the calculation of the temperature is found in Appendix A.4.

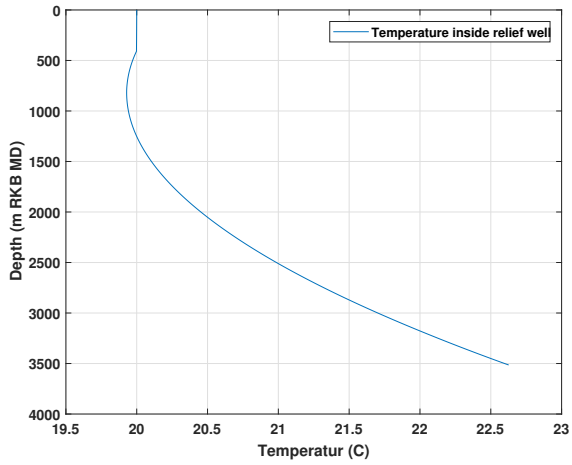

Figure 6.11: Well 1a - Temperature inside the relief well

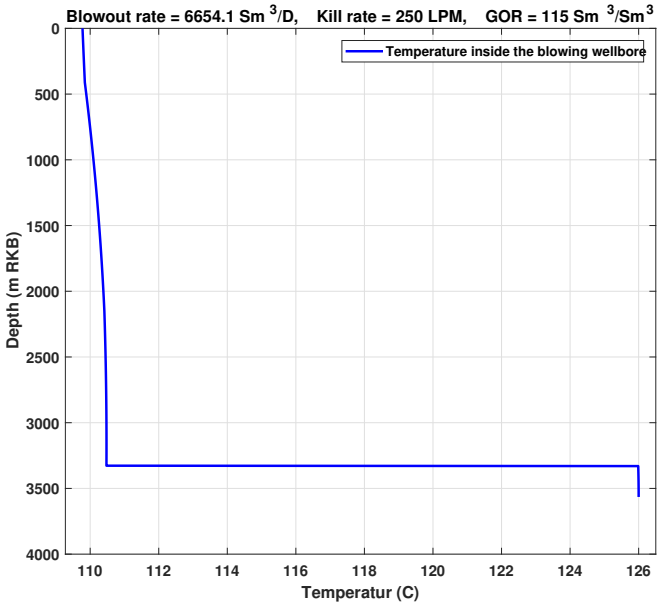

Figure 6.12: Well 1a - Temperature inside the blowing wellbore

Step 6-9
The well/increment iterative process is conducted calculating the pressure drop over all the 1170 length increments in the same manner as shown in the blowout procedure, with one exception the kill fluid is also flowing. In this example, the kill fluid is flowing with 250 LPM from the interception point and up to surface (3330 to 0 m RKB), no kill fluid is assumed to flow below the interception point. The kill fluid has a density of 1.8 s.g. and a viscosity of 10 cp. Below the interception point only hydrocarbons are flowing, this assumption is backed up in Appendix A.8.1. More details can be found in the blowout procedure.

Step 10
When the pressure increase is calculated for all the 1170 length increments the flowing bottom hole pressure is obtained for the used blowout rate and kill rate. The pressure profile after the first well iteration with a kill rate of 250 LPM is shown in figure 6.13 a), the pressure change per distance is shown in figure 6.13 b).

By examining the pressure change plot one can see the effect of no kill fluid below the interception point (3330 m RKB) by a reduction in each curve. This is caused by a lighter fluid mixture, a lower flow rate and probably a lower viscosity. The flowing bottom hole pressure is calculated to 142.5 bar with a resulting blowout rate of 6380 Sm^3/d. A kill fluid rate of 250 LPM increased the flowing bottom hole pressure with 23.9 bar and reduced the blowout rate with 274 Sm^3/d.

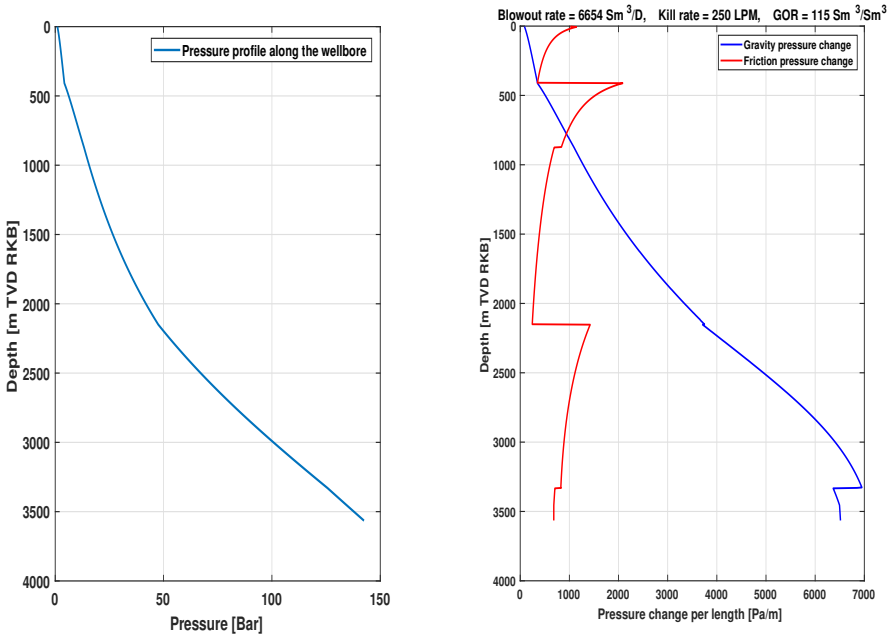

(a) **(b)**

Figure 6.13: Well 1a - blowout to surface - kill with 250 LPM first iteration: a) Pressure profile, b) Pressure change along the wellbore

Step 11

Since the assumed blowout rate of 6654 Sm^3/d used from step 3 to 10 does not equal the calculated blowout rate of 6380 Sm^3/d in step 10, it is clear that equilibrium is not met. Step 3 to 10 is repeated with the new blowout rate (6380 Sm^3d) and the same kill rate (250 LPM), until the assumed and calculated blowout rate equal each other within a 1 Sm^3/d margin.

Step 12

Three more blowout loops were conducted with a kill rate of 250 LPM before the assumed blowout rate equalled the calculated blowout rate within a 1 Sm^3/d margin. The pressure profiles for the four iterations are shown in figure 6.14. Table 6.10 shows the used blowout rate, the resulting FBHP and calculated blowout rate for each iteration. The equilibrium blowout rate for a kill rate of 250 LPM is 6412.9 Sm^3/d. The pressure loss along the wellbore and the reservoir production is now in equilibrium with the kill rate of 250 LPM, i.e. if the kill rate remains 250 LPM the blowout rate will remain constant at 6412.9 Sm^3/d (assuming the reservoir does not lose any pressure support).

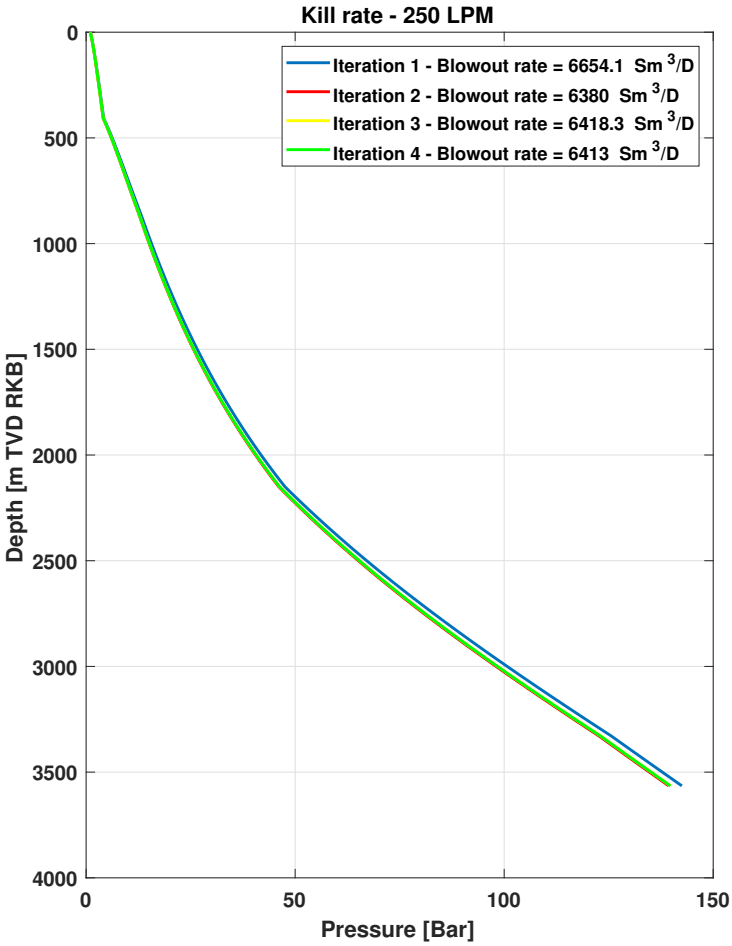

Figure 6.14: Well 1a - pressure profile for a kill rate of 250 LPM

Table 6.10: Well 1a - blowout rates and FBHP for a kill rate of 250 LPM

Iteration	Blowout rate used	Calculated blowout rate	Flowing bottom hole pressure
-	[Sm3/D]	[Sm3/D]	[Bar]
1	6654.2	6380.0	142.5
2	6380.0	6418.4	139.4
3	6418.4	6412.9	139.8
4	6412.9	6413.7	139.8

Step 13

Since the reservoir and well have met an equilibrium with a kill rate of 250 LPM and the blowout rate is higher than zero, the well is not killed. The kill rate is increased to 500 LPM and the blowout rate is set to the initial blowout rate of 6654 Sm^3/d as if the 250 LPM kill rate simulation never happened. The reason behind setting the blowout rate to the initial blowout rate is to be sure that the kill rate simulated can kill the well without any prior steps. Step 3 to 12 is repeated with the new kill rate and the initial blowout rate until the blowout rate equal 0.

The described procedure was repeated 17 times and the kill rate was increased with 250 LPM each loop, until the final kill rate of 4500 LPM. The equilibrium blowout rate for each of the different kill rates is presented visually in figure 6.15 and numerically in table 6.11.

Table 6.11: Well 1a - Kill rate iteration loop results

Kill Rate [LPM]	**Blowout rate used [SM3/D]**	**Blowout rate calculated [SM3/D]**	**Flowing bottom hole pressure [Bar]**
0	6654.4	6654.1	118.6
250	6413.0	6413.7	139.7
500	6150.9	6151.7	160.0
750	5874.3	5874.6	179.7
1000	5602.0	5602.0	199.0
1250	5328.9	5329.3	218.4
1500	5055.2	5055.1	237.9
1750	4784.5	4783.7	257.1
2000	4514.9	4514.5	276.2
2250	4245.8	4245.6	295.3
2500	3976.4	3975.8	314.5
2750	3702.5	3701.9	333.9
3000	3422.9	3422.4	353.8
3250	3134.2	3133.7	374.3
3500	2827.2	2826.4	396.1
3750	2491.7	2490.8	419.9
4000	2103.4	2102.5	447.5
4250	1554.5	1553.5	486.4
4500	0.2	0.0	622.5

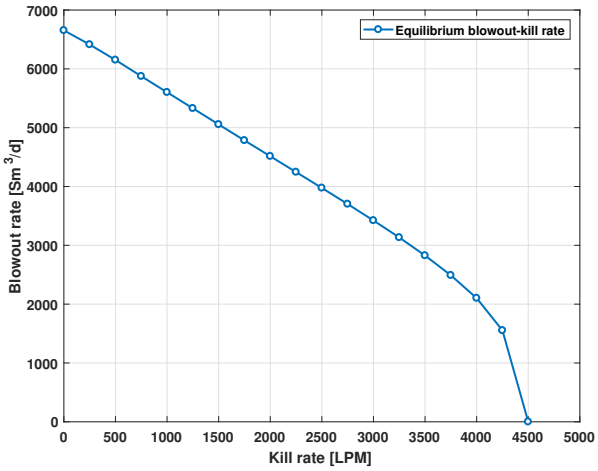

Figure 6.15: Well 1a - Kill rate iteration loop visualised

The final kill rate

The final kill rate iteration loop with a kill rate of 4500 LPM is shown in figure 6.16 and table 6.12. The iteration loop started with the initial blowout rate (6654 Sm^3/d) from the blowout procedure. The kill rate remained constant at 4500 LPM and an equilibrium between the blowout rate and the kill rate was obtained for each kill rate iteration.
In iteration number 20 the calculated blowout rate was zero, but to be sure the kill rate of 4500 LPM was able to keep the well killed one more iteration with a negligible blowout rate of 1 STB/d was used. Iteration number 21 shows that a kill rate of 4500 LPM is able to keep the well dynamically killed, i.e. the friction pressure from the kill rate must be present or the well will begin to flow once more. If the density of the kill fluid is high enough so the hydrostatic pressure exceeds the reservoir pressure the well is killed.

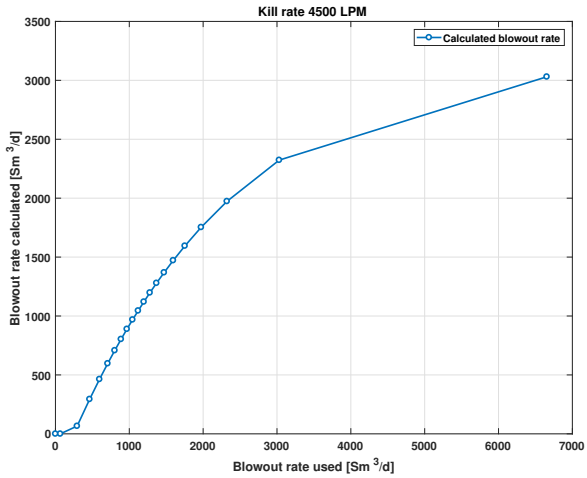

Figure 6.16: Well 1a - The final kill rate blowout rate vs kill rate

Table 6.12: Well 1a - The last blowout rate iteration loop for a kill rate of 4500 LPM

Iteration	Kill Rate [LPM]	Blowout rate used [SM3/D]	Blowout rate calculated [SM3/D]	Flowing bottom hole pressure [Bar]
1	4500	6654.2	3030.2	381.7
2	4500	3030.2	2323.1	431.9
3	4500	2323.1	1973.3	456.7
4	4500	1973.3	1753.0	472.4
5	4500	1753.0	1594.9	483.6
6	4500	1594.9	1471.5	492.4
7	4500	1471.5	1368.8	499.6
8	4500	1368.8	1279.3	506.0
9	4500	1279.3	1197.6	511.8
10	4500	1197.6	1120.3	517.3
11	4500	1120.3	1044.8	522.7
12	4500	1044.8	968.5	528.1
13	4500	968.5	889.0	533.7
14	4500	889.0	803.1	539.8
15	4500	803.1	707.6	546.6
16	4500	707.6	596.7	554.5
17	4500	596.7	463.2	564.0
18	4500	463.2	293.7	576.0
19	4500	293.7	66.0	592.2
20	4500	66.0	0.0	615.5
21	4500	0.2	0.0	622.6

In this example the reservoir pressure is 597 Bar, the FBHP is calculated to 622.5 bar, where friction pressure accounts for 17.6 bar (2.8%) and the gravitational pressure accounts for 604 bar (97.2 %). This means a kill fluid density of 1800 kg/m^3 is enough to statically kill the well, when the entire wellbore is filled with only kill fluid. The pressure at the interception point is 606.9 bar.
In a real dynamic kill procedure, the pump rate is reduced when the FBHP exceeds the reservoir pressure, leaving some hydrocarbons in the wellbore. The reduction of the pump rate is done to avoid fracturing the weakest formation and a static kill fluid is circulated into the wellbore. Since the created simulator is based on a stationary model and not a transient model, it is not possible to determine the exact point the FBHP exceeds the reservoir pressure and the required time to get there.

If the kill density was 1700 kg/m^3 a kill rate of 5750 LPM is required to kill the well. The FBHP is then 598.5 bar (1.5 Bar above the reservoir pressure), where the hydrostatic pressure account for 571.3 bar and the friction pressure accounts for 26.3 bar. By turning the pumps off the friction pressure is lost and only the hydrostatic pressure remains. Assuming that all the fluid flow is stopped the exact moment the pumps are turned off, the bottom hole pressure would equal the hydrostatic pressure of 571.3 bar. The corresponding reservoir influx is 364.5 Sm^3/d, calculated with the IPR. If the mud pumps are not turned back on the wellbore will gradually be emptied for kill fluid and a full blowout of 6654 Sm^3/d would reoccur.

6.3.7 Calculation of the required mud pump pressure

The theory behind the calculation of the required mud pump discharge pressure and the required energy input are presented in Appendix A.7. Only the results specific to the example is presented in this section.

By using the same parameters as the kill simulation in the previous section, the flowing pressure at the interception point was 606.9 bar, the kill fluid density was 1.8. s.g. and the true vertical depth of the interception point was 3330 m TVD RKB. The resulting hydrostatic pressure of the kill fluid is 588 bar at the interception point. The pressure differential between the hydrostatic pressure and the flowing pressure is 18.9 bar, which is supplied by the mud pumps.

The friction pressure over the two different flow paths are shown for option 1 - the annulus in table 6.13 and option 2 - inside of the drill string in table 6.14. A kill rate of 4500 LPM was used together with the relief well trajectory presented earlier. The calculated friction pressure when pumping through the drill string is almost twice the size of the annular flow path. The calculated required mud pump pressure for both cases are not particular high and should not be a problem for a modern drilling unit. For higher kill rates the friction pressure will increase. The required energy input to the mud pumps are 2213 HP and 3885 HP for the annulus flow and drill string flow, respectively.

Table 6.13: Well 1a - relief well friction pressure - annulus flow path

parameter **unit**	**OD** **in**	**ID** **in**	**Length** **m MD**	**Pressure** **Bar**
Surface lines	4.0	0.0	75.0	11.8
Kill/choke line	3.5	0.0	410.0	67.9
Casing - DP	8.8	5.5	2964.5	82.5
Casing - BHA	8.8	6.5	60.0	4.6
Casing - OH	8.8	0.0	80.0	0.3
Δp **- interception point**			0.0	18.9
Sum			3514.5	186.0

Table 6.14: Well 1a - relief well friction pressure - drill string flow path

parameter **unit**	**OD** **in**	**ID** **in**	**Length** **m MD**	**Pressure** **Bar**
Surface lines	4.0	0.0	75.0	11.8
Drill pipe	4.0	0.0	3374.5	288.0
BHA	4.0	0.0	60.0	9.4
Casing - OH	8.8	0.0	80.0	0.3
Δp **- interception point**			0.0	18.9
Sum			3514.5	328.3

Required mud volume to kill the well
One big limitation in the created simulator is that it only calculates a stationary flow, i.e. it does not take time into account. The simulator assumes stationary conditions where only one blowout rate and one kill rate are used for each blowout iteration loop. When a kill procedure is initiated the wellbore fluid consist only of hydrocarbons, seconds after the kill is initiated the wellbore fluid consist of both hydrocarbons and kill fluid, but only hydrocarbons are flowing out of the wellhead. The first kill fluid will not flow out of the wellhead after some time, dependent on the flow rate and wellbore length, often in a 10 - 30 minute range.

Since the simulator does not take time into account, it impossible to determine how long the dynamic kill procedure will take and the required kill volume to reach a dynamic kill is unknown. Some approximations can of course be done when calculating the required time, but a transient model is preferred.

When the well is dynamically killed hydrocarbons may still be present in the wellbore. To ensure that the wellbore is free for hydrocarbon and the hydrostatic bottom hole pressure is higher than the reservoir pressure, the well is circulated with a static kill fluid. The static kill mud has a density that ensure the hydrostatic pressure exceeds the reservoir pressure and are below the fracture pressure of the weakest formation.

A normal practice is to circulate the well two times bottom-up with the static kill mud to ensure that the wellbore is free of hydrocarbons. The wellbore volume for an unrestricted open hole is 259 m^3 and the annulus volume is 206.5 m^3. The required mud volume consumption when circulating to a static kill is 518m^3. The total required mud volume of the rig is two times the wellbore volume added with the required mud volume to reach dynamic kill.

6.4 Step 8 - generation of the report

When all the different blowout scenarios and kill scenarios are calculated an automatically generated report for the simulations is created. An example of the report for all the different scenarios for the example well is shown in Appendix B.

6.5 Comparison of the different simulation combinations

The calculated blowout rate to surface in the example above was conducted with the multiphase pressure correlation ”Olgjenka” and the Standing-PVT set. The created simulator offers the opportunity to choose the Orkiszewski pressure correlation and the Glasø-PVT set as well, in total four possible combinations. The simulator calculates the blowout rate through two different flow channels: open hole or annulus with two different release locations: surface or seabed. How the different combinations affect the calculated blowout rate is discussed below.

Surface blowout - Open hole

A blowout to surface is simulated with the four different combinations, figure 6.17 shows the pressure profile for the IPR-VLP-matched end results for the different combinations for a surface blowout through open/cased hole. The numerical values of the end results are shown in table 6.15 together with the required number of blowout iteration loops to reach the equilibrium. By examining the well profiles one can see that the different combinations are almost identical, small variations are present. The combination "Orkiszewski - Glasø" slightly over predict the wellbore pressure along the wellbore compared to the other combinations. The end results for all the different combinations are consisting, with a total difference of 57 Sm^3/d from the highest to the lowest blowout rate. The Glasø-PVT set give the highest calculated FBHP and the lowest blowout rate for both pressure correlations. The Olgjenka correlation predicts a higher pressure increase caused by friction than the Orkiszewski correlation. The Standing PVT-set predicts a higher friction pressure than the Glasø PVT-set. The number of iterations loops to reach equilibrium only differ with 1 loop for the different multiphase pressure correlations.

Table 6.15: Well 1a - Open hole surface blowout - end results for the different simulation combinations

Multiphase correlation **PVT correlation**	**Olgjenka** **Standing**	**Olgjenka** **Glasø**	**Orkiszewski** **Standing**	**Orkiszewski** **Glasø**
Blowout rate $[Sm^3/d]$	6654.2	6622.7	6679.4	6625.2
FBHP [Bar]	118.6	121.6	116.2	121.3
Gravity pressure inc. [%]	77.6	79.3	82.9	84.6
Friction pressure inc. [%]	22.4	20.7	17.2	15.4
Iteration-loops	6	6	5	5

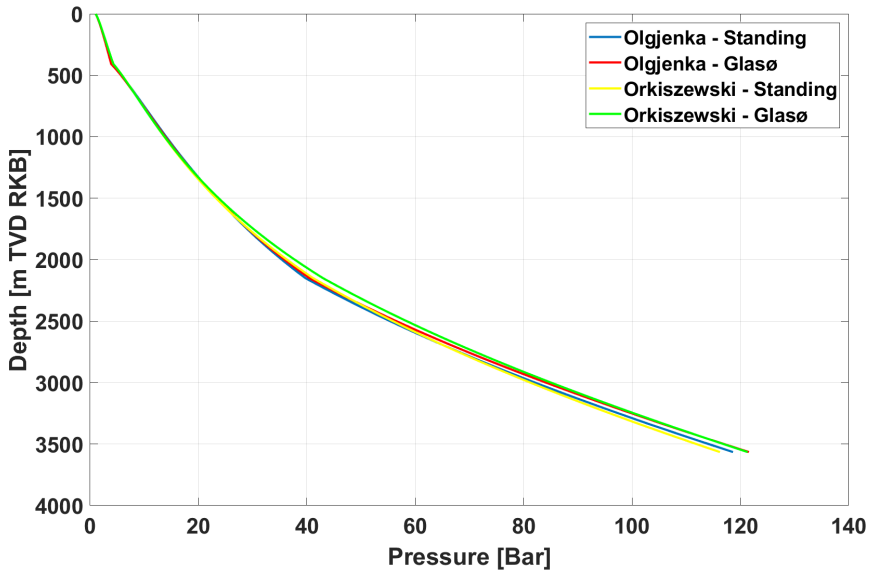

Figure 6.17: Well 1a - Open hole surface blowout - pressure profile for the different combinations

Seabed blowout - Open hole

To investigate how the different combinations behave under higher pressure, the same experiment was conducted for a blowout to seabed. The IPR-VLP matched pressure profile for each of the combinations are presented in figure 6.18 and table 6.16. The same behavior is observed where the combination "Orkiszewski-Glasø" predicts the highest pressure profile and the combination "Olgjenka-Standing" predicts the lowest pressure profile, the trends are more visible in this scenario. The difference in the calculated blowout rate between the highest and lowest prediction is 153 Sm^3/D. The Olgjenka-Standing combination predicts the highest frictional pressure increase. The difference in the required number of iteration loops to reach equilibrium between the two multiphase correlations is large. The Olgjenka correlation reaches equilibrium faster than the Orkiszewski correlation, the reason is caused by a pressure discontinuity in the Orkiszewski correlation. The pressure discontinuity and the method used to go around it is further discussed in Appendix A.9.

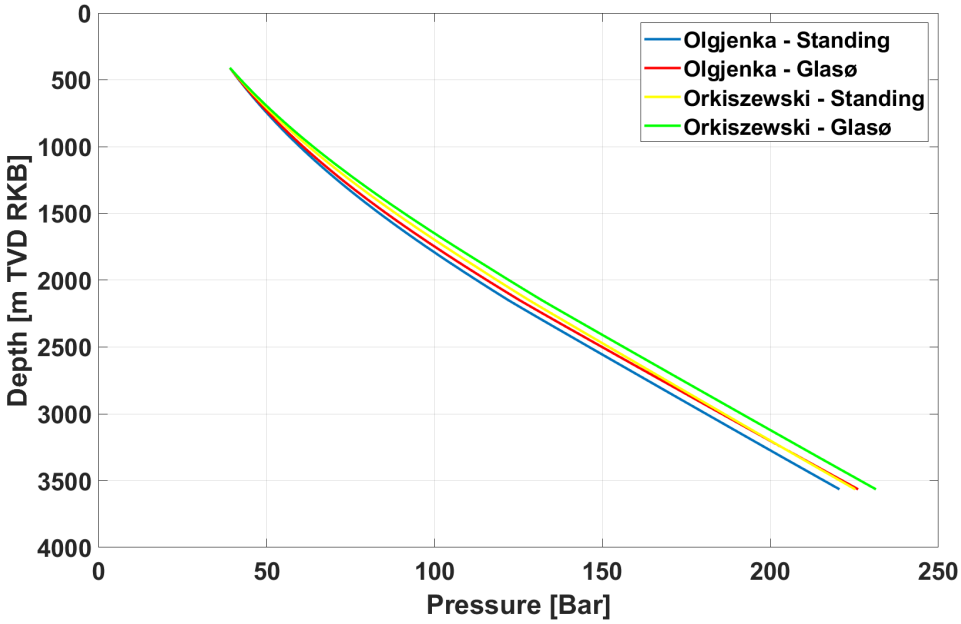

Figure 6.18: Well 1a - Open hole seabed blowout - pressure profile for the different combinations

Table 6.16: Well 1a - Open hole seabed blowout - end results for the different simulation combinations

Multiphase correlation / **PVT correlation**	**Olgjenka** **Standing**	**Olgjenka** **Glasø**	**Orkiszewski** **Standing**	**Orkiszewski** **Glasø**
Blowout rate [Sm^3/d]	5299.9	5221.6	5233.8	5147.0
FBHP [Bar]	220.5	226.1	225.2	231.4
Gravity pressure inc. [%]	95.8	96.1	97.2	97.4
Friction pressure inc. [%]	4.2	3.9	2.8	2.6
Iteration-loops	4	3	19	18

Surface blowout - Annulus

When a drill string is present in the wellbore an annulus is created, how the different combinations behaves for annulus flow to surface is shown in figure 6.19 and table 6.17. One obvious difference is that the Orkiszewski correlation calculates a lower friction drop in the annulus than the Olgjenka correlation. The two PVT-sets gives a small difference between the multiphase pressure correlations. The total difference is 430 Sm^3/d. The Olgjenka correlations requires more iterations than the Orkiszewski correlation to reach equilibrium. The frictional pressure increase is around 50 $\%$ for the four different combinations and the same trend as earlier where Olgjenka-Standing predicts the highest frictional pressure is observed.

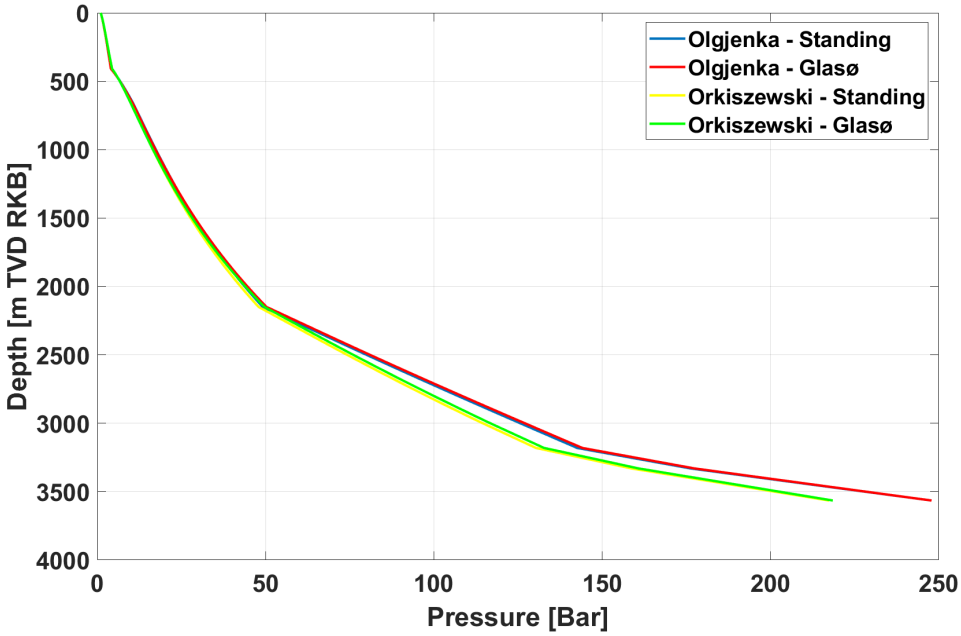

Figure 6.19: Well 1a - Annulus surface blowout - pressure profile for the different combinations

Table 6.17: Well 1a - Annulus surface blowout - end results for the different simulation combinations

Multiphase correlation **PVT correlation**	**Olgjenka** **Standing**	**Olgjenka** **Glasø**	**Orkiszewski** **Standing**	**Orkiszewski** **Glasø**
Blowout rate $[Sm^3/d]$	4914.4	4916.0	5344.1	5328.2
FBHP [Bar]	247.9	247.9	217.4	218.5
Gravity pressure inc. [%]	45.4	47.0	50.9	53.0
Friction pressure inc. [%]	54.7	53.0	49.1	47.0
Iteration-loops	34	31	7	7

Seabed blowout - Annulus

How the four different simulation combinations predict the blowout rate for a seabed blowout through annulus is shown in table 6.18 with the well profiles in figure 6.20. The same trends are observed as earlier. The difference in the blowout calculations are 300 Sm^3/d from the highest rate to the lowest rate.

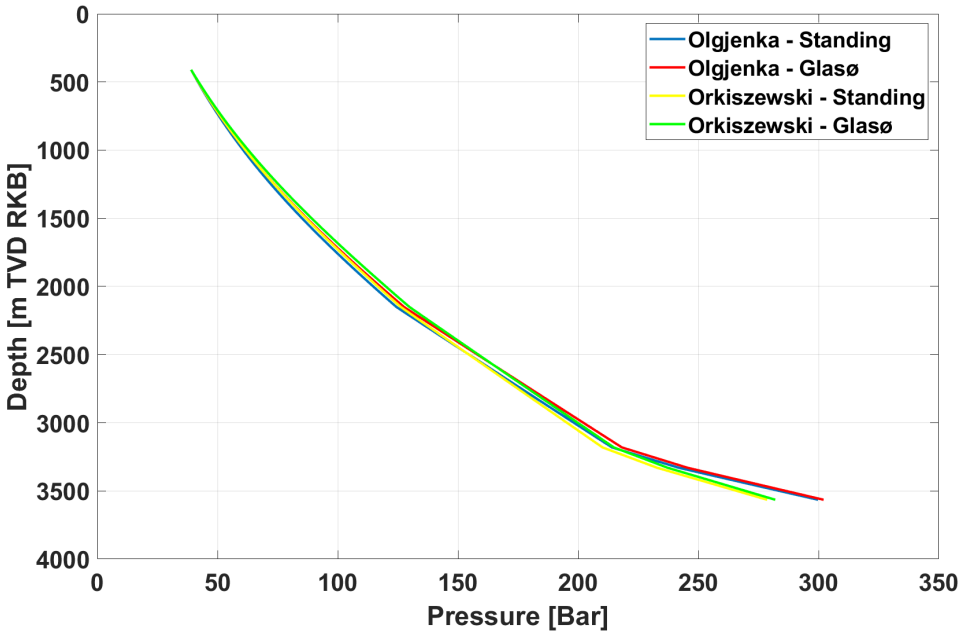

Figure 6.20: Well 1a - Annulus seabed blowout - pressure profile for the different combinations

Table 6.18: Well 1a - Annulus seabed blowout - end results for the different simulation combinations

Multiphase correlation **PVT correlation**	**Olgjenka** **Standing**	**Olgjenka** **Glasø**	**Orkiszewski** **Standing**	**Orkiszewski** **Glasø**
Blowout rate [Sm^3/d]	4183.3	4151.0	4481.4	4434.0
FBHP [Bar]	299.8	302.1	278.7	282.0
Gravity pressure inc. [%]	67.1	68.8	74.3	75.9
Friction pressure inc. [%]	32.9	31.2	25.7	24.1
Iteration-loops	14	14	9	9

IPR-VLP matching with Olgjenka-Standing

By using the combination Olgjenka - Standing on the four blowout scenarios table 6.19 and figure 6.21 are obtained. Table 6.19 shows the numerical values of the IPR-VLP matched blowouts and figure 6.21 shows the IPR-VLP matched curves for each of the blowout scenarios. The surface blowout through open hole has as expected the highest blowout rate, while the annulus blowout to seabed has the lowest blowout rate. The surface

through annulus blowout has as expected the highest frictional pressure. This is caused by a longer length and more free gas which creates a higher fluid velocity compared to the seabed blowout through annulus. The reason behind the higher gravity pressure increase in the blowout to seabed between both the open hole scenarios is caused by a higher back pressure (water column) which results in less free gas. The amount of less gas creates a higher average fluid density through the entire wellbore, which surpasses the hydrostatic pressure caused by the extra length for the blowout to surface.

Table 6.19: IPR - VLP matched end results for the four blowout scenarios with the combination Olgjenka - Standing

Blowout location **Flow path**	**Surface** **Open hole**	**Seabed** **Open hole**	**Surface** **Annulus**	**Seabed** **Annulus**
Blowout rate $[Sm^3/d]$	6654.2	5299.9	4914.4	4183.3
FBHP [Bar]	118.6	220.5	247.9	299.8
Pressure increase [Bar]	117.6	181.5	246.8	260.8
Gravity pressure inc. [Bar]	91.3	173.9	111.9	175.1
Friction pressure inc. [Bar]	26.3	7.7	134.9	85.8
Gravity pressure inc. [%]	77.6	95.8	45.4	67.1
Friction pressure inc. [%]	22.4	4.2	54.7	32.9

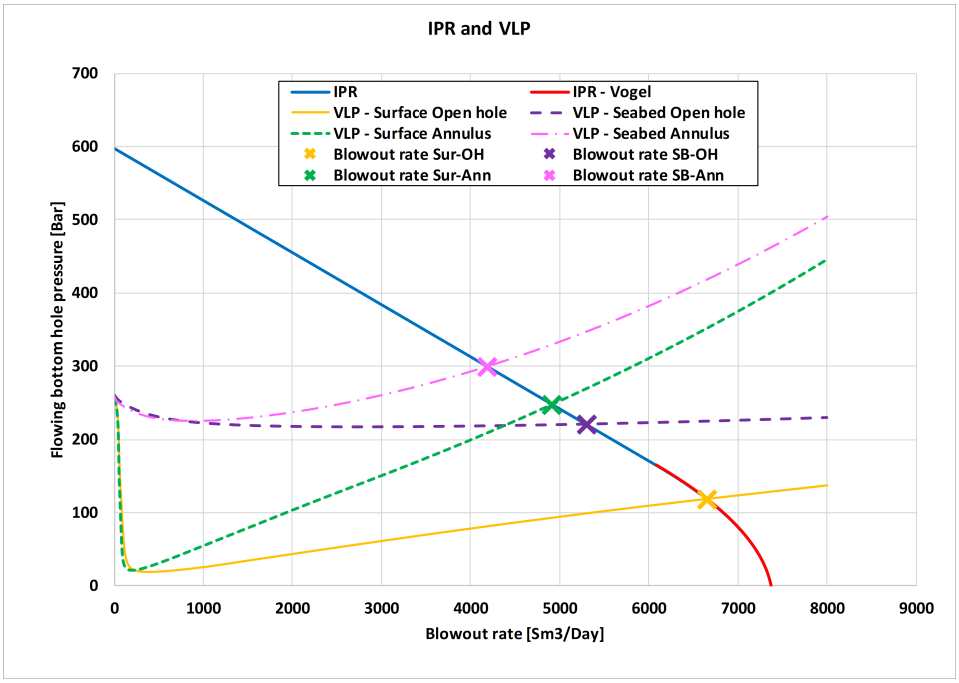

Figure 6.21: Well 1a - IPR-VLP matching for the different blowout scenarios with the Olgjenka-Standing combination

Chapter 7

Simulation results

This chapter presents the input data for 17 simulated wells and the result from the created simulator for both blowout rates and kill rates. The information from the wells are taken from several blowout and kill simulations conducted by companies specialized in blowout and kill. The results from the created simulator are compared with the professional obtained results. Four calibration formulas are created for the kill rates and are based on the professional listed kill rates and the input parameters for each well. Two calibration formulas for each of the two multiphase pressure correlations, one for each blowout release point. Only the Standing PVT-correlation set is used since it gave the highest blowout rate in section 6.5.

7.1 Available simulations

As a part of the planning phase of each well, a requirement from NORSOK is to have a blowout and kill simulation that shows if the planned well can be killed in the event of a blowout. The simulations must be based on realistic reservoir properties and the planned well design. Several companies in the petroleum industry are specialized in different kinds of simulations, such as blowout and kill. Most of these companies use the multiphase flow simulator "Olga-Well-Kill" by Schlumberger, which is viewed as a state of the art software within the field. Several blowout and kill simulations conducted on behalf of Aker BP have been provided to be used in this master thesis. Most of these simulations are based upon exploration wells which results in vertical wells. All the wells are anonymized and are located all around the Norwegian continental shelf.

7.2 Input data

An overview over the range of the input parameters used in the simulator are presented in table 7.1. The parameters for each well are shown in table 7.2 to 7.5.

Table 7.1: Range of input parameters used in the simulator

Parameter	Unit	Minimum	Maximum
Total depth	**m RKB TVD**	1020	4022
Water depth	**m MSL**	67	497
Oil gravity	**s.g.**	0.806	0.945
Gas gravity	**s.g.**	0.628	1.291
GOR	**Sm3/Sm3**	16	475
Saturation pressure	**Bar**	52	375
Productivity index	**Sm/d/bar**	1	875
AOF	**Sm3/d**	465	100000
Reservoir temperature	**C**	30	138
Reservoir pressure	**Bar**	105	709

Table 7.2: Input data - Well and rig data

Rig and well properties					Average well diameter	
Well	**Total depth**	**Water depth**	**Rig elevation**	**Riser ID**	**TVD to surface**	**TVD to seabed**
	m TVD RKB	**m MSL**	**m MSL**	**in.**	**in.**	**in.**
Well 1a	3565	386	24	18	11.57	10.82
Well 1b	3442	386	24	18	11.68	10.91
Well 2	2070	338	40	18	10.21	8.76
Well 3	2046	103	40	18	11.34	11.06
Well 4	3132	114	30	18	10.36	10.10
Well 5	3513	110	22	18	11.68	11.50
Well 6	1559	497	20	18	11.63	8.70
Well 7	2852	82.5	25	18	8.97	8.72
Well 8a	1720	346	40	18	10.52	8.71
Well 9	1020	112	30	18	9.72	8.79
Well 10	1715	393	40	18	13.07	11.72
Well 11	3744	112	55	18	8.97	8.74
Well 12	3520	432	22	18	9.81	8.69
Well 13	3401	122	55	18	10.46	10.23
Well 14a	2334	112	55	18	9.05	8.66
Well 14b	2334	112	55	18	9.05	8.66
Well 15	4022	67	55	18	8.85	8.74

Table 7.3: Input data - Well design

Well	Production casing			Liner			Open hole
	OD in.	ID in.	Shoe m TVD RKB	OD in.	ID in.	Shoe m TVD RKB	Diameter in.
Well 1a	13.375	12.5	2150	9.625	8.7	3330	8.5
Well 1b	13.375	12.5	2150	9.625	8.7	3320	8.5
Well 2	9.625	8.7	2024				8.5
Well 3	13.375	12.5	1160	9.625	8.7	1990	8.5
Well 4	13.375	12.5	1100	9.625	8.7	2881	8.5
Well 5	14	13.25	2100	9.625	8.7	3370	8.5
Well 6	9.625	8.7	1285				8.5
Well 7	9.625	8.7	2810				8.5
Well 8	9.625	8.7	1260				8.5
Well 9	9.625	8.7	1010				8.5
Well 10	13.375	12.5	1300	9.625	8.7	1520	8.5
Well 11	9.625	8.7	3680				8.5
Well 12	9.625	8.7	3000				8.5
Well 13	13.375	12.5	1500				8.5
Well 14a	9.625	8.7	1200				8.5
Well 14b	9.625	8.7	1200				8.5
Well 15	9.625	8.7	3990				8.5

Table 7.4: Input data - Reservoir fluid

Well	Oil gravity	Gas gravity	GOR	Saturation pressure
	s.g.	s.g.	Sm3/Sm3	Bar
Well 1a	0.838	1.200	115	165
Well 1b	0.838	1.200	115	165
Well 2	0.823	1.291	162	205
Well 3	0.849	0.735	90	178
Well 4	0.870	1.143	67	105
Well 5	0.806	0.882	475	327
Well 6	0.876	0.702	54	120
Well 7	0.881	1.143	27	59
Well 8	0.812	1.020	152	141
Well 9	0.913	0.628	16	52
Well 10	0.945	0.735	30	110
Well 11	0.854	0.645	334	375
Well 12	0.848	0.702	219	373
Well 13	0.847	0.986	335	282
Well 14a	0.849	0.735	90	182
Well 14b	0.849	0.735	90	182
Well 15	0.826	0.980	142	180

Table 7.5: Input data - Reservoir productivity

Well	Productivity Index	AOF	Reservoir temperature	Reservoir pressure
	Sm3/d/bar	Sm^3/d	**Celsius**	**Bar**
Well 1a	14	7374	126	597
Well 1b	3	1400	121	587
Well 2	4	465	70	220
Well 3	142	14000	63	178
Well 4	10	2800	108	317
Well 5	23	8907	127	528
Well 6	22	2200	49	151
Well 7	10	3180	110	344
Well 8	875	100000	72	168
Well 9	1	3180	30	105
Well 10	12	1570	50	178
Well 11	16	6141	136	552
Well 12	158	54000	138	507
Well 13	17	4400	120	380
Well 14a	129	19300	73	231
Well 14b	43	7000	73	231
Well 15	16	12333	138	709

7.3 Blowout results

All the presented wells have available blowout rates simulated by different companies in the industry. The professional listed blowout rates are used for comparison with the blowout rates calculated in the created simulator. Some of the professional conducted simulations did not present the flowing bottom hole pressure, and the pressure was calculated with the same inflow performance relationship as used in the created simulator. Two multiphase pressure correlation have been used in the comparison, the Olgjenka correlation and the Orkiszewski correlation. For PVT calculations the Standing PVT-set was chosen. The theory behind the calculations is not presented in this section, see section 6.3 and Appendix A.5 A.6 for more details.

7.3.1 Open hole to surface

A blowout to surface through an open/cased wellbore is commonly the worst-case scenario due to a low back pressure compared to a seabed blowout, and a lower friction pressure caused by less restrictions in the flow path compared to an annulus flow. In total 15 different wells were simulated plus 2 additional wells with an altered reservoir productivity.

The blowout rates for both the multiphase pressure correlation and the professional listed blowout rates for a surface blowout through open hole are presented in table 7.6. The calculated blowout rates for both multiphase correlations come close to the professional listed blowout rates, some key statistical values are presented in table 7.7. The Olgjenka correlation had a better accuracy than the Orkiszewski correlation, with an average error of -1.1% compared to -11.2%. Both methods under predicted the blowout rates. The absolute error for the different methods were 20.2% and 13.9% for Orkiszewski and Olgjenka, respectively.

The calculated flowing bottom hole pressure (FBHP) have a higher error for both methods. The fact that the calculated blowout rate and the FBHP are interconnected, and that the errors are remarkable different could indicate that the professional listed simulations does not calculate the inflow performance relationship the same way as described in this thesis, Appendix A.2.

Table 7.6: Blowout rates - Open hole to surface

Well	Professional		Orkiszewski		Olgjenka	
	Oil rate Sm^3/d	FBHP Bara	Oil rate Sm^3/d	FBHP Bara	Oil rate Sm^3/d	FBHP Bara
Well 1a	6964	70.3	6849	98.7	6654	118.6
Well 1b	1347	21.7	1190	149.6	1384	30.1
Well 2	450	25.2	351	97.9	461	8.0
Well 3	11847	58.7	7039	119.8	9867	88.1
Well 4	2144	100.4	1603	162.1	2319	92.4
Well 5	8256	99.1	8252	108.8	7860	145.6
Well 6	1450	78.1	1338	85.3	2012	26.5
Well 7	1560	188.0	1437	195.7	1712	167.3
Well 8	20831	171.1	29531	161.2	15880	176.8
Well 9	9	89.0	7	91.1	7	91.1
Well 10	916	102.4	514	135.7	1075	87.5
Well 11	5670	145.0	5695	141.3	5514	164.6
Well 12	22710	363.3	20005	380.4	18214	391.8
Well 13	4167	62.8	3698	129.1	4009	89.7
Well 14a	12237	129.9	10245	148.5	9473	155.5
Well 14b	5561	71.4	2852	163.6	4993	97.0
Well 15	7005	63.9	9382	261.8	9049	282.3

Table 7.7: Blowout statistics - Open hole to surface

Correlation Parameter Unit	Blowout rate Difference Sm^3/d	Error %	FBHP Difference Bar	Error %
Orkiszewski - average	-184	-11.2	46.5	99.8
Absolute average	1491	20.2	48.1	100.8
Absolute max	8700	48.7	197.9	589.5
Olgjenka - Average	-744	-1.1	21.9	29.6
Absolute average	1113	13.9	35.1	49.4
Absolute max	4951	38.7	218.4	341.7

7.3.2 Open hole to seabed

The blowout rates for both multiphase pressure correlations and the professional listed blowout rates for a seabed blowout through open hole are presented in table 7.8. The calculated blowout rates for both multiphase correlations come close to the professional listed blowout rates, some key statistical values are presented in table 7.9. The Orkiszewski correlation had a slightly better accuracy than the Olgjenka correlation with an average error of -7.2% compared to -7.6%. The absolute maximum difference was almost twice as high in Olgjenka than in Orkiszewski. Both methods under predicted the blowout rates. The absolute average error for the different methods were 11.9% and 13.9% for Orkiszewski and Olgjenka, respectively. The calculated flowing bottom hole pressures (FBHP) have a much better accuracy for the seabed blowout than a surface blowout.

Table 7.8: Blowout rates - Open hole to seabed

Well	**Professional**		**Orkiszewski**		**Olgjenka**	
	Oil rate Sm^3/d	**FBHP Bara**	**Oil rate** Sm^3/d	**FBHP Bara**	**Oil rate** Sm^3/d	**FBHP Bara**
Well 1a	5462	198.5	5233	225.2	5300	220.5
Well 1b	1022	202.5	991	223.3	1012	215.6
Well 2	213	155.7	277	131.3	298	122.6
Well 3	10691	74.9	9594	91.5	9182	96.5
Well 4	1480	174.1	1151	205.8	1468	175.2
Well 5	8241	102.7	8132	121.0	7844	146.9
Well 6	1390	82.0	482	128.9	489	128.5
Well 7	1270	213.0	1304	209.4	1365	203.1
Well 8	18165	174.2	16468	176.1	14262	178.6
Well 9	8	89.0	8	88.6	8	88.7
Well 10	355	148.8	326	151.1	328	151.0
Well 11	5660	146.0	5695	141.3	5499	166.3
Well 12	22200	366.7	19627	382.8	17789	394.4
Well 13	4114	72.0	4062	81.6	3971	95.2
Well 14a	11808	134.2	10069	150.1	9175	158.2
Well 14b	5202	88.4	4785	105.0	4673	109.1
Well 15	9701	204.3	9410	260.0	9035	283.2

Table 7.9: Blowout statistics - Open hole to seabed

Correlation	**Blowout rate**		**FBHP**	
Parameter	**Difference**	**Error**	**Difference**	**Error**
Unit	Sm^3/d	**%**	**Bar**	**%**
Orkiszewski - Average	-551	-7.2	14.5	11.6
Absolute average	567	11.9	18.4	14.0
Absolute max	2573	65.3	55.7	57.2
Olgjenka - Average	-899	-7.6	18.0	15.2
Absolute average	920	13.9	23.1	18.3
Absolute max	4411	64.8	78.9	56.8

7.3.3 Annulus to surface

The blowout rates for both multiphase pressure correlations and the professional listed blowout rates for a surface blowout through annulus are presented in table 7.10. The calculated blowout rates for both multiphase correlations come close to the professional listed blowout rates, some key statistical values are presented in table 7.11. The Olgjenka correlation had a better accuracy than the Orkiszewski correlation with an average error of -6.7% compared to -10.5%. The absolute maximum difference for both methods were close to each other. Both methods under predicted the blowout rates. The absolute average error for the two methods were 27.3% and 34.8% for Orkiszewski and Olgjenka, respectively. Olgjenka is the correlation with the highest overall accuracy.

Table 7.10: Blowout rates - Annulus to surface

Well	Professional		Orkiszewski		Olgjenka	
	Oil rate Sm^3/d	FBHP Bara	Oil rate Sm^3/d	FBHP Bara	Oil rate Sm^3/d	FBHP Bara
Well 1a	6229	143.2	5432	211.1	4915	247.8
Well 1b	1336	33.8	1278	109.8	1351	64.0
Well 2	440	36.5	416	57.6	452	22.7
Well 3	7585	114.2	6027	129.5	4827	140.3
Well 4	1846	134.8	1787	144.5	1802	143.0
Well 5	6761	219.2	5523	288.7	4703	325.9
Well 6	560	125.3	1361	83.8	1720	58.0
Well 7	1500	190.0	1469	192.4	1434	196.1
Well 8	10139	183.4	4834	189.4	4461	189.8
Well 9	9	89.0	7	90.7	7	90.7
Well 10	805	111.8	483	138.2	1025	92.4
Well 11	4440	276.0	4095	295.7	3657	327.1
Well 12	7920	456.8	5972	469.1	5105	474.5
Well 13	4100	74.2	2930	199.7	2841	206.5
Well 14a	7062	176.8	3459	204.0	3577	203.1
Well 14b	4198	125.7	3281	146.3	2795	165.1
Well 15	7005	369.0	6124	462.4	5671	490.3

Table 7.11: Blowout statistics - Annulus to surface

Correlation	Blowout rate		FBHP	
Parameter	Difference	Error	Difference	Error
Unit	Sm^3/d	%	Bar	%
Orkiszewski - average	-1027	-10.5	32.5	36.2
Absolute average	1121	27.3	37.4	40.1
Absolute max	5305	143.0	125.5	224.7
Olgjenka - Average	-1270	-6.7	34.0	24.7
Absolute average	1436	34.8	45.8	37.5
Absolute max	5678	207.2	132.3	178.3

7.3.4 Annulus to seabed

The blowout rates for both multiphase pressure correlations and the professional listed blowout rates for a seabed blowout through annulus are presented in table 7.12. The calculated blowout rates for both multiphase correlations come close to the professional listed blowout rates, some key statistical values are presented in table 7.13. The Orkiszewski correlation had a better accuracy than the Orkiszewski correlation with an average error of -15.1% compared to -20.3%. The absolute maximum difference for the two methods varied with about 900 Sm^3/d. Both methods under predicted the blowout rates. The absolute average error for the two methods were 17.9% and 23.8% for Orkiszewski and Olgjenka, respectively. Orkiszewski is the correlation with the highest overall accuracy.

Table 7.12: Blowout rates - Annulus to seabed

Well	**Professional**		**Orkiszewski**		**Olgjenka**	
	Oil rate Sm^3/d	**FBHP Bara**	**Oil rate** Sm^3/d	**FBHP Bara**	**Oil rate** Sm^3/d	**FBHP Bara**
Well 1a	5201	217.0	4481	278.6	4183	299.7
Well 1b	1035	199.3	981	226.8	1006	217.9
Well 2	261	137.9	282	129.3	309	117.9
Well 3	7047	119.7	5577	133.7	4528	142.9
Well 4	1489	173.8	1164	204.6	1344	187.2
Well 5	6736	220.7	5457	291.8	4696	326.2
Well 6	610	116.0	470	129.4	493	128.4
Well 7	1230	217.0	1323	207.5	1270	212.9
Well 8	9529	184.6	4908	189.3	3975	190.4
Well 9	8	89.0	8	88.3	8	88.3
Well 10	367	147.8	322	151.4	322	151.4
Well 11	4430	277.0	4166	290.4	3651	327.4
Well 12	7740	458.0	5946	469.2	4987	475.3
Well 13	4060	80.5	3202	177.3	2821	208.0
Well 14a	6890	178.1	4511	195.8	3475	203.9
Well 14b	4027	131.2	3256	153.0	2682	167.9
Well 15	7103	363.2	6250	454.7	5669	490.4

Table 7.13: Blowout statistics - Annulus to seabed

Correlation	**Blowout rate**		**FBHP**	
Parameter	**Difference**	**Error**	**Difference**	**Error**
Unit	Sm^3/d	**%**	**Bar**	**%**
Orkiszewski - average	-909	-15.1	27.1	17.0
Absolute average	923	17.9	29.3	18.3
Absolute max	4621	48.5	96.8	120.3
Olgjenka - Average	-1314	-20.3	36.8	22.3
Absolute average	1325	23.8	39.7	24.3
Absolute max	5554	58.3	127.5	158.4

7.4 Kill results

7.4.1 Professional kill simulations

The different blowout and kill simulations conducted by the professional companies often only give the worst-case scenario for a given well. The worst-case scenario can be either a gas blowout instead of an oil blowout, a different well design, different reservoir properties or the number of reservoirs. Several of the wells used in this master thesis is not the worst-case scenario, and the resulting number of simulations to be used for comparison is only seven wells for each of the blowout release points. Since the simulator "Olga-Well-Kill" is developed through multiple decades it would be a great achievement if the created blowout and kill simulator in this thesis come close to the results.

The professional simulated kill rates for a blowout release through open/cased hole to surface is presented in table 7.14 for the seven available wells. The professional simulated kill rates with a release point to seabed is presented in table 7.15 for the seven available wells for this scenario. These tables are used as a reference in the comparison with the kill rates simulated in the created simulator. Note that in total 11 different wells are listed where three wells are common for both release points.

Table 7.14: Professional kill simulation - Open hole to surface

	Density S.G.	**Kill rate LPM**	**Density S.G.**	**Kill rate LPM**	**Density S.G.**	**Kill rate LPM**	**Density S.G.**	**Kill rate LPM**
Well 1a	2.2	4500	2.0	5750	1.9	7750	1.8	11000
Well 3	1.8	4500	1.6	4000				
Well 8a	1.8	9000	1.6	10500				
Well 10	1.4	2500	1.3	2500	1.2	3500		
Well 13	2.0	6600	1.8	8000	1.6	11000		
Well 14a	2.0	4500	1.8	5250	1.6	6375	1.4	8375
Well 15	2.2	5500	2.1	6750	2.08	7000		

Table 7.15: Professional kill simulation - Open hole to seabed

	Density S.G.	**Kill rate LPM**	**Density S.G.**	**Kill rate LPM**	**Density S.G.**	**Kill rate LPM**	**Density S.G.**	**Kill rate LPM**
Well 1a	2.00	4500	1.90	6000				
Well 6	1.50	7800	1.15	10300				
Well 8a	1.80	5000	1.60	6000				
Well 9	1.26	2400						
Well 11	1.92	4450						
Well 12	1.95	7500	1.80	8700	1.60	11100		
Well 14a	2.00	3375	1.80	4000	1.60	4875	1.40	6750

7.4.2 Olgjenka kill simulations

The multiphase pressure correlation Olgjenka and the Standing PVT-set are used together for the presented results in this section. A more detailed description of the kill procedure is described in section 6.2.3 and 6.3.6, only the results are presented in this section. The kill rates are calculated with the created simulator and a calibration formula is created to increase the accuracy between the created simulator and the professional results.

Open hole to surface

The kill fluid densities and the required simulated kill rates for a blowout through open/-cased hole with a surface release point are shown in table 7.16. By comparing the simulated rates with the listed professional rates in table 7.14, table 7.17 is obtained. By examining table 7.17 one can see that the simulated results under predicts the required kill rate for all wells except Well 13. The average error is 26%, while the average absolute error is close to 50%. Well 10 shows that a kill rate of only 250 LPM is required to kill the well, which is most likely a flaw in the simulator.

Table 7.16: Olgjenka kill simulation - Open hole to surface

	Density S.G.	**Kill rate LPM**	**Density S.G.**	**Kill rate LPM**	**Density S.G.**	**Kill rate LPM**	**Density S.G.**	**Kill rate LPM**
Well 1a	2.20	2500	2.00	3250	1.90	3750	1.80	4500
Well 3	1.80	2000	1.60	2500				
Well 8a	1.80	6000	1.60	7250				
Well 10	1.40	250	1.30	250	1.20	250		
Well 13	2.00	9750	1.80	14750	1.60	23500		
Well 14a	2.00	3500	1.80	4000	1.60	5000	1.40	6250
Well 15	2.20	4500	2.10	5000	2.08	5250		

Table 7.17: Olgjenka kill simulation - Surface - Statistics

Well	**Difference LPM**	**Absolute difference LPM**	**Error %**	**Absolute error %**
Well 1a	-3750	3750	-49.7	49.7
Well 3	-2000	2000	-46.5	46.5
Well 8a	-3125	3125	-32.1	32.1
Well 10	-2583	2583	-91.0	91.0
Well 13	7467	7467	81.9	81.9
Well 14a	-1438	1438	-23.2	23.2
Well 15	-1500	1500	-23.0	23.0
Total average	-993	3126	-26.0	49.4

Table explanation
The calculated values in table 7.17 and similar tables presented later in this thesis are calculated with the following equations. The ”difference” value presented in table 7.17 is the difference between the simulated kill rate and the professional kill rate averaged for each well, calculated with equation 7.1. The ”absolute difference” is included to account for wells where the simulation is under predicted and over predicted for the different kill fluid densities. The ”error” equals the difference over the professional listed kill rate, calculated with equation 7.2. The total average is based on all the 21 different simulated kill rates.

$$\Delta q_{kill,w} = \sum_{i=1}^{N} \frac{q_{kill,i} - q_{kill,i,p}}{N} \tag{7.1}$$

$$\epsilon_w = \sum_{i=1}^{N} \frac{1}{N} \frac{q_{kill,i} - q_{kill,i,p}}{q_{kill,i,p}} \tag{7.2}$$

$$\Delta q_{T,avg} = \sum_{i=1}^{T} \frac{q_{kill,i} - q_{kill,i,p}}{T} \tag{7.3}$$

$$\epsilon_{T,avg} = \sum_{i=1}^{T} \frac{1}{T} \frac{q_{kill,i} - q_{kill,i,p}}{q_{kill,i,p}} \tag{7.4}$$

Δq - Difference between simulated kill rate and professional simulated kill rate
ϵ - Error of the simulated kill rate compared to the professional simulated kill rate
Subscripts: w - well, p - professional, i - one of the simulations,
N - number of simulations for one well,
T - total number of simulations conducted for the given scenario.

Open hole to seabed

The kill fluid densities and the required simulated kill rates for a seabed blowout through open/cased hole are shown in table 7.18. By comparing the simulated rates with the listed professional rates in table 7.14, table 7.19 is obtained.

By examining table 7.19 one can see that the simulated results under predicts the required kill rate for all wells, with 2650 LPM in average. In average the simulation under predict the required kill rate with 40%. The same error as observed in the surface section with a kill rate of only 250 LPM is observed for Well 6 and Well 9.

Table 7.18: Olgjenka kill simulation - Open hole to seabed

	Density S.G.	**Kill rate LPM**	**Density S.G.**	**Kill rate LPM**	**Density S.G.**	**Kill rate LPM**	**Density S.G.**	**Kill rate LPM**
Well 1a	2.00	2500	1.90	3000				
Well 6	1.50	250	1.15	250				
Well 8a	1.80	4000	1.60	4500				
Well 9	1.26	250						
Well 11	1.92	3000						
Well 12	1.95	5750	1.80	6250	1.60	7500		
Well 14a	2.00	3000	1.80	3500	1.60	4000	1.40	5250

Table 7.19: Olgjenka kill simulation - Seabed - Statistics

Well	**Difference LPM**	**Absolute difference LPM**	**Absolute Error %**	**Error %**
Well 1a	-2500	2500	-47.2	47.2
Well 6	-8800	8800	-97.2	97.2
Well 8a	-1250	1250	-22.5	22.5
Well 9	-2150	2150	-89.6	89.6
Well 11	-1450	1450	-32.6	32.6
Well 12	-2600	2600	-28.0	28.0
Well 14a	-813	813	-15.9	15.9
Total average	-2650	2650	-40.2	40.2

7.4.3 Olgjenka calibrated kill simulations

The average simulated kill rate error in both kill scenarios were not accurate enough and the accuracy of the simulator should be improved. The fact that the kill rate is as low as 250 could indicate a problem with the simulator. One way to increase the accuracy is to calibrate the created simulator with the results from the professional simulator based on the common input data. Several parameters used in the calculation process are unknown such as: the kill fluid viscosity, the inner diameter of each casing, relative roughness of each pipes and the kill fluid temperature. It is likely that the professional listed rates also have a safety margin.

To account for the impact of the unknown parameters and the most likely safety factor used in the professional simulations a calibration is conducted. Several calibration methods were tested without success. The first failed calibration method was a simple kill rate calibration factor based on the average error calculated in table 7.17 and table 7.19, e.g. an error of 0.50 would give a calibration factor of 1.5 multiplied with the calculated kill rate. The second failed calibration method used a calibrated friction factor to adjust the friction pressure increase along the wellbore, this calibration factor was used in the multiphase pressure calculation. Both these methods gave a small accuracy improvement, but still not satisfactory.

A calibration method which proved successful was to use a calibration factor for the calculated pressure increase over each length iterations, e.g. if a calculated pressure increase over 10 ft is 3 psi, the calculated 3 psi is multiplied with the calibration factor (C_{dp}). The calibration factor is multiplied with the calculated pressure increase over each length increment and not the total flowing bottom hole pressure to account for the PVT physics, such as a gas going out of solution.

A series of simulations for each kill density and resulting kill rate in the different wells were required to match the simulated kill rate with the professional kill rates. The calibration factor for a surface kill is presented in figure 7.20 and a seabed kill in table 7.21. A calibration factor higher than one will reduce the calculated kill rate, and a calibration factor lower than one will reduce the calculated kill rate. Since most of the wells under predicted the kill rate most of the calibration factors are less than one.

Table 7.20: Kill rate calibration factor - Olgjenka - Open hole to surface

Well	Density S.G.	C_dp -	Density S.G.	C_dp -	Density S.G.	C_dp -	Density S.G.	C_dp -	C_dp Average
Well 1a	2.2	0.836	2.0	0.862	1.9	0.872	1.8	0.859	0.857
Well 3	1.8	0.703	1.6	0.803					0.753
Well 8a	1.8	0.828	1.6	0.813					0.820
Well 10	1.4	0.779	1.3	0.835	1.2	0.894			0.836
Well 13	2.0	1.094	1.8	1.119	1.6	1.134			1.116
Well 14a	2.0	0.921	1.8	0.921	1.6	0.921	1.4	0.906	0.917
Well 15	2.2	0.931	2.1	0.906	2.08	0.906			0.915

Table 7.21: Kill rate calibration factor - Olgjenka - Open hole to seabed

	Density S.G.	C_dp -	Density S.G.	C_dp -	Density S.G.	C_dp -	Density S.G.	C_dp -	C_dp Average
Well 1a	2.0	0.921	1.9	0.946					0.934
Well 6	1.5	0.648	1.2	0.742					0.695
Well 8a	1.8	0.911	1.6	0.911					0.911
Well 9	1.3	0.850							0.850
Well 11	1.9	0.850							0.850
Well 12	2.0	0.859	1.8	0.844	1.6	0.813			0.839
Well 14a	2.0	0.972	1.8	0.938	1.6	0.955	1.4	0.922	0.947

Calibration formula - Open hole to surface

The averaged calibration factor was used together with the input data as presented in section 7.2 to create a calibration formula. The formula should be valid to use for several wells and not only those used in this thesis. The number of wells the calibration formula is based upon may of course be questioned and it cannot be argued that more wells is preferable. By looking further into the calibration factors in table 7.20 a common trend is that the calibration factor is increasing with decreasing density, this was however neglected due to the number of data points. With more data points a calibration formula for a lower range of densities and a higher range of densities would be beneficial.

The averaged calibration factors were plotted against the input data and a best fit linear regression were conducted for all input parameters. The correlation between the calibration factor and each of the input parameters is quantified with the root mean square value (R^2). Table 7.22 shows how well each of the input parameters correlates with the calibration factor and the four parameters chosen for further use in the development of a calibration formula. The linear regression for each of the four chosen parameters are presented in figure 7.1 to figure 7.4.

Table 7.22: Olgjenka - Open hole to surface - Linear regression

Parameter	Unit	R^2	Used further
Total depth	**[m TVD RKB]**	0.30	Yes
Depth to seabed	**[m MSL]**	0.16	
Average diameter	**[in.]**	0.15	
Oil gravity	**[s.g.]**	0.01	
Gas gravity	**[s.g.]**	0.06	
GOR	**[Sm3/Sm3]**	0.69	Yes
Saturation pressure	**[Bar]**	0.68	Yes
Productivity Index	**[Sm3/d/bar]**	0.11	
AOF	**[Sm3/d]**	0.09	
Reservoir temperature	**[Celsius]**	0.31	
Reservoir pressure	**[Bar]**	0.10	
Intersection point	**[m TVD]**	0.00	
IP/TD	**[%]**	0.52	Yes
p_s / p_r	**[%]**	0.03	

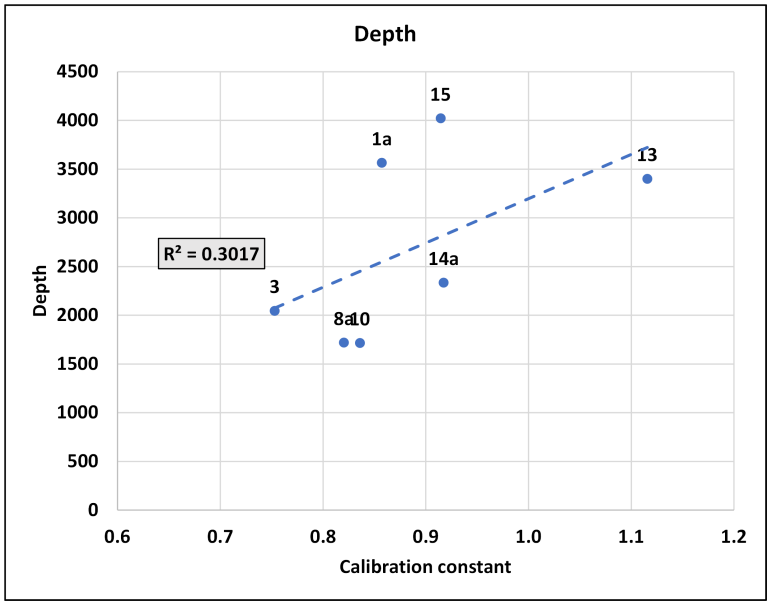

Figure 7.1: Olgjenka calibration - Surface - Total depth

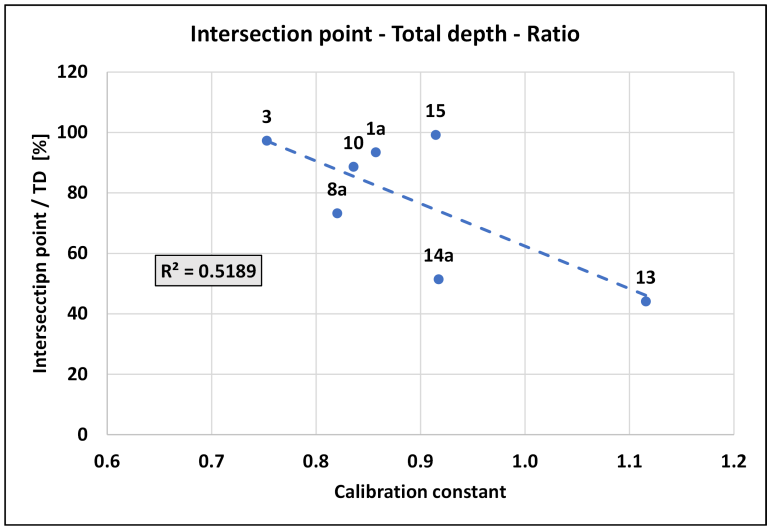

Figure 7.2: Olgjenka calibration - Surface - Intersection point - Total depth ratio

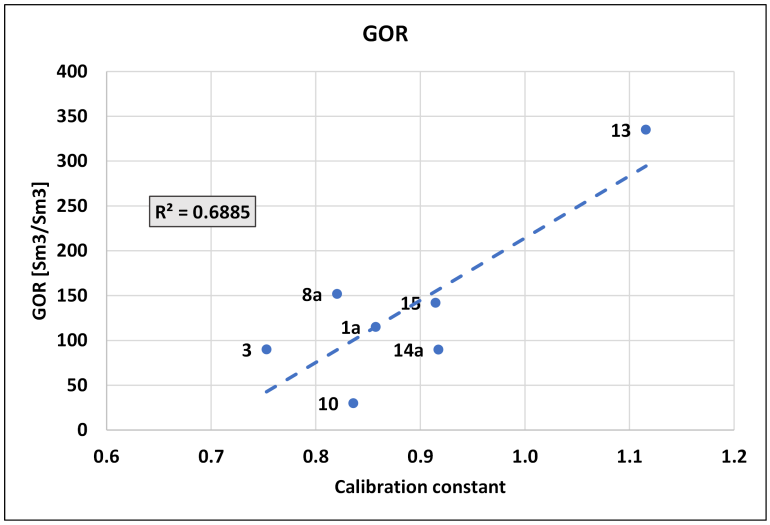

Figure 7.3: Olgjenka calibration - Surface - GOR

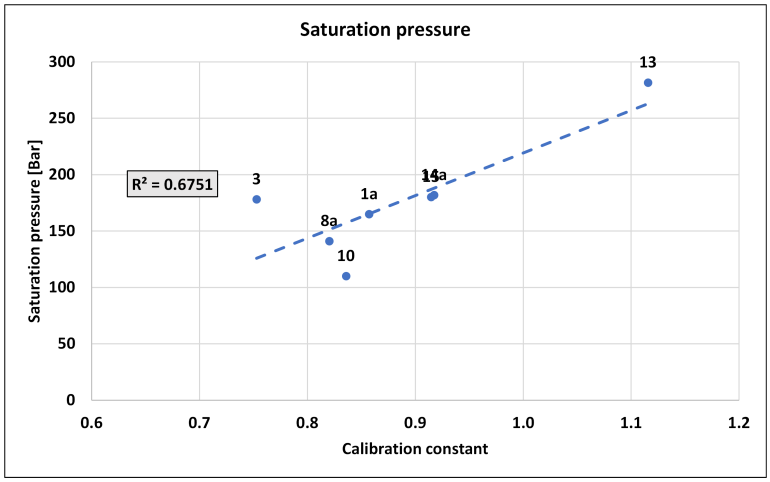

Figure 7.4: Olgjenka calibration - Surface - Saturation pressure

To create the calibration formula a non-linear regression tool in Matlab was used together with the four input parameters and the averaged calibration factor. The used Matlab function is called ”fitnlm” and finds the coefficients that gives a best fit between a chosen equation and a given data set. The data set used is shown in table 7.23, where the calibration factor is the target to be matched with the four input parameters. The chosen calibration formula is presented in equation 7.5. The coefficients which gives the lowest error is presented in table 7.24 together with the R^2-value for the non-linear regression and the p-value.

Table 7.23: Input data for non-linear regression - Olgjenka - Surface

C_dp	Well	Total depth [m TVD RKB]	Saturation pressure [Bar]	GOR [Sm3/Sm3]	IP/TD [%]
0.857	**Well 1a**	3565.0	164.8	115.0	93.4
0.753	**Well 3**	2046.0	178.0	90.0	97.3
0.820	**Well 8a**	1720.0	141.0	152.0	73.3
0.836	**Well 10**	1715.0	110.0	30.0	88.6
1.116	**Well 13**	3401.0	281.6	335.0	44.1
0.917	**Well 14a**	2334.0	181.8	89.8	51.4
0.915	**Well 15**	4022.0	180.0	142.0	99.2

$$C_{dp} = b_1 + b_2 TD + b_3 R_t + b_4 p_s + b_5 \frac{IP}{TD} \tag{7.5}$$

C_{dp} - Calibration factor [-]
TD - Total depth [m TVD RKB]
R_t - Total gas-oil-ratio [Sm^3/Sm^3]
p_s - Saturation pressure of the oil [Bar]
IP/TD - Intersection point - total depth fraction [$\%$]

Table 7.24: Calibration formula coefficients - Olgjenka - Surface

b1	b2	b3	b4	b5	R-squared	p-value
9.69E-01	6.13E-05	-2.16E-04	3.51E-04	-3.27E-03	0.90	0.19

Calibrated values - Open hole to surface
By using the calibration factor formula together with the input data for the seven wells as shown in table 7.23 the estimated calibration factors presented in table 7.25 are obtained. The best predicted value comes close to the actual calibration factor for all the wells with an averaged absolute difference equal to 0.03 and the highest difference is -0.06 (Well 10). The true calibration factor is within the range of P10 and P90 for all the wells.

The best predicted calibration factor gives the best predicted kill rate. The true calibration factor has a 90$\%$ probability to be above the estimated P90 value. The resulting kill rate from the P90 calibration will be an upper bound. The true calibration factor has a 10$\%$ probability to be above the estimated P10 value, the resulting kill rate will be a lower bound.

Table 7.25: Calculated calibration factors - Olgjenka - Surface

Well	Best prediction	P90	P10
Well 1a	0.89	0.811	0.963
Well 3	0.77	0.652	0.887
Well 8a	0.86	0.753	0.963
Well 10	0.77	0.692	0.850
Well 13	1.09	0.978	1.203
Well 14a	0.94	0.822	1.050
Well 15	0.90	0.810	0.995

Calibrated kill rates - Open hole to surface

The resulting best predicted kill rates are presented in table 7.26 for the different wells with a surface blowout release. Table 7.27 shows the difference between the best predicted kill rate and the professional listed kill rates together with the error.

Compared to the uncalibrated kill rates the absolute difference is almost halved. The average absolute error is less than 9%, if Well 10 is neglected. Well 10 which initially had a calculated kill rate of 250 is now highly over predicted with more than 3 times the professional listed kill rate. In total the calibration was a success, but the highly over prediction of Well 10 cause a concern which should be further investigated.

Table 7.26: Olgjenka Calibrated kill simulation - Open hole to surface

	Density S.G.	Kill rate LPM	Density S.G.	Kill rate LPM	Density S.G.	Kill rate LPM	Density S.G.	Kill rate LPM
Well 1a	2.20	3750	2.00	5000	1.90	7000	1.80	9750
Well 3	1.80	3750	1.60	4500				
Well 8a	1.80	7750	1.60	9000				
Well 10	1.40	6500	1.30	12000	1.20	16500		
Well 13	2.00	6500	1.80	8500	1.60	12750		
Well 14a	2.00	4500	1.80	5000	1.60	6250	1.40	7500
Well 15	2.20	5750	2.10	6500	2.08	6750		

Table 7.27: Olgjenka calibrated kill simulation - Surface- Statistics

Well	Difference LPM	Absolute difference LPM	Error %	Absolute error %
Well 1a	-875	875	-12.7	12.7
Well 3	-125	625	-2.1	14.6
Well 8a	-1375	1375	-14.1	14.1
Well 10	8833	8833	303.8	303.8
Well 13	717	783	6.9	7.9
Well 14a	-313	313	-4.3	4.3
Well 15	-83	250	-0.9	3.9
Total average	983	1826	39.5	51.1
Total average*	-325	624	-4.6	8.9

* Without Well 10

Calibration formula - Open hole to seabed

The calibration procedure for the required kill rate of a seabed blowout is the same as described for the surface calibration. This section describes the same procedure, but with less details. For the full detailed explanation see the calibration of the surface kill rate.

The calibration factors for the different wells and densities are shown in table 7.21, the averaged calibration factors are on the right end of the table. The averaged calibration factors are used to create the calibration formula. To be able to select the four best input parameters to be used in a non-linear regression for the calibration formula, a linear regression was conducted on the input parameters. The linear correlation between the input parameters and the seabed calibration factors are shown in table 7.28. The total depth was used instead of parameters with a better correlation due to its importance. The length of the well highly impact the hydrostatic pressure and the friction pressure.

Table 7.28: Olgjenka - Open hole to seabed - Linear regression

Parameter	Unit	R^2	Used further
Total depth	**[m TVD RKB]**	0.08	Yes
Depth to seabed	**[m RKB]**	0.19	Yes
Average diameter	**[in.]**	0.15	
Oil gravity	**[s.g.]**	0.24	Yes
Gas gravity	**[s.g.]**	0.26	Yes
GOR	**[Sm3/Sm3]**	0.01	
Saturation pressure	**[Bar]**	0.00	
Productivity Index	**[Sm3/d/bar]**	0.09	
AOF	**[Sm3/d]**	0.09	
Reservoir temperature	**[Celsius]**	0.07	
Reservoir pressure	**[Bar]**	0.07	
Intersection point	**[m TVD]**	0.02	
IP/TD	**[%]**	0.10	
p_s / p_r	**[%]**	0.09	

To create the calibration formula a non-linear regression tool in Matlab was used together with the four input parameters and the averaged calibration factor. The data set used is shown in table 7.29 and the calibration formula is shown in equation 7.6. The required units to be used are shown in table 7.29. The coefficients which gives the lowest error are presented in table 7.30 together with the R^2-value for the non-linear regression and the p-value. The root mean square is slightly smaller for the seabed calibration coefficients compared to the surface coefficients, but a correlation of 0.83 is considerable accurate.

Table 7.29: Input data for non-linear regression

C_dp	Well	Total depth [m TVD RKB]	Water depth [m MSL]	Oil gravity [s.g.]	Gas gravity [s.g.]
0.934	**Well 1a**	3565.0	386.0	0.838	1.200
0.695	**Well 6**	1559.0	497.0	0.876	0.702
0.911	**Well 8a**	1720.0	346.0	0.812	1.020
0.850	**Well 9**	1020.0	112.0	0.913	0.628
0.850	**Well 11**	3744.0	112.0	0.854	0.645
0.839	**Well 12**	3520.0	432.0	0.848	0.702
0.947	**Well 14a**	2334.0	112.0	0.849	0.735

$$C_{dp} = b_1 + b_2 TD + b_3 D_{sb} + b_4 \gamma_o + b_5 \gamma_g \tag{7.6}$$

Table 7.30: Calibration formula - Olgjenka - Seabed

b1	b2	b3	b4	b5	R-squared	p-value
1.45E+00	5.28E-06	-3.98E-04	-7.95E-01	2.38E-01	0.83	0.31

Calibrated values - Open hole to seabed

By using the calibration factor formula together with the input data for the seven wells as shown in table 7.29 the estimated calibration factors presented in table 7.31 are obtained. The best predicted value comes close to the actual calibration factor for all the wells with an average absolute difference equal to 0.03 and the highest difference is +0.05 (Well 13). The true calibration factor is within the range of P10 and P90 for all the wells.

Table 7.31: Calculated calibration coefficients - Olgjenka - Seabed

Well	Best prediction	P90	P10
Well 1a	0.93	0.82	1.05
Well 3	0.73	0.64	0.83
Well 8a	0.92	0.81	1.02
Well 10	0.83	0.73	0.94
Well 13	0.90	0.81	0.99
Well 14a	0.79	0.70	0.88
Well 15	0.92	0.84	0.99

Calibrated kill rates - Open hole to seabed

The resulting best predicted kill rates are presented in table 7.32 for the different wells with a seabed blowout release. Table 7.33 shows the difference between the best predicted kill rate and the professional listed kill rates together with the error.

The calibrated kill rates to seabed are close to the professional listed kill rates, the under prediction and over prediction in the different wells almost cancel each other out making the difference only -17 Sm^3/d. The total absolute error is reduced to almost one third, from 40.2% to 15.6 %. The wells with the highest error are the wells that use the lowest kill fluid density (1.2-1.5 s.g.). The problem with the highly over prediction as observed in the surface calibration is not present in the seabed calibration.

Table 7.32: Olgjenka calibrated kill simulation - Open hole to seabed

	Density S.G.	Kill rate LPM	Density S.G.	Kill rate LPM	Density S.G.	Kill rate LPM	Density S.G.	Kill rate LPM
Well 1a	2.00	3750	1.90	6750				
Well 6	1.50	2750	1.15	10500				
Well 8a	1.80	4750	1.60	5750				
Well 9	1.26	3250						
Well 11	1.92	3750						
Well 12	1.95	8750	1.80	10000	1.60	11750		
Well 14a	2.00	3750	1.80	4500	1.60	5500	1.40	7000

Table 7.33: Olgjenka calibrated kill simulation - Seabed - Statistics

Well	Difference LPM	Absolute difference LPM	Error %	Absolute error %
Well 1a	0	750	-2.1	14.6
Well 6	-2425	2625	-31.4	33.3
Well 8a	-250	250	-4.6	4.6
Well 9	850	850	35.4	35.4
Well 11	-700	700	-15.7	15.7
Well 12	1067	1067	12.5	12.5
Well 14a	438	438	10.0	10.0
Total average	-17	917	1.4	15.6

7.4.4 Orkiszewski kill simulations

The multiphase pressure correlation Orkiszewski (A.5.2) and the Standing PVT-set (A.6.1) are used together for the presented results in this section. A more detailed description of the kill procedure is described in section 6.2.3 and 6.3.6, only the results are presented in this section. The calculated kill rates are presented based on the theory presented in this thesis and the kill rates are calibrated with the professional simulated kill rates to obtain a higher accuracy. This section covers the same information as the Olgjenka section, but with the calculated results obtained with the Orkiszewski multiphase pressure correlation instead.

Open hole to surface
The kill fluid densities and the simulated kill rates calculated with the Orkiszewski correlation for a blowout through open/cased hole with a surface release point are shown in table 7.34. By comparing the simulated rates with the professional rates in table 7.14, table 7.35 is obtained.

By examining table 7.35 one can see that the simulated results under predicts the required kill rate for most wells. The average error is -6%, while the average absolute error is more than 50%. Well 10 shows that a kill rate of only 250 LPM is required to kill the well, which also was observed for the required kill rate to surface with the Olgjenka-correlation.

Table 7.34: Orkiszewski kill simulation - Open hole to surface

	Density S.G.	Kill rate LPM	Density S.G.	Kill rate LPM	Density S.G.	Kill rate LPM	Density S.G.	Kill rate LPM
Well 1a	2.20	2000	2.00	2750	1.90	3250	1.80	4250
Well 3	1.80	2500	1.60	3250				
Well 8a	1.80	7500	1.60	9000				
Well 10	1.40	250	1.30	250	1.20	250		
Well 13	2.00	13250	1.80	21000	1.60	34000		
Well 14a	2.00	4000	1.80	5000	1.60	6250	1.40	7750
Well 15	2.20	6750	2.10	6750	2.08	6750		

Table 7.35: Orkiszewski kill simulation - Surface - Statistics

Well	Difference LPM	Absolute difference LPM	Absolute Error %	Error %
Well 1a	-4188	4188	-56.8	56.8
Well 3	-1375	1375	-31.6	31.6
Well 8a	-1500	1500	-15.5	15.5
Well 10	-2583	2583	-91.0	91.0
Well 13	14217	14217	157.4	157.4
Well 14a	-375	375	-6.3	6.3
Well 15	333	500	6.4	8.8
Total average	567	3614	-6.1	53.2

Open hole to seabed

The kill fluid densities and the required simulated kill rates for a seabed blowout through open/cased hole with the Orkiszewski correlation are shown in table 7.36. By comparing the simulated rates with the professional rates in table 7.15, table 7.37 is obtained. By examining table 7.37 one can see that the simulated results under predicts the required kill rate with -1667 LPM in average or -25% in average. The 250 LPM kill rate error as observed in the required surface kill rates is observed for Well 6 and Well 9.

Table 7.36: Orkiszewski kill simulation - Open hole to seabed

	Density S.G.	Kill rate LPM	Density S.G.	Kill rate LPM	Density S.G.	Kill rate LPM	Density S.G.	Kill rate LPM
Well 1a	2.00	2500	1.90	3500				
Well 6	1.50	250	1.15	250				
Well 8a	1.80	5000	1.60	6250				
Well 9	1.26	250						
Well 11	1.92	3500						
Well 12	1.95	7500	1.80	8500	1.60	10250		
Well 14a	2.00	3500	1.80	4250	1.60	5250	1.40	7000

Table 7.37: Orkiszewski kill simulation - Seabed - Statistics

Well	Difference LPM	Absolute difference LPM	Error %	Absolute Error %
Well 1a	-2250	2250	-43.1	43.1
Well 6	-8800	8800	-97.2	97.2
Well 8a	125	125	2.1	2.1
Well 9	-2150	2150	-89.6	89.6
Well 11	-950	950	-21.3	21.3
Well 12	-350	350	-3.3	3.3
Well 14a	250	250	5.3	5.3
Total average	-1667	1833	-25.1	28.5

7.4.5 Orkiszewski calibrated kill simulations

Calibration formula - Open hole to surface

The calibration procedure for the Orkiszewski correlation is the same as described for the Olgjenka calibration. This section will describe the same procedure, but with less details. For the full detailed explanation see section 7.4.3.

The calibration factors for the different wells and densities are shown in table 7.38 together with the averaged calibration factors on the right end of the table. The averaged calibration factors are used to create the calibration formula. To be able to select the four best

input parameters to be used in a non-linear regression for the calibration formula, a linear regression was conducted on the input parameters. The correlation between the input parameters and the seabed calibration factors are shown in table 7.39. The total depth was used instead of parameters with a better correlation due to its importance. The length of the well highly impact the hydrostatic pressure and the friction pressure.

Table 7.38: Kill rate calibration factor - Open hole to surface

	Density S.G.	**C_dp -**	**Density S.G.**	**C_dp -**	**Density S.G.**	**C_dp -**	**Density S.G.**	**C_dp -**	**C_dp Well average**
Well 1a	2.2	0.828	2.0	0.878	1.9	0.905	1.8	0.921	0.883
Well 3	1.8	0.734	1.6	0.911					0.823
Well 8a	1.8	0.916	1.6	0.931					0.924
Well 10	1.4	0.783	1.3	0.838	1.2	0.900			0.840
Well 13	2.0	1.175	1.8	1.216	1.6	1.200			1.197
Well 14a	2.0	0.972	1.8	0.982	1.6	0.992	1.4	0.982	0.982
Well 15	2.2	0.982	2.1	0.972	2.1	0.972			0.975

Table 7.39: Orkiszewski - Open hole to surface - Linear regression

Parameter	**Unit**	R^2	**Used further**
Total depth	**[m TVD RKB]**	0.24	Yes
Depth to seabed	**[m RKB]**	0.18	
Average diameter	**[in.]**	0.26	
Oil gravity	**[s.g.]**	0.09	
Gas gravity	**[s.g.]**	0.06	
GOR	**[Sm3/Sm3]**	0.82	Yes
Saturation pressure	**[Bar]**	0.76	Yes
Productivity Index	**[Sm3/d/bar]**	0.02	
AOF	**[Sm3/d]**	0.09	
Reservoir temperature	**[Celsius]**	0.28	
Reservoir pressure	**[Bar]**	0.06	
Intersection point	**[m TVD]**	0.02	
IP/TD	**[%]**	0.60	Yes
p_s / p_r	**[%]**	0.00	

To create the calibration formula a non-linear regression tool in Matlab was used together with the four input parameters and the averaged calibration factor. The data set used is shown in table 7.40 and the calibration formula is shown in equation 7.7. The required units to be used are shown in table 7.40. The coefficients which gives the lowest error are presented in table 7.41 together with the R^2-value for the non-linear regression and the p-value. The root mean square is 0.96 and is the highest of all the four calibration formulas.

Table 7.40: Input data for non-linear regression

C_dp	Well	Total depth [m TVD RKB]	Saturation pressure [Bar]	GOR [Sm3/Sm3]	IP/TD [%]
0.883	**Well 1a**	3565.0	164.8	115.0	93.4
0.823	**Well 3**	2046.0	178.0	90.0	97.3
0.924	**Well 8a**	1720.0	141.0	152.0	73.3
0.840	**Well 10**	1715.0	110.0	30.0	88.6
1.197	**Well 13**	3401.0	281.6	335.0	44.1
0.982	**Well 14a**	2334.0	181.8	89.8	51.4
0.975	**Well 15**	4022.0	180.0	142.0	99.2

$$C_{dp} = b_1 + b_2 TD + b_3 p_s + b_4 R_t + b_5 \frac{IP}{TD} \tag{7.7}$$

Table 7.41: Calibration formula coefficients - Orkiszewski - Surface

b1	b2	b3	b4	b5	R-squared	p-value
1.01E+00	4.34E-05	-1.58E-04	6.31E-04	-3.06E-03	0.96	0.079

Calibrated values - Open hole to surface

By using the calibration factor formula together with the input data for the seven wells as shown in table 7.40 the estimated calibration factors presented in table 7.42 are obtained. The best predicted value comes close to the actual calibration factor for all the wells with an average absolute difference equal to 0.02 and the highest difference is +0.04 (Well 1a). The true calibration factor is within the range of P10 and P90 for all the wells.

Table 7.42: Calculated calibration coefficients - Orkiszewski - Surface

Well	Best prediction	P90	P10
Well 1a	0.93	0.87	0.98
Well 3	0.83	0.75	0.91
Well 8a	0.94	0.86	1.01
Well 10	0.81	0.76	0.87
Well 13	1.19	1.11	1.27
Well 14a	0.98	0.91	1.06
Well 15	0.94	0.88	1.01

Calibrated kill rates - Open hole to surface

The resulting best predicted kill rates are presented in table 7.43 for the different wells with a surface blowout release. Table 7.44 shows the difference between the ”best predicted” kill rate and the professional kill rates together with the error. All the wells show a significant increase in accuracy except Well 10. When excluding Well 10 the average error is only -2.1%, while the average absolute error is reduced to less than one third, from 53.2% to 14.1 %. Well 10 was problematic in the surface section with the Olgjenka correlation as well.

Table 7.43: Orkiszewski calibrated kill simulation - Open hole to surface

	Density S.G.	**Kill rate LPM**	**Density S.G.**	**Kill rate LPM**	**Density S.G.**	**Kill rate LPM**	**Density S.G.**	**Kill rate LPM**
Well 1a	2.20	2750	2.00	3750	1.90	5500	1.80	10500
Well 3	1.80	4250	1.60	5250				
Well 8a	1.80	8000	1.60	9500				
Well 10	1.40	500	1.30	9250	1.20	17750		
Well 13	2.00	6250	1.80	8250	1.60	11000		
Well 14a	2.00	4250	1.80	5250	1.60	6500	1.40	8250
Well 15	2.20	7250	2.10	8250	2.08	8250		

Table 7.44: Orkiszewski calibrated kill simulation - Surface- Statistics

Well	**Difference LPM**	**Absolute difference LPM**	**Error %**	**Absolute error %**
Well 1a	-1625	1625	-26.8	26.8
Well 3	500	750	12.8	18.4
Well 8a	-1000	1000	-10.3	10.3
Well 10	6333	7667	199.0	252.4
Well 13	-33	200	-0.7	2.8
Well 14a	-63	125	-1.3	2.3
Well 15	1500	1500	24.0	24.0
Total average	745	1838	26.6	48.2
Total average*	-186	821	-2.1	14.1

*Without Well 10

Calibration formula - Open hole to seabed

The calibration procedure for the Orkiszewski correlation is exactly the same as described for the Olgjenka calibration. This section will describe the same procedure, but with less details, for the full detailed explanation see section 7.4.3. .

The calibration factors for the different wells and densities are shown in table 7.45 together with the averaged calibration factors on the right side of the table. The averaged calibration

factors are used to create the calibration formula. To be able to select the best four input parameters to be used in a non-linear regression for the calibration formula, a linear regression was conducted on the input parameters. The correlation between the input parameters and the seabed calibration factors are shown in table 7.46. A non-linear regression was conducted on the four parameters: oil gravity, AOF, reservoir temperature and the fraction IP/TD, the corresponding R^2-value was 0.694 which is considerably lower than the other calibrations. A trial and error process were conducted on the different input parameters to find the calibration formula with the highest R^2-value, the chosen input parameters are shown in table 7.46.

Table 7.45: Kill rate calibration factor - Orkiszewski - Open hole to seabed

Well	**Density S.G.**	**C_dp -**	**Density S.G.**	**C_dp -**	**Density S.G.**	**C_dp -**	**Density S.G.**	**C_dp -**	**C_dp Well average**
Well 1a	2.0	0.936	1.9	0.974					0.955
Well 6	1.5	0.699	1.2	0.831					0.765
Well 8a	1.8	1.013	1.6	1.013					1.013
Well 9	1.3	0.861							0.861
Well 11	1.9	0.911							0.911
Well 12	2.0	0.992	1.8	0.992	1.6	0.969			0.984
Well 14a	2.0	1.013	1.8	1.013	1.6	1.028	1.4	1.008	1.015

Table 7.46: Orkiszewski - Open hole to seabed - Linear regression

Parameter	**Unit**	R^2	**Used further**
Total depth	**[m TVD RKB]**	0.15	Yes
Depth to seabed	**[m RKB]**	0.03	Yes
Average diameter	**[in.]**	0.01	
Oil gravity	**[s.g.]**	0.50	Tried
Gas gravity	**[s.g.]**	0.16	Tried
GOR	**[Sm3/Sm3]**	0.11	
Saturation pressure	**[Bar]**	0.11	
Productivity Index	**[Sm3/d/bar]**	0.27	
AOF	**[Sm3/d]**	0.38	Yes
Reservoir temperature	**[Celsius]**	0.19	Tried
Reservoir pressure	**[Bar]**	0.09	
Intersection point	**[m TVD]**	0.03	
IP/TD	**[%]**	0.23	Yes
p_s / p_r	**[%]**	0.01	

To create the calibration formula a non-linear regression tool in Matlab was used together with the four input parameters and the averaged calibration factor. The data set used is shown in table 7.47 and the calibration formula is shown in equation 7.8. The required units to be used are shown in table 7.47. The coefficients which gives the lowest error is

presented in table 7.48 together with the R^2-value for the non-linear regression and the p-value. The root mean square is smaller than the surface calibration coefficients, but a correlation of 0.853 is considerable accurate.

Table 7.47: Input data for non-linear regression

C_dp	Well	Total depth [m TVD RKB]	Water depth [m MSL]	AOF [Sm3/d]	IP/TD [%]
0.955	**Well 1a**	3565	386	7374	93.4
0.765	**Well 6**	1559	497	2200	82.4
1.013	**Well 8a**	1720	346	100000	73.3
0.861	**Well 9**	1020	112	3180	99.0
0.911	**Well 11**	3744	112	6141	98.3
0.984	**Well 12**	3520	432	54000	85.2
1.015	**Well 14a**	2334	112	19300	51.4

$$C_{dp} = b_1 + b_2 T_r + b_3 \gamma_o + b_4 AOF + b_5 \frac{IP}{TD} \tag{7.8}$$

Table 7.48: Calibration formula coefficients - Orkiszewski - Seabed

b1	b2	b3	b4	b5	R-squared	p-value
9.93E-01	4.32E-05	-2.21E-04	1.61E-06	-1.84E-03	0.853	0.272

Calibrated values - Open hole to seabed

By using the calibration factor formula together with the input data for the seven wells as shown in table 7.29 the estimated calibration factors presented in table 7.49 are obtained. The best predicted value comes close to the actual calibration factor for all the wells with an average absolute difference equal to 0.03 and the highest difference is +0.05 (Well 1a). The true calibration factor is within the range of P10 and P90 for all the wells.

Table 7.49: Calculated calibration coefficients - Orkiszewski - Seabed

Well	Best prediction	P90	P10
Well 1a	0.90	0.83	0.98
Well 6	0.80	0.70	0.90
Well 8a	1.02	0.91	1.12
Well 9	0.84	0.73	0.94
Well 11	0.96	0.87	1.05
Well 12	0.98	0.90	1.06
Well 14a	1.01	0.89	1.12

Calibrated kill rates - Open hole to seabed

The resulting best predicted kill rates are presented in table 7.50 for the different wells with a seabed blowout release. Table 7.51 shows the difference between the ”best predicted” kill rate and the professional listed kill rates together with the error. The calibration was not as successful as for the three other calibrations, but all the averaged parameters except the average absolute error have decreased. The average error has decreased from -25% to 13.6 %, the absolute error has increased from 28.5% to 33%. The average difference before the calibration was -1667 LPM it is now 350 LPM, the absolute difference has decreased with 400 LPM. Well 1a and Well 9 responded badly on the calibration with an increase in the absolute error.

Table 7.50: Orkiszewski calibrated kill simulation - Open hole to seabed

	Density S.G.	Kill rate LPM	Density S.G.	Kill rate LPM	Density S.G.	Kill rate LPM	Density S.G.	Kill rate LPM
Well 1a	2.00	8500	1.90	12250				
Well 6	1.50	500	1.15	11750				
Well 8a	1.80	4250	1.60	5000				
Well 9	1.26	5500						
Well 11	1.92	4000						
Well 12	1.95	7750	1.80	8750	1.60	10500		
Well 14a	2.00	3250	1.80	4250	1.60	5000	1.40	6750

Table 7.51: Orkiszewski calibrated kill simulation - Seabed - Statistics

Well	Difference LPM	Absolute difference LPM	Error %	Absolute error %
Well 1a	5125	5125	96.5	96.5
Well 6	-2925	4375	-39.8	53.8
Well 8a	-875	875	-15.8	15.8
Well 9	3100	3100	129.2	129.2
Well 11	-450	450	-10.1	10.1
Well 12	-100	300	-0.5	3.1
Well 14a	63	125	1.3	3.1
Total average	350	1713	13.6	32.9
Total average*	154	1507	5.4	26.0

* - Without well 9

Chapter 8

Discussion

In general, the created blowout and kill simulator shows promising results compared to the standard industry simulator. The summarized statistics for the created simulator with the two different multiphase correlations are shown in table 8.1.

The Olgjenka correlation gave the lowest error for the average of all the blowout scenarios with an average error of -7.5% compared to Orkiszewski's error of -11%. The average uncalibrated Orkiszewski kill error was -15.6%, almost half of Olgjenka with an average error of -33.1%. The Olgjenka correlation responded better to the calibration than Orkiszewski's correlation. The average calibrated Olgjenka error was 16.2%, while Orkiszewski had an increase in the average error to 20.1%. Well 10 was problematic in the calibration for both correlations and is the reason of the increased error in the calibrated Orkiszewski. The average calibrated errors without the outlier wells (Well 9 and Well 10) are -3.0% and 1.65% for Olgjenka and Orkiszewski, respectively. The absolute average errors are 12.7% for Olgjenka and 20.0% for Orkiszewski, without the outlier wells.

Table 8.1: Summarized errors for the different scenarios

Multiphase correlation	**Olgjenka**		**Orkiszewski**	
Scenario (↓)	**Error**	**Absolute error**	**Error**	**Absolute error**
Unit (→)	**%**	**%**	**%**	**%**
Surface blowout - OH	-1.1	13.9	-11.2	20.2
Seabed blowout - OH	-7.6	13.9	-7.2	11.9
Surface blowout - Ann	-20.3	23.8	-15.1	17.9
Seabed blowout - Ann	-1.1	13.9	-11.2	20.2
Surface kill	-26	49.4	-6.1	53.2
Calibrated surface kill	31	44.4	26.6	48.2
Calibrated surface kill*	-4.9	11.1	-2.1	14.1
Seabed kill	-40.2	40.2	-25.1	28.5
Calibrated seabed kill	1.4	15.6	13.6	32.9
Calibrated seabed kill*	-1.0	14.2	5.4	26

* - Without Well 10 or Well 9

Due to the overall performance of the two multiphase correlations, it seems like Olgjenka is the more accurate of the two. Another factor where Olgjenka is superior to the Orkiszewski correlation is in the simulation time, especially in the surface section. The Orkiszewski require an additional iterative process when calculating the pressure increase over one length increment compared to the Olgjenka correlation, which is the reason of the increased simulation time. The Olgjenka correlation does not use an iterative process over each length increment, but due to the nature of the correlation it is not necessary for small length increments, which only affect the PVT parameters. The created simulator uses a length increment of 10ft as standard, but for longer length increments it is advised that an iterative process is added to the Olgjenka correlation.

The Orkiszewski correlation is slightly altered compared to the original correlation published by (Orkiszewski, 1967). The changes made to the correlation are related to a pressure discontinuity in the correlation and an error that creates a negative density, further details are presented in Appendix A.9.

Listed below are some possible reasons that can cause errors:

- The input data are outside the range of what the Orkiszewski correlation is based upon.
- The professional listed blowout rates are not the true values and only simulations.
- Several parameters used in the professional simulations are unknown, some parameters are internal diameter of the pipes, the kill fluid temperature and the kill fluid viscosity.
- The PVT correlation used in the professional simulator is not the same as the either the Glasø correlation or the Standing correlation.
- Several of the investigated wells consist of more than one reservoir, the created simulator combines the two reservoirs into one.
- At least one of the wells (Well 6) is not a single-phase reservoir fluid, a gas cap is present.
- The simulations have used a kill rate step of 250 LPM which may result in a too high kill rate of the different simulations.
- Several thousand lines of codes are written as a part of the simulator. It cannot be excluded that one or more mistakes are made in the coding, even when the code is checked several times.
- The created simulator does not use a transient model which could affect the calculated kill rate. The used stationary model follows the same trend as a transient model, see Appendix A.8.2.
- Due to a big difference in the accuracy of the blowout rate and the accuracy of the calculated flowing bottom hole pressure it is assumed that the professional simulation calculates inflow performance relationship in a different way than the created simulator.
- The calibration formulas should be calculated with dimensionless parameters

Chapter 9

Conclusion

The main part of this thesis is about the created blowout and kill simulator and the comparison with the professional conducted simulations, some key elements are:

- A simulator is created that everyone with Excel and a Matlab license can use. The simulator is easy to use and require no knowledge of the software Matlab, all changes to the input data are intuitive and made in Microsoft Excel. The results of each simulation are presented as an automatically generated report as a PDF-file.
- The simulator gives the user a choice to choose between two multiphase pressure correlations and two PVT-correlation sets. Any combinations show promising results.
- In total 17 wells were simulated in the created simulator and compared against the common industry simulator for blowout and kill. Simulations were conducted for two different flow paths (open/cased hole and annulus) for both a surface and seabed blowout release point. The average error of the blowout rate for the four different combinations was -7.5% for the combination Olgjenka-Standing and -11.0% for the combination Orkiszewski-Standing.
- 7 wells were simulated for a kill through open/cased hole to surface with a total of 21 different kill fluid densities. These simulations were compared against simulations conducted in the common industry simulator, "Olga-Well-Kill". The average error for the combination Olgjenka-Standing was -26.0% and -6.1% for the combination Orkiszewski-Standing.
- A calibration formula was created based on the input data and an adjustment factor required to obtain the same kill rates as the professional listed kill rates. The calibrated kill rates for an open/cased hole kill to surface gave an average error of 31.0% for the combination Olgjenka-Standing and 26.6% for the combination Orkiszewski-Standing. Well 9 responded poorly on the calibration and is viewed as

an outlier, the average errors without the outlier are -4.9% for Olgjenka and -2.1% for Orkiszewski.

- 7 wells were simulated for a kill through open/cased hole to seabed with a total of 15 different kill fluid densities. These simulations were compared against simulations conducted in the common industry simulator. The average error for the combination Olgjenka-Standing was -40.2% and -25.1% for the combination Orkiszewski-Standing.
- A calibration formula was created based on the input data and an adjustment factor required to obtain the same kill rates as the professional listed kill rates. The calibrated kill rates for an open/cased hole kill to seabed gave an average error of 1.4% for the combination Olgjenka-Standing and 13.6% for the combination Orkiszewski-Standing. Well 9 responded poorly on the calibration and is viewed as an outlier, the average errors without the outlier are -1.0% for Olgjenka and 5.4% for Orkiszewski.
- The simulator provides a minimum kill rate (P90) and a maximum kill rate (P10) based on statistics from the calibration process. The professional listed kill rate lies between the minimum and maximum for all simulations. The minimum and maximum values can become unrealistic low or high and it is assumed that more wells to calibrate the kill rates with will reduce the uncertainty.
- The simulator should be improved in several areas which is discussed in the chapter of "Further work". The area that required the most improvement is to implement a transient model to the simulator so the required time to reach dynamic kill can be obtained.

Chapter 10

Further work

Even though the created simulator shows promising results more work should be conducted and implemented in the simulator. The list below consists of a prioritized order that should have the biggest impact on the simulator.

1. A transient model should be implemented to be able to calculate the required mud volume to reach dynamic kill. This will also allow for a more detailed pump schedule. It is believed that the obtained kill rate from the simulator can be used and a transient model is not required to be run for every kill rate, e.g. if the calculated kill rate is 4500 LPM a transient model should be used on the 4500 LPM and not 250 LPM, 500 LPM, etc... Using the transient model only to obtain the required pumping time will be highly efficient and will reduce the total simulation time.

2. The simulator is only aimed towards vertical wells, but an adjustment to include both deviated and horizontal wells should be implemented. For a small inclination ($< 20^{\circ}$) both the Olgjenka and Orkiszewski correlation may be used, but for higher deviations only the Olgjenka correlation should be used. The reason why Orkiszewski should not be used for high deviated is related to the flow regimes the correlation is based upon.

3. Currently the simulator only accounts for oil as the reservoir fluid and the reservoir productivity for a gas well is not implemented. The possibility to account for a gas reservoir or a reservoir consisting of both gas and liquid should be added.

4. Often the drilled reservoir will penetrate several productive zones and as of now only one reservoir is used in the simulator. The possibility to add two or more productive zones should be present in a blowout and kill simulator.

5. The calibration process of the kill rate should include more professional conducted simulations to increase the accuracy of the simulator. The possibility to create a dimensionless calibration formula should be investigated.

6. A flow path through the inside of the drill string should be implemented to the simulator.
7. The calculation of the temperature profile should include the heat gain caused by friction and the calculated thermal conductivity should be based on the entire wellbore and not just the lowest thermal conductivity. The temperature of the surrounding formation in contact with the wellbore should also be properly calculated and not assumed constant.
8. The Glasø PVT correlation set should be simulated in the same manner as the Standing PVT correlation set and a comparison of the results should give the optimum PVT correlation to be used. The presented comparison for well 1a with a surface blowout gave small variations with the different PVT-sets.
9. The simulator provides the opportunity to calculate the productivity index (J) based on reservoir parameters and reservoir fluid parameters. The productivity calculator has not been compared to the professional simulations and the accuracy of the calculations are unknown.
10. Several multiphase pressure correlations can be included in the simulator, some examples are the correlation by (Duns and Ros, 1963), (Hagedorn and Brown, 1965) and (Beggs and Brill, 1973). It will be easy to implement these codes in the created simulator, only one additional script is required for each of the correlations. These pressure correlations should also be checked against the professional kill simulations.

Bibliography

Abdul-Majeed, G.H., Abu Al-Soof, N.B., 2000. Estimation of gas–oil surface tension. Journal of Petroleum Science and Engineering 27, 197–200. doi:10.1016/S0920-4105(00)00058-9.

AddEnergy, 2018. Well control and blowout support .

Ansari, A.M., Sylvester, N.D., Sarica, C., S., O., Brill, J., 1994. A comprehensive mechanistic model for upward two-phase flow in wellbores. Society of Petroleum Engineers doi:10.2118/20630-PA.

Asheim, H., 1986. Mona, an accurate two-phase well flow model based on phase slippage. Society of Petroleum Engineers doi:10.2118/12989-PA.

Asheim, H., 2018a. Chapter 9 - Multiphase flow .

Asheim, H., 2018b. Tpg4245 - production wells - inflow limitations .

Asheim, H., 2020. Lille-Olga: Transient tofasestrømning i røyr.

Aziz, K., Govier, G.W., 1972. Pressure drop in wells producing oil and gas. Petroleum Society of Canada doi:10.2118/72-03-04.

Baxendell, P.B., Thomas, R., 1961. The calculation of pressure gradients in high-rate flowing wells. Society of Petroleum Engineers doi:10.2118/2-PA.

Beggs, D.H., Brill, J.P., 1973. A study of two-phase flow in inclined pipes. Society of Petroleum Engineers doi:10.2118/4007-PA.

Biria, S., 2013. Prediction of Pressure Drop in Vertical Air/Water Flow in the Presence/Absence of Sodium Dodecyl Sulfate as a Surfactant. URL: https://etd.ohiolink.edu/pg_10?0::NO:10:P10_ACCESSION_NUM:dayton1375217183. [Online; accessed 28. Apr. 2020].

Brechan, B.A., Corina, A.N., Gjersvik, T.B., Sangesland, S., Skalle, P., 2017. Tpg4215 drilling engineering drilling, completion, intervention and pa –design and operations.

Cinco-Ley, H., Ramey, Jr., H.J., Miller, F.G., 1975. Pseudo-skin Factors for Partially-Penetrating Directionally-Drilled Wells. Society of Petroleum Engineers doi:10.2118/5589-MS.

Colebrook, C.F., 1939. Turbulent flow in pipes, with particular reference to the transition region between the smooth and rough pipe laws. Journal of the Institution of Civil Engineers 11, 133–156. URL: https://doi.org/10.1680/ijoti.1939.13150, doi:10.1680/ijoti.1939.13150.

Danenberger, E.P., 1993. Outer Continental Shelf Drilling Blowouts, 1971-1991. Offshore Technology Conference doi:10.4043/7248-MS.

DrillingFormulas, 2014. Learn about Maximum Surface Pressure in Well Control (MASP, MISICP and MAASP). URL: http://www.drillingformulas.com/learn-about-maximum-surface-pressure-in-well-control-masp-misicp-and-maasp. [Online; accessed 23. Oct 2019].

Duns, H., Ros, N.C.J., 1963. Vertical flow of gas and liquid mixtures in wells. World Petroleum Congress .

EgnineeringToolbox, 2020. Mixing Fluids. URL: https://www.engineeringtoolbox.com/mixing-fluids-temperature-mass-d_1785.html. [Online; accessed 25. Apr. 2020].

EngineeringToolbox, 2020a. Specific Heat of some Liquids and Fluids. URL: https://www.engineeringtoolbox.com/specific-heat-fluids-d_151.html. [Online; accessed 24. Apr. 2020].

EngineeringToolbox, 2020b. Thermal Conductivities of Heat Exchanger Materials. URL: https://www.engineeringtoolbox.com/heat-exchanger-material-thermal-conductivities-d_1488.html. [Online; accessed 23. Apr. 2020].

Equinor, 2019. Equinor fact sheet - what are capping stacks. URL: https://www.equinor.com/content/dam/statoil/documents/australia/gab-project/equinor-fact-sheet-what-are-capping-stacks.pdf. [Online; accessed 2. Nov. 2019].

Evensen, K., 2013. Surface Seismic While Drilling - A new method for relief well drilling. Master's thesis. NTNU. URL: https://ntnuopen.ntnu.no/ntnu-xmlui/handle/11250/2400765.

Fancher, G.H., Brown, K.E., 1963. Prediction of pressure gradients for multiphase flow in tubin. Society of Petroleum Engineers doi:10.2118/440-PA.

Feteke, 2014. Skin. URL: http://www.fekete.com/san/webhelp/welltest/webhelp/Content/HTML_Files/Reference_Materials/Skin.htm#Skin_due_to_inclination. [Online; accessed 8. Dec. 2019].

Flores, V., Dailey, P., Todd, D., Mathur, R., Donadieu, B., 2014. Relief Well Planning. Society of Petroleum Engineers doi:10.2118/168029-MS.

Fossmark, M.G., 2011. Multiphase-flow correlation ability to model vertical lift performance. Master Thesis UIS .

olje og gass, N., .

Glaso, O., 1980. Generalized Pressure-Volume-Temperature Correlations. Journal of Petroleum Technology 32, 785–795. doi:10.2118/8016-PA.

Gomes, D., Nilsen, M.S., Frøyen, J., Bjørkevoll, K.S., Lage, A.C.V.M., Fjelde, K.K., Sui, D., 2018. A Transient Flow Model for Investigating Parameters Affecting Kick Behavior in OBM for HPHT Wells and Backpressure MPD Systems Volume 8: Polar and Arctic Sciences and Technology; Petroleum Technology. URL: https://doi.org/10.1115/OMAE2018-77547, doi:10.1115/OMAE2018-77547.

Grace, R.D., 2017. Chapter three - pressure control procedures while tripping, in: Grace, R.D. (Ed.), Blowout and Well Control Handbook (Second Edition). second edition ed.. Gulf Professional Publishing, Boston, pp. 99 – 120. URL: http://www.sciencedirect.com/science/article/pii/B9780128126745000031, doi:https://doi.org/10.1016/B978-0-12-812674-5.00003-1.

Gray, H., 1974. Vertical flow correlation in gas wells. In User manual for API 14B, Subsurface controlled safety valve sizing computer program .

Griffith, P., 1962. Two-phase flow in pipes. Society of Petroleum Engineers .

Griffith, P., Wallis, G.B., 1961a. Two-Phase Slug Flow. Journal of Heat Transfer 83, 307–318. doi:10.1115/1.3682268.

Griffith, P., Wallis, G.B., 1961b. Two-Phase Slug Flow. J. Heat Transfer 83, 307–318. doi:10.1115/1.3682268.

Guan, S.W., Shaw, B., 2011. Insulation for flowlines and risers. URL: http://www.ccop.or.th/download/PETRAD/PETRAD58_2011-01/Paper21_ShiweiWilliamGuan_BrederoShaw.pdf. [Online; accessed 24. Apr. 2020].

Hagedorn, A.R., Brown, K.E., 1965. Experimental study of pressure gradients occurring during continuous two-phase flow in small-diameter vertical conduits. Society of Petroleum Engineers doi:10.2118/940-PA.

Hall, K., Yarborough, L., 1973. A New EOS for Z-factor Calculations,Oil and Gas. Oil Gas .

Helmenstine, A.M., 2020. Specific Heat Capacity in Chemistry. ThoughtCo URL: https://www.thoughtco.com/definition-of-specific-heat-capacity-605672.

Krieg, D., 2018. What is a Blowout? Oilfield Basics URL: https://oilfieldbasics.com/2018/10/11/what-is-a-blowout.

Larsen, R., 2018. Insulation for flowlines and risers.

LatamEnergy, 2019. Internacional,Halliburton, Oil Spill Response Ltd (OSRL) y Trendsetter Engineering han firmado un Memorando de Entendimiento. URL: http://www.latam-energy.com/2017/05/31/internacionalhalliburton-oil-spill-response-ltd-osrl-y-trendsetter-engineering-han-firmado-un-memorando-de-entendimiento. [Online; accessed 2. Nov. 2019].

Madrid, M., Matson, A., 2014. How Offshore Capping Stacks Work. Way Ahead 10, 25–27. doi:10.2118/0114-025-TWA.

Mathisen, V.A., 2019. Well Control - Blowout and Kill Simulator.

Mian, M.A., 1992. Petroleum Engineering Handbook for the Practicing Engineer. Number v. 2 in Petroleum Engineering Handbook for the Practicing Engineer, PennWell Books. URL: https://books.google.no/books?id=SX6PTJq5I04C.

Moody, L., 1944. Friction factors for pipe flow. Transactions of American Society Mechanical Engineers .

Mostofi, M., 2019. Well control lecture .

Mukherjee, H., Brill, J.P., 1985. Pressure Drop Correlations for Inclined Two-Phase Flow. Journal of Energy Resources Technology 107, 549–554. doi:10.1115/1.3231233.

Mukherjee, H., Brill, J.P., 1999. Multiphase Flow in Wells. Society of Petroleum Engineers .

Muskat, M., 1937. The Flow of Heterogeneous Fluids Through Porous Media. Physics .

OffshoreMagazine, 2006. Overcoming difficult thermal challenges in deeper waters. URL: https://www.offshore-mag.com/subsea/article/16754582/overcoming-difficult-thermal-challenges-in-deeper-waters. [Online; accessed 24. Apr. 2020].

Oliasoft, 2018. Oliasoft Launches Blowout & Kill Simulations. URL: https://www.oliasoft.com/2018/04/08/oliasoft-launches-blowout-kill-simulations. [Online; accessed 24. May 2020].

Orkiszewski, J., 1967. Predicting two-phase pressure drops in vertical pipe. Society of Petroleum Engineers doi:10.2118/1546-PA.

Pabst, W., 2004. Fundamental considerations on suspension rheology. Ceram. Silik. 48, 6–13. URL: https://www.researchgate.net/publication/285023667_Fundamental_considerations_on_suspension_rheology.

Petrowiki, 2019. Formation damage - PetroWiki. URL: https://petrowiki.org/Formation_damage. [Online; accessed 8. Dec. 2019].

Poettman, F.H., Carpenter, P.G., 1952. The multiphase flow of gas, oil, and water through vertical flow strings with application to the design of gas-lift installations. American Petroleum Institute .

ProductionTechnology, 2017. Multiphase flow correlations - Production Technology. URL: https://production-technology.org/multiphase-flow-correlations. [Online; accessed 28. Apr. 2020].

Ranold, 2018. Technical report - blowout and dynamic wellkill simulations - well xxx.

Sadenwater, D., 2014. API RP17W Subsea Capping Stacks. Offshore Technology Conference doi:10.4043/25415-MS.

Senapati, P.K., Panda, D., Parida, A., 2009. Predicting Viscosity of Limestone-Water Slurry. Journal of Minerals and Materials Characterization and Engineering 08. doi:10.4236/jmmce.2009.83018.

Sintef, 2020. SINTEF Offshore Blowout Database - SINTEF. URL: https://www.sintef.no/en/projects/sintef-offshore-blowout-database. [Online; accessed 15. Apr. 2020].

Solgren, J.W., 2014. Multiphase Blowout Simulation Model. Master's thesis. NTNU.

Souza, W.J., Santos, K.M.C., Cruz, A.A., Franceschi, E., Santana, C.C., 2015. Effect of water content, temperature and average droplet size on the settling velocity of water-in-oil emulsions. Braz. J. Chem. Eng. 32, 455–464. doi:10.1590/0104-6632.20150322s00003323.

Standing, M., 1980. Volumetric and Phase Behavior of Oil Field Hydrocarbon Systems. Society of Petroleum Engineers of AIME.

Standing, M.B., 1947. A Pressure-Volume-Temperature Correlation For Mixtures Of California Oils And Gases. American Petroleum Institute URL: https://www.onepetro.org/conference-paper/API-47-275.

Standing, M.B., Katz, D.L., 1942. Density of Natural Gases. Transactions of the AIME 146, 140–149. doi:10.2118/942140-G.

Sutton, R.P., 2005. Fundamental PVT Calculations for Associated and Gas-Condensate Natural Gas Systems. Society of Petroleum Engineers doi:10.2118/97099-MS.

Tang, B., Zhu, C., Xu, M., Chen, T., Hu, S., 2018. Thermal conductivity of sedimentary rocks in the Sichuan basin, Southwest China. Energy Explor. Exploit. 37. doi:10.1177/0144598718804902.

Vasquez, M., Beggs, H.D., 1980. Correlations for Fluid Physical Property Prediction. Journal of Petroleum Technology 32, 968–970. doi:10.2118/6719-PA.

Vogel, J.V., 1968. Inflow Performance Relationships for Solution-Gas Drive Wells. Journal of Petroleum Technology 20, 83–92. doi:10.2118/1476-PA.

Warriner, R.A., Cassity, T.G., 1988. Relief-Well Requirements To Kill a High-Rate Gas Blowout From a Deepwater Reservoir (includes associated paper 19889). Journal of Petroleum Technology 40, 1602–1608. doi:10.2118/16131-PA.

Whitson, C.H., Burlé, M.R., 2000. Phase behavior. SPE Monograph Series 20, 22,24.

WildWellControl, 2019. Relief Well Engineering. URL: https://wildwell.com/engineering/relief-well. [Online; accessed 2. Nov. 2019].

Willson, S.M., Nagoo, A.S., Sharma, M.M., 2013. Analysis of Potential Bridging Scenarios During Blowout Events. Society of Petroleum Engineers doi:10.2118/163438-MS.

Appendix A

Theory

In this Appendix the theory included in the blowout and kill simulator is presented. How the theory is used in the simulator is presented in chapter 6. Some of the theory included was a part of a project thesis (Mathisen, 2019) written the fall of 2019, further details see chapter 1.

A.1 Productivity index

The productivity index accounts for both the rock and fluids parameters and quantifies the production rate relative to the pressure drop between the reservoir and the flowing bottom hole pressure. Several equations are published to account for different scenarios such as natural drive, water drive and gas cap drive as well as different reservoir fluids. The relationship between the productivity index, flow rate and pressure drop is shown in equation A.1. Equation A.2 shows the relationship based on rock and fluids properties for a natural drive. The skin factor (S) can account for different scenarios such as: drilling induced damage, an inclined well, partly penetration of the reservoir, well placement and permeability anisotropy. The skin factor can be beneficial (negative) or detrimental(positive) for the total productivity. When the reservoir fluid is gas equation A.3 must be used, which require a steady-state production. (Mian, 1992; Asheim, 2018b)

$$J = \frac{q}{p_e - p_{wf}} \tag{A.1}$$

$$J = \frac{k_o h}{\mu_o B_o [LN(r_e/r_w) - 3/4 + S]} \tag{A.2}$$

$$J = \frac{q_g}{p_e^2 - p_{wf}^2} = \frac{T_{sc} k_g h}{p_{sc} (\mu_g z)_{avg} T_f LN(r_e/r_w)} \tag{A.3}$$

Skin factor determination - Partly penetration

The skin factor can adjust the productivity index to account for several effects as discussed above. In section 4.3 it was discussed that exploration wells have a higher chance of encountering a blowout situation compared to production wells. It can be assumed that in many cases of exploration well drilling, the well does not fully penetrate the entire height of the reservoir. If the productivity index for a fully penetrated reservoir is used a too high blowout rate will be calculated, instead the skin factor for a partly penetrated reservoir should be used to account for the reduction in productivity. It is also incorrect to reduce and match the reservoir height with the penetration height in the calculations due to non-radial flow in the lower parts of the well. A partly penetrating well and the reservoir fluid flow direction is shown in figure A.1.

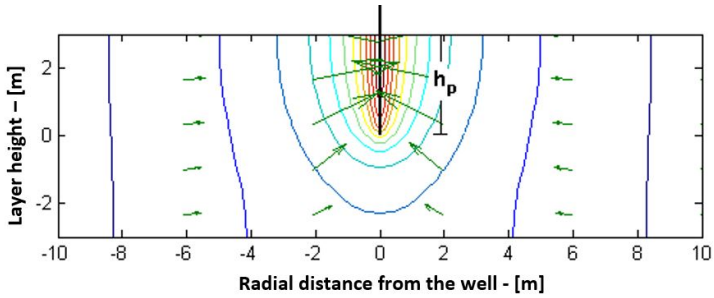

Figure A.1: The flow direction in a partly penetrating well, courtesy of (Asheim, 2018b)

To account for the partly penetrating well (Muskat, 1937) presented an equation for the flow rate based on the gamma function as shown in equation A.4. By approaching the gamma function and single out the effect of the partly penetrating well (Asheim, 2018b) showed that the skin factor due to partly penetration can be expressed as equation A.5. (Muskat, 1937)

$$Q = \frac{2\pi kh\Delta p}{\frac{\mu}{2\bar{h}}\left(2log(\frac{4h}{r_w}) - log\left(\frac{\Gamma(0.875\bar{h})\Gamma(0.125\bar{h})}{\Gamma(1-0.875\bar{h})\Gamma(1-0.125\bar{h})}\right)\right) - log\frac{4h'}{r_e}} \tag{A.4}$$

$$S \approx \left(\frac{1-\bar{h}}{\bar{h}}\right)LN(\frac{4h}{r_w}) - \frac{1}{2\bar{h}}LN\left(\frac{(1-0.875\bar{h})(1-0.125\bar{h})}{(0.875\bar{h})(0.125\bar{h})}\right) \tag{A.5}$$

To easier show the effect of partly penetration (Muskat, 1937) presented figure A.2, which shows the production rate, reservoir height and partly penetration for two different well sizes. For a 6inch well with a reservoir height of 170 feet the production rate for a fully penetrating well is 2400 STB/Day, while for a 25%-penetration the production rate is only 900 STB/day. This represents a reduction in 62.5%, which makes it evident that partly penetration is important to account for.

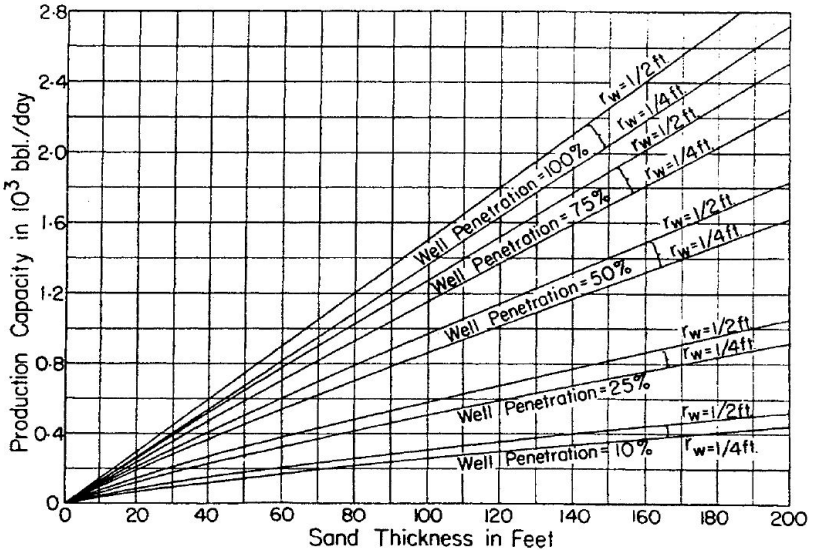

Figure A.2: The effect of partly penetration on production rate, courtesy of (Muskat, 1937)

Skin factor determination - Inclined well/reservoir

The relative angle between the bedding plane and the well is often not perfectly orthogonal as most of the equations for the productivity index assume. The well will penetrate a longer interval compared to a vertical well. The well can be drilled vertically, but the bedding plane of the reservoir can deviate from horizontal due to faulting and other geomechanically impacts. Even if the bedding plane is in the horizontal direction the well can be drilled inclined or horizontally. The difference in the angle will result in a longer penetration length of the reservoir and a deviation from a radial flow direction towards the wellbore. By introducing a geometric skin factor these beneficial effects can be accounted for, i.e. resulting in a negative skin factor which will increase the calculated productivity. Cinco-Ley et al. (1975) presented equation A.6 based on empirical values that accounts for the inclination of the well. This equation introduces a geometric skin factor and the equation is valid for an inclination less than 75 degrees. (Asheim, 2018b; Feteke, 2014)

$$S_i = -\left(\frac{\theta}{41}\right)^{2.06} - \left(\frac{\theta}{56}\right)^{1.865} log\left(\frac{h}{100 r_w}\right) \tag{A.6}$$

Skin factor determination - invasion

When the reservoir section is drilled the particles in the drilling mud will cause invasion into the reservoir. This invasion helps to build up the important mud cake, but even when the mud cake is removed prior to production some particles will be left in the pores causing a pore-blockage and a reduction in the permeability, illustrated in figure A.3. This will reduce the productivity of the well and the related skin factor will be positive, typically in the range of 0-50. Some beneficial treatments may be conducted such as fracturing and

acid treatments which will increase the permeability and thus the productivity of the well. (Feteke, 2014)

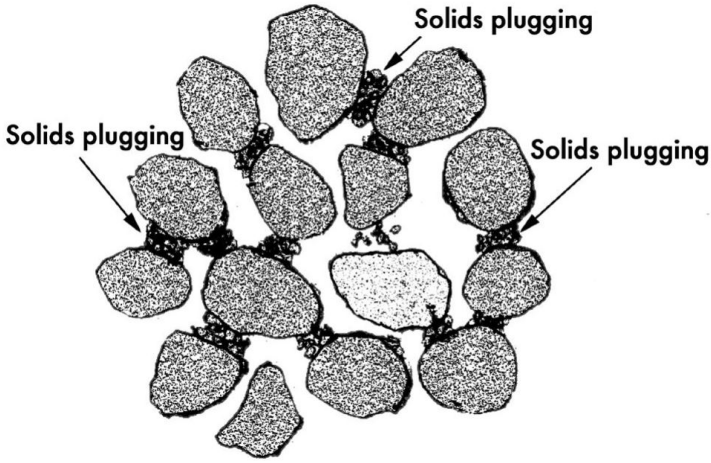

Figure A.3: Pore-blockage due to invasion of mud particles, courtesy of (Petrowiki, 2019)

A.2 Inflow performance relationship

The inflow performance relationship is used to determine the production rate for an interval of the flowing bottom hole pressure, it is a function of the pressure drop and the productivity index. A typical IPR-curve is shown in figure A.4. With a flowing bottom hole pressure higher than the saturation pressure of the reservoir fluid the shape of the IPR-curve is linear, but when the pressure is below the saturation pressure a quadratic form is observed. The maximum flow rate q_{max} is a theoretical value which will never be obtained since the flowing bottom hole pressure always is greater than zero. The actual flowing bottom hole pressure depends on several factors such as the fluid density and the total flowing friction when producing.

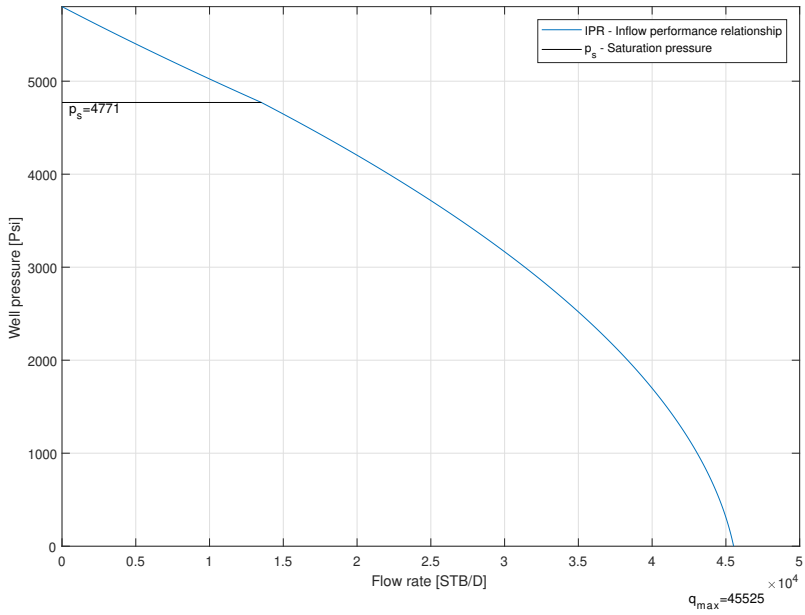

Figure A.4: Inflow performance relationship curve

When the flowing bottom hole pressure is above the saturation pressure the flow will follow the Darcy law and can be expressed as equation A.7. When the well pressure falls below the saturation pressure some alterations must be done. (Vogel, 1968) published a study presenting the behavior of the IPR curve when the pressure falls below the saturation pressure. Vogel showed that an extrapolation of the linear IPR-trend will result in too high flow rates, approximately 1.8 times too high, e.g. equation A.8. Vogel presented equation A.9 which represents the behavior of the inflow performance relationship for pressures lower than the saturation pressure. The method presented by Vogel use the saturation pressure as the datum and the q_o from equation A.9 will not show the total flow rate if the reservoir pressure is greater than the saturation pressure.

$$q_o = J(p_r - p_{wf}) \tag{A.7}$$

$$q_{max} = \frac{q_{max,linear}}{1.8} \tag{A.8}$$

It is possible to combine the IPR curve above and below the saturation pressure by taking the production at saturation conditions into account by using equation A.10. (Vogel, 1968; Asheim, 2018b)

$$\frac{q_{o,v}}{q_{max}} = 1 - 0.2\left(\frac{p_{wf}}{p_s}\right) - 0.8\left(\frac{p_{wf}}{p_s}\right)^2 \tag{A.9}$$

$$q_{o,tot} = q_s + q_{o,v} = J(p_r - p_s) + q_{o,v} \tag{A.10}$$

A.3 Wellbore trajectory

The wellbore trajectory is a vital part of most well designs. The reservoir target might be a trusted fault resulting in a small target area. If the wellbore does not penetrate the target area the wellbore will not produce hydrocarbons or with partly penetration the well will produce poorly. During the development of huge fields, several hundred wells might be drilled within a small area making it of high importance to keep track of where the well to be drilled are located compared to the other wells in the area, to avoid an unintentional intersection. (Brechan et al., 2017)

There are several ways to calculate the wellbore trajectory, some more accurate and complicated than others. Some of these survey calculation methods are: (Brechan et al., 2017)

- Tangential
- Average angle
- Radius of curvature
- Balanced tangential
- Minimum curvature

To calculate the wellbore trajectory in the simulator a simplification is made that the well follows a constant azimuth. This allows one to calculate the well path with the use of the radius of curvature survey method.

Radius of curvature
The radius of curvature assumes that one can calculate the curve of a cylinder to approximate the curve between two survey points in the wellbore. If one look in the vertical plane of the cylinder one can view the system as a part of a circle with length L and angle θ. The angle θ will have the same fraction of a total circle (360°) as the length for this given angle will have over the total circumference, see figure A.5 as an illustration. By setting these facts equal each other equation A.11 is obtained. By rearranging the equation and saying that the angle/length equals a constant angle increase over a length increment equation A.12 is obtained.

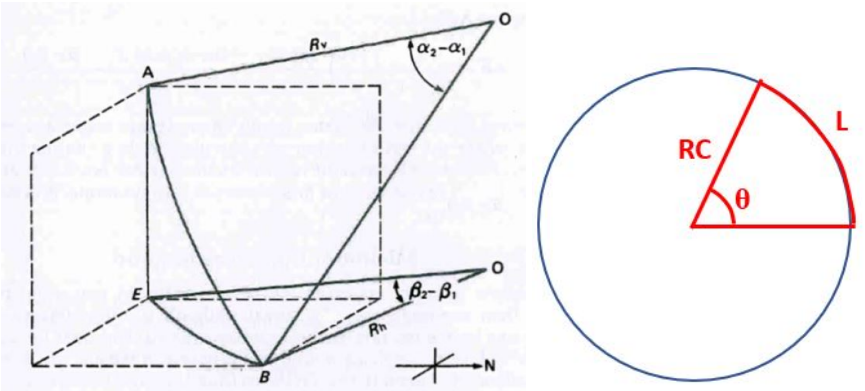

Figure A.5: Left: illustration of the radius of curvature principle, courtesy of (Brechan et al., 2017). Right: part of a circle

$$\frac{\theta}{360} = \frac{L}{2\pi RC} = \frac{Length}{Circumference} \tag{A.11}$$

$$RC = \frac{180 * 30}{\pi B} \tag{A.12}$$

RC = radius of curvature [m]
B = Build up rate [deg/30m]

Example
The theory is best described by an example. Looking on the relief well trajectory from well 1a, presented in figure A.6. The wellbore trajectory is based on the parameters presented in table A.1, where the interception point represents the total vertical depth of the wellbore trajectory. The wellbore can be described by four different sections: The vertical section, the build section, the hold section and the drop section.

Table A.1: Parameters used to calculate the wellbore trajectory

Relief well trajectory		
Parameter	**Unit**	**Value**
Kick of point	[m RKB]	500
Interception point	[m RKB]	3330
Distance North	[m]	900
Distance East	[m]	435
Build up rate	degree/30m	2
Max build up rate	degree	20
Drop rate	degree/30m	2
Max drop rate	degree	20

By using the fact that the starting location and end location is known, one can calculate the wellbore trajectory. The radius of curvature is calculated by equation A.12 and equals 859.4 m for both the build and drop section.

Build section
The horizontal departure and vertical departure can be calculated by simple trigonometric relationships for a triangle and circle. The right triangle for the build section, partly covered by the azimuth plot, has an angle equal to the build angle (20°), which allows the usage of simple triangle trigonometric. The vertical departure is described by equation A.13, the horizontal departure by equation A.14 and the total length (MD) by equation A.15.

$$\Delta z_b = sin(\theta_b) * RC_b = sin(20) * 859.4 = 294m \tag{A.13}$$

$$\Delta H_b = RC - RC_b * cos(\theta_b) = 859.4 * (1 - cos(20)) = 51.8m \tag{A.14}$$

$$\Delta MD_b = \frac{\theta_b}{360} * 2\pi RC_b = \frac{20}{360} * 2 * \pi * 859.4 = 300m; \tag{A.15}$$

Drop section
In this case the drop section uses the same parameter values as the build section and the calculated values will be the same, presented by equation A.16 to A.18

$$\Delta z_d = sin(\theta_d) * RC_d = sin(20) * 859.4 = 294m \tag{A.16}$$

$$\Delta H_d = RC_d - RC * cos(\theta_d) = 859.4 * (1 - cos(20)) = 51.8m \tag{A.17}$$

$$\Delta MD_d = \frac{\theta_d}{360} * 2\pi RC_d = \frac{20}{360} * 2 * \pi * 859.4 = 300m; \tag{A.18}$$

Hold section The total horizontal departure can be calculated by using the distance north and distance east, represented by equation A.19. The horizontal departure for the hold section is the remaining departure when the horizontal departure in the build and drop section is subtracted. The same goes for the vertical departure in the hold section. The horizontal, vertical and total departure for the hold section is represented by equation A.20 to A.22

$$H = \sqrt{N^2 + E^2} = \sqrt{900^2 + 435^2} = 999.6m \tag{A.19}$$

$$\Delta H_h = H - H_b - H_d = 999.6 - 51.8 - 51.8 = 896m \tag{A.20}$$

$$\Delta z_h = TVD - KOP - z_b - z_d = 3330 - 500 - 294 - 294 = 2242m \quad \text{(A.21)}$$

$$\Delta MD_h = \sqrt{\Delta H_h^2 + \Delta z_h^2} = \sqrt{896^2 + 2242^2} = 2414m \quad \text{(A.22)}$$

The total length of the wellbore trajectory equals the total length of each section. For the example well the total length equals 3514m MD.

$$MD = MD_v + MD_b + MD_h + MD_d = 500 + 300 + 2414 + 300 = 3514mMD \quad \text{(A.23)}$$

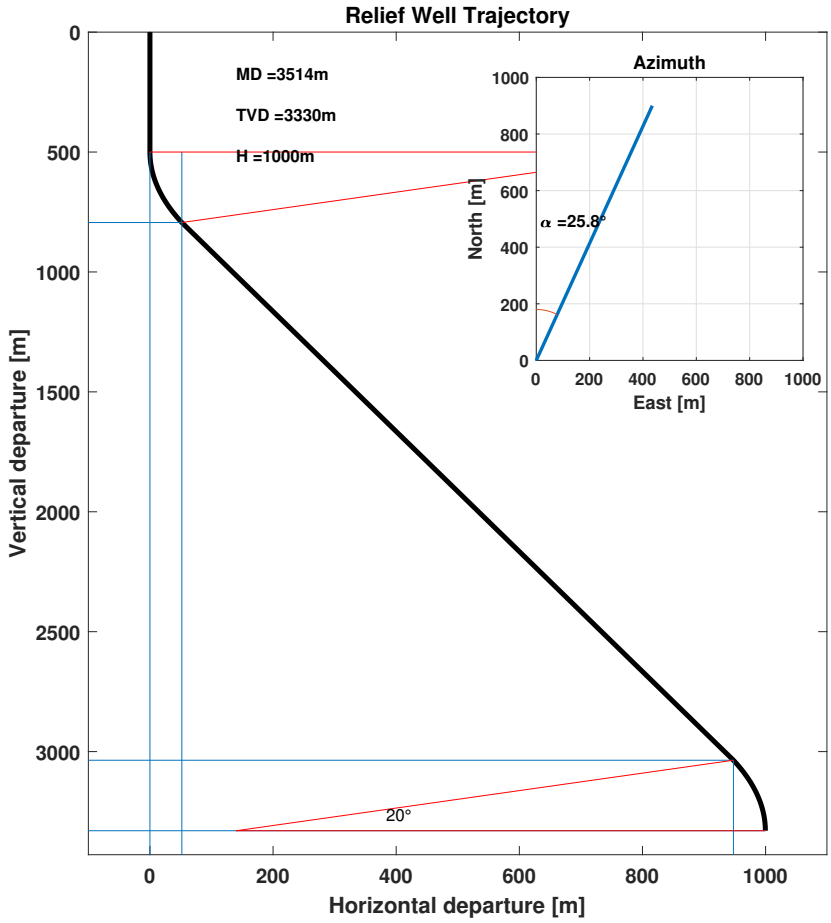

Figure A.6: Wellbore trajectory for the relief well used in the simulation of well 1a

A.4 Temperature profile calculation

The temperature is an important factor in the calculation of the bottom hole pressure, which makes it important to a blowout and kill simulator. The temperature impacts the density and the viscosity of the fluid, which gives a direct impact on both the hydrostatic pressure and the friction pressure. This makes the knowledge of the temperature profile along the wellbore critical for a blowout and kill simulator.

During a blowout, the reservoir fluid initial has a temperature equal to the reservoir temperature, but as the fluid flow through the wellbore some heat will be lost. The rate of heat loss is affected by the temperature difference of the flowing fluid and the temperature of the surrounding formation, and the thermal conductivity of the system. The heat capacity of the flowing fluid determines the temperature for a given heat loss.

The temperature profile of the formation surrounding the wellbore can be estimated by the geothermal gradient, calculated from the seabed to the reservoir. Different parts of the wellbore will release different amounts of heat as the fluid flow through.

Temperature equation

The heat flow is affected by the surface area in contact with a conductor and the temperature difference between the fluid and the conductor element, for a pipe the relationship is shown in equation A.24. How the heat flow will affect the temperature of the flowing fluid is expressed by equation A.25, which considers the heat capacity of the fluid and the mass rate. Equation A.25 does not consider the heat gain due to friction or the of effect fluid expansion. (Asheim, 2018b)

$$dQ = -U(T - T_s)\pi D dx \tag{A.24}$$

dQ - Heat flow [W]
U - Thermal conductivity [W/(m*K)]
T - T_s - Temperature difference between the fluid inside the pipe and the temperature outside [K]
D - Diameter of pipe [m]
dx - Length increment [m]

$$dQ = c_p \dot{m} dT \tag{A.25}$$

c_p - Heat capacity of the fluid [J/(kg*K)]
$\dot{m}$ - Mass rate - [kg/s]
dT - Temperature difference for the fluid inside the pipe[K]

By setting the two equations above equals each other, equation A.26 is obtained, describing the temperature change over a length increment of flow inside a pipe. To be able to use

the equation in a numerical scheme it must be discretised, as shown in equation A.27 for a wellbore system. The equation is solved to give the temperature for the next increment, which can be used directly in a numerical scheme, the solved equation is presented in equation A.28. The parameter (i+1) represents the next increment, while (i) represent the current increment.

$$\frac{dT}{dx} = -\frac{U\pi D}{c_p \dot{m}}(T - T_s) \tag{A.26}$$

$$\frac{T(i+1)_w - T(i)_w}{x(i+1) - x(i)} = -\frac{U\pi D}{c_p \dot{m}}[T(i)_w - T_s(i)] \tag{A.27}$$

$$T(i+1)_w = T(i)_w - \frac{U\pi D}{c_p \dot{m}}[T(i)_w - T_s(i)] * [x(i+1) - x(i)] \tag{A.28}$$

T_w - wellbore fluid temperature [K]
T_s - Temperature in the surrounding formation [K]
x - depth [m TVD RKB]

Parameters used in the temperature equation
This section describes the different parameters used in the temperature equation and how these parameters are adjusted to the blowout and kill simulator. All the different parts of a well should be included in the temperature calculations, however several simplifications are made to the system in the simulator. An illustration of the actual well system and the simplified system used in the temperature calculations are shown in figure A.7. The simplified system neglects the effect of pipe-in-pipe, i.e. the casings surrounding the production casing. In an actual well the annulus behind the production casing will consist partly of cement and the rest will be drilling mud, in the simplified system it is assumed that cement covers the entire length. An assumption that the temperature outside the concrete in the simplified system equals the temperature of the formation is also made.

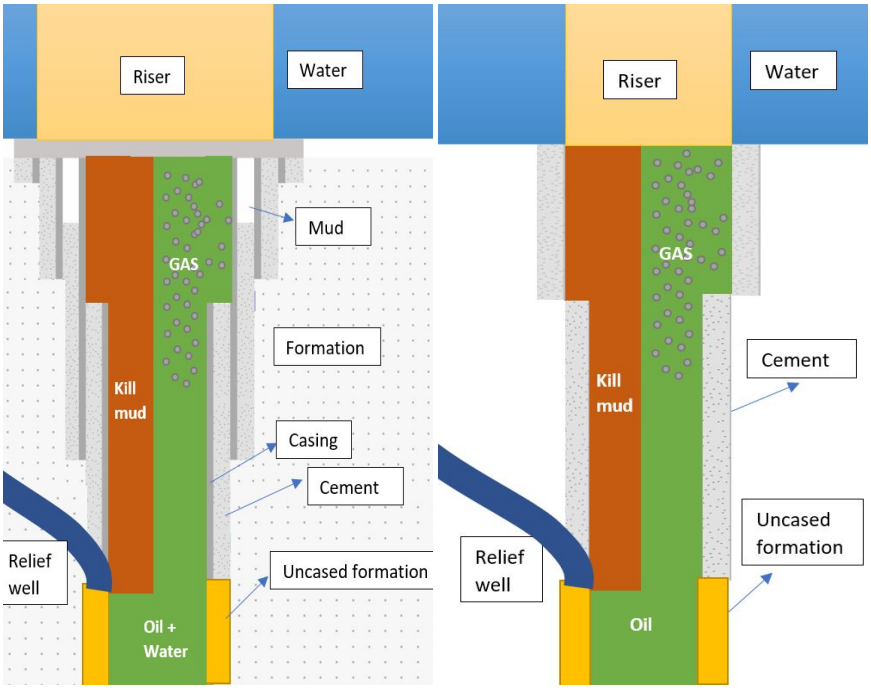

Figure A.7: On the left is an actual well system, on the right side is a simplified system used in the temperature calculation

Thermal conductivity - U

The thermal conductivity of a material is a quantification of how much heat the material can conduct. Insulated materials have a low thermal conductivity, approaching zero, while different materials used in heat exchangers will have a higher thermal conductivity, allowing it to exchange heat more quickly. Table A.2 shows the thermal conductivity of some common materials.(EngineeringToolbox, 2020b)

In the system used for temperature calculation the different parts of the well can be viewed in figure A.7. The true thermal conductivity should be calculated based on the principle of thermal conductivity in a parallel system. In the simplified system the thermal conductivity is set equal the thermal conductivity for the material with the lowest thermal conductivity in the given section. The open hole section may consist of several types of lithologies for the different wells run in the simulator, a list of some common lithology types and the thermal conductivity are presented in table A.3.

Assuming that the reservoir consist of sandstone and a production casing is set in the caprock slightly above the reservoir, one can assume that thermal conductivity value of sandstone, 3.06 (W/m*K), may be used to cover the entire open hole section. For the cased hole section, the cement behind the casing will have the lowest thermal conductivity. Using

Table A.2: Thermal conductivity of some common materials, courtesy of (EngineeringToolbox, 2020b; Guan and Shaw, 2011; Larsen, 2018)

Material	**Thermal conductivity W/(m*K)**
Copper	386
Aluminium	205 - 250
Red Brass (85 Cu - 15 Zn)	159
Carbon Steel	45
Stainless Steel, type 304 (18 Cr - 8 Ni)	16
Polypropylene	0.1 - 0.22
Quartz mineral	3
Portland Cement	0.29
Cement API - Class G	0.95
Rock, solid	2 to 7
Rock, porous volcanic (Tuff)	0.5 - 2.5
Thermotite Riser insulation	0.21 - 0.24
Rock Wool insulation	0.045
Insulated steel pipe	0.024 - 0.033

an API grade G cement will provide a thermal conductivity of 0.95 (w/m*K). If the riser is insulated with the "Thermotite"-insulation system one can assume a thermal conductivity of 0.24 (W/m*K). The thermal conductivity of the choke and kill lines on the relief well can be approximated by an insulated steel pipe. (Tang et al., 2018; Larsen, 2018; Guan and Shaw, 2011; OffshoreMagazine, 2006)

Table A.3: Thermal conductivity of different lithologies from the Sichuan basin, courtesy of (Tang et al., 2018)

Lithology	**Number of samples**	**Range [W/(m K)]**	**Mean ± SD [W/(m K)]**
Dolomite	109	1.91–5.55	3.55 ± 0.71
Limestone	87	1.74–4.64	2.53 ± 0.44
Sandstone	108	1.74–5.24	3.06 ±0.73
Mudstone	85	1.69–3.89	2.57 ±0.42
Shale	15	1.80–3.14	2.48 ± 0.33
Anhydrite	7	2.39–4.40	3.60 ± 0.64

Heat capacity - c_p

One definition on the specific heat capacity is: "Specific heat capacity is the amount of heat energy required to raise the temperature of a substance per unit of mass. The specific heat capacity of a material is a physical property." (Helmenstine, 2020). The units used in this master thesis is [J/kg/K] for the different specific heat capacities. The heat capacity is affected by temperature, pressure and the type of substance. For a light oil with 149 $^{\circ}C$,

(EngineeringToolbox, 2020a) report a heat capacity of 2300 [J/kg/K] and for a temperature of 15 $^{\circ}C$ it is 1800 [J/kg/K]. In the simulator a heat capacity of the oil is assumed to be 2300 [J/kg/K] and constant, but the "Simulator - input file" gives the opportunity to change it. The kill fluid is assumed to have the same heat capacity as water, 4200 [J/kg/K]. Above the intersection point, the hydrocarbons and the kill fluid will mix. The mixture specific heat capacity is calculated with equation A.29, and it is used as a parameter in the temperature equation.

$$c_{p,mix} = c_{p,HC} * \frac{\dot{m}_{HC}}{\dot{m}_{mix}} + c_{p,kill} \frac{\dot{m}_{kill}}{\dot{m}_{mix}} \tag{A.29}$$

Mass rate - $\dot{m}$
The mass rate is a measure of how much mass is flowing per time unit, a unit of [kg/s] is used for the temperature calculations. The mass rate can easily be calculated with the flow rate and the density of each phase. Since the mass rate entering the wellbore must be the same as the mass rate leaving the wellbore, given no leaks along the well path, one can use the surface densities and surface flow rates. Equation A.30 calculates the mass rates for the hydrocarbons. The mass flow rate of the kill fluid is calculated by equation A.31, and the mixture flow rate is presented in equation A.32.

$$\dot{m}_{HC} = \dot{m}_{Oil} + \dot{m}_{gas} = q_{o,s}\rho_o + q_{g,s}\rho_g \tag{A.30}$$

$$\dot{m}_{kill} = \rho_{kill} q_{kill} \tag{A.31}$$

$$\dot{m}_{mix} = \dot{m}_{kill} + \dot{m}_{HC} \tag{A.32}$$

$\dot{m}_i$ - Mass rate of the hydrocarbons $[m/s]$
$q_{i,s}$ - Surface flow rate of oil $[Sm^3/s]$
ρ_i - Surface density of oil $[kg/m^3]$
The subscripts represent the following: o = oil, g = gas, HC = Hydrocarbons, kill = kill fluid and mix = the mixture of HC and kill fluid.

Diameter available for fluid flow - D
The diameter affects both the fluid velocity and the surface area of the fluid in contact with the conducting element, i.e. for a constant thermal conductivity an increase of diameter will increase the heat loss. For a system where the drill pipe is in the wellbore, i.e. an annulus is present, it is assumed that the diameter in the temperature equation only contribute to the surface area in contact with the section wall.

The diameter is set equal to the internal diameter of the borehole for the given depth. The diameter of the riser section equals the internal diameter of the riser, if the well uses a liner the diameter used for this section will equal the internal diameter of the liner for the liner section only.

The temperature in the surrounding formation - T_s
The temperature in the surrounding formation or surrounding water is based on a simple linear relationship. In the "Simulator - input file" it is possible to specify the seabed temperature, the surface temperature of the water and the reservoir temperature. A geothermal gradient is calculated from the reservoir to the seabed using equation A.33. The same is conducted for a geothermal gradient in the water. The temperature in the surrounding formation is calculated with equation A.34. The calculated temperature will equal the temperature in the formation "far away" from the wellbore, which is an approximation. The true temperature close to the wellbore will be slightly affected by the temperature inside the wellbore.

$$G_f = \frac{T_r - T_{sb}}{TVD} \tag{A.33}$$

$$T_s = T_r - G_f * x \tag{A.34}$$

G_f - Geothermal gradient of the formation $[^\circ C/mTVD]$
$T_{r,sb}$ - Temperature of reservoir or seabed $[^\circ C]$
T_s - Temperature in the surroundings $[^\circ C]$
x - Total vertical depth above the reservoir [m TVD]

Comments to the temperature calculations
Since the section change is only a function of the depth, and the simulator uses a predefined step size some sections may be placed a few meters wrong, e.g. if a section is changed in 3000m and the previous increment depth is 2999, the section change is conducted at a depth of 3002m for a step size of 3. Using a low step size will make this negligible, but at the cost of a longer simulation time.

The injected kill fluid will have another temperature than the reservoir fluid at the interception point. The kill fluid temperature is calculated on the same principles as above, but some small alterations. The initial temperature is assumed to equal the inside temperature of the mud pits (assumed to be $20^\circ C$) and the flowing geometry will equal that of the relief well, i.e. a longer well with a S-trajectory. The kill fluid flow through the kill and choke lines down to the seabed. When the kill fluid and reservoir fluid mixes at the interception point the resulting mixture temperature is calculated based on equation A.35. An assumption is made that there is not kill fluid below the interception point and the temperature below the intersection point is unaffected by the temperature above. (EgnineeringToolbox, 2020)

$$T_{IP,mix} = \frac{\dot{m}_{HC} * c_{p,HC} * T_{HC,IP} + \dot{m}_{kill} * c_{p,kil} * T_{kill,IP}}{\dot{m}_{HC} * c_{p,HC} + \dot{m}_{kill} * c_{p,kill}} \tag{A.35}$$

Table A.4: Add caption

Parameter	Symbol	Unit	Value
Thermal conductivity of Sandstone	U	W/(m*K)	2.37
Thermal conductivity of cased interval	U	W/(m*K)	0.58
Thermal conductivity of choke line	U	W/(m*K)	0.033
Heat capacity of hydrocarbon mix	C_p	J/kg/K	2300
Heat capacity of kill fluid	C_p	J/kg/K	4200
Temperature of injected kill fluid	T	°C	20

A.5 Multiphase flow correlations

A.5.1 Multiphase flow introduction

For the greater part of the last half a century several correlations to predict the pressure loss in a multiphase fluid system have been developed. Most of these are empirical correlations that have been develop with different approaches and experimental data. This makes it of greatest importance to be aware of what these correlations are based upon, and thus what their limitations of use are. Some of these correlations are based solely upon vertical wells which should make it evident that it should not be used to calculate the pressure drop in a horizontal well, or highly inclined well for that matter. The same can be said for a correlation purely based on dry gas measurements should under no circumstances be used for a black oil well. Some of the most common multiphase flow correlations used today are shown in table A.5

The different correlations can either be categorized as empirical or mechanistic with the following definitions.

- "Empirical models: based on experimental data and dimensional analysis." (Fossmark, 2011)
- "Mechanistic models: based on simplified mechanistic (physical) considerations like conservation of mass and energy." (Fossmark, 2011)

Single-phase flow theory

The single-phase flow is easier to understand than multiphase flow. Most of the theory applicable to single-phase flow is also valid for multiphase flow, with some adjustments. It is important to have a good understanding of the single-phase flow theory before going into the more complex multiphase flow theory. The pressure loss gradient in a single-phase flow system consists of three different terms: a gravity term, a friction term and an acceleration term. This can easily be shown by using conservation of mass and Newton's first law. (Mukherjee and Brill, 1999)

$$\left(\frac{dp}{dL}\right)_t = \left(\frac{dp}{dL}\right)_g + \left(\frac{dp}{dL}\right)_f + \left(\frac{dp}{dL}\right)_a = -\rho g sin(\theta) - \frac{f\rho v^2}{2d} - \rho v \frac{dv}{dL} \tag{A.36}$$

Table A.5: Common multiphase flow correlation in the industry, presented by (Fossmark, 2011; Mukherjee and Brill, 1999)

Correlation	Category	Flow regime considered	Slip Considered	Flow Direction
(Poettman and Carpenter, 1952)	Empirical	No	No	Vertical
(Baxendell and Thomas, 1961)	Empirical	No	No	Vertical
(Fancher and Brown, 1963)	Empirical	No	No	Vertical
(Duns and Ros, 1963)	Empirical	Yes	Yes	Vertical
(Hagedorn and Brown, 1965)	Empirical	No	Yes	Vertical
(Orkiszewski, 1967)	Empirical	Yes	Yes	Vertical
(Aziz and Govier, 1972)	Empirical	Yes	Yes	All
(Beggs and Brill, 1973)	Empirical	Yes	Yes	All
(Gray, 1974)	Empirical	No	Yes	Vertical
(Mukherjee and Brill, 1985)	Empirical	Yes	Yes	All
(Asheim, 1986)	Empirical	No	Yes	All
Petroleums Experts (1,2,3)	Empirical	Yes	Yes	All
(Ansari et al., 1994)	Mechanistic	Yes	Yes	All
Petroleums Experts (4,5)	Mechanistic	Yes	Yes	All
Hydro 3-phase	Mechanistic	Yes	Yes	All
OLGAS	Mechanistic	Yes	Yes	All

The gravity term $\left(\frac{dp}{dL}\right)_g$ is dependent on the density of the fluid, the gravity acceleration and the inclination. It can be expressed with the following equation, where θ is the inclination relative to a horizontal position, e.g. vertical $\rightarrow \theta = 90$. The gravity term often contributes with 80-95$\%$ of the pressure gradient in wells, (Mukherjee and Brill, 1999).

$$\left(\frac{dp}{dL}\right)_g = -\rho g sin(\theta) \tag{A.37}$$

The acceleration term $\left(\frac{dp}{dL}\right)_a$ can in most cases be neglected, due the small contribution it gives in the total pressure loss. In some cases, the contribution of the acceleration term is not insignificant and have to be evaluated, commonly when the fluid velocity change rapidly such as in the upper part of gas wells with a low back pressure. The one-dimensional pressure gradient can be expressed as.

$$\left(\frac{dp}{dL}\right)_a = -\rho v \frac{dv}{dL} \tag{A.38}$$

The friction term $\left(\frac{dp}{dL}\right)_f$ is caused by friction or shear stress (τ) between the fluid and the pipe wall, as shown by equation A.39. A typical method to determine the wall shear stress is to introduce a dimensionless friction factor f. This dimensionless friction factor is defined as "the ratio of the wall shear stress to the kinetic energy of the fluid per unit volume" (Mukherjee and Brill, 1999). A well-known friction factor is the Fanning friction factor f_f or the Moody friction factor that is four times as large, $f_m = 4f_f$. By

combining equation A.39 and A.40, one can show that the friction gradient is a function of the dimensionless friction factor resulting in the well-known Darcy-Waisbach equation, equation A.41, (Mukherjee and Brill, 1999).

$$\left(\frac{dp}{dL}\right)_f = -\tau\frac{\pi d}{A} \tag{A.39}$$

$$f_m = \frac{\tau}{\rho v^2/8} \longrightarrow \tau = f\frac{\rho v^2}{8} \tag{A.40}$$

$$\left(\frac{dp}{dL}\right)_f = -\left(f\frac{\rho v^2}{8}\right)\left(\frac{\pi d}{\pi d^2/4}\right) = -\frac{f\rho v^2}{2d} \tag{A.41}$$

How the friction factor is calculated depends on if the flow is either laminar or turbulent, an illustration of these flow regimes is shown in figure A.8. The flow regime can be determined by the value of the Reynolds number N_{Re}, calculated with equation A.42. Table A.6 shows the boundary conditions for the different flow regimes.

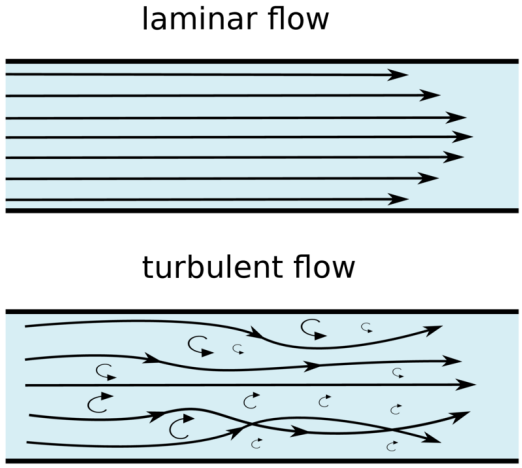

Figure A.8: Laminar and turbulent flow regime, courtesy of (**?**)

$$N_{Re} = \frac{\rho v d}{\mu} \tag{A.42}$$

Table A.6: single-phase flow regimes with boundaries

Flow regime	Reynolds numbers
Laminar flow	$2000 < N_{Re}$
Transition zone	$2000 < N_{Re} < 4000$
Turbulent flow	$N_{Re} < 4000$

For laminar flow, the friction term can be calculated by introducing the Poiseuille equation, equation A.43, that show the velocity as a function of the pressure gradient. By combining the Poiseuille equation and equation A.41 one can show that the friction term is only a function of the Reynolds number in laminar flow. This makes the friction gradient straight forward to calculate and mainly dependent on the viscosity, velocity and pipe diameter, as expressed with equation A.45.

$$v = \frac{d^2}{32\mu}\left(\frac{dp}{dL}\right) \tag{A.43}$$

$$f = \frac{64\mu}{\rho v} = \frac{64}{N_{Re}} \tag{A.44}$$

$$\left(\frac{dp}{dL}\right)_f = \frac{4}{d}\frac{16}{N_{Re}}\frac{1}{2}\rho v^2 = 32\frac{\mu v}{d^2} \tag{A.45}$$

Calculating the friction term in the transition zone or the turbulent regime is more complicated than the method used in the laminar flow. The effective wall roughness ϵ/d is an important contributor to the friction factor which will determine the friction loss. Several empirical correlations have been suggested and one of the most used ones are the Colebrook equation, equation A.46, (Colebrook, 1939). When solving the Colebrook equation as done in equation A.47, an iterative process is required to calculate the friction factor. Starting with an assumed value for the friction factor f_{est} and iterating until the value of f_{est} equals the calculated friction factor within the required accuracy (Colebrook, 1939).

$$\frac{1}{\sqrt{f}} = 1.74 - 2LOG\left(\frac{2\epsilon}{d} + \frac{18.7}{N_{Re}\sqrt{f}}\right) \tag{A.46}$$

$$f_c = \left[1.74 - 2LOG\left(\frac{2\epsilon}{d} + \frac{18.7}{N_{Re}\sqrt{f_{est}}}\right)\right]^{-2} \tag{A.47}$$

Another method to obtain the friction factor is to use the Moody diagram shown in figure A.9, which is a graphical representation of equation A.41 and A.46. One can clearly see that there are only small changes in the friction factor for the fully turbulent regime, which can be explained by the second term within the LOG in equation A.46 goes to zero and the equation becomes the equation proposed by Nikuradse, equation A.48 (Colebrook, 1939;

Mukherjee and Brill, 1999). When the friction factor is determined equation A.41 can be used to calculate the friction gradient.

$$\frac{1}{\sqrt{f}} = 1.74 - 2LOG\left(\frac{2\epsilon}{d}\right) \tag{A.48}$$

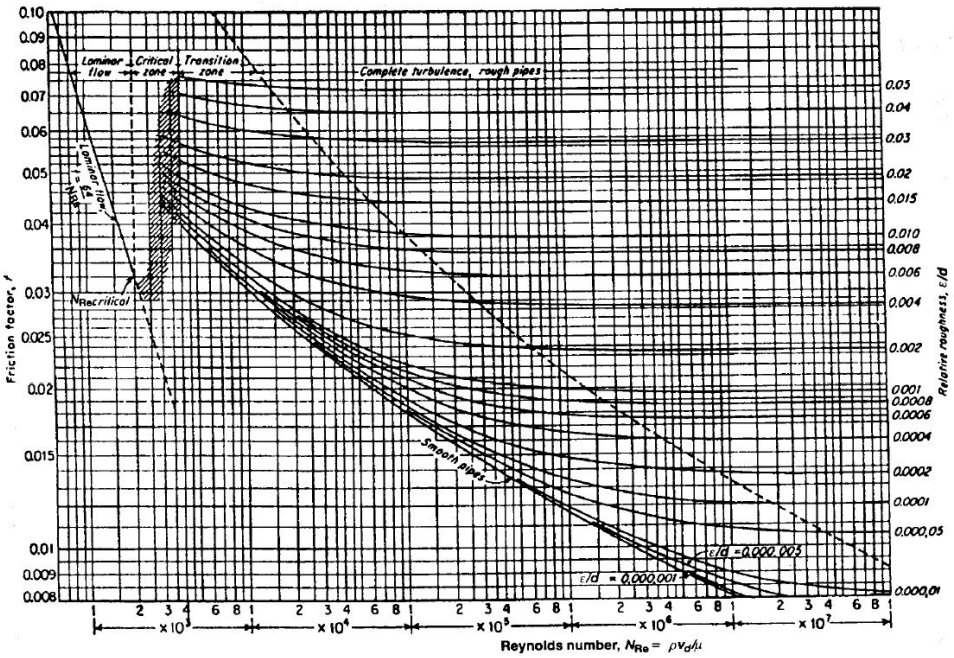

Figure A.9: The Moody diagram used to determine the friction factor based on the relative roughness and the Reynolds number (Mukherjee and Brill, 1999)

The single-phase flow theory presented are a simplification of the actual flow in a petroleum system, not considering the behavior of non-Newtonian fluids and the possibility of flow in the annulus. In a single-phase petroleum system, the oil or gas behaves as a non-Newtonian fluid, several correlations have been developed to best describe the different behaviors, such as the Bingham model and the Power law model. Regarding the flow in annulus a hydraulic diameter is commonly used, but this does not take into the eccentricity of the pipe, i.e. the position of the inner pipe relative to the outer pipe. Although the theory presented are a simplification of the actual single-phase flow it gives a brief introduction into some of the ideas and concepts implemented in several of the multiphase flow correlations. (Mukherjee and Brill, 1999)

Multiphase flow summary

Several of the empirical correlations shown in table A.5 follow the same basic principle

to calculate the total pressure gradient as discussed in the single-phase flow theory. A total pressure gradient that consist of three different terms, a gravity term, a friction term and an acceleration term, is the used energy balance equation for most of the empirical correlations. How each of these terms are determined differ slightly in each correlation.

$$\left(-\frac{dP}{dZ}\right) = g\rho_s sin(\theta) + \frac{f_{tp}\rho_{tp}v_m^2}{2d} + \frac{\rho_s}{2g}\frac{dv_m^2}{dL} \tag{A.49}$$

The main difference in most of the correlations are how the following terms are calculated or obtained ρ_s, f_{tp}, ρ_{tp} and v_m. The density in the gravity term ρ_s is commonly referred to as a slip density and is a function of the density of each of the phases and the liquid holdup H_L. The liquid holdup is defined as the liquid volume over the total volume for a small length of pipe, it is commonly measured in the experiments conducted and a correlation is presented. Only a few correlations separate between the two-phase density and the slip density.

$$\rho_s = H_L\rho_L + (1 - H_L)\rho_g \tag{A.50}$$

The friction term is commonly dependent on the flow regime and the liquid holdup. The method to determine the flow regime differs in each of the correlations, but a flow regime chart presented by (Duns and Ros, 1963) are the basis for vertical flow and are dependent on the gas superficial velocity compared to the liquid superficial velocity. How the friction factor is determined differs in the different correlations, but a common feature is to adjust the flow properties in such a manner that the moody diagram, figure A.9, is valid for the multiphase flow.

The main difference between calculating the pressure loss in a single fluid system and a multiphase fluid system is due to the pressure loss caused by the slippage between the different phases. In multiphase flow there are not only the two flow regimes laminar and turbulent, but several flow regimes dependent on the amount of gas to liquid, the inclination of the pipe also plays a vital role in the flow regime behavior. (Mukherjee and Brill, 1999)

Several of the empirical correlation consider the flow regime. (Duns and Ros, 1963) described several flow regimes for vertical wells and (Beggs and Brill, 1973) described different flow regimes for horizontal and deviated wells. The vertical flow regimes are presented in figure A.10 and the horizontal flow regimes in figure A.11.

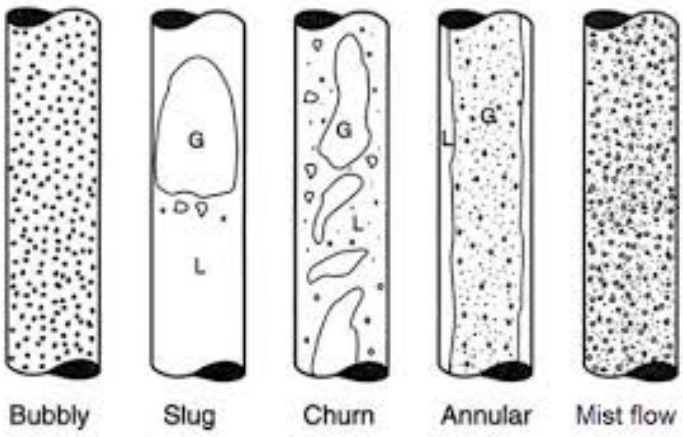

Figure A.10: Flow regimes observed for a vertical well, courtesy of (Duns and Ros, 1963)

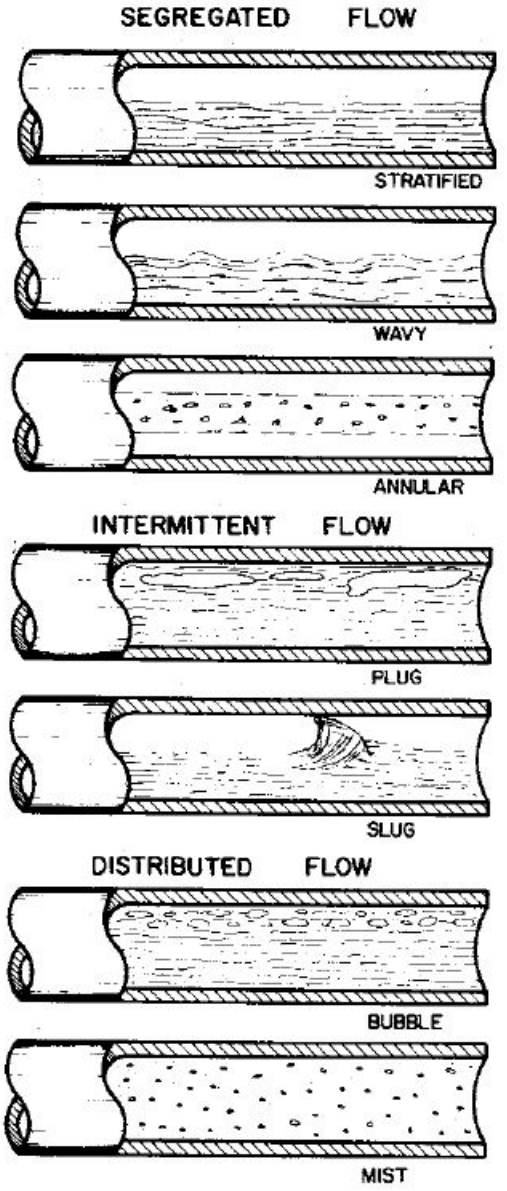

Figure A.11: Flow regimes observed for a deviated and horizontal flow, courtesy of (Beggs and Brill, 1973)

Common procedure

Most of the different multiphase correlations are based on a common procedure to calculate the pressure drop. This procedure is listed below and the difference between the different correlations is in step 3 to step 8.

1. Begin at a known elevation with known values for the flow rate and pressure, commonly at either the wellhead or the bottom of the well.
2. For a given length increment ΔL, assume a value for the pressure loss Δp, or the opposite way.
3. Calculate the average pressure, i.e. the pressure in the middle of the increment. If not isothermal flow, calculate the average pressure in the middle of the increment as well.
4. Calculate all the phase behavior of the fluids, gas and liquid properties such as GOR, B_o, B_g, μ_L, v_{sg}, v_{sL} ρ_l and ρ_g for the average pressure and temperature.
5. If flow regime is considered, determine the flow regime for the selected increment.
6. If slip is considered in the correlation, calculate the liquid holdup H_L, this step is usual different in the different correlations.
7. Obtain a value for the friction factor f or f_{tp}, this step is usual different in the different correlations.
8. Calculate the total pressure gradient $\frac{dp}{dL}$.
9. Calculate ΔL from the total pressure gradient and the assumed Δp from step 2.
10. If the calculated value for ΔL does not match the assumed value in step 2 within the wanted accuracy, assume a new value for Δp and repeat step 3-9.
11. If the calculated value for ΔL equals the assumed value from step 2, start the procedure from step 2 for a new increment, until the entire wellbore has been calculated.

A.5.2 Okriszewski's correlation

Orkiszewski developed a new procedure to calculate the pressure drop in a multiphase flow system. The method differentiates between the different flow regimes described by (Duns and Ros, 1963) and calculate the pressure gradient by using previously known correlations for each regime. This is with an exception for the flow regime slug flow where the author has modified a correlation by (Griffith and Wallis, 1961a) to include a friction term based on a liquid distribution coefficient. The different correlations used, and the respective flow regimes used in the procedure by Orkiszewski are shown in table A.7. The procedure presented by (Orkiszewski, 1967) is based on measurements from 148 well conditions presented by different authors. In all of the 148 wells almost 95% included the flow regime slug flow, which the author redeemed the most important flow regime to be measured. Table A.8 show the well conditions used and compare the method presented by Orkiszewski, (Duns and Ros, 1963) and (Hagedorn and Brown, 1965). The method developed by Orkiszewski is shown to be more precise than both Duns & Ros and Hagedorn & Brown, with more than half the standard deviation.

Table A.7: Orkiszewski's method: Flow regime and correlations

Flow Regime	**Method**
Bubble flow	(Griffith, 1962)
Slug flow (density term)	(Griffith and Wallis, 1961b)
Slug flow (friction gradient term)	(Orkiszewski, 1967)
Transition flow	(Duns and Ros, 1963; Orkiszewski, 1967)
Annular mist flow	(Duns and Ros, 1963)

Table A.8: Range of parameters used in the paper and a comparison between the method described and two previous methods, (Orkiszewski, 1967)

	Prediction Method		
	This Method	Duns and Ros	Hagedorn and Brown
Over-all Results			
(148 Well conditions)			
Avg. error, percent	— 0.8	+ 2.4	+ 0.7
Std. deviation, percent	10.8	27.0	24.2
Results from Grouped Data Sources			
Table 1 — Heavy-Oil Wells (22 Wells, low to medium velocities, 10 to 20° API oils)			
Avg. error, percent	— 1.2	+22.7	+16.4
Std. deviation, percent	10.4	18.7	41.4
Baxendell-Thomas[8] (1 Well, 25 rates mostly high velocities, 34° API oil)			
Avg. error, percent	— 2.1	+ 2.3	+ 8.7
Std. deviation, percent	11.1	20.0	12.7
Fancher-Brown[6] (1 Well, 20 rates medium to high velocities, 95 percent water cut)			
Avg. error, percent	+ 0.3	+ 1.7	+ 5.4
Std. deviation, percent	11.8	32.1	10.8
Hagedorn-Brown[9] (1 Well, medium to high velocities, 16 water runs, 16 oil runs of 10 to 100 cp oil)			
Avg. error, percent	+ 0.1	—16.9	+ 1.2
Std. deviation, percent	8.2	36.6	10.3
Poettmann-Carpenter[1] (49 Wells, low to medium velocities, 15 wells high water cut, rest 36 to 54° API oils)			
Avg. error, percent	— 1.0	+ 5.8	—13.0
Std. deviation, percent	12.0	12.4	22.2

Procedure

Step 1
Choose a point in the drill string with known depth, flow rate, temperature and pressure. This is commonly either the wellhead or bottom-hole.

Step 2
Obtain a temperature gradient for the well, a straight line can be used.

Step 3
Discretize the well bore into several increments and assume a pressure drop for a given length in the first increment, i.e. Δp_k over the length ΔD_k. Calculate the average pressure in the middle of increment.

$$\bar{p} = \frac{p_k + p_{k-1}}{2} = p_{k-1} + 0.5\Delta p_k \tag{A.51}$$

$$\bar{D} = D_{k-1} + \Delta D_k \tag{A.52}$$

Step 4
Calculate the temperature in the middle of the increment, i.e. at the depth $\bar{D}$.

Step 5
Obtain correct fluid properties for the temperature and pressure in the middle of the increment. Some of the fluid properties needed are: B_o, B_w, B_g, R_s, z and μ_l. Several correlations are available, and the ones that best fit the flowing fluid should be used

Step 6
Determine what flow regime that are present in the increment, the boundaries for the different flow regimes are shown in table A.9. The bubble flow boundary is retrieved from (Griffith and Wallis, 1961a), while the three other boundaries comes from (Duns and Ros, 1963). These three boundaries have been described in the section regarding Duns and Ros, but for the sake of easiness it is included here.

Table A.9: Boundaries between the different flow regimes (Orkiszewski, 1967)

Flow Regime	**Boundaries**
Bubble flow	$q_g/q_t < L_B$
Slug flow	$q_g/q_t > L_B$ and $v_{gD} < L_s$
Transition flow	$L_m > v_{gD} > L_s$
Mist flow	$v_{gD} > L_m$

The upper boundary for the bubble flow can be calculated with the equations below. Note that the lower limit for the value L_B is 0.13, i.e. $L_B \geq 0.13$.

$$L_B = 1.071 - 0.2218\frac{v_t^2}{d_h} \tag{A.53}$$

$$L_S = 50 + 36 v_{gD}\frac{q_L}{q_g} \tag{A.54}$$

$$L_M = 75 + 84(v_g\frac{q_L}{q_g})^{0.75} \tag{A.55}$$

$$v_{gD} = q_g \sqrt[4]{\frac{\rho_L}{\sigma g}}/A_p \tag{A.56}$$

Step 7
Determine the average density and friction loss gradient based on the flow regime found in the previous step.
Step 7a - Bubble flow
Calculate the void fraction of gas with equation A.57. v_s (Griffith and Wallis, 1961b)

suggested that a value of v_s=0.8 ft/sec is a good assumption. The equations below and figure A.12 are used to determine the friction factor.

$$F_g = \frac{1}{2}[1 + \frac{q_t}{v_s A_p} - \sqrt{(1 + \frac{q_t}{v_s A_p})^2 - \frac{4q_g}{v_s A_p}}] \tag{A.57}$$

$$\bar{\rho} = (1 - F_g)\rho_L + F_g \rho_g \tag{A.58}$$

$$\tau_f = f_{tp} \frac{v_L^2}{2 g_c d_h} \tag{A.59}$$

$$v_L = \frac{q_L}{A_p(1 - F_g)} \tag{A.60}$$

$$N_{Re} = \frac{1488 \rho_L d_h v_L}{\mu_L} \tag{A.61}$$

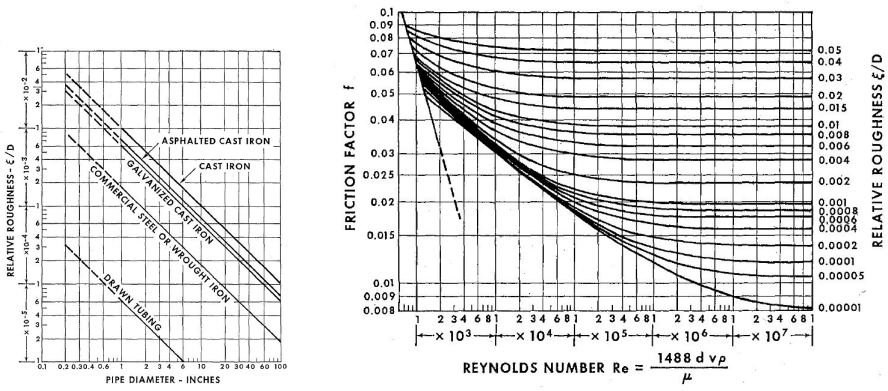

(a) **(b)**

Figure A.12: Relative roughness for typical materials and the moody diagram for two phases (Orkiszewski, 1967)

Step 7b - Slug Flow

The average density can be found by using the equation below, where v_b is the bubble rise velocity and the Γ is the liquid distribution coefficient, an empirical coefficient correlated from oilfield data. The bubble rise velocity can be calculated by equation A.63 when the coefficients C_1 and C_2 are found from figure A.13 and A.14. Since v_b is used to calculate N_b that is used to find C_2, v_b must be obtained by an iterative process and the first v_b value need to be assumed, v_b=1.75 is a good start. Since figure A.14 only show a limited range of the Reynold number the figure has been extrapolated and C_2 can be calculated by equation A.67 to A.70.

$$\bar{\rho} = \frac{w_t + \rho_L v_b A_p}{q_t + v_b A_p} + \Gamma \rho_L \tag{A.62}$$

$$v_b = C_1 C_2 \sqrt{g d_h} \tag{A.63}$$

$$N_b = \frac{1488 \rho_L d_h v_b}{\mu_L} \tag{A.64}$$

$$N_{Re} = \frac{1488 q_t \rho_L d_h}{A_p \mu_L} \tag{A.65}$$

$$q_t = q_L + q_g = Q_o B_o + Q_w B_w + Q_g B_g \tag{A.66}$$

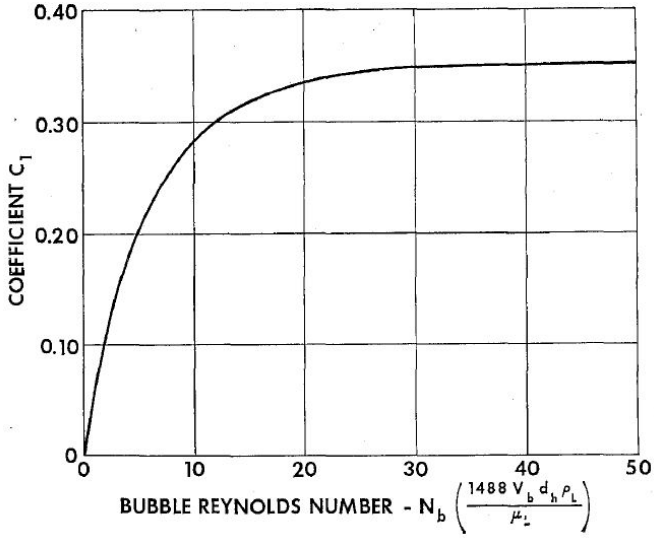

Figure A.13: Bubble rise velocity coefficient 1, (Orkiszewski, 1967)

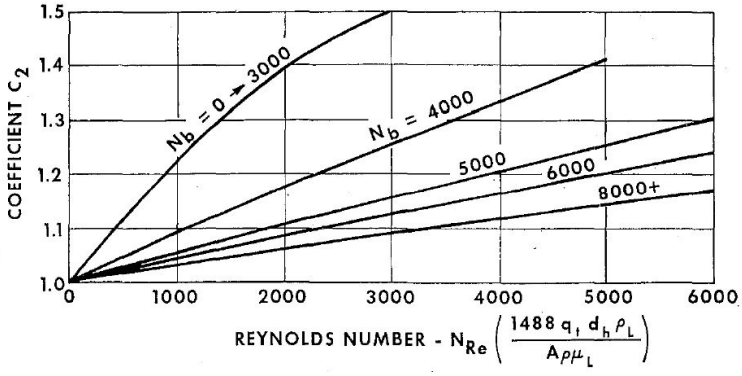

Figure A.14: Bubble rise velocity coefficient 2, (Orkiszewski, 1967)

The extrapolated equations for figure A.14 are:
When $N_b \leq 3000$

$$v_b = (0.546 + 8.74 \cdot 10^{-6} N_{Re}) \sqrt{g d_h} \tag{A.67}$$

When $N_b \geq 8000$

$$v_b = (0.35 + 8.74 \cdot 10^{-6} N_{Re}) \sqrt{g d_h} \tag{A.68}$$

When $3000 < N_b < 8000$

$$v_{bi} = (0.251 + 8.74 \cdot 10^{-6} N_{Re}) \sqrt{g d_h} \tag{A.69}$$

$$v_b = \frac{1}{2} v_{bi} + \sqrt{v_{bi}^2 + \frac{13.59 \mu_L}{\rho_L \sqrt{d_h}}} \tag{A.70}$$

Orkiszewski provide different equations for the liquid distribution coefficient Γ depending on what liquid is the continuous phase and the total velocity pipe velocity v_t. Table A.10 show the relationship between the velocity, liquid phase and the equations. The equations shown in table A.10 are based on data from (Hagedorn and Brown, 1965), a graphical presentation of the data is shown in figure A.15.

Table A.10: Liquid distribution coefficient equation relationship

Continuous liquid phase	v_t	Equation
Water	<10	A.71
Water	>10	A.72
Oil	<10	A.73
Oil	>10	A.74

$$\Gamma = \frac{0.013 Log(\mu_L)}{d_h^{1.38}} - 0.681 + 0.232 Log(v_t) - 0.428 Log(d_h) \tag{A.71}$$

$$\Gamma = \frac{0.045 Log(\mu_L)}{d_h^{0.799}} - 0.709 - 0.162 Log(v_t) - 0.888 Log(d_h) \tag{A.72}$$

$$\Gamma = \frac{0.0127 Log(\mu_L + 1)}{d_h^{1.415}} - 0.284 + 0.167 Log(v_t) + 0.113 Log(d_h) \tag{A.73}$$

$$\Gamma = \frac{0.0274 Log(\mu_L + 1)}{d_h^{1.371}} + 0.161 + 0.569 Log(d_h) - Log(v_t)[\frac{0.01 Log(\mu_L + 1)}{d_h^{1.571}} + 0.397 + 0.63 Log(d_h)] \tag{A.74}$$

The liquid distribution coefficient is limited to equation A.75, but if $v_t > 10ft/sec$ equation A.76.

$$\Gamma \geq -0.065 \tag{A.75}$$

$$\Gamma \geq -\frac{v_b A_p}{q_t + v_b A_p}(1 - \frac{\bar{\rho}}{\rho_L}) \tag{A.76}$$

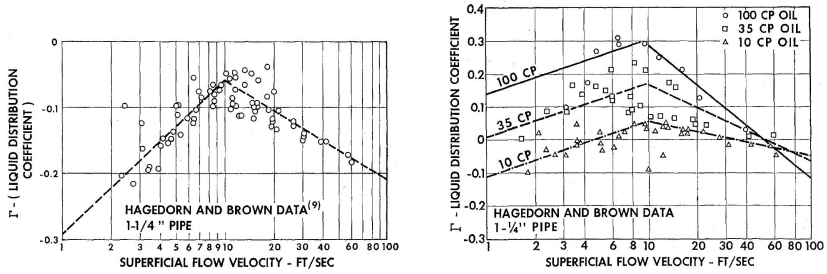

(a) **(b)**

Figure A.15: The liquid distribution coefficient Γ for a) water and b) oil (Orkiszewski, 1967)

Now everything required to calculate the average density in equation A.62 are available. Without going into how the friction loss gradient τ_f is derived the author postulate the following equation. The only missing quantity is the friction factor f, which can be obtained by using the two-phase Reynolds number and the Moody diagram, e.g. figure A.12 and equation A.65. The Colebrook equation can also be used instead of the Moody diagram.

$$\tau_f = \frac{f\rho_L v_t^2}{2g_c d_h}\left[\frac{q_L + v_b A_p}{q_t + v_b A_p} + \Gamma\right] \tag{A.77}$$

The author states that this new method to calculate the complex nature of the friction loss in the slug flow regime implicitly account for the following terms when the liquid distribution coefficient is accounted for: (Orkiszewski, 1967)

1. "Liquid is distributed in three phases: the, the film around the gas bubble and in the gas bubble as entrained droplets. A change in this distribution will change the net friction losses."
2. "The friction loss has essentially two contributions, one from the liquid slug and the other from the liquid film."
3. "The bubble rise velocity approaches zero as mist flow is approached"

Step 7c - Transition flow

The first description of how to calculate the pressure loss in the transition flow regime were (Duns and Ros, 1963). The method to calculate the pressure loss in this regime is to first calculate the pressure loss in both the slug flow and mist flow regime, then interpolate

between these values with respect to v_{gD} and the boundaries for the transition zone L_s and L_m. Orkiszewski presented this interpolation with the following equation

$$\bar{\rho} = \frac{L_M - v_{gd}}{L_M - L_s}[\bar{\rho}]_{slug} + \frac{v_{gd} - L_s}{L_M - L_s}[\bar{\rho}]_{mist} \tag{A.78}$$

$$\bar{\tau}_f = \frac{L_M - v_{gd}}{L_M - L_s}[\bar{\tau}_f]_{slug} + \frac{v_{gd} - L_s}{L_M - L_s}[\bar{\tau}_f]_{mist} \tag{A.79}$$

Step 7d - Mist flow
As described in the section regarding Duns and Ros the author assume no slip between the liquid and the gas in the mist flow regime, this makes the flowing gas fraction close to unity and can be calculated with equation A.80. When F_g is calculated the average density can be obtained.

$$F_g = \frac{1}{1 + \frac{q_L}{q_g}} \tag{A.80}$$

$$\bar{\rho} = (1 - F_g)\rho_L + F_g\rho_g \tag{A.81}$$

Duns and Ros described that the true problem with the mist flow was to determine the effective wall roughness ϵ/D due to the wavy liquid film on the side walls. The upper boundary for the relative roughness caused by the wavy liquid film is 0.5 and the lower boundary is the effective roughness of the pipe itself which can be obtained by figure A.12. Orkiszewski proposed the following set of equations to determine the relative roughness. When a value for ϵ/D is obtained the friction factor can be found by using figure A.12. (Duns and Ros, 1963) extrapolated the moody diagram for $\epsilon > 0.05D$ with equation A.85. When the friction factor is obtained the friction loss gradient can be calculated with equation A.86.

$$N = 4.52 \cdot 10^{-7}\left(\frac{v_g\mu_L}{\sigma}\right)^2\frac{\rho_g}{\rho_L} \tag{A.82}$$

When $N < 0.005$:

$$\frac{\epsilon}{D} = 34\frac{\sigma}{\rho_g v_g^2 d_h} \tag{A.83}$$

When $N > 0.005$:

$$\frac{\epsilon}{D} = 174.8\frac{\sigma N^{0.302}}{\rho_g v_g^2 d_h} \tag{A.84}$$

$$f = \frac{1}{(4LOG_{10}(0.27\epsilon/D))^2} + 0.067\left(\frac{\epsilon}{D}\right)^{1.173} \tag{A.85}$$

$$\tau_f = f\frac{\rho_g v_g^2}{2g_c d_h} \tag{A.86}$$

Step 8
Calculate the incremental depth change ΔD from the following equation by using the assumed values for $\bar{p}$ and Δp_k from step 3 and the calculated values $\bar{\rho}$ and τ_f from step 7.

$$\Delta D = 144\left[\frac{\Delta p_k(1-\frac{w_t q_g}{4637A_t^2\bar{p}})}{\bar{\rho}+\tau_f}\right] \tag{A.87}$$

Step 9
If the calculated value for ΔD does not equal the assumed value for ΔD_k in step 3, an iteration process starting from step 3 where a new value for ΔD_k needs to be assumed until the two values for ΔD is within the required accuracy.

Step 10
Calculate the pressure p_k and the depth D_k.

$$p_k = p_{k-1} + \Delta p_k \tag{A.88}$$

$$D_k = D_{k-1} + \Delta D_k \tag{A.89}$$

Step 11
Repeat the procedure starting from step 3, until the pressure over the entire length of the wellbore has been calculated.

Nomenclature and subscripts as used by (Orkiszewski, 1967)

NOMENCLATURE

A_p = flow area of pipe, sq ft
B_o = oil formation volume factor, bbl/STB
C_1, C_2 = parameters used to calculate bubble rise velocities from Eq. C-5, dimensionless, to be evaluated from Figs. 8 and 9
d_h = hydraulic pipe diameter ($4 \times A_p$/wetted perimeter), ft
D = depth from wellhead, ft
ΔD = increment of depth, ft
f = Moody friction factor, dimensionless, to be evaluated from Fig. 6
F_g = flowing gas fraction, dimensionless
g = acceleration of gravity, ft/sec^2
g_c = gravitational constant, ft-lb(mass)/lb(force)-sec^2
$(L)_B$ = bubble-slug boundary, dimensionless
$(L)_M$ = transition-mist boundary, dimensionless
$(L)_S$ = slug-transition boundary, dimensionless
N_b = 1,488 $v_b d_h \rho_L / \mu_L$, bubble Reynolds number, dimensionless
N_{Re} = 1,488 $v D_h \rho / \mu$, Reynolds number, dimensionless
p = pressure, psia
Δp = pressure drop, psi
$\overline{p}$ = average pressure, psia
p_{pc} = pseudo-critical pressure, psia
p_r = reduced pressure, dimensionless
P = pressure, lb/sq ft
q = volumetric flow rate, cu ft/sec
q_o = oil rate, B/D
R = produced GOR, scf/STB
R_s = solution gas, scf/STB
T_{pc} = pseudo-critical temperature, °R
T_r = reduced temperature, dimensionless
$\overline{T}$ = average temperature, °F
v = fluid velocity, ft/sec
v_b = bubble rise velocity (velocity of rising gas bubble relative to preceding liquid slug), ft/sec
v_{bz} = base bubble rise velocity for Eq. C-9, ft/sec
v_s = slip velocity (difference between average gas and liquid velocities), ft/sec
v_{gD} = $q_g \left(^4\sqrt{\rho_L / g\sigma}\right) / A_p$, dimensionless gas velocity
z = gas compressibility factor, dimensionless
γ = fluid specific gravity, dimensionless
Γ = liquid distribution coefficient, to be evaluated from Eqs. C-11 through C-16, dimensionless
μ = viscosity, cp
ξ/D = Moody pipe relative roughness factor (Fig. 7) and Duns-Ros mist flow factor (Eqs. C-21 and C-22), dimensionless
ρ = density, lb/cu ft
$\overline{\rho}$ = average flowing density, lb/cu ft
τ_f = friction-loss gradient, lb/sq ft/ft
σ = surface tension, lb/sec^2

SUBSCRIPTS

g = gas
L = liquid
o = oil
t = total

Figure A.16: Nomenclature and subscripts as used by (Orkiszewski, 1967)

A.5.3 Olgjenka

In the simulator one of the two multiphase pressure drop correlation is the Olgjenka - correlation. The theory presented in this section is based on the theory presented by (Asheim, 2018a) and (Asheim, 2020). Only the stationary part of the Olgjenka correlation is used.

Based on the PVT-values and the surface flow rates the down hole flow rate of each phase can be calculated.

$$q_{o,dh} = q_{o,s} * B_o \tag{A.90}$$

$$q_{g,dh} = q_{g,s} * (R_t - R_s) * B_g \tag{A.91}$$

$$q_{k,dh} = q_{k,s} * B_k \tag{A.92}$$

$q_{i,dh}$ - Down hole fluid rate $[m^3]$
$q_{i,s}$ - Surface fluid rate under standard conditions $[Sm^3]$
B_i - Formation volume factor $[m^3/Sm^3]$
R_t - Total Gas-Oil-Ratio $[Sm^3/Sm^3]$
R_s - Solution Gas-Oil-Ratio $[Sm^3/Sm^3]$
Subcripts: o - oil, g-gas, k - kill, dh - downhole, s-surface or solution, t - total.

The superficial velocities of the two phases, gas and liquid, and the mixture can be calculated with equation A.93 to A.95. The superficial velocity assumes that the fluid-phase is alone in the cross-section, the true fluid-phase velocity is different. The superficial gas velocity is calculated for the down hole gas rate, while the superficial liquid velocity is calculated based on both the oil and kill fluid flowing at the given depth.

$$v_{sg} = \frac{q_{g,dh}}{A} \tag{A.93}$$

$$v_{sl} = \frac{q_{o,dh} + q_{k,dh}}{A} \tag{A.94}$$

$$v_{sm} = v_{sg} + v_{sl} \tag{A.95}$$

$v_{s,i}$ - Superficial velocity of fluid phase i [m/s]
A - Cross section area of the pipe $[m^2]$
subscripts: g - gas, l - liquid, m - mixture

The flux fraction is a measure of the how much of each phase (gas or liquid) that flows. The flux fraction for each of the phases is calculated with equation A.96 and A.97.

$$\lambda_l = \frac{v_{sl}}{v_{sm}} = \frac{q_{o,dh} + q_{k,dh}}{q_{o,dh} + q_{k,dh} + q_{g,dh}} \tag{A.96}$$

$$\lambda_g = \frac{v_{sg}}{v_{sm}} = \frac{q_{g,dh}}{q_{o,dh} + q_{k,dh} + q_{g,dh}} \tag{A.97}$$

The mixture density, liquid fraction and two-phased density is calculated with equation A.98 to A.100.

$$\rho_m = \rho_g * \lambda_g + \rho_l * \lambda_l \tag{A.98}$$

$$y_l = \pm\frac{1}{2}\sqrt{\left(\frac{v_{sg}}{v_o} + C_o\frac{v_{sl}}{v_o} - 1\right)^2 + 4C_o\frac{v_{sl}}{v_o}} - \frac{1}{2}\left(\frac{v_{sg}}{v_o} + C_o\frac{v_{sl}}{v_o} - 1\right) \tag{A.99}$$

$$\rho_{tp} = \rho_g * (1 - y_l) + \rho_l * y_l \tag{A.100}$$

ρ_m - Mixture density $[kg/m^3]$
y_l - Liquid fraction [-]
C_o - Distribution parameter for bubbles in flow, commonly in the range [1.0, 1.2]
v_o - Buoyancy velocity of gas bubbles [m/s]
ρ_{tp} - two phased fluid velocity $[kg/m^3]$
ρ_i - Density of phase i $[kg/m^3]$

The density of the liquid mix, mixture of oil and kill fluid, can be calculated with equation A.101.

$$\rho_l = \frac{\rho_o * q_{o,dh} + \rho_k * q_{k,dh}}{q_{o,dh} + q_{k,dh}} \tag{A.101}$$

ρ_i - Down hole density of liquid i $[kg/m^3]$

The buoyancy velocity of gas bubbles may be approximated with equation A.102. The equation is mainly used to calculate the buoyancy velocity for a gas bubble in a stagnant liquid (Asheim, 2018a). An assumption is made that this equation can be used to approximate the bubble buoyancy velocity with fluid flow in the simulator.

$$v_o = 1.53\left(\frac{g\sigma * 10^{-3}(\rho_l - \rho_g)}{\rho_l^2}\right)^{0.25} \tag{A.102}$$

v_o - Buoyancy velocity of gas bubbles [m/s]
g - Gravitation acceleration $[m/s^2]$
σ - Interfacial tension [dynes/cm]
ρ_i - Density of phase i $[kg/m^3]$

The pressure gradient is calculated with equation A.103, which is reduced to equation A.104 if the acceleration is neglected.

$$-\frac{dp}{dx} = \rho_{tp}g_x + \frac{1}{2}f_{tp}\frac{\rho_m}{d}v_m^2 + \rho_g v_{sg}\frac{dv_g}{dx} + \rho_l v_{sl}\frac{dv_l}{dx} \tag{A.103}$$

$$-\frac{dp}{dx} = \rho_{tp} g_x + \frac{1}{2} f_{tp} \frac{\rho_m}{d} v_m^2 \tag{A.104}$$

$\frac{dp}{dx}$ - The pressure gradient [Pa/m]
g_x - Inclination adjusted gravity $[m/s^2]$
f_{tp} - Two-phase friction factor
d - Diameter of pipe $[m]$

The two-phase friction factor can be calculated with equation A.105, where f is calculated in the same manner as a single-phase fluid, either by correlations or charts and C_tp is a correction factor for two-phase flow. The single-phase friction can be calculated with equation A.106 for laminar flow, i.e. a Reynolds number lower than 2300, or the Colebrook equation for turbulent flow. The moody chart may also be used to calculate the single-phase friction factor. The laminar or turbulent flow regime is determined by the two-phase Reynolds number, shown in equation A.107. (Colebrook, 1939; Moody, 1944)

$$f_{tp} = f C_{tp} \tag{A.105}$$

$$f = \frac{0.16}{Re_m^{0.172}} \tag{A.106}$$

$$Re_m = \frac{\rho_m v_{sm} d}{\mu_g \lambda_g + \mu_l \lambda_l} \tag{A.107}$$

$$C_{tp} = \frac{\rho_g}{\rho_m} \frac{\lambda_g^2}{y_g} + \frac{\rho_l}{\rho_m} \frac{\lambda_l^2}{y_l} \tag{A.108}$$

f - Single-phase friction factor [-]
C_{tp} - Two-phase friction factor correlation number []
Re_m - Two-phase Reynolds number [-]
μ, i - Viscosity of phase i [Pa-s]
y_g - Gas fraction (1-y_l) [-]

A.6 PVT - Correlations

In this simulator it is possible to choose between two different sets of PVT correlations, the Glasø-set and the Standing set. These two PVT correlations are based on (Glaso, 1980) and (Standing, 1947). The correlations predict the saturation pressure (p_b), solution gas-oil-ratio R_s and the oil formation volume factor below the saturation pressure B_o. The two correlations are based on different types of oils. The Glasø correlation is based upon North Sea oils, while the Standing correlation is based on California crude oil.

More fluid properties must be included to have a fully operational PVT-simulator. Properties such as: the oil formation volume factor above the saturation pressure (B_o), The gas formation volume factor (B_g) the density of both oil and gas phase ($\rho_{o,g}$), the viscosity of both oil and gas phase ($\mu_{o,g}$) and the interfacial tension between the two-phases (σ) should be included.

The two sets of PVT correlations available in this simulator uses the same correlations to calculate the different fluid properties described above. The value of most of these properties will be different between the two PVT sets since they are a function of the solution GOR and oil formation volume factor.

A.6.1 The Standing set

The standing PVT correlation, (Standing, 1947), is based on 22 different Californian crude oils. 122 different data points were used to determine to PVT-relationships presented below. The range of the different parameters used to obtain the correlation are presented in table A.11.

Table A.11: Standing PVT - range of parameters

Parameter	Unit	Range
Bubble point pressure	Psia	130 - 5000
Total GOR	SCF/STB	20 - 1425
Temperature	F	100 - 258
Gas gravity	s.g. (air=1.0)	0.59 - 0.95
API oil gravity	API	16.5 - 63.8
Oil gravity	s.g. (Water = 1.0)	0.725 - 0.956

Bubble point / Saturation pressure

$$p_b = 18.2 * \left(\left(\frac{R_t}{\gamma_g} \right)^{0.83} * \frac{10^{0.00091T}}{10^{0.0125\gamma_{API}}} - 1.4 \right) \tag{A.109}$$

$$\gamma_{API} = \frac{141.5}{\gamma_o} - 131.5 \tag{A.110}$$

p_b - Saturation pressure of the oil [Psia]
R_t - Total gas-oil-ratio [SCF/STB]
γ_g - Specific gravity of phase gas [-]
γ_o - Oil specific gravity [-]
γ_{API} - API density of the oil [° API]
T - Temperature of the fluid [$°F$]

Solution - gas-oil-ratio
By solving the saturation pressure equation for R_t equation A.111 is obtained, giving the relationship for the solution gas-oil-ratio for all different pressures.

$$R_s = \left(\left(\frac{p}{18.2} + 1.4 \right) * \frac{10^{0.0125\gamma_{API}}}{10^{0.00091T}} \right)^{1/0.83} * \gamma_g \tag{A.111}$$

R_s - Solution Gas-Oil-Ratio [SCF/STB]
p - Pressure of the fluid [Psia]

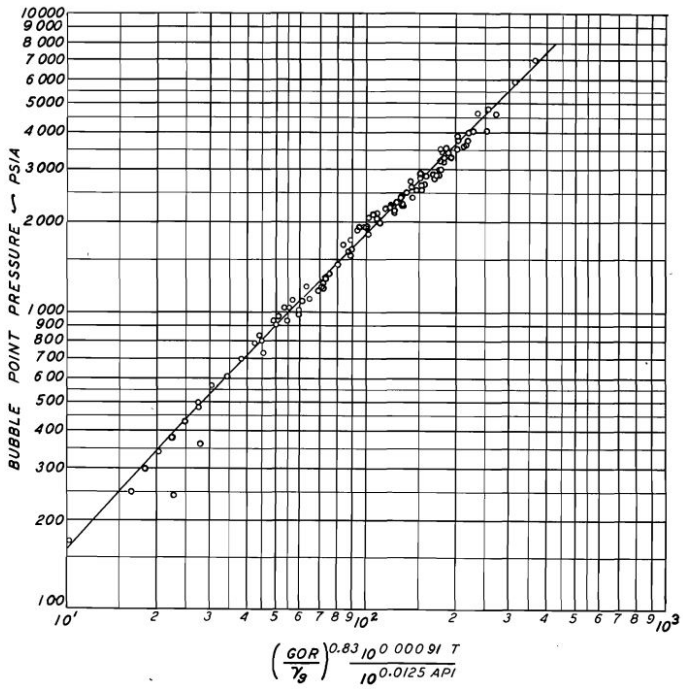

Figure A.17: Standing PVT - bubble point pressure relationship, courtesy of (Standing, 1947)

The oil formation volume factor - B_o - saturated

$$B_o = 0.972 + 1.47 * 10^{-4} * \left(R_s (\frac{\gamma_g}{\gamma_o})^{0.5} + 1.25 * T \right)^{1.175} \tag{A.112}$$

B_o - Oil formation volume factor [RB/STB]

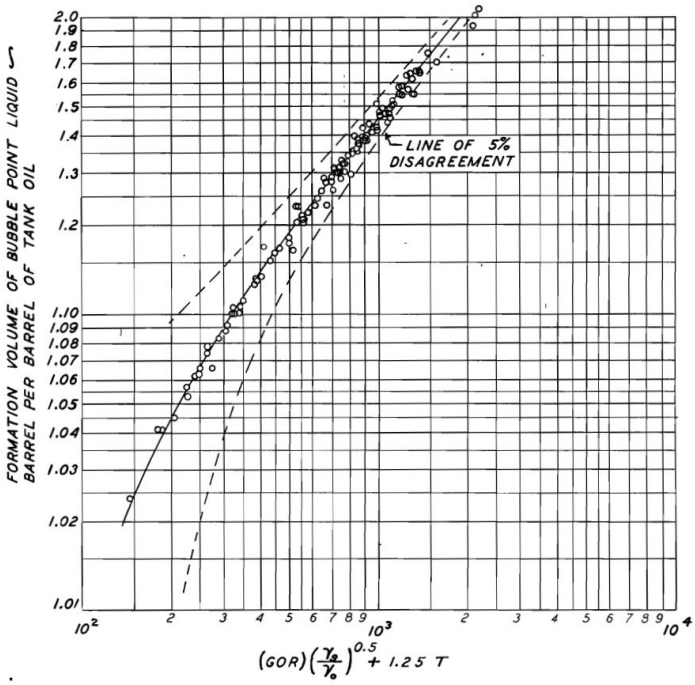

Figure A.18: Standing PVT - Oil formation volume factor relationship, courtesy of (Standing, 1947)

A.6.2 The Glasø correlation

In the article (Glaso, 1980) a PVT correlation is described, this correlation is based upon six different oils from the Norwegian continental shelf with the experimental quantities as shown in table A.12.

Table A.12: Experimental quantities used in the Glasø correlation

Parameter	Unit	Symbol	Range
Total Gas-Oil ratio	SCF/STB	R_t	497-2036
Gas specific gravity	-	γ_g	0.74 - 0.92
Oil specific gravity	-	γ_o	0.80 - 0.93
Oil formation volume factor	bbl/STB	B_o	1.25 - 2.11
Reservoir temperature	$^\circ F$	T	150 - 280
Saturation pressure @ 150°F	psia	p_b	1804 - 6684
Viscosity @ 150°F	cp	μ	0.76 - 37.1

Bubble point pressure
The saturation / bubble point pressure is a measure of when the first gas bubble goes out of solution. The saturation pressure for the different oil mixtures is plotted in figure A.19 and a regression analysis resulted in equation A.113 and A.114.

$$LOG(p_b) = 1.7669 + 1.7447 LOG(p_b^*) - 0.30218 LOG(p_b^*)^2 \tag{A.113}$$

$$p_b^* = \left(\frac{R}{\gamma_g}\right)^{0.816} \cdot \frac{T^{0.172}}{\gamma_{API}^{0.989}} \tag{A.114}$$

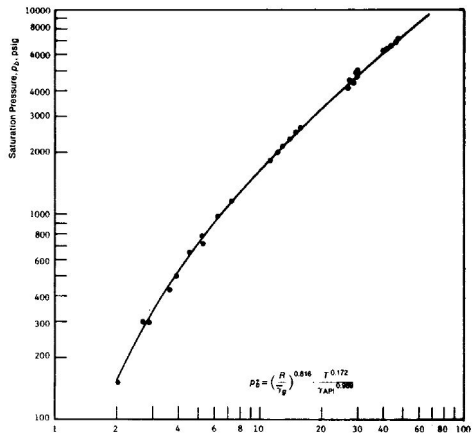

Figure A.19: Measured saturation pressures, courtesy of (Glaso, 1980)

Solution gas-oil-ratio
When the pressure is below the saturation pressure some of the gas is free gas and less gas will be in solution in the oil, a new saturation pressure for the liquid composition will be present. Equation A.113 and A.114 can be altered to calculate the given solution gas-oil-ratio for the pressure. Since equation A.113 is a quadratic equation two solution must be considered with the following boundaries R_s = [0, R_t]. It can be shown that the only viable solution based on the boundaries uses the + part of equation A.115. The solution gas-oil-ratio can be calculated with equation A.115 and A.116. The free gas in the wellbore is the difference between R_t and R_s, adjusted from standard conditions to the conditions in the well.

$$LOG(p^*) = \frac{-1.7447 \pm \sqrt{1.7447^2 - 4 \cdot (-0.30218) \cdot (1.7669 - LOG(p))}}{2 \cdot (-0.30218)} \quad \text{(A.115)}$$

$$R_s = \left(\frac{p^* \cdot \gamma_g^{0.816} \cdot \gamma_{API}^{0.989}}{T^{0.172}} \right)^{\frac{1}{0.816}} \quad \text{(A.116)}$$

Oil formation volume factor
The oil formation volume factor is a parameter that indicates how much the oil will shrink when going from down hole conditions to stock tank conditions. The factor accounts for gas in solution, temperature effects and compressibility. Glasø plotted the measured results in figure A.20 and obtained equation A.117 and A.118 from regression analysis.

$$LOG(B_{ob} - 1) = -6.58511 + 2.91329LOG(B_{ob}^*) - 0.27683LOG(B_{ob}^*)^2 \quad \text{(A.117)}$$

$$B_{ob}^* = R\left(\frac{\gamma_g}{\gamma_o} \right)^{0.526} + 0.968T \quad \text{(A.118)}$$

The correlation presented by Glasø does not give any procedure on how to calculate the oil formation volume factor, B_o, when the pressure is greater than the saturation pressure of the oil. The correlation given by (Vasquez and Beggs, 1980) is used to account for the compressibility under these conditions and the calculated bubble point formation volume factor is an important input to the calculations. The correlation by (Vasquez and Beggs, 1980) will not be discussed any further in the thesis. The

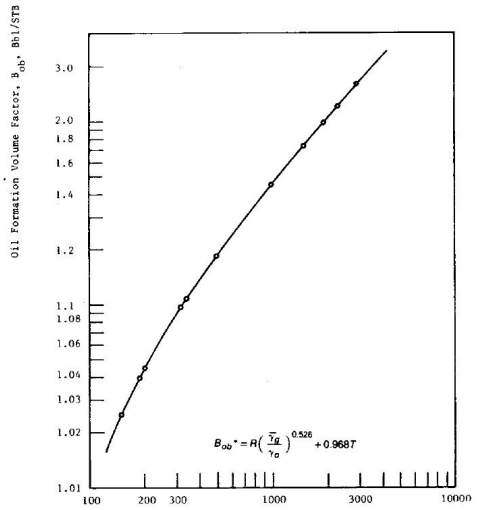

Figure A.20: Measured vs calculated B_o, courtesy of (Glaso, 1980)

A.6.3 Common for both PVT-sets

Dead oil viscosity
The dead oil viscosity is the viscosity of the gas free oil, i.e. when no gas is in solution $R_s = 0$. Glasø conducted a regression analysis on the viscosity from the different fields for a temperature range of 50 to 300 $^\circ$F. Equation A.119 can be used to calculate the dead oil viscosity of North Sea oils. Since (Standing, 1947) did not present any way to calculate the dead oil viscosity, Glasø's correlation is used to calculate the dead oil viscosity in both PVT-sets.

$$\mu_{oD} = c \cdot LOG(\gamma_{API})^d \tag{A.119}$$

With the following equations for the c and d values:

$$c = 3.141 \cdot 10^{10} \cdot T^{-3.444} \tag{A.120}$$

$$d = 10.313 \cdot LOG(T) - 36.447 \tag{A.121}$$

The Glasø correlation does not give a procedure on how to calculate the viscosity when gas is in solution or when the pressure is greater than the saturation pressure. The dead oil viscosity is an important input parameter to calculate the viscosity at different conditions. When gas is in solution and the pressure is less than the saturation pressure the correlation presented by (Standing, 1980) is used. For pressures greater than the saturation pressure the (Vasquez and Beggs, 1980)-correlation will be used.

Saturated oil viscosity, p $< p_b$
When gas goes out of solution of the oil phase, the oil phase will get a higher viscosity. A simple saying is "that the oil loses it's lubrication when the gas goes out of solution", i.e. the gas makes the oil less viscous.

Standing presented a method to calculate the viscosity below the saturation pressure in (Standing, 1980), shown by (Whitson and Burlé, 2000). The details will not be discussed in this thesis, but only the calculation procedure. The viscosity below the saturation pressure of the original reservoir fluid, i.e. the saturation pressure for the current oil mixture, is obtained with equation A.122 to A.124.

$$\mu_{ob} = A_1(\mu_{oD})^{A_2} \tag{A.122}$$

$$A_1 = 10^{-(7.4*10^{-4})}R_s + (2.2 * 10^{-7}) * R_s^2 \tag{A.123}$$

$$A_2 = \frac{0.68}{10^{(8.62*10^{-5})}R_s} + \frac{0.25}{10^{(1.1*10^{-3})}R_s} + \frac{0.062}{10^{(3.74*10^{-3})}R_s} \tag{A.124}$$

Undersaturated oil viscosity, p $> p_b$
When the pressure is greater than the saturation pressure the oil mixture will be compresses. This compression will make the oil more viscous. (Vasquez and Beggs, 1980) presented a method to calculate the oil viscosity above the saturation pressure. The procedure is to use equation A.125 to A.126, more details can be found in the original article. The Standing correlation is used to calculate the saturated oil viscosity used in equation A.125.

$$\mu_o = \mu_{ob}(\frac{p}{p_b})^m \tag{A.125}$$

$$m = 2.6 * p^{1.187} * exp(-11.513 - 8.98 * 10^{-5}p) \tag{A.126}$$

μ_o - Undersaturated oil viscosity, at pressure p [cp]
μ_{ob} - Oil viscosity at saturation pressure (p_b) [cp]
p - Fluid pressure [psia]
p_b - Saturation pressure [psia]
R_s - Solution GOR [SCF/STB]

Undersaturated Oil formation volume factor, p $> p_b$
As the pressure increase the oil will be more compressed and the volume it occupies decreases. When going from a low pressure to the saturation pressure gas goes in solution which have a larger opposite effect than the compressibility, which results in a volume increase. When the oil mixture reaches the saturation pressure, no more gas goes into solution, and the compressibility is the only factor affecting the volume occupation of the oil

mixture. The oil formation volume factor will reduce as a function of the oil compressibility. The article by (Vasquez and Beggs, 1980) present a method to calculate the oil FVF above the saturation pressure.

$$B_o = B_{ob} exp(C_o(p_b - p)) \tag{A.127}$$

$$C_o = \frac{-1433.0 + 5.0R_s + 17.2T - 1180.0\gamma_g + 12.61\gamma_o}{p * 10^5} \tag{A.128}$$

B_o - Oil FVF [RB/STB]
B_{ob} - Oil FVF at saturation pressure [RB/STB]
C_o - Oil compressibility [vol/vol-psi]
R_s - Solution GOR [SCF/STB]
T - Temperature [$^\circ F$]

Gas formation volume factor
The gas formation volume factor (B_g) describe the shrinkage of gas compared to standard conditions, it is based upon the real gas law. (Whitson and Burlé, 2000) present equation A.129 to calculate the gas FVF, which is reduced to equation A.130 with the units presented below.

$$B_g = \left(\frac{p_{sc}}{T_s c}\right)\frac{ZT}{p} \tag{A.129}$$

$$B_g = 0.02827\frac{ZT}{p} \tag{A.130}$$

B_g - Gas formation volume factor [ft^3/SCF]
T_{sc} - Temperature at standard condition = 520 $^\circ R$
T - Temperature of gas $^\circ R$
p_{sc} - Pressure at standard conditions = 14.7 psia
p - Pressure of gas [psia]
Z - Gas compressibility factor [-]

The gas compressibility factor (Z) is calculated based on the gas pseudocritical properties calculated with the correlation presented by (Sutton, 2005), calculated with equation A.131 and A.132. Converted to reduced pressure and reduce temperature with equation A.133 and A.134. The Z-factor is obtained by a procedure presented by (Hall and Yarborough, 1973), which is a representation of the Standing-Katz chart, presented in figure A.21. The procedure by (Hall and Yarborough, 1973) will not be described.

$$T_{pc} = 169.2 + 349.5\gamma_g - 74.0\gamma_g^2 \tag{A.131}$$

$$p_{pc} = 756.8 - 131\gamma_g - 3.6\gamma_g^2 \tag{A.132}$$

$$p_r = \frac{p}{p_{pc}} \tag{A.133}$$

$$T_r = \frac{T}{T_{pc}} \tag{A.134}$$

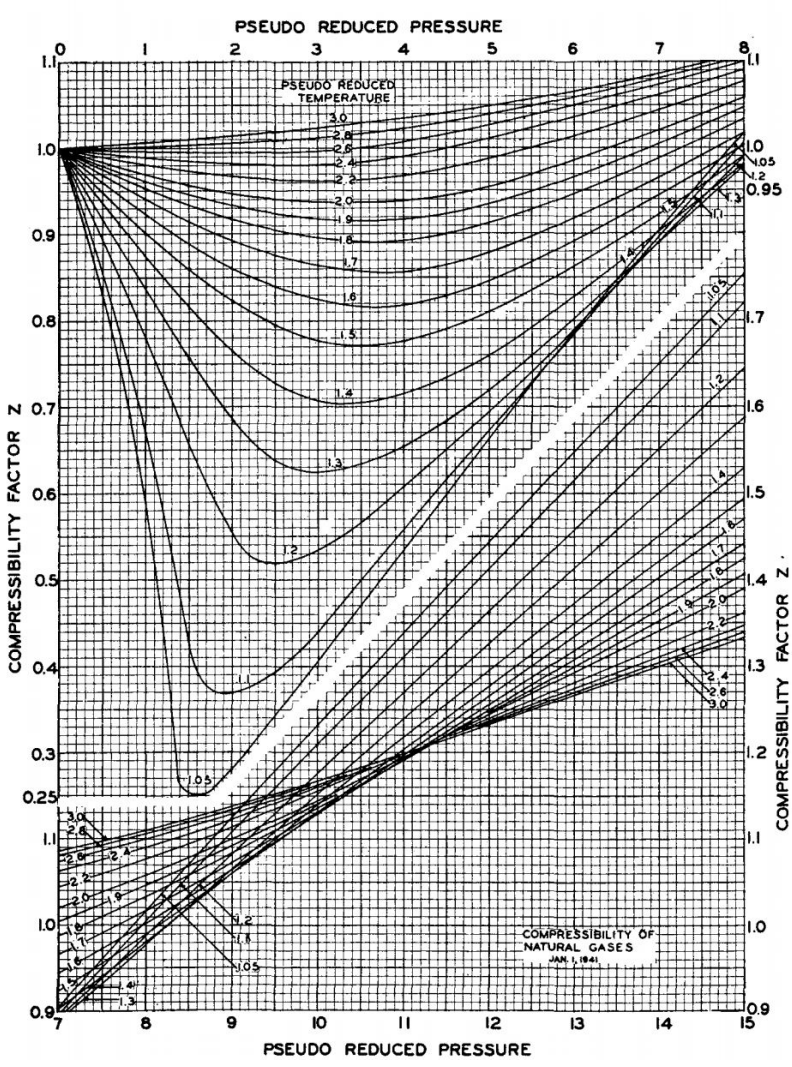

Figure A.21: The Standing-Katz chart to determine the Z-factor, courtesy of (Standing and Katz, 1942)

Oil density
The oil density can be calculated with equation A.135, which is based on the black-oil theory (Whitson and Burlé, 2000). This equation assumes that the gas does not contain any oil.

$$\rho_o = \frac{62.428\gamma_o + 0.0136\gamma_g R_s}{B_o} \tag{A.135}$$

ρ_o - Oil density [lb/ft^3]
γ_i - Specific gravity of phase i [s.g.]
R_s - Solution gas-oil-ratio [SCF/STB]

Gas Density
The gas density is approximated with the gas formation volume factor and the gas specific gravity. Equation A.136 is used to calculate the gas density. (Whitson and Burlé, 2000)

$$\rho_g = \frac{\rho_{g,s}}{B_g} = \frac{\rho_{air}\gamma_g}{B_g} = 0.0765\frac{\gamma_g}{B_g} \tag{A.136}$$

ρ_g - Gas density [lb/ft^3]
$\rho_{g,s}$ - Surface gas density [lb/ft^3]
ρ_{air} - Density of air [lb/ft^3]

Interfacial Tension
The interfacial tension is a parameter that describe the tension between two phases. (Abdul-Majeed and Abu Al-Soof, 2000) gives a procedure on how to calculate the interfacial tension between oil and gas, equation A.137 to A.140. The correlation has an average error of 0.64% and an absolute error of 7.28% from the data points used in the article. The splitting of equation A.138 and A.139 based on the solution GOR will cause an irregularity for the interfacial tension, easily visible when plotting the interfacial tension vs. the saturation pressure.

$$\sigma_{od} = (1.11591 - 0.00305 * T) * (38.085 - 0.259\gamma_{API}) \tag{A.137}$$

When $R_s < 50\ Sm^3/Sm^3$

$$\frac{\sigma_o}{\sigma_{od}} = \frac{1}{1 + 0.02549R_s^{1.0157}} \tag{A.138}$$

When $R_s >= 50\ Sm^3/Sm^3$

$$\frac{\sigma_o}{\sigma_{od}} = 32.0436R_s^{-1.1367} \tag{A.139}$$

$$\sigma_o = \frac{\sigma_o}{\sigma_{od}} \sigma_{od} \tag{A.140}$$

σ_{od} - Dead oil surface tension [dynes/cm]
σ_o - Surface tension of live oil [dynes/cm]
T - Temperature [$^\circ C$]
γ_{api} - Api gravity [$^\circ API$]
R_s - Solution GOR [Sm^3/Sm^3]

A.7 Pumping capacities

It is important to know if the mud pumps pumping the kill fluid through the relief well are able pump the calculated kill rate. The kill fluid goes down the relief well and up the blowing wellbore. Three limitations that can become a problem are: 1. The required kill rate - the mud pumps may not be able to pump that high, 2. The required pressure to pump the kill fluid and 3. The required energy input to the mud pump.

Kill rate
The kill rate must be high enough to dynamically kill the blowing well and not too high so the weakest formation fractures. The kill rate is calculated as described in the kill rate procedure.

Pump pressure
Commonly the highest required pump pressure is observed when the hydrocarbon influx from the reservoir stops, (Warriner and Cassity, 1988) describes it as ”Maximum pump pressure during the kill operation will occur during the transition from the dynamic to the hydrostatic kill phase.”. This is a two sided cause, first the reservoir is not able to give pressure support since the bottom hole pressure has exceeded the reservoir pressure, and secondly the pressure in the interception point has increased due to the increased content of kill fluid in the blowing wellbore. The increased kill fluid content reduces the hydrostatic difference of the relief well and blowing well, and the U-tubing effect is minimal.

A typical pump pressure vs time graph is shown in figure A.22, where the sudden drop is the transition from dynamic kill to static kill where the pump rate is reduced.

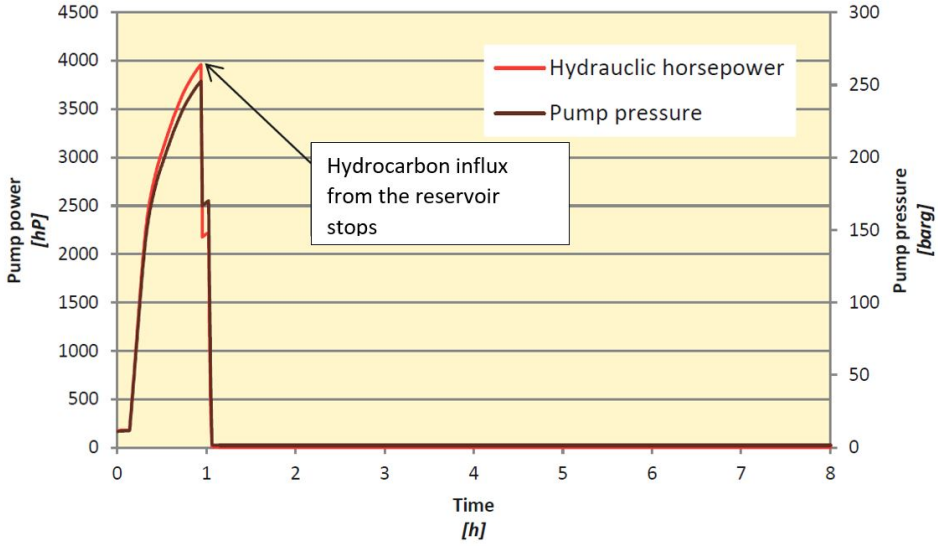

Figure A.22: A typically pump pressure vs time chart, courtesy of (Ranold, 2018)

The required mud pump discharge pressure is a function of the hydrostatic pressure difference between the two wells and the frictional pressure through the entire flow system, it can mathematically be described with equation A.141. (Warriner and Cassity, 1988)

$$p_{mp} = p_{IP} - p_{IP,h} + \sum_{i=1}^{n} p_{f,i} \tag{A.141}$$

p_{mp} - mud pump pressure
p_{IP} - Flowing pressure at the interception point between the blowing well and the relief well
$p_{IP,h}$ - Hydrostatic pressure at the interception point for the relief well
$p_{f,i}$ - Frictional pressure for the different flow path segments through the relief well

The difference between the flowing pressure at the interception point and the hydrostatic pressure at the same depth is easily calculated when the pressure profile along the wellbore already is obtained. The hydrostatic pressure is just a function of the density, the true vertical depth and the gravitational constant.

The mud pumps must also supply the frictional pressure loss from the pump outlet through the relief well to the interception point and through the blowing well. The frictional pressure loss through the blowing well is accounted for in the flowing pressure at the interception point as calculated by the kill procedure. The simulator calculates the friction pressure through the relief well for two different flow paths, 1. surface lines, choke/ kill line and annulus, 2. surface line and drill pipe. Since the kill fluid is single-phase the Darcy-Weisbach friction loss equation may be used, equation A.142. (Mukherjee and Brill, 1999)

$$\Delta p = \left(f_D \frac{\rho}{2} \frac{v^2}{D_h} \right) L \tag{A.142}$$

Δp - Differential friction pressure [Pa]
f_D - Darcy friction factor
ρ - Fluid density [kg/m^3]
D_h - Hydraulic diameter [m]
L - Length -[m]

When the friction pressure is calculated over the different flow segments and the difference between the hydrostatic and flowing pressure is known the maximum mud pump pressure is obtained. The mud pump pressure output and the pump rate are dependent on the liner configuration of the mud pump, which will not be discussed further. A typical relationship between the mud pump pressure and pump rate capacity are shown in figure A.23.

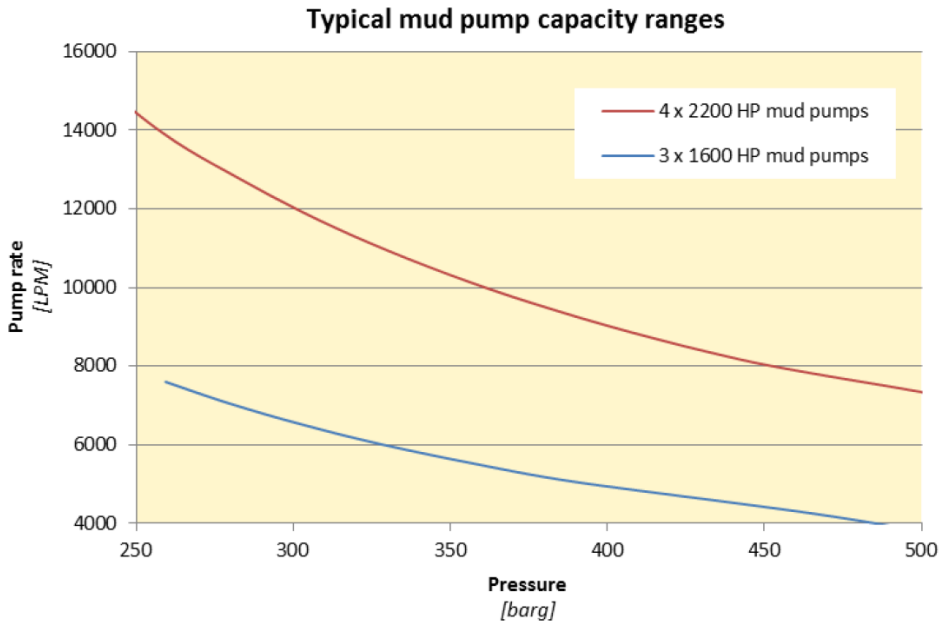

Figure A.23: Caption

The normal killing procedure is to pump through the annulus and connect one pump to the drill string for pressure monitoring. If the kill rate exceeds what the pumps can pump, the cement unit can be used to pump through the drill string. It is also possible to connect several units (the rig and supply ships) through a relief well injection spool (RWIS) to overcome the high kill rate and/or high mud pump pressure requirements. The principle of the RWIS is presented in figure A.24. During some dynamic kill operation two relief wells is required.

Required energy input
When the required maximum mud pump pressure is calculated the required energy output of the generators can be calculated with equation A.143. The pump efficiency factor is assumed to be 0.85 (85%).

$$HP = 1.341 \frac{\Delta p \cdot Q}{600\nu} \tag{A.143}$$

HP - Horsepower [HP]
Δp - Pressure differential [Bar]
Q - Pump rate [LPM]
ν - pump efficiency factor

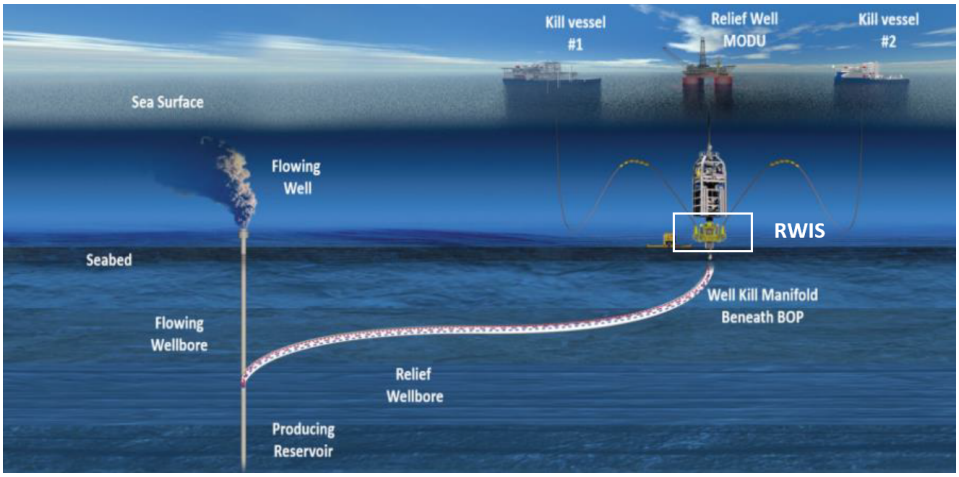

Figure A.24: The Relief Well Injection Spool, courtesy of (AddEnergy, 2018)

A.8 Assumptions

A.8.1 Only oil flows below the intersection point

One assumption which may be brutally wrong is that no kill fluid is below the intersection point during the kill procedure. Since the kill fluid has a higher density than the hydrocarbons, it will sink down due to the gravitational forces. During a blowout and kill procedure the hydrocarbon velocity below the intersection point may be high enough to avoid the settling of kill fluid. Some theory to back this up:

The terminal settling velocity of a sphere can be calculated based on Stoke's law, equation A.144. Some of the assumptions that must be fulfilled are: Laminar flow, spherical particles, homogeneous material and that the particles do no not interfere with each other.

$$v_s = \frac{gD^2(\rho_s - \rho_f)}{18\mu} \tag{A.144}$$

v_s - Terminal settling velocity [m/s]
g - Gravitational acceleration 9.81 $[m/s^2]$
D - Diameter of the sphere [m]
ρ_s - Density of the sphere $[kg/m^3]$
ρ_f - Density of the surrounding fluid $[kg/m^3]$
μ - Dynamic viscosity of the surrounding fluid [kg/(m*s)]

The article (Souza et al., 2015) gives a simple relationship between the water content of an oil-water mixture and the water droplets size.

$$d_w = 0.986WC - 9.104 \tag{A.145}$$

d_w - Water droplet size [µm]
WC - Water content [$\%$]

By using a simple example where the kill fluid has a density of 1800 kg/m^3, the oil has a density of 850 kg/m^3, oil viscosity of 2cp and a kill fluid content of 60$\%$ one can calculate the settling velocity of a kill fluid drop. This require the assumption that the kill fluid behave as water. All the different additives of a kill fluid will most likely make this assumption poor even for a water based kill mud.

By using equation A.145 the calculated diameter of the kill fluid drops is 50.1 µm. By the use of Stoke's law, equation A.144, the terminal settling velocity of a kill fluid drop is $v_s = \frac{9.81*(50.1*10^{-6})^2*(1800-850)}{18*2*10^{-3}}$ = $6.5 * 10^{-4}$ m/s.
With a settling velocity of $6.5 * 10^{-4} m/s$ it takes 25.6 minutes for the drop to sink 1m in a stagnant fluid. In some cases, the last casing and the target for the interception point is set in the caprock above the reservoir with only a few meters down to the reservoir. The distance between the last casing shoe and the top of the reservoir is rarely less than 5m, requiring two hours for the first kill fluid drop to reach the top of the reservoir. The blowout rate is determined by the bottom hole pressure and even with the entire 5m filled with kill fluid only small increase is made to the pressure. During a blowout and kill situation the fluids are flowing, the viscous forces from the upwards hydrocarbon flow will drag the sinking kill fluid drop upwards.

The assumption is still that below the interception point only hydrocarbons flow, how low can the blowout rate be for an 8.5"-section for this assumption to be valid based on the example above? A fluid velocity equal to the sinking velocity of the kill fluid drop shall be able to make the drop stagnant, a higher fluid velocity shall be able to lift the drop. The flow rate in a pipe is easily calculated with equation A.146.

$$q = v * A = v * \frac{\pi}{4} * D^2 * 0.0254^2 \tag{A.146}$$

By setting v = $6.5 * 10^{-4} m/s$ and D= 8.5" the calculated flow rate is $2.38 * 10^{-5}$ m^3/s or 2.06 m^3/day. Having a blowout rate of only 2.06 m^3/day is small and a realistic blowout will most likely have a higher blowout rate.

Based on this example the assumption that there is no kill fluid below the interception point may not be too bad during the actual kill process. Even if the kill fluid is allowed to sink, it will sink with a low velocity and the impact it will have on the bottom hole pressure is marginal during the time scale of a dynamic kill procedure. When the well is killed and the bottom hole pressure is higher than the reservoir pressure, no hydrocarbons will flow from the reservoir. This will allow the kill fluid droplets to sink, filling the wellbore between the interception point and the reservoir with kill fluid.

A.8.2 Justification of a stationary simulation model

One limitation in the created simulator is that only a stationary model is used and not a transient model. As discussed several times in the thesis this should not affect the required kill rate, but only the possibility to obtain the required time to reach dynamic kill. In this section a small justification of why the stationary model should give the correct kill rate is presented.

A stationary model assumes that the same fluid that enters the bottom of the well are the same as leaves the outlet at all times. The stationary model accounts for gas that goes out of solution.

A transient model includes the time, and the fluid that enters the wellbore does not have to equal the fluid that leaves the wellbore. For a couple of minutes after the mud pumps are started and kill fluid is injected into the blowing wellbore, only hydrocarbons flow out of the wellbore.

In section 6.3.6 the detailed kill rate procedure was explained for Well 1a. If a kill rate is not high enough to stop the blowout an equilibrium blowout rate will occur based on the flowing bottom hole pressure and the inflow performance relationship. Table 6.11 show the equilibrium blowout rate for each kill rate in the example. In the example the original blowout rate was 6654 Sm^3/day, an equilibrium was met for the kill rate of 4250 LPM and the resulting blowout rate was 1553 Sm^3/day. The well is clearly not killed.

A kill rate of 4500 LPM was enough to kill the well. Table 6.12 shows the flowing bottom hole pressure and the corresponding rate after each blowout iteration loop for a constant kill rate. In the first iteration it is assumed that the blowout rate is equal to the original blowout rate (6654 Sm^3/day) without injected kill fluid, the FBHP was 118.6 bar. The calculated flowing bottom hole pressure after the first iteration was 381.7 bar. It is a fact that the FBHP increases as the kill fluid is injected, and the corresponding blowout rate decreases. The reservoir will never produce a constant blowout rate for the duration it takes from the kill fluid is first injected until it flows out of the well head. After 2 minutes of injecting, $9m^3$ of kill fluid is injected, which certainly will increase the FBHP and decrease the blowout rate. A transient model can simulate this behavior, but a stationary model cannot, i.e. a transient model is able to reduce the blowout rate for each time unit.

Table 6.12 shows that the simulator is not able to find an equilibrium between the kill rate of 4500 LPM and a blowout rate greater than zero. If one looks at the entire blowout iteration loop in this table, the same behavior as a transient model is observed. The kill rate is always 4500 LPM and the blowout rate is decreasing, one may call it a semi-transient model.

However, it cannot be argued that a fully transient model is preferred. This will give the required pumping time to reach dynamic kill. One can also calculate the hydrocarbon content in the wellbore when hydrocarbon influx stops, and the pressure profile will be much more accurate.

A.9 Alterations done to the Orkiszewski's correlation

In the development of the blowout and kill simulator several struggles related to the multiphase pressure calculation with Orkiszewski's method were encountered. Three of these obstacles is discussed below as well as the alterations done to the original correlation given by (Orkiszewski, 1967). One possible reason for encountering these obstacles is that the high flow rates of a blowout and kill situation is outside the viable range of parameters in the Orkiszewski correlation.

Pressure discontinuity
One of the flaws are that the correlation have a discontinuity in the calculation procedure, which may cause instability during the inflow performance relationship - vertical lift performance matching(ProductionTechnology, 2017). This pressure discontinuity is observed during the simulation of several wells used in this master thesis, one example is presented in table A.13. This example illustrates that by increasing the used blowout rate with $1 * 10^{-4}$ STB/d the calculated FBHP can increase with 4.52 psi when the pressure discontinuity is hit, while for the different flow rate increases the FBHP only increase with $4*10^{-5}$ psi. The pressure discontinuity in this example represents a change of $\frac{4.52}{4*10^{-4}} * 100$ = 11,300,000% compared to the normal pressure change.

Table A.13: Orkiszewski correlation pressure discontinuity

Calculated Blowout rate [STB/day]	Used blowout rate [STB/day]	Flowing bottom hole pressure [psig]
8156.52737	8123.6646	3924.35489
8156.52696	8123.6647	3924.35493
8156.52656	8123.6648	3924.35498
8118.99091	8123.6649	3928.80762
8118.9905	8123.665	3928.80766
8118.9901	8123.6651	3928.80771

The liquid distribution coefficient
Another big disadvantage with the Orkiszewski correlation is observed for high flow rates, where the liquid distribution coefficient becomes largely negative. This will cause the calculated average density to become negative as well. The same observation was discussed by (Biria, 2013), who recommended the use of a a new equation to calculate the liquid distribution factor, equation A.147 to replace the equations presented by (Orkiszewski, 1967). The new equation does not remove the problem with a too large negative liquid distribution coefficient. A way to solve the problem is too choose a lower limit for the parameter. By further investigating the liquid distribution coefficient charts presented by (Orkiszewski, 1967), shown in figure A.25, one can see that the lowest liquid distribution coefficient is -0.1 and -0.22 for oil and water, respectively. The velocities used in these charts ranges from 1-60 [ft/s]. It will be wrong to use the same equations as presented by Orkiszewski for flow rates that extend beyond the range used in the original paper.

$$\Gamma = \frac{0.013log(\mu_L)}{d^{1.38}} - 0.287 - 0.162log(v_m) - 0.428log(d) \tag{A.147}$$

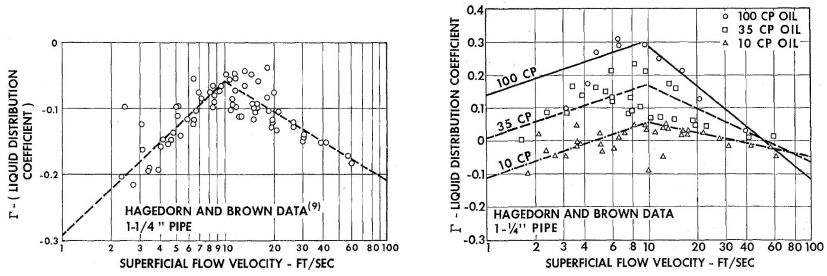

(a) **(b)**

Figure A.25: The liquid distribution coefficient Γ for a) water and b) oil (Orkiszewski, 1967)

To be able to account for the viscosity and diameter in the determination of a lower bound of the liquid distribution coefficient, one approach is to use the original equations published by (Orkiszewski, 1967) and set the velocity to maximum 100 ft/s. Another approach which does not take the viscosity or diameter into account is to choose a minimum value based on the plots shown in figure A.25. Both these methods have been tested out, but without success. For high flow rates the density term can still become negative.

Since Orkiszewski refer that the density term in the slug flow phase comes from (Griffith and Wallis, 1961b), the original equation for the density term is used. The density term used in slug flow presented by (Griffith and Wallis, 1961b) is shown in equation A.148. The implementation of the (Griffith and Wallis, 1961b) original density term for slug flow in the Orkiszewski multiphase pressure calculations was a success, the density is no longer negative for high flow rates, even without adjusting the original equations for the liquid distribution factor. The density term in equation A.148 is used to calculate the average density before equation A.76 is used.

$$\rho_a = \rho_l \left[\frac{q_l + v_b A_p}{q_l + q_g + v_b A_p} \right] + \left[\frac{\rho_g q_g}{q_l + q_g + v_b A_p} \right] \tag{A.148}$$

ρ_a - Average density term in slug flow [lb/ft^3]
ρ_i - Density of phase i [lb/ft^3]
q_i - Down hole flow rate of phase i [ft^3/s]
v_b - Bubble rise velocity [ft/s]
A_p - Cross section area of the pipe [ft^2]

Bubble rise velocity

Orkiszewski presented a procedure to calculate the bubble rise velocity based on the work of (Griffith and Wallis, 1961b), see equation A.63 to A.70. This procedure is used to calculate the C_1 and C_2 coefficients presented in figure A.26 which are used in equation A.149 to calculate the bubble rise velocity. At higher flow rates the Reynolds number will become high, which affect the calculations of the bubble rise velocity and the Bubble Reynolds number (N_b), i.e. an infinite Reynolds number will result in an infinite bubble rise velocity and Bubble Reynolds number.

$$v_b = C_1 C_2 \sqrt{g D_p} \tag{A.149}$$

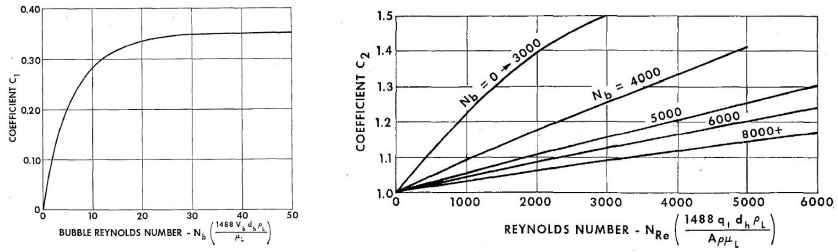

(a) **(b)**

Figure A.26: C1 and C2 coefficient for bubble rise velocity , (Orkiszewski, 1967)

One can see from right side of figure A.26 that a trend is present where the slope decreases with an increasing Bubble Reynolds number. In the original paper by (Griffith and Wallis, 1961b) this trend was discussed, "It seems logical, though, that as the velocity profile becomes flatter at large pipe Reynolds number, C_2 should approach 1. This appears to be the case" (Griffith and Wallis, 1961b). On the left side of figure A.26 the c_1 coefficient approach 0.35 for a relatively low Bubble Reynolds number. By using these values in equation A.149 and a pipe diameter of 12" the bubble rise velocity becomes 1.99 ft/s. The experimental apparatus used by (Griffith and Wallis, 1961b) varied the pipe diameter between 1/2, 3/4 and 1 in. how well this correlation applies to larger pipes such as production casing or drilling riser in the event of a blowout is not described.

Appendix B

Automatically generated blowout and kill report

In this Appendix chapter the automatically generated blowout and kill report from well 1a is presented. The calculations of the blowout rate and the kill rate for surface blowout were gone detailed gone through in chapter 6. All the other scenarios calculated are presented in the generated report. The generated report is the end result of the simulator.

Blowout and kill report

Well 1a

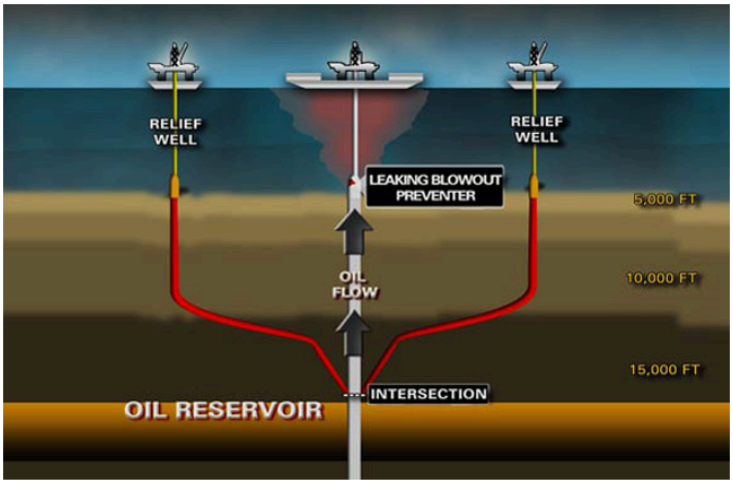

Created in

MATLAB R2020a

Vetle Arild Mathisen

27-May-2020

Chapter 1. Preface

This report is a product of a master thesis written by Vetle Arild Mathisen at NTNU during the spring of 2020. The master thesis describes the theory behind the simulator and how the simulator works. This automatically generated report is based on the structure of the blowout and kill reports provided by Ranold.

Table of Contents

Chapter 2. Input values

Most of the data input given from the user are shown in Table 2.1 to Table 2.8. The entire simulation is based upon the provided information. The input data covers rig elevation, well design, relief well design, reservoir fluid and reservoir productivity parameters.

Table 2.1. General rig/seabed values

Total depth	Wellhead depth	Seabed depth	Rig floor elevation	Pressure at wellhead
m RKB TVD	m RKB TVD	m MSL	m RKB	Bar
3565	410	386	79	39

The well design used in the simulation is shown in Table 2.2, when the fluid flow through the annulus the drill string design shown in Table 2.3 is used together with the inner diameter of the surrounding casing at each depth. Figure 2.1 shows the well schematic for the used well.

Table 2.2. Well design

Well section	OD	ID	Top	Bottom
Unit	[in]	[in]	[m RKB]	[m RKB]
Riser	18	18	0	410
Casing	30	28	410	470
Casing	20	18	410	1200
Casing	13.375	12.5	410	2150
Casing	9.625	8.7	2150	3330
Open Hole	8.5	8.5	3330	3565

Table 2.3. Drill string components

Drill string part	OD	ID	Top	Bottom
Unit	[in]	[in]	[m RKB]	[m RKB]
BHA	7	4	3180	3330
Drill pipe	6	4	0	3180

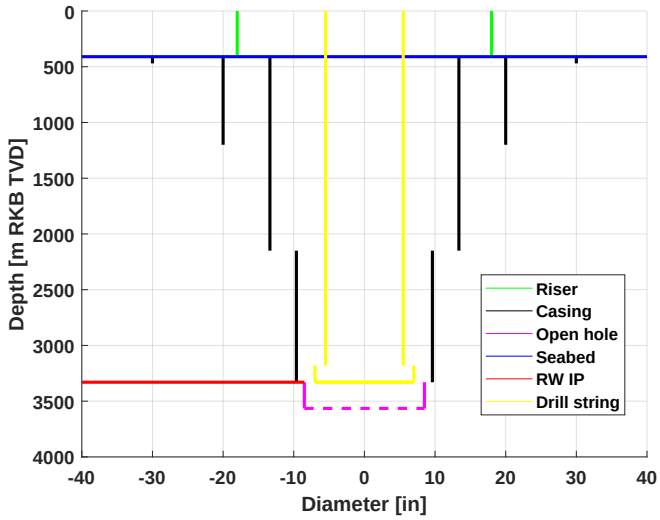

Figure 2.1. Well schematic of the simulated well

A relief well is used to kill the well and a simplified relief well trajectory is used for the simulated kill process. The relief well trajectory is used to calculate the maximum required mud pump pressure and the heat change of the kill fluid. Table 2.4 presents the different parts of the relief well where the kill fluid flows through. The relief well trajectory is a simple build, hold and drop trajectory and is based on the parameters shown in Table 2.5. The calculated relief well trajectory is presented in Figure 2.2.

Table 2.4. Rellief well design

Drill string part	OD	ID	Top	Bottom
Unit	[in]	[in]	[m RKB]	[m RKB]
Surface lines	5	4	0	75
Kill and choke lines	4	3.5	0	410
Casing	9.625	8.75	0	3330
Drill pipe	5.5	4	0	3190
BHA	6.5	4	3190	3250

Table 2.5. Rellief well trajectory parameters

IP	KOP	Northing	Easting	BU rate	Build angle	Drop rate	Drop angle
m RKB	m RKB	m	m	deg/30m	deg	deg/30m	deg
3330	500	900	435	2	20	2	20

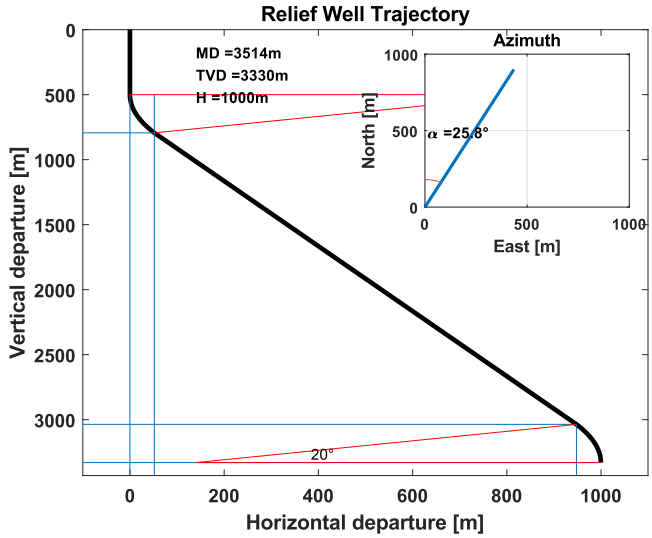

Figure 2.2. Relief well trajectory used in the simulations

The reservoir fluid is important in the calculation of the flowing bottom hole pressure and the resulting blowout rate. Table 2.6 shows the used reservoir fluid and reservoir productivity parameters. The saturation pressure of the of the fluid is only used for the inflow performance relationship, a calculated saturation pressure is used for the multiphase pressure calculations. More on how the different reservoir fluids behave for the given temperature and pressure is presented in Chapter 2.

Table 2.6. Reservoir fluid and reservoir productivity parameters

Oil gravity	Gas gravity	GOR	Saturation pressure	Reservoir pressure	PI	AOF
s.g.	s.g.	Sm3/Sm3	Bar	Bar	Sm3/d/bar	Sm3/d
0.838	1.2	115	165	597	14	7374

The interception point between the relief well and the blowing well is shown in Table 2.7 together with the viscosity and density of the kill fluid. The number of kill fluid density steps gives the number of different kill densities simulated. The density increase is linear going from the minimum to maximum density.

Table 2.7. Parameters for kill simulation

Intersection Point	Kill fluid viscosity	Kill fluid density range min	Kill fluid density max	Number of kill fluid density steps
m RKB	cp	s.g.	s.g.	-
3330	10	1.8	2.2	4

Several material properties used in the simulation are shown in Table 2.8. These material properties are not an input from the user, but assumed in the simulator.

Table 2.8. Properties of different materials used in the simulation

Parameter	Unit	Value
Thermal conductivity of Sandstone	W/(m*K)	3.06
Thermal conductivity of cased interval	W/(m*K)	0.95
Thermal conductivity of choke line	W/(m*K)	0.033
Heat capacity of hydrocarbon mix	J/kg/K	2300
Heat capacity of kill fluid	J/kg/K	4200
Temperature of injected kill fluid	°C	20
Temperature of seabed	°C	4
Temperature of sea surface	°C	15
Thermal conductivity of riser	W/(m*K)	0.24
Roughness of steel pipes	in	0.00177
Roughness of formation	in	0.06

The created simulator gives the user the opportunity to choose between two multiphase pressure drop correlations and two PVT correlations sets. The chosen correlations are presented in Table 2.9.

Table 2.9. Chosen correlations used in this simulation

Correlation type	Chosen correlation
Multiphase pressure drop correlation	Olgjenka
PVT correlation set	Standing

Chapter 3. Temperature, inflow performance relationship and reservoir fluid

3.1. Temperature

The temperature in the surrounding formation is an important factor when calculating the heat loss of the flowing fluid. The temperature of the surrounding formation is presented in figure 3.1. The calculated temperature inside the blowing wellbore for a surface blowout is presented in figure 3.2. During a kill process the temperature of the kill fluid and the blowing fluid will mix, thus knowing the temperature of the kill fluid is important. The calculated temperature profile of the kill fluid is shown in figure 3.3 for the relief well with a kill rate as shown on the top of the figure.

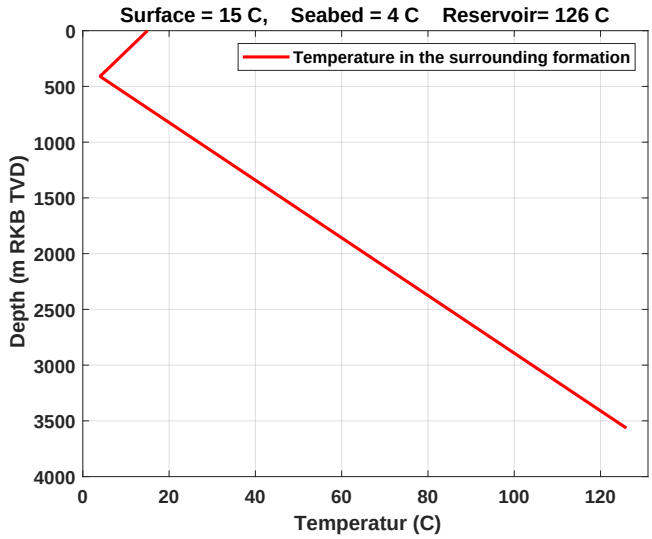

Figure 3.1. Calculated temperature inside the wellbore during openhole blowout

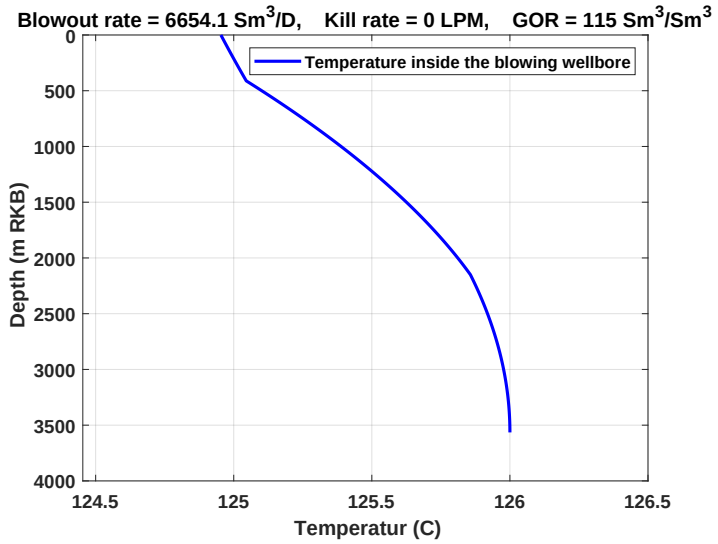

Figure 3.2. Calculated temperature inside the wellbore during openhole blowout

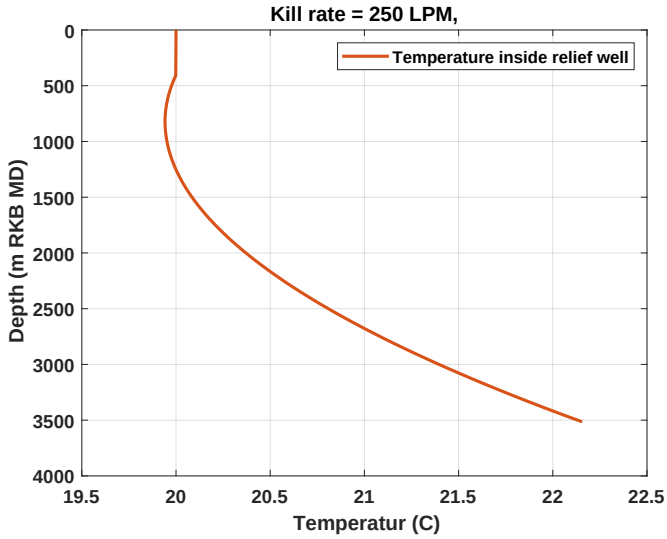

Figure 3.3. Calculated temperature inside the relief well with the kill rate as shown

3.2. Inflow performance relationship

The inflow performance relationship is based on the simple Darcy equation when the flowing bottom hole pressure is above the saturation pressure and the Vogel equation when the flowing bottom hole pressure is below the saturation pressure. The inflow performance relationship is used together with the flowing bottom hole pressure to determine the blowout rate. The figure below shows the inflow performance relationship for the simulation and is based on the input values. The productivity index (J), which is a quantification of how much the reservoir is able to produce for a given drawdown (reservoir pressure - bottom hole pressure), the absolute open flow potential (AOF) which is an theoretical value for the maximum blowout rate is also presented in the figure. The AOF will never happen since the flowing bottom hole pressure always will be greater than zero due to the hydrostatic pressure and the friction of the flowing fluid.

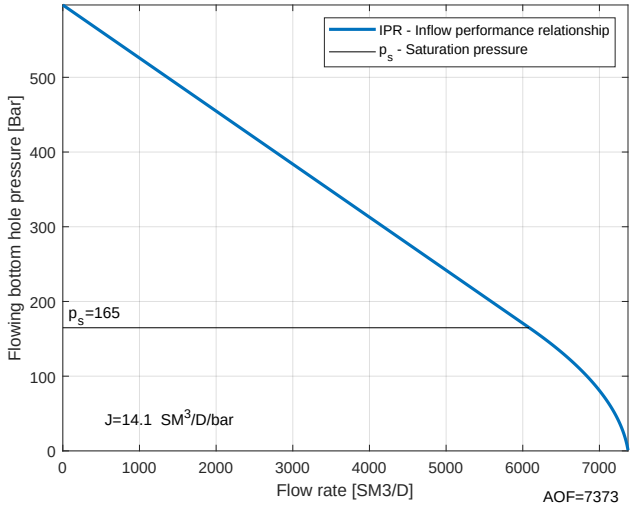

Figure 3.4. Inflow performance relationship

3.3. Reservoir fluid - PVT

Some of the most important pressure-volume-temperature (PVT) properties used in the simulator is presented below. The pressure ranges from reservoir pressure to surface pressure. The parameters are shown with three different temperatures: the reservoir temperature, the interception point temperature of the kill fluid and an average of the two temperature. In the simulator the actual temperature profile at each depth is used to calculate the PVT properties.

The PVT properties are calculated with the Standing-correlation as chosen by the user.

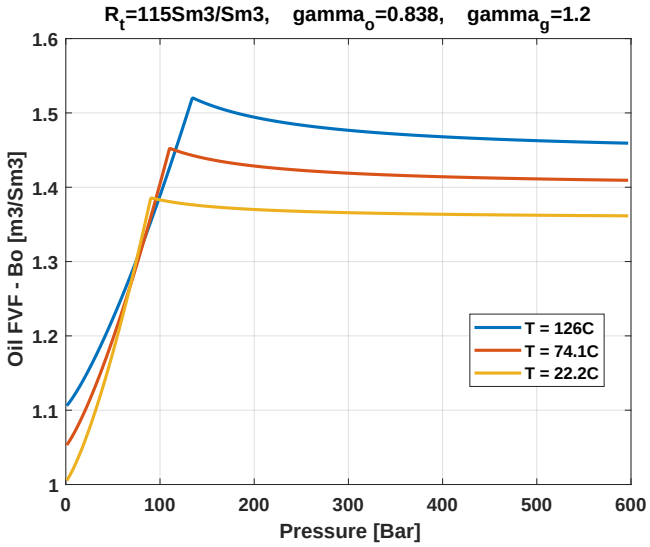

Figure 3.5. Calculated oil formation volume factor (Bo), from reservoir pressure to atmospheric pressure

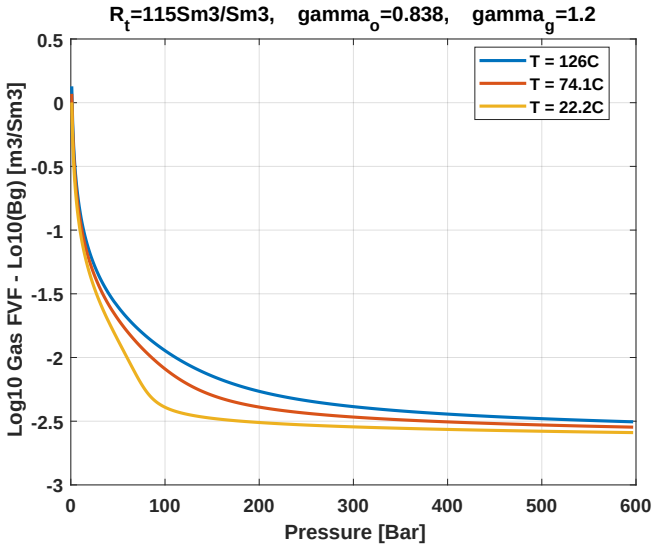

Figure 3.6. Calculated gas formation volume factor (Bg), from reservoir pressure to atmospheric pressure

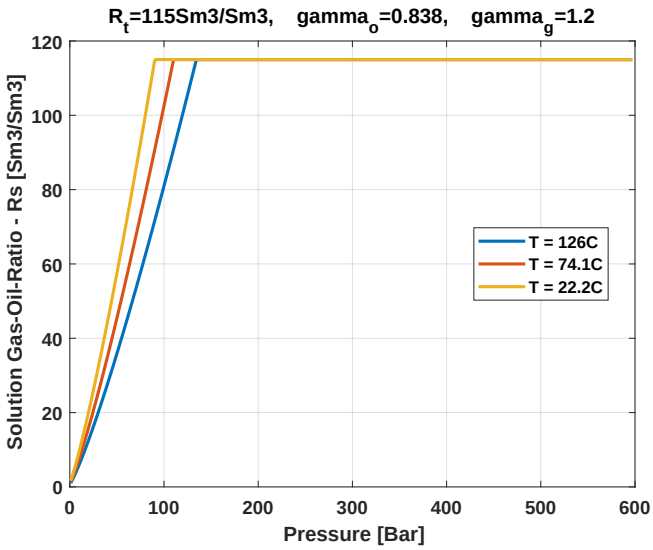

Figure 3.7. Calculated solution Gas-Oil-Ratio (Rs), from reservoir pressure to atmospheric pressure

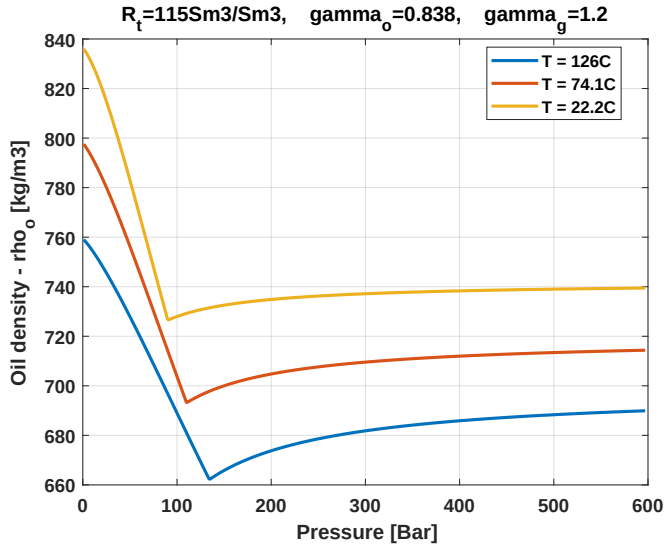

Figure 3.8. Calculated oil density, from reservoir pressure to atmospheric pressure

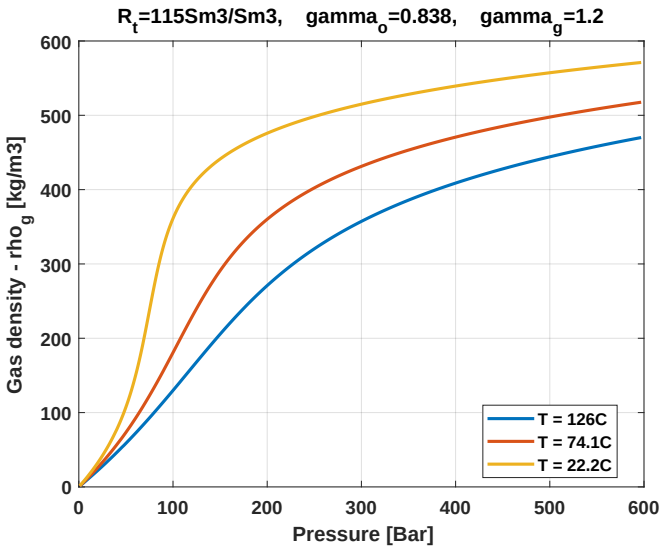

Figure 3.9. Calculated gas density, from reservoir pressure to atmospheric pressure

Chapter 4. Blowout rates

A blowout release point may be located either on the surface, seabed or underground. The underground blowout is neglected in this simulator. The reservoir fluid may flow through three different channels: through an open/cased hole, through the inside of the drill string or in the annulus. The flow path through drill pipe is not calculated in this simulator. The three different blowout flow paths are shown in figure 4.1. The reservoir may either be fully penetrated or partly penetrated, the partly penetration is not used in this simulation. The blowout preventor (BOP) may be open or partly closed, since an open BOP status is more conservative the restricted BOP is not included. Based on more than 30 years of blowout statistics figure 4.2 is created which present the risk of each blowout combination.

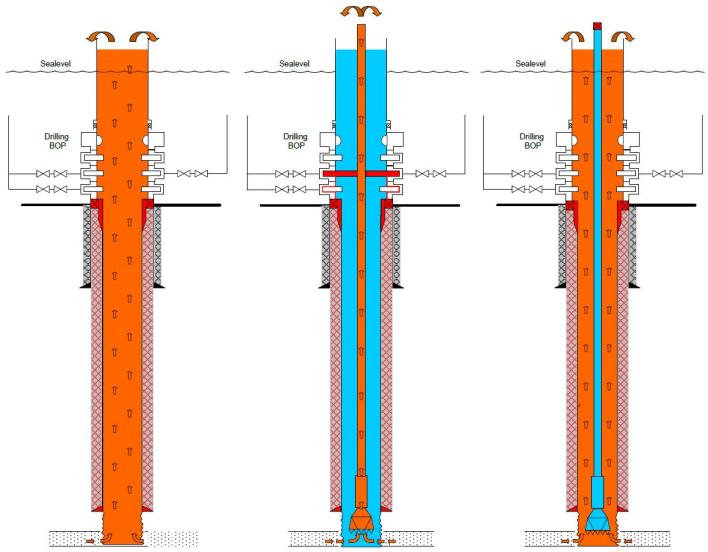

Figure 4.1: possible blowout flow paths, courtecy of Ranold.

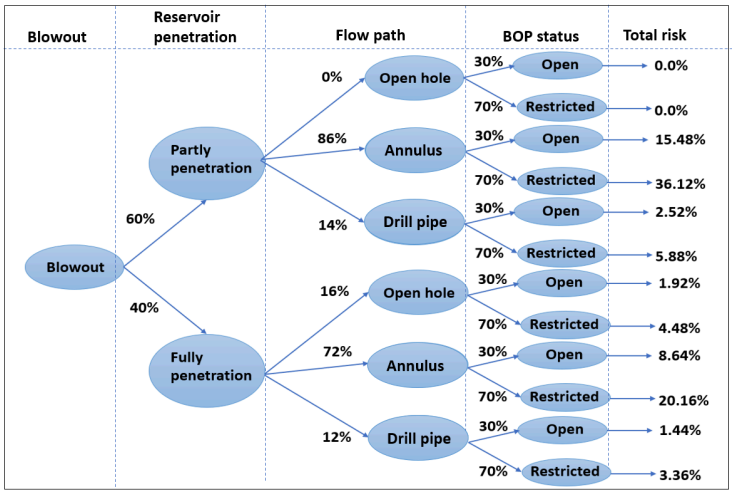

Figure 4.2: Blowout risk statistics for appraisal wells from the last 30 years.

The calculated blowout rates for this simulation is presented in Table 3.1 for the different blowout scenarios listed. These blowout rates are based upon the concept of IPR-VLP-matching. The inflow performance relationship (IPR) quantify how much the reservoir is able to produce for a given bottom hole pressure. The vertical lift performance (VLP) quantify the required pressure the well need to be able to produce/lift a given fluid rate. Figure 4.3 illustrate the process of IPR-VLP-matching for a general well. The interception between the IPR and the VLP gives the highest rate the reservoir can produce that the well is able to lift out, the resulting rate is called the blowout rate

The multiphase pressure drop correlation Olgjenka is used together with the Standing - PVT correlation the calculate the flowing bottom hole pressure. The user can choose between two multiphase pressure correlations: Olgjenka and Orkiszewski and two PVT correlation sets: Standing or Glasø. The combination of correlations will affect the calculated results slightly.

Table 4.1. Blowout rates

Blowout type	Oil rate	Gas rate	FBHP	Risked oil rate	Risked gas rate
Unit	Sm3/D	MSm3/D	Bar	Sm3/D	MSm3/D
Open hole to seabed	5300	0.6	220.5	101.8	0
Open hole to surface	6654	0.8	118.6	127.8	0
Annulus to seabed	4183	0.5	299.8	361.4	0
Annulus to surface	4915	0.6	247.8	424.7	0

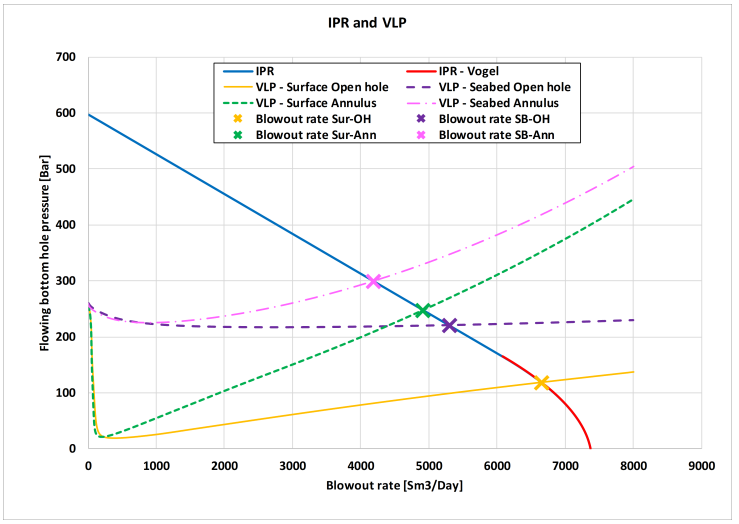

Figure 4.3: The IPR-VLP-matching process for the different blowout scenarios.

Chapter 5. Kill rates

The kill rate is calculated in the same way as the blowout rate, but kill fluid is present above the interception point. The increased flow rate due to the kill fluid increases the friction loss, and the higher weight of the kill fluid increase the hydrostatic pressure. The calculated kill rates for the simulated well is shown in Table 5.1 for an open/cased hole to seabed and in Table 5.2 for a open/cased hole to surface. The required kill rate to stop an annulus blowout or a drillpipe blowout was neglected since the open hole is the most conservative scenario.

During the development of the simulator a calibration factor formula was created. This formula is used to calibrate the kill rates based on several simulations conducted by the industry standard blowout and kill simulators. The "best prediction" gives the best predicted kill rate based on the calibration formula, "Not adjusted" gives the calculated kill rate based on the multiphase pressure drop calculations without any calibrations. The higher and lower rate gives the P10 and P90 distributed kill rates

Table 5.1. Kill rates - Open/cased hole to seabed

Prediction	Calibration constant value	Kill density	Kill rate	Kill density	Kill rate	Kill density	Kill rate	Kill density	Kill rate	Kill density	Kill rate
[-]	[-]	[s.g]	[LPM]	[s.g]	[LPM]	[s.g]	[LPM]	[s.g]	[LPM]	[s.g]	[LPM]
Best prediction	0.93452	1.8	9500	1.9	6750	2	3750	2.1	2750	2.2	2250
Higher rate	0.82096	1.8	14500	1.9	12750	2	10750	2.1	8500	2.2	6000
Lower rate	1.0481	1.8	3000	1.9	2250	2	2000	2.1	1750	2.2	1500
Not adjusted	1	1.8	5750	1.9	3000	2	2500	2.1	2000	2.2	1750

Table 5.2. Kill rates - Open/cased hole to surface

Prediction	Calibration constant value	Kill density	Kill rate	Kill density	Kill rate	Kill density	Kill rate	Kill density	Kill rate	Kill density	Kill rate
[-]	[-]	[s.g]	[LPM]	[s.g]	[LPM]	[s.g]	[LPM]	[s.g]	[LPM]	[s.g]	[LPM]
Best prediction	0.88689	1.8	9500	1.9	6500	2	5000	2.1	4250	2.2	3750
Higher rate	0.81064	1.8	13500	1.9	11500	2	9000	2.1	6250	2.2	5000
Lower rate	0.96314	1.8	5250	1.9	4250	2	3750	2.1	3250	2.2	3000
Not adjusted	1	1.8	4500	1.9	3750	2	3250	2.1	3000	2.2	2500

Chapter 6. Kill rates and pumping capacities - best prediction

The required maximum mud pump discharge pressure for the different kill rates and kill fluid density are shown for the best predicted value. The pressure at the interception point and the flowing bottom hole pressure are also shown. Table 6.1 shows the values for a seabed blowout and Table 6.2 shows the value for a surface blowout. The required maximum mud pump discharge pressure is calculated for two flow paths. The first flow path goes through surface lines, down choke and kill line and through the annulus. The other flow path goes through the surface lines and through the inside of the drill string.

One limitation to the simulator is that the simulator does not use a transient model, making the required time to kill the well impossible to obtain. The rig must be able to store enough kill fluid to be able to kill the well, but the required amount to reach dynamic kill is not calculated. When the well is dynamically killed a new mud is injected to ensure no hydrocarbons are left in the wellbore and the hydrostatic pressure exceeds the reservoir pressure. Two times the wellbore volume is used for this static circulation and the volume is presented the two tables below.

Table 6.1. Kill rates and pumping capacity - Open hole to seabed - Best prediction

Kill fluid density	Kill rate	IP Pressure	FBHP	Max pump pressure - annulus	Energy input - annulus	Max pump pressure - drill string	Mud volume - static
s.g.	LPM	Bar	Bar	Bar	HP	Bar	m3
1.8	9500	584	597.8	615.4	15372.1	1146.5	517.9
1.9	6750	583.7	597.5	303.6	5388.5	595.2	517.9
2	3750	601.3	615.2	53.2	525	154.6	517.9
2.1	2750	625.6	639.4	< 30	< 500	52.6	517.9
2.2	2250	651.8	665.6	< 30	< 500	<30	517.9

Table 6.2. Kill rates and pumping capacity - Open hole to surface - Best prediction

Kill fluid density	Kill rate	IP Pressure	FBHP	Max pump pressure - annulus	Energy input - annulus	Max pump pressure - drill string	Mud volume - static
s.g.	LPM	Bar	Bar	Bar	HP	Bar	m3
1.8	9500	584	597.8	614.3	15344.6	1145.4	517.9
1.9	6500	583.7	597.5	280.3	4791.1	551.8	517.9
2	5000	601.3	615.2	151.2	1987.2	324.6	517.9
2.1	4250	625.6	639.4	96.2	1075.3	229.7	517.9
2.2	3750	651.8	665.6	62.4	614.9	172.4	517.9

Chapter 7. References

Front page picture - relief-well|Coastal Care. URL:https://coastalcare.org/2010/08/feds-no-timeline-for-completing-gulf-relief-well/relief-well-2. [Online; accessed 19. May 2020].-

Master Thesis - Mathisen, V. 2020. Blowout and kill simulator for vertical wells, NTNU.

Ranold - Ranold, 2018. Technical report - blowout and dynamic wellkill simulations.

Appendix C

Matlab code

This Appendix chapter describes all the different scripts used in the created simulator. In total 32 scripts with varied size are required to run the simulations. The different script names, the purpose of each script and the size of each script is presented in table C.1. In the rest of this Appendix chapter the actual Matlab scripts are presented. The scripts ”Olgjenka_correlation” and ”zfak” are taken from (Asheim, 2020). The ”Olgjenka_correlation” script is altered, but some parts of the original code remains, while the ”zfak” script is unaltered.

Table C.1: The different scripts used in the simulator

Script name	Code lines	Purpose
The_Simulator	324	Get input file, prepare the different blowout and kill scenarios
Build_Relief_well	170	Get the relief well trajectory
Sort_well	17	Create a vector of depth vs diameter for the wetted tubulars
IPR	135	Calculate the inflow performance relationship
Prod_index	48	Calculate the productivity index
Plot_well	55	Plot the wellbore only in contact with the flowing fluid
Run_non_linear_reg	47	Calculate the kill rate calibration factor
Run_scenario	347	Calculate the blowout rate and or kill rate for the scenario
Get_Temperature2	166	Get the temperature profiles in the wellbore and the formation
Get_IP_Temperature2	113	Get the temperature profile in the relief well
retrieve_diameter	34	Obtain the outer and inner diameter for the chosen depth
Orkiszewski _correlation	391	Calculate the pressure increase from Orkiszewski's correlation
Standing_PVT	144	Calculate PVT properties from the Standing correlation
Glaso_PVT	162	Calculate PVT properties from the Glasø correlation
zfak	52	Obtain the gas z-factor
colebrook	54	Calculate the friction factor with colebrook equation
Olgjenka_correlation	95	Calculate the pressure increase from the Olgjenka correlation
getBlowoutRate	22	Calculate the blowout rate for the given FBHP
Find_next_blowout _rate	68	Find the next blowout rate script 1
Find_next_blowout _rate_hard	202	Find the next blowout rate script 2
Find_next_blowout _rate_hard_blowout	80	Find the next blowout rate script 3
Report_preparator	161	Prepare the calculated data to be presented in the report
Report_plotter	163	Plot the figures that are used in the report
Plot_actual_well	78	Plot the well design used
RW_pump_annulus	92	Calculate the friction pressure in the annulus
RW_pump_dp	92	Calculate the friction pressure in the drillstring
report_gen	384	Generate the blowout and kill report
AOF_to_PI	17	Calculate the productivity index from the AOF
API2Gravity	3	Calculate the specific gravity from the API gravity
gravity2API	3	Calculate the API gravity from the specific gravity
PI_to_AOF	17	Calculate the AOF from the productivity index
Wellbore_volume	16	Calculate the volume of the wellbore
	3752	Lines of code and 32 scripts in total

Listing C.1: The_Simulator

```
%% This file will ask for input data within a excel file and run
%  the entire script for the blowout and kill simulator
clc
clear all
close all
%% Data from excel
global plot_this num raw
dbstop if error
set(groot,'defaultFigureVisible','off')
plot_this = "no";

[file,path]=uigetfile('.xlsm','',pwd);
location = char(strcat(path,file));
[num, raw, ~] = xlsread(location,'Locked','B4:T78');

if num(1,3)>0
    num(:,1)=[];
end

Kill_steps=num(16,6);

Sim_steps=4+2*Kill_steps;  %Total number of simulations
Kill_dens = num(13,6) + [zeros(1,4), repmat((0:Kill_steps)*num(15,6),1,2)];
tic
Matrix_blowout=strings([1,8]);
Header1 = [{'Blowout rate - OH to seabed'},{'FBHP'},{'Blowout rate - OH to surface'},{'FBHP'},{'Blowout rate - Annulus to seabed'},{'FBHP'},{'Blowout rate - Annulus to surface'},{'FBHP'}];
Header2 = [{'[Sm3/d]'},{'[Bar]'},{'[Sm3/d]'},{'[Bar]'},{'[Sm3/d]'},{'[Bar]'},{'[Sm3/d]'},{'[Bar]'}];
Matrix_blowout = [Header1; Header2; Matrix_blowout];


Matrix_kill_seabed=strings([4,2*(Kill_steps+1)]);
Header1 = repmat([{'Kill density'}, {'Kill rate'}],1,Kill_steps+1);
Header2 = repmat([{'[s.g]'}, {'[LPM]'}],1,Kill_steps+1);

Matrix_kill_seabed=[Header1; Header2; Matrix_kill_seabed];
Header1 = [{'Prediction'}, {'Calibration constant value'}];
Header2 = [{' [ - ]'}, {'[ - ]'}];
```

```
Col_12 = [Header1; Header2; strings([4,2])];

Matrix_kill_seabed = [Col_12, Matrix_kill_seabed];
Col_1 = [{'Best prediction'}, {'Higher rate'}, {'Lower rate'}, {'Not adjusted'}];
Matrix_kill_seabed(3:end,1) = Col_1;
Matrix_kill_surface=Matrix_kill_seabed;

Load_max = 4+8+8*Kill_steps;
Load_now = 0;

Blowout_rel = ["Seabed", "Surface", "Seabed", "Surface"];

Drill_p = ["No", "No", "Yes", "Yes"];


fprintf(' \n \n \n')
for N_sim = 1:(Sim_steps+2)

clearvars -except num N_sim raw Matrix_kill_surface Matrix_kill_seabed Kill_steps Kill_dens Sim_steps plot_this N_blowout i_simulated Blowout_rel Drill_p Matrix_blowout path  num_case raw_case N_cases N_case N_kills Matrix_cases Matrix_cases_result f_vektor Matrix_f f_ad f_adjust Loading Load_tot f_results going adjustment_dp dp_IP_seabed  dp_IP_surface Pressure_IP_surface Pressure_BH_surface Pressure_IP_seabed Pressure_BH_seabed Load_now Load_max
close all
%Loading=Loading+1;
%fprintf('Loading %1.0f of %1.0f \n', Loading, Load_tot)
% D           - Total depth [ft]
% D_wh        - Depth of well head [ft]
% d_t         - Tubing dia   meter [in]
% gamma_o     - Specific gravity of oil
% gamma_API   - API gravity of oil
% gamma_g     - Specific gravity of gas
% R_t         - Total gas-oil-ratio [SCF/STB]
% p_wh        - Wellhead backpressure [psig]
% q_os        - Surface flow rate of oil [STB/D]
% q_ws        - Surface flow rate of water [STB/D]
% T_s         - Flowing surface temperature [F]
% T_bh        - Flowing bottom hole temperature [F]


```

```
74
75      %User answers
76      global gamma_o gamma_API gamma_g gamma_k R_t q_os q_ws
            g_c T_bh T_s D DS D_sb well_sorted Drill_pipe
            Blowout_release Length_IP RW RW_t; % variables that
            are constant
77      global Materials Simulate p_s_true p_r  Depth_IP
            PVT_sim kill_viscosity
78
79
80
81  Unit = string(raw(5,6));
82  Wellhead = string(raw(6,6));
83  PI_calc = string(raw(7,6));
84
85
86  if N_sim < 5
87  Simulate = "Blowout" ;  %raw(5,9);
88  Drill_pipe = Drill_p(N_sim); %string(raw(8,6));
89  Blowout_release = Blowout_rel(N_sim); %string(raw(9,6));
90  elseif N_sim >4 && N_sim <= (5+Kill_steps)
91  Simulate = "Blowout and Kill" ;
92  Drill_pipe = "No";
93  Blowout_release = "Seabed";
94  else
95  Simulate = "Blowout and Kill" ;
96  Drill_pipe = "No";
97  Blowout_release = "Surface";
98  end
99  gamma_k = Kill_dens(N_sim);
100
101 %Materials
102 Materials = num(5:15,17);
103
104
105 %Well values
106 D = num(1,2) ; % ft
107 D_wh=num(2,2); %ft %ft RKB
108 D_sb=num(3,2)+num(7,2); %ft RKB
109 p_wh =num(4,2); %psi
110 T_s = num(5,2); %F
111 T_bh = num(6,2); %F
112 Rig_elevation= num(7,2); %must be changed to rig floor
        elevation
113
```

```
114
115
116
117 %Reservoir fluid values
118 gamma_o = num(24,2);
119 gamma_API = gravity2API(gamma_o);
120 gamma_g = num(25,2);
121 R_t = num(26,2); %SCF/STB
122 q_os = num(27,2); % STB/D
123 q_ws = num(28,2); % STB/D
124 p_s_true = num(29,2); %psi
125
126
127
128
129 %Productivity Index
130 %Reservoir rock values
131 if PI_calc == "Yes"
132 k=num(12,2); % mD
133 beta= num(13,2);
134 h_res = num(14,2)*0.3048;% m
135 h_p = num(15,2)*0.3048;  % m
136 theta = num(16,2); % Degree
137 r_e = num(17,2);%*0.3048; %m
138 r_w = num(18,2);%*0.3048; %m
139 p_r = num(19,2)/14.5038; % Bar
140 elseif PI_calc == "No"
141 % User given productivty index
142 J=num(57,2);          % STB/D/Psi
143 p_r = num(58,2)/14.5038; %bar
144 elseif PI_calc == "No - AOF"
145 AOF = num(59,2); %STB/D
146 p_r = num(58,2)/14.5038;  %Bar
147 %p_s_true = 164.8*14.5; %psi
148 J = AOF_to_PI(AOF,p_r,p_s_true); %STB/D/psi
149 end
150
151 Excel = string([D/3.28084, D_sb/3.28084, 8.7 , gamma_o,
        gamma_g, R_t/5.6145, p_s_true/14.5, J/0.433667, num
        (59,2)*0.159, (T_bh -32)*5/9, p_r]);
152
153 %Relief well and kill fluid
154 Depth_IP = num(12,6); %ft
155 kill_viscosity = num(14,6); %cp
156 gamma_k_step = num(15,6);
```

```
Kill_steps = num(16,6);
%Length_IP = num(17,6); %ft


if strcmp(Simulate,'Blowout and Kill')
%Relief well program
% [OD , ID, top, shoe, relative roughness] [in, in, ft RKB,
    ft RKB, -]
RW_sur = [num(26,5), num(26,6), num(26,7), num(26,8), num
    (26,9)];
RW_CL = [num(22,5), num(22,6), num(22,7), num(22,8), num
    (22,9)];
RW_csg = [num(23,5), num(23,6), num(23,7), num(23,8), num
    (23,9)];
RW_dp = [num(24,5), num(24,6), num(24,7), num(24,8), num
    (24,9)];
RW_bha = [num(25,5), num(25,6), num(25,7), num(25,8), num
    (25,9)];
RW = [RW_sur; RW_CL; RW_csg; RW_dp; RW_bha];

%Relief well trajectory
KOP = num(68,2); %m
Coord = [num(69,2),num(70,2)]; %Distance [North, East]
B_rate = num(71,2); %build up rate deg/30m
B_max = num(72,2);  % Maximum build angle
D_rate = num(73,2); % Drop rate deg/30m
D_max = num(74,2);  %Maxiumum drop angle

RW_value = [Depth_IP,KOP,Coord(1),Coord(2),B_rate,B_max,
    D_rate,D_max];

[RW_t] = Build_Relief_well(B_max,B_rate,D_max,D_rate,KOP,
    Depth_IP/3.28084,Coord); %Relief well trajectory [x,TVD,
    MD]-[m]
end
%Casing and open hole values
% [OD , ID, top, shoe, relative roughness] [in, in, ft RKB,
    ft RKB, -]
Riser = [num(35,1), num(35,2), num(35,3), num(35,4),num
    (35,5)];
csg2 = [num(36,1), num(36,2), num(36,3), num(36,4),num
    (36,5)];
csg3 = [num(37,1), num(37,2), num(37,3), num(37,4),num
    (37,5)];
csg4 = [num(38,1), num(38,2), num(38,3), num(38,4),num
```

```
    (38,5)];
csg5 = [num(39,1), num(39,2), num(39,3), num(39,4),num
    (39,5)];
Open_hole = [num(40,1), num(40,2), num(40,3), num(40,4),num
    (40,5)];
Well=[Riser;csg2;csg3;csg4;csg5;Open_hole];
Well(all(Well==[0,0,0,0,0],2),:)=[]; %remove empty rows
Well(all(isnan(Well),2),:)=[];


Top_OH = num(find(raw(1:end,1) == "Open Hole",1)-1,3)
    /3.28084; %m

%Riser and seabed
if Wellhead == "Wet wellhead"
D_sea = num(52,2);    % ft RKB
Riser_ID = num(53,2); % in
else
    Well = Well(2:end,:); %Remove riser if dry wellhead
end

[well_sorted] = sort_well(Well);
well_sorted(:,[3,4]) = round(well_sorted(:,[3,4]),0);



%Drill string values
% [OD , ID, length, top, shoe, relative roughness] [in, in,
     ft, ft RKB, ft RKB, - ]
DS_BHA = [num(46,1), num(46,2), num(46,3), num(46,4), num
    (46,5),num(46,6)];
DS_DP = [num(47,1), num(47,2), num(47,3), num(47,4), num
    (47,5),num(47,6)];
DS = [DS_DP; DS_BHA] ;

  Plot_well


% Numerical simulation alternative
N = num(62,3);
Residual_pressure_crit = num(63,3);
```

```
227
228 %Some general values
229 g_c = 32.2; % ft/sec^2
230 %Given productivity index
231 %% Values from blowout calculator
232 adjustment_orki = 1.0;
233 adjustment_kill = 1.0; %4/gamma_k;
234 adjustment_dp = 1.0 ;
235 IPR
236
237
238 PVT_sim = raw(9,6);
239
240 Multiphase = raw(8,6);
241 if strcmp(Simulate,"Blowout")
242  n_cals=1;
243 else
244 %n_cals=4;
245 n_cals=4;
246 end
247
248 for i_cal = 1:n_cals
249 %q_os = 4060/0.159;
250 Run_non_linear_reg
251 q_kill_add1 = 250; %num_case(N_case,col_dens+1); % 250; %
       LPM
252 q_kill_i = 0 ; % STB/D
253
254 if strcmp(Simulate,"Blowout")
255 adjustment_dp = 1;
256 else
257 adjustment_dp = result_non_linear(i_cal);
258 %adjustment_dp=1;
259 end
260 max_kill_rate = 30000;
261 p_bh = 0.8*p_r *14.5; %FBHP
262 q_os = getBlowoutRate(p_bh, p_r, p_s_true/14.5, q_max,q_s,J
       ); %STB/D
263 %Simulation=['Simulation: ', char(Simulate), ',    Blowout
       release point: ', char(Blowout_release), ',    Drill
       string in wellbore: ', char(Drill_pipe), ',  Multiphase:
        ', char(Multiphase), ',  PVT: ', char(PVT_sim)]
264 %Run_VLP
265
266 Load_now = Load_now + 1;
```

```
lineLength_load = fprintf('Simulation %1.0f of %1.0f \n', Load_now, Load_max);

Run_scenario

Rate_matrix(all(Rate_matrix=="0",2)==1,:)=[]; %remove rows that are non zero



if N_sim < 5
Matrix_blowout(3,N_sim*2-1) = round(double(Rate_matrix(end,3)),0);
Matrix_blowout(3,N_sim*2) = round(double(Rate_matrix(end,4)),1);


elseif N_sim >4 && N_sim <= (5+Kill_steps)
if N_sim == 6
    a=0;
end
%Seabed kill
Matrix_kill_seabed(i_cal+2,2) = adjustment_dp;
Matrix_kill_seabed(i_cal+2,(N_sim-3)*2-1) = gamma_k;
Matrix_kill_seabed(i_cal+2,(N_sim-3)*2) = round(double(Rate_matrix(end,1)),0);
if i_cal ==1 %best prediction
   dp_IP_seabed(N_sim-4) = double(Rate_matrix(end,5)) - gamma_k*Depth_IP/3.28084*9.81*10^-2;
   pressure_IP_seabed(N_sim-4) = double(Rate_matrix(end,5));
   pressure_BH_seabed(N_sim-4) = double(Rate_matrix(end,4));
end

else
%Surface kill
Matrix_kill_surface(i_cal+2,2) = adjustment_dp;
Matrix_kill_surface(i_cal+2,(N_sim-4-Kill_steps)*2-1) = gamma_k;
Matrix_kill_surface(i_cal+2,(N_sim-4-Kill_steps)*2) = round(double(Rate_matrix(end,1)),0);

 if i_cal ==1 %best prediction
   dp_IP_surface(N_sim-(5+Kill_steps)) = double(Rate_matrix
```

```
        (end,5)) - gamma_k*Depth_IP/3.28084*9.81*10^-2;
302     Pressure_IP_surface(N_sim-(5+Kill_steps)) = double(
            Rate_matrix(end,5));
303     Pressure_BH_surface(N_sim-(5+Kill_steps)) = double(
            Rate_matrix(end,4));
304 end
305
306 end
307
308 fprintf(repmat('\b',1,lineLength_load))
309 fprintf(' \n \n \n')
310 Going="No";
311 end
312
313 end
314
315 toc
316
317 Report_preparator
318
319 report_gen
320
321
322 fprintf('\n \n Simulation is finished and the blowout
        report is created \n \n')
```

Listing C.2: Build_Relief_well

```
1  function [RW_t] = Build_Relief_well(B_max,B,D_max,D,KOP,
       Depth_IP,Coord)
2  % Will get the well trajectory for a S-well that are a
       given distance
3  % from the blowing well, it will have a maximum building
       angle
4  % and will intersect the blowing well with a minimum of 5
       degree offset
5  % compare to the blowing well
6  global RW_fig
7  %% Input
8  % KOP - Kick of point [ft]
9  % B_max - maximum building angle
10 % B - Build up rate degree/30m
11 % D_max - maximum drop angle
12 % D - Drop rate degree/30m
13 % kCord - Offsett kordinate from blowing well [North, East]
14
```

```
%Output RW_t - Relief well trajectory [x,TVD,MD] [m]

global plot_this


% clear
% close all
% format bank
% KOP=500;
% Depth_IP = 2200;
% B=2.5;
% D=2.5;
% B_max=45;
% D_max = 45;
% Coord = [900,435];
% %Coord = [1800,900];


% First build
RC_b = 180*30 / (pi*B); % m
z_b = sind(B_max)*RC_b;  %Vertical departure [m]
x_b = RC_b - cosd(B_max)*RC_b;  %Horizontal departure [m]
L_b =  pi*RC_b*2 * B_max/360; % measured depth [m]

%First drop
RC_d = 180*30 / (pi*D); % m
z_d = sind(D_max)*RC_d;  %Vertical departure
x_d = RC_d - cosd(D_max)*RC_d;  %Horizontal departure
L_d =  pi*RC_d*2 * D_max/360; % measured depth [m]

% North - East plane
N = Coord(1) ;
E = Coord(2) ;

x_tot = sqrt(N^2+E^2); % Total horizontal departure [m]

azi = atand(E/N); %Azimuth - degrees from north

if azi<0
    azi=360-azi;
end



% Tangentional section
```

```
x_t = x_tot - x_b - x_d;
z_tot=Depth_IP; %total vertical departure
z_t = z_tot - KOP - z_b - z_d;
L_t = sqrt(z_t^2 + x_t^2); %Measured depth [m]

MD = KOP + L_b + L_d + L_t;
% Entire well

x_k = zeros(100,1);
z_k=linspace(0,KOP);

t = linspace(0,B_max);
r=RC_b;
x_build = x_k(end) + r-r*cosd(t) ;
z_build = z_k(end) + r*sind(t) ;
MD_build = KOP + pi*RC_b*2 * t/360; % measured depth [m]


x_tan = linspace(x_build(end),x_build(end)+x_t);
z_tan = linspace(z_build(end),z_build(end)+z_t);
x = linspace(0,x_t);
y = linspace(0,z_t);
MD_tan = MD_build(end) + sqrt(x.^2 + y.^2);


t = linspace(0,D_max);
r=-RC_d;
x_drop = x_tan(end) + x_d + r-r*cosd(t) ;
z_drop = z_tan(end) + z_d + r*sind(t) ;
MD_drop = MD_tan(end) + pi*RC_d*2 * t/360; % measured depth
    [m]

x_drop=flip(x_drop);
z_drop=flip(z_drop);


%Output
x=[x_k;x_build';x_tan';x_drop'];
z = [z_k'; z_build';z_tan';z_drop'];
MD_vector = [z_k'; MD_build'; MD_tan'; MD_drop'];

RW_t=round([x,z,MD_vector],1);

%% Plot
if strcmp(plot_this,"Yes")
```

```
RW_fig = figure('Name','RW_fig');
figure(RW_fig)
plot(x,z,'k','LineWidth',3)
title('Relief Well Trajectory')
set(gca, 'YDir','reverse','Fontsize',12,'fontweight','bold')
axis([-100 (x_tot+100) 0 (z_tot + 100)])



line([0,0],[KOP,z_tot+100])
line([x_b,x_b],[KOP,z_tot+100])
line([-100,x_b],[z_b+KOP,z_b+KOP])
line([x_tan(end),x_tan(end)],[z_tan(end),z_tot+100])
line([-100,x_tan(end)],[z_tan(end),z_tan(end)])
line([-100,x_tot],[z_tot,z_tot])


hold on
build_x = [0,RC_b,x_b];
build_y = [KOP, KOP, KOP+z_b];
plot(build_x,build_y,'r')

str1=char(strcat(string(round(B_max,0)),char(176)));
%text(RC_b-0.3*RC_b,KOP+0.1*KOP, str1) %'Units','normalized')
text(RC_b/(x_tot+200)-0.05,(z_tot-KOP)/(z_tot+100), str1, 'Units','normalized')

hold on
drop_x = [x_tot,x_tot - RC_d,x_tan(end)];
drop_y = [z_tot, z_tot, z_tan(end)];
plot(drop_x,drop_y,'r')

str1=char(strcat(string(round(D_max,0)),char(176)));
text((x_tot - 0.6*RC_d)/(x_tot+200), 0.05 , str1,'Units','normalized')

xlabel('Horizontal departure [m]')
ylabel('Vertical departure [m]')


str1=char(strcat('MD = ', string(round(MD,0)),'m'));
text(0.2,0.95, str1 ,'Units','normalized','Fontsize',10,'fontweight','bold')
```

```
str1=char(strcat('TVD = ', string(round(z_tot,0)),'m'));
text(0.20,0.90, str1 ,'Units','normalized','Fontsize',10,'
    fontweight','bold')
str1=char(strcat('H = ', string(round(x_tot,0)),'m'));
text(0.20,0.85, str1 ,'Units','normalized','Fontsize',10,'
    fontweight','bold')

ax1 = axes('Position',[0.6 0.6 0.28 0.28],'Box','on');

plot([0,E],[0,N],'LineWidth',2)
title('Azimuth')
ylabel('North [m]')
xlabel('East [m]')
axis([0 max(Coord)+100 0 max(Coord)+100])
hold on
t = linspace(90,90-azi);
r=N/5;
x = r*cosd(t) ;
y = r*sind(t) ;
plot(x,y)

str1=char(strcat('\alpha =', string(round(azi,1)),char(176)
    ));
text(x(10)/(E+100),N/2/abs(N), str1 ,'Units','normalized','
    Fontsize',10,'fontweight','bold')
grid on
set(gca,'Fontsize',10,'fontweight','bold')
else
end

end
```

Listing C.3: Sort_well

```
function [well_sorted] = sort_well(Well)

% Shall give the tubulars that are connected, i.e riser,
    production casing,
% liners and open hole
%Well [OD, ID, Start, Shoe]

Start_depth = unique(Well(:,3));

well_sorted=zeros(length(Start_depth),5);
for i = 1:length(Start_depth)

```

```
    I = Well(:,3)==Start_depth(i);
    row = find(I==1);
    well_sorted(i,:) = Well(row(end),:);

end
end
```

Listing C.4: IPR

```
%% Input and output

% Input
% p_r         - Reservoir pressure [bar]
% r_w         - Well radius [m]
% r_e         - Drainage radius [m]
% h_res       - Reservoir layer height [m]
% h_p         - Penetration height of reservoir [m]
% k           - Permeability [mD]
% beta        - Permeability anisotropy factor[-]
% theta       - Inclination [degrees, vertical = 0]
% R_t         - Total Producing GOR [SCF/SBL]
% gamma_g     - Specific gas gravity [-]
% gamma_o     - Specific oil gravity [-]
% T           - Reservoir temperature [F]

% Output
% q_ov        - Surface flow rate vector [STB/D]
% p_wv        - Flowing bottom hole pressure vector [psig]
% A chart of the Inflow Performance Relationship
%%
global IPR_fig

T=T_bh;
p = p_r*14.5038; % Conversion from bar to psi

if p_s_true > 0 && PI_calc == "Yes"

[p_s, Bo,R_s, mu_o] = Glaso_2(R_t, T, gamma_g, gamma_o,p,
   p_s_true);
elseif PI_calc == "Yes"


[p_s, Bo,R_s, mu_o] = Glaso(R_t, T, gamma_g, gamma_o,p);
end
R_t_old=R_t;

```

```
if PI_calc == "Yes"
J = Prod_index(r_w, r_e, h_res, h_p, k, beta, Bo, mu_o,
    theta);
else
J = J/0.433667; %SM3/D/bar
p_s = p_s_true;
end
p_s=p_s/14.5038;


%dp = 1/14.5038;  %delta p psi]
q_max = J*p_s/1.8 ;  % SM3/D

N = round(p_r); %round(p_r/dp);
p_w=linspace(N,1,N); p_w(1)=p_r;
q_o=zeros(N,1);

q_s = J*(p_r-p_s);
if q_s <0
    q_s = 0;
end

for i=1:N
% if i>1
% p_w(i)= p_r-dp*i;
% end


if p_w(i) >= p_r
q_o(i)=0;
elseif p_w(i) > p_s
q_o(i) = J*(p_r-p_w(i));
elseif p_w(i) <= p_s
q_o(i) = q_s +(1-0.2*p_w(i)/p_s - 0.8*(p_w(i)/p_s)^2)*q_max
    ;
end

end


%% Plot section
a=0;
if strcmp(plot_this,"Yes")
IPR_fig = figure('Name','IPR_fig');
if strcmp(Unit,"Oil field units")
```

```
p_w=p_w*14.5038; %psi
q_o = q_o/0.159; %STB

IPR_fig=figure('Name','IPR_fig')
IPR_fig=figure(IPR_fig)
plot(q_o,p_w,'LineWidth',2)
ylim([0 inf])
xlim ([0 inf])
grid on
ylabel('Flowing bottom hole pressure [Psi]')
xlabel('Flow rate [STB/D]')
line([0,q_o(find((round(p_w)==round(p_s*14.5038)),1))],[p_s
    *14.5038,p_s*14.5038],'Color','black')
legend('IPR - Inflow performance relationship','p_s -
    Saturation pressure')
str1=char(strcat('p_s=', string(round(p_s*14.5038))));

text(0.01,p_s/p_r + 0.03, str1 ,'Units','normalized')
str2=char(strcat('AOF=', string(round(q_o(end)))));
text(0.85,-0.1, str2 ,'Units','normalized')


str2=char(strcat('J=', string(round(J*0.433667,1)),' STB/D/
    psi'));
text(0.1,0.1, str2 ,'Units','normalized')

elseif strcmp(Unit,"Semi-SI units")



IPR_fig=figure('Name','IPR_fig')
IPR_fig=figure(IPR_fig)
plot(q_o,p_w,'LineWidth',2)
ylim([0 inf])
xlim([0 inf])
grid on
ylabel('Flowing bottom hole pressure [Bar]')
xlabel('Flow rate [SM3/D]')
line([0,q_o(find((round(p_w)==round(p_s)),1))],[p_s,p_s],'
    Color','black')
legend('IPR - Inflow performance relationship','p_s -
    Saturation pressure')
str1=char(strcat('p_s=', string(round(p_s))));

text(0.01,p_s/p_r+0.03, str1 ,'Units','normalized')
```

```
str2=char(strcat('AOF=', string(round(q_o(end)))));
text(0.85,-0.1, str2 ,'Units','normalized')


str2=char(strcat('J=', string(round(J,1)),'  SM^3/D/bar'));
text(0.075,0.075, str2 ,'Units','normalized')

p_w=p_w*14.5038; %psi
q_o = q_o/0.159; %STB
end

else
end


R_t = R_t_old;
```

Listing C.5: Prod_index

```
function J = Prod_index(r_w, r_e, h_res, h_p, k, beta, Bo,
    mu_o, theta)
% This script calculates the productivity index
%% Input and Output

% Input
% r_w         - Well radius [m]
% r_e         - Drainage radius [m]
% h_res       - Reservoir layer height [m]
% h_p         - Penetration height of reservoir [m]
% k           - Permeability [mD]
% Bo          - Oil formation volume factor [sm3/sm3]
% mu_o        - Oil viscosity [cp]
% beta        - Permeability anisotropy factor[-]
% theta       - Inclination [degrees, vertical = 0]

% Ouput
%J           - Productivity index [SM3/D/Bar]
%% Conversion
mu_o=mu_o * 10^-3 ; %cp to pas
k=k*10^-15;
h_f = h_p/h_res ;
C = 2*pi*k*h_res/(mu_o*Bo) ;


%% Adjusting for partly penetrating the reservoir
if h_f<1
```

```
S_c = (1-h_f)/h_f *log(4*h_res/r_w) - 0.5/h_f*log((1-0.875*
    h_f)*(1-0.125*h_f)/(0.875*0.125*h_f^2));
else
S_c = 0;
end


%% Adjusting for inclination and anisotrophy
if theta> 0 && theta <= 75 && beta ~= 1
S_i = -(theta/41)^2.06 -(theta/56)^1.865 * log10(beta*h_res
    /(100*r_w));
elseif theta> 0 && theta <= 75
S_i = -(theta/41)^2.06 -(theta/56)^1.865 * log10(h_res
    /(100*r_w));
elseif theta==0
S_i=0;
else
S_i = 0;
fprintf('Use horizontal well')
end

S_t = S_i + S_c ;

J = C/(log(r_e/r_w)-0.75+S_t)*24*3600*10^5; %SM3/D/Bar
end
```

Listing C.6: Plot_well

```
%D = 3000;

x =linspace(D,0,300);

for i = 1:length(x)
D_avg=x(i);
[ID_csg, OD_DS] = retrieve_diameter(well_sorted,DS,D_avg,
    Drill_pipe) ;


ID(i)=ID_csg;
OD(i)=OD_DS;

end



if strcmp(Unit,"Semi-SI units")
```

```
    x = x/3.28084; % Convert feet to meter
end


if Drill_pipe == "Yes"
figure()
plot(ID,x,'blue','LineWidth',2)
hold on
plot(-OD,x,'black','LineWidth',2)
hold on
plot(-ID,x,'blue','LineWidth',2)
hold on
plot(OD,x,'black','LineWidth',2)
hold on
plot([-ID(1),ID(1)],[x(1),x(1)],'blue','LineWidth',2)
hold on
plot([-OD(1),OD(1)],[x(1),x(1)],'black','LineWidth',2)

legend('Casing/Riser/Open hole','Drill string','Location',
    'Best')
else
figure()
plot(ID,x,'blue','LineWidth',2)
hold on
plot(-ID,x,'blue','LineWidth',2)
hold on
plot([-ID(1),ID(1)],[x(1),x(1)],'blue','LineWidth',2)
hold on
legend('Casing/Riser/Open hole','Location', 'Best')
end

if strcmp(Unit,"Semi-SI units")
    ylabel('Depth [m RKB]')
else
    ylabel('Depth [ft RKB]')
end
xlabel('Diameter [in]')
set(gca, 'YDir','reverse','Fontsize',14,'fontweight','bold'
    )
grid on
```

Listing C.7: Run_non_linear_reg.m

```


%ypred er den predikerte verdien
```

```
4  % yci er konfidens intervallet for denne verdien, om ikke
       annet er gitt  s
5  % er den innen 95% conficence interval.
6
7  %konfidens intervallet kan endres ved    endre alpha
       verdien fra 0.05, 0.05 = 95%
8  % [ypred,yci] = predict(mdl,Xnew,'Alpha',0.05)
9
10
11
12 %Matrix_new = [Total depth, GOR, Saturation pressure]
13 %              [m, sm3/sm3, Bar]
14
15 % my_regress= 'y~ b1+ b2*x1 + b3*x2 + b4*x3';
16 % beta0 = ones(4,1);
17 % model_1 = fitnlm(Matrix,target,my_regress,beta0)
18 AOF = PI_to_AOF(J*0.433667,p_r,p_s_true);
19
20 if strcmp(Blowout_release,'Surface') && strcmp(Multiphase,'
       Olgjenka')
21 load('non_linear_models')
22 Matrix_new = [D/3.28084,p_s_true/14.5, R_t /5.6145833,
       Depth_IP/D*100];
23 [ypred, yci] = predict(non_linear_OH_Surface_Olgjenka,
       Matrix_new,'Alpha',0.20);
24 result_non_linear=[ypred yci 1];
25 % gives [best prediction, and min/max within 95% confidence
       , no change]
26
27 elseif strcmp(Blowout_release,'Seabed') && strcmp(
       Multiphase,'Olgjenka')
28 load('non_linear_models')
29 Matrix_new = [D/3.28084,num(3,2)/3.28084, gamma_o, gamma_g
       ];
30 [ypred, yci] = predict(non_linear_OH_Seabed_Olgjenka,
       Matrix_new,'Alpha',0.20);
31 result_non_linear=[ypred yci 1];
32
33 elseif strcmp(Blowout_release,'Surface') && strcmp(
       Multiphase,'Orkiszewski')
34 load('non_linear_models')
35 Matrix_new = [D/3.28084,p_s_true/14.5, R_t /5.6145833,
       Depth_IP/D*100];
36 [ypred, yci] = predict(non_linear_OH_Surface_Orkiszewski,
       Matrix_new,'Alpha',0.20);
```

```
result_non_linear=[ypred yci 1];

elseif strcmp(Blowout_release,'Seabed') && strcmp(
    Multiphase,'Orkiszewski')
load('non_linear_models')
Matrix_new = [D/3.28084,num(3,2)/3.28084, AOF*0.159,
    Depth_IP/D*100];
[ypred, yci] = predict(non_linear_OH_Seabed_Orkiszewski,
    Matrix_new,'Alpha',0.20);
result_non_linear=[ypred yci 1];


end
```

Listing C.8: Run_scenario

```
%% prepare well for simulation
Depth=round(D,0);
Depth_wh = round(D_wh/5,0)*5;
Depth_sb = round(D_sb/5,0)*5;
dL = num(62,3); % ft



if strcmp(Simulate,"Blowout and Kill") && strcmp(
    Blowout_release,"Seabed")
     a=0;
elseif strcmp(Simulate,"Blowout and Kill") && strcmp(
    Blowout_release,"Surface")
     a=0;
end


if strcmp(Blowout_release,"Seabed")
N = fix((Depth-Depth_sb)/dL) +1;
Pressure_kill = zeros(1,N)';
X = linspace(Depth_sb,Depth,N);
Pressure_kill(1) = p_wh;
else
N = fix(Depth/dL) +1;
Pressure_kill = zeros(1,N)';
X = linspace(0,Depth,N);
Pressure_kill(1) = 14.7;
end
dL = X(2)-X(1);

```

```
29
30 dp=10; %psia
31
32
33 q_kill_i2=q_kill_i;
34
35 % Vectors to store date from the different conditions/loops
36
37 dp_kill = zeros(1,N)';
38 Flow_regime_kill = string(zeros(1,N)');
39 Density_avg= zeros(1,N)';
40 Density_liquid = zeros(1,N)';
41 Depth_kill= zeros(1,N)'; Depth_kill(1)=0;
42 Outer_D_kill= zeros(1,N)';
43 Inner_D_kill= zeros(1,N)';
44 Roughness_kill = zeros(1,N)';
45 dp_grav = zeros(1,N)';
46 dp_f = zeros(1,N)';
47 p_sat = zeros(1,N)';
48 yl = zeros(1,N)';
49 yk = zeros(1,N)';
50 kill_rate = zeros(1,N)';
51 Gamma_phase = string(zeros(1,N)');
52 Gamma = string(zeros(1,N)');
53 Bo = zeros(1,N)';
54 R_s = zeros(1,N)';
55 v_mix = zeros(1,N)';
56 mu_l = zeros(1,N)';
57 fric_factor = zeros(1,N)';
58
59 q_o_dh = zeros(1,N)';
60 q_g_dh = zeros(1,N)';
61 q_k_dh = zeros(1,N)';
62 q_t_dh = zeros(1,N)';
63
64 kill_rate_two = zeros(1,10)';
65 Blow_rate_two = zeros(1,10)';
66 Blow_rate_used = zeros(1,10)';
67 Blow_rate_next = zeros(1,10)';
68 pressure_IP = zeros(1,10)';
69 Pressure_kill_two = zeros(1,10)';
70 v_mix_table = zeros(1,10)';
71 q_o_table =zeros(1,10)';
72 q_g_table =zeros(1,10)';
73 q_k_table =zeros(1,10)';
```

```
q_t_table =zeros(1,10)';

k=0;
Q=0;
lineLength = fprintf('Kill rate step %1.0f \n', Q);
S=0;
Killed_once="No";
sim_failed="No";
Simple_kill = "Yes";


q_os_bo = 100;
Header = [{'Depth'}, {'Pressure'},{'Pressure change'},{'
    Outer Diameter'},{'Inner Diameter'}, {'Flow Regime'}, {'
    Density of mixture'},{'Density of liquid'}, {'Relative
    Roughness'}, {'dp_f'}, {'dp_grav'}, {'liquid fraction'},
     {'kill fluid fraction'},{'Kill rate'},{'Gamma phase'},{
    'Gamma'},{'Bo'},{'Rs'},{'mu_l'},{'Friction factor'}];
Header2 = [{'[Feet]'}, {'[psia]'},{'[psi]'},{'[in]'},{'[in]
    '}, {'[in]'}, {'[lb/ft3]'},{'[lb/ft3]'}, {'[-]'}, {'[psi
    ]'}, {'[psi]'}, {'[-]'}, {'[-]'},{'LPM'},{'-'},{''},{'-'
    },{'SCF/STB'},{''},{''}];
Matrix_big=string([Header ; Header2]);

lineLength_W=0;

%% Kill rate loop start
while q_os_bo > 0
Q=Q+1;

if Q==1;
q_kill_i=0;
end

clear Matrix_W Blowout_W Blowout_W_used Pressure_W
    Difference_W_CU Difference_W_UC Pressure_W_used
    Pressure_W_Perc
fprintf(repmat('\b',1,lineLength))
lineLength = fprintf('Kill rate step %1.0f - %1.0f LPM \n',
     Q, q_kill_i*0.159/1.44);


Overwrite = 'No';
New_if='No';
WL = 0;
```

```
Higher = 'Yes';
Numb_W = 1;
Change_W="No";
Neg_FBHP_W="No";
Restart_W = "No";


k=k+1;

W=0;
delta_q=5000; % to start the while loop
lineLength_W=0;

%% Blowout loop start
while abs(delta_q) > 1/0.159 && strcmp(sim_failed,'No');

fprintf(repmat('\b',1,lineLength_W))
lineLength_W = fprintf('Blowout step - %1.0f - %1.0f Sm^3/d
    \n', W, q_os*0.159);

    W=W+1;
    if round(q_os)==34181
        a=0;
    end

T = get_Temperature2(Depth,D_sb, Top_OH,Depth_IP, q_kill_i,
   X);
T = flip(T);
dp=10;

%% Well loop start
for i= 2:N %Calculate the pressure in the well going from
   bottom to WH
D_avg = 0.5*(X(i)+X(i-1)); % ft
T_avg = 0.5*(T(i)+T(i-1)); % ft

if D_avg <= Depth_IP % To check if the flow rate from the
   relief well
  if Q == 1  %% always calculate the blowout rate first.
  q_kill=0;
  else
  q_kill = q_kill_i;
  end
else
    q_kill = 0;
```

```
end


[ID_csg, OD_DS,~] = retrieve_diameter(well_sorted,DS,D_avg,
    Drill_pipe); %Retrieve inner and outer flow area
d_h = (ID_csg - OD_DS)/12; % ft Hydraulic diameter
A_p = pi/4 * (ID_csg^2 - OD_DS^2); % in^2

if D_avg > well_sorted(end,2)
    rel_rough = Materials(11)/ID_csg;
else
    rel_rough = Materials(10)/ID_csg;
end


%Updating vectors with data storage
Depth_kill(i)=D_avg; %ft
Outer_D_kill(i) = round(ID_csg,3);% in
Inner_D_kill(i) = round(OD_DS,3); %in
Roughness_kill(i) = rel_rough;
kill_rate(i) = q_kill*159/(24*60); %lpm
p_old = Pressure_kill(i-1); %psia




%angle = -90; %90 degrees downwards
if strcmp(Multiphase,'Orkiszewski')
[dp,Flow_regime_kill(i),Density_avg(i),Density_liquid(i),
    dp_f(i),dp_grav(i),yl(i),yk(i),Gamma_phase(i),Bo(i), R_s
    (i),mu_l(i),fric_factor(i),p_sat(i),Gamma(i)] =
    Orkiszewski_correlation(D_avg, T_avg, p_old, dp,dL, d_h,
    A_p,rel_rough,q_kill, gamma_k);
elseif strcmp(Multiphase,'Olgjenka')
[dp,fric_factor(i),Density_liquid(i),mu_l(i),Density_avg(i)
    ,yl(i),v_mix(i),q_o_dh(i), q_g_dh(i), q_k_dh(i),q_t_dh(i
    ),Bo(i),R_s(i)] = Olgjenka_correlation(D_avg, T_avg,
    p_old,dL, d_h,rel_rough,q_kill,A_p);
end
dp=dp*adjustment_dp;


if Depth_kill(i) > Depth_kill(i-1) % if going from surface
    to bot
    Pressure_kill(i) = Pressure_kill(i-1) + dp *
```

```
        adjustment_orki ;
else
    Pressure_kill(i) = Pressure_kill(i-1) - dp*
        adjustment_orki;
end

dp_kill(i) = dp;
if isnan(dp)|| isreal(dp)== 0 || Q >= 300 || W >=2000  ||
    q_kill_i*0.159/1.44 >= max_kill_rate

%Find the reason why it failed
 if isreal(dp)== 0
   reason = 'The calculate dp became imaginary';
 elseif isnan(dp)
     reason = 'The calculated dp was NaN';
 elseif Q >= 300
      reason = ['The kill rate became unrealistics high - '
          , num2str(Q*250),'LPM'];
 elseif W>= 1000
     reason = ['An equilibrium between the wellbore and
         reservoir used more than', num2str(W),'iterations'
         ];
  elseif q_kill_i*0.159/1.44 >= max_kill_rate
  reason = ['Required kill rate exceeded the maximum kill
      rate of', num2str(max_kill_rate),'LPM'];
end
    warning('foo:bar',['The Simulation of file - "'  char(
        file), '" was unsuccesfull.\n Reason: ' reason])
sim_failed="Yes";
break
end


end % end for i
%% Well loop finished / Next part of blowout loop

%Create a matrix with different values along the entire
    wellbore
Matrix_kill = [Depth_kill,round(Pressure_kill,3),round(
    dp_kill,3), Outer_D_kill, Inner_D_kill, Flow_regime_kill
    , round(Density_avg,2),round(Density_liquid,2),
    Roughness_kill,dp_f, dp_grav,yl,yk,kill_rate,Gamma_phase
    ,Gamma,Bo,R_s, mu_l,fric_factor];
Header = [{'Depth'}, {'Pressure'},{'Pressure change'},{'
    Outer Diameter'},{'Inner Diameter'}, {'Flow Regime'}, {'
```

```
    Density of mixture'},{'Density of liquid'}, {'Relative
    Roughness'}, {'dp_f'}, {'dp_grav'}, {'liquid fraction'},
     {'kill fluid fraction'},{'Kill rate'},{'Gamma phase'},{
    'Gamma'},{'Bo'},{'Rs'},{'mu_l'},{'Friction factor'}];
Header2 = [{'[Feet]'}, {'[psia]'},{'[psi]'},{'[in]'},{'[in]
    '}, {'[in]'}, {'[lb/ft3]'},{'[lb/ft3]'}, {'[-]'}, {'[psi
    ]'}, {'[psi]'}, {'[-]'}, {'[-]'},{'LPM'},{'-'},{'-'},{''
    },{'SCF/STB'},{''},{''}];
Matrix_kill = [Header;Header2;Matrix_kill];


% Calculate the blowout rate from IPR based on bottom hole
    pressure
q_os_bo = getBlowoutRate(Pressure_kill(end), p_r, p_s,
    q_max,q_s,J);
q_os_used = q_os;

 if strcmp(Simple_kill,'Yes')
%Script to find the blowout rate for the next loop
 Find_next_blowout_rate
 elseif strcmp(Simple_kill,'No') && Q==1
Find_next_blowout_rate_hard_blowout
 elseif strcmp(Simple_kill,'No') && Q>1
Find_next_blowout_rate_hard
 end


end %end while W

%% Blowout loop finish / next part of kill rate loop




fprintf(repmat('\b',1,lineLength_W))

kill_rate_two(Q) = q_kill_i*159/(24*60)/adjustment_kill;
Blow_rate_two(Q) = q_os_bo;
Blow_rate_next(Q) = q_os;
Blow_rate_used(Q) = q_os_used;
Pressure_kill_two(Q) = Pressure_kill(end);


q_kill_i = q_kill_i + q_kill_add1*(24*60)/159*
    adjustment_kill;  %q_kill_add1*adjustment_kill;
```

```
clear Matrix_kill

Matrix_kill = [Depth_kill,round(Pressure_kill,1),round(
    dp_kill,3), Outer_D_kill, Inner_D_kill, Flow_regime_kill
    , round(Density_avg,2),round(Density_liquid,2),
    Roughness_kill,dp_f, dp_grav,yl,yk,kill_rate,Gamma_phase
    ,Gamma,Bo,R_s, mu_l,fric_factor];
Header = [{'Depth'}, {'Pressure'},{'Pressure change'},{'
    Outer Diameter'},{'Inner Diameter'}, {'Flow Regime'}, {'
    Density of mixture'},{'Density of liquid'},{'Relative
    Roughness'}, {'dp_f'}, {'dp_grav'}, {'liquid fraction'},
     {'kill fluid fraction'},{'Kill rate'},{'Gamma phase'},{
    'Gamma'},{'Bo'},{'Rs'},{'mu_l'},{'Friction factor'}];
Header2 = [{'[Feet]'}, {'[psia]'},{'[psi]'},{'[in]'},{'[in]
    '}, {'[in]'}, {'[lb/ft3]'},{'[lb/ft3]'}, {'[-]'}, {'[psi
    ]'}, {'[psi]'}, {'[-]'}, {'[-]'},{'LPM'},{'-'},{'-'},{''
    },{'SCF/STB'},{''},{''}];
Matrix_kill = [Header;Header2;Matrix_kill];


%Storing the values used for every flowrate for the entire
    wellbore

pressure_IP(Q) = round(double(Matrix_kill(min(find(Depth_IP
    <Depth_kill==1))+2,2)),1);
v_mix_table(Q) = mean(v_mix);
q_o_table(Q) = mean(q_o_dh);
q_g_table(Q) = mean(q_g_dh);
q_k_table(Q) = mean(q_k_dh);
q_t_table(Q) = mean(q_t_dh);
flow_table = [q_o_table, q_g_table, q_k_table, q_t_table];









Rate_matrix = [round(kill_rate_two,1),string(round(
    Blow_rate_used,3)), string(round(Blow_rate_two,3)),round
    (Pressure_kill_two,3),string(pressure_IP), string(
    v_mix_table*3.82084)];

Header = [{'Kill Rate'}, {'Blowout rate used'},{'Blowout
```

```
    rate calculated'},{'Bottom hole pressure'},{'Pressure at
     IP'},{'[Mixture velocity]'}];
279 Header2 = [{'[LPM]'}, {'[STB/D]'},{'[STB/D]'},  {'[psi]'},{
    '[psi]'},{'[ft/s]'}];
280 Rate_matrix = [Header;Header2;Rate_matrix];
281
282 if strcmp(Unit,"Semi-SI units")
283 Rate_matrix = [round(kill_rate_two,2),string(round(
    Blow_rate_used*0.159,3)), string(round(Blow_rate_two
    *0.159,3)),round(Pressure_kill_two/14.503,3),string(
    round(pressure_IP/14.5,1)), string(v_mix_table)];
284
285 Header = [{'Kill Rate'}, {'Blowout rate used'},{'Blowout
    rate calculated'},{'Bottom hole pressure'},{'Pressure at
     IP'},{'Mixture velocity'}];
286 Header2 = [{'[LPM]'}, {'[SM3/D]'},{'[SM3/D]'}, {'[Bar]'},{'
    [Bar]'},{'[m/s]'}];
287 Rate_matrix = [Header;Header2;Rate_matrix];
288 end
289
290 if Q == 1
291     Matrix_initial = Matrix_kill;
292 end
293
294 if strcmp(Simulate,'Blowout')
295     q_os_bo=0;
296 elseif strcmp(sim_failed,'Yes')
297     Rate_matrix(end,:)="failed";
298 q_os_bo=0;
299 end
300
301
302 Header1 = [{'Calculated Blowout rate'}, {'Blowout rate used
    '}, {'FBHP'}];
303 Header2 = [{'Sm3/D'}, {'Sm3/D'}, {'Bar'}];
304 Matrix_W = string(round([Blowout_W'*0.159, Blowout_W_used
    '*0.159,Pressure_W'/14.5],1));
305 Matrix_W = [Header1; Header2; Matrix_W];
306
307
308   q_os = double(Rate_matrix(3,3))/0.159; %STB/day
309
310 if Q==1
311 q_kill_i=q_kill_i2;
312 end
```

```

end %end for Q
%% End of kill rate loop / convert units to SI start


if strcmp(sim_failed,'Yes')==0
fprintf(repmat('\b',1,lineLength_W))
fprintf(repmat('\b',1,lineLength))
end


% Convert to SI units
if strcmp(Unit,"Semi-SI units")

Header1 = [{'Calculated Blowout rate'}, {'Blowout rate used
    '}, {'FBHP'}];
Header2 = [{'Sm3/D'}, {'Sm3/D'}, {'Bar'}];
Matrix_W = string(round([Blowout_W'*0.159, Blowout_W_used
    '*0.159,Pressure_W'/14.5],1));
Matrix_W = [Header1; Header2; Matrix_W];


Matrix_big(3:end,1)=round(double(Matrix_big(3:end,1))
    /3.28084,3);
Matrix_big(2,1) = {' [m] '};

Matrix_big(3:end,2)=round(double(Matrix_big(3:end,2))
    /14.5,3);
Matrix_big(2,2) = {' [bar] '};

Matrix_big(3:end,3)=round(double(Matrix_big(3:end,3))
    /14.5,2);
Matrix_big(2,3) = {' [bar] '};

Matrix_big(3:end,7)=round(double(Matrix_big(3:end,7))
    *16.0184,2);
Matrix_big(2,7) = {' [kg/m3] '};

Matrix_big(3:end,8)=round(double(Matrix_big(3:end,8))
    *16.0184,2);
Matrix_big(2,8) = {' [kg/m3] '};
end
```

Listing C.9: Get_Temperature2

```
function T = get_Temperature2(Depth,D_sb, Top_OH,Depth_IP,
```

```
     q_kill,X)
% This script shall calculate the temperature along the blowing wellbore.
% This shall be based on thermal conductivity and flow rates, at the
% intersection point between the blowing well and the relief well, the
% temperature will be mixed based on heat capacities of each of the fluid
% and the mass rate of the different fluids.

%Input
% Depth - Reservoir depth [ft RKB]
% D_sb  - Seabed depth [ft RKB]
% Top_OH - Depth of the last casing shoe/top of open hole [ft RKB]
% Depth_IP - Depth of intersection point between well and relief well
% gamma_k - kill fluid specific gravity [s.g.]
% q_kill - rate of kill fluid [STB/D]
% X - depth vector for the wellbore [ft RKB]

%Output
%T - a temperature vector for the entire wellbore [F]


global q_os gamma_o gamma_g gamma_k R_t T_bh T_s plot_this
global well_sorted DS Drill_pipe Materials Simulate Fig_temp Fig_temp_sur

X=flip(X)';

q_o=q_os*0.159/86400; %m3/s
q_g = q_os*R_t*0.0283168/86400;
rho_o=gamma_o*1000; %kg/m3
rho_g = gamma_g*1.225; %kg/m3
m_rate_hc =q_o*rho_o + q_g*rho_g; % kg/s



cp_HC=Materials(4); % varmekapasitet (J/kg/K)
cp_k = Materials(5);
T_st = Materials(8); %seawater surface temperature [celsius]

```

```
T_sw=(T_s-32)*5/9; % Temperatur i havet C
T_res=(T_bh-32)*5/9; % Temperatur, fluidstr m fra br nnen


U_csg = Materials(2); % W/mK
U_OH = Materials(1);  % W/mK
U_riser = Materials(9); % W/mK
Depth_IP = Depth_IP/3.28084;


if strcmp(Simulate,'Blowout and Kill') && q_kill>0
%T_IP = get_IP_temperature(q_kill,gamma_k,Depth,Depth_IP);
    %degree C
 T_IP = get_IP_Temperature2(q_kill);
else
T_IP = T_res;
end



Depth=round(Depth,0);
Depth_sb = round(D_sb/5,0)*5;

N = length(X);


T = zeros(N,1);
x = zeros(N,1);
Diam = zeros(N,1);
T_around = zeros(N,1);
Kill_rate = zeros(N,1);
G = (T_res - T_sw)/((Depth-Depth_sb)/3.28084); %Geothermal
    gradient C/m
G_s = (T_st-T_sw)/(Depth_sb/3.28084); %Water-geothermal
    gradient C/m
Depth=Depth/3.28084;


T(1) = T_res;
x(1) = Depth;
T_around(1) = T_res;

for i=2:length(X)
    D_avg = X(i)/3.28084; %meter
    x(i) = D_avg; %Depth vector in meter
```

```
80
81  if D_avg > D_sb/3.28084
82  Ta = T_res - G*(Depth - D_avg); %Celsius
83  else
84  Ta = T_sw + G_s*(Depth_sb/3.28084 - D_avg);
85  end
86
87  if D_avg < Depth_IP
88      q_k = q_kill*0.159/86400;
89  else
90      q_k = 0;
91  end
92
93     m_rate_k = q_k*gamma_k*1000; %kill fluid mass rate [kg/s
           ]
94     m_rate_m = m_rate_hc + m_rate_k;          %mixture mass
           rate [kg/s]
95     cp_m = m_rate_hc/m_rate_m * cp_HC + m_rate_k/m_rate_m *
           cp_k;
96
97  [ID_csg, OD_DS,~] = retrieve_diameter(well_sorted,DS,D_avg
       *3.28084,Drill_pipe); %Retrieve inner and outer flow
       area
98  d_h = (ID_csg - OD_DS)*0.0254; % m Hydraulic diameter
99  %d_h = ID_csg*0.0254;
100
101 if D_avg >= Top_OH
102     U = U_OH;
103 elseif D_avg < D_sb/3.28084
104     U = U_riser;
105 else
106     U = U_csg;
107 end
108
109  T(i) = T(i-1) - U*pi*d_h/(cp_m*m_rate_m)*(T(i-1)-Ta)*(X(i
        -1)-X(i))/3.28084;
110 if x(i) < Depth_IP && x(i-1) > Depth_IP
111    T_ip_m =  (m_rate_hc*cp_HC*T(i) + m_rate_k*cp_k*T_IP)/(
           m_rate_hc*cp_HC + m_rate_k*cp_k); %mixture
           temperature [c]
112 % T_ip_m =  (m_rate_hc*cp_HC*T(i-1) + m_rate_k*cp_k*T_IP)/(
       m_rate_hc*cp_HC + m_rate_k*cp_k); %mixture temperature [
       c]
113  T(i) = T_ip_m;
114 %else
```

```
%    T(i) = T(i-1) - U*pi*d_h/(cp_m*m_rate_m)*(T(i-1)-Ta)*(
    X(i-1)-X(i))/3.28084;
end

Diam(i) = d_h;
T_around(i) = Ta;
Kill_rate(i) = q_k;

end %end for i

Matrix= [x,T,Diam,T_around,Kill_rate];

if strcmp(plot_this,"Yes")


%
% Fig_Bo = figure('Name','Fig_Bo');
% figure(Fig_Bo);
 set(groot, 'DefaultFigureVisible', 'off')
Fig_temp=figure('Name','Fig_temp');
figure(Fig_temp)
plot(T,x,'b','LineWidth',2)
% hold on
% plot(T_around,X/3.28084)

ylabel('\bf Depth (m RKB)')
xlabel('\bf Temperatur (C)')
set(gca,'Ydir','reverse')
legend('Temperature inside the blowing wellbore')
xlim([min(T)-0.5, max(T)+0.5])
title(['Blowout rate = ',num2str(round(q_o*86400,1)),' Sm
    ^3/D,','    Kill rate = ',num2str(round(q_kill
    *0.159*25/36,1)),' LPM,' ,'    GOR = ',num2str(round(R_t
    /5.614583,1)),' Sm^3/Sm^3'])
set(gca,'Fontsize',12,'fontweight','bold')
grid on


Fig_temp_sur=figure('Name','Fig_temp_sur');
figure(Fig_temp_sur)
plot(T_around,x,'r','LineWidth',2)
grid
ylabel('\bf Depth (m RKB TVD)')
xlabel('\bf Temperatur (C)')
set(gca,'Ydir','reverse')
```

```
set(gca,'Fontsize',12,'fontweight','bold')
xlim([0, max(T_around)+5])
legend('Temperature in the surrounding formation')
title(['Surface = ',num2str(round(T_st)),' C,','    Seabed
    = ',num2str(round(T_sw,0)),' C' ,'    Reservoir= ',
    num2str(round(T_res,0)),' C'])
grid on
else
end

T=T*9/5 + 32; %Convert to Fahrenheit

end
```

Listing C.10: Get_IP_Temperature2

```
 function T_IP = get_IP_Temperature2(q_kill)
% This script shall calculate the temperature along the
    blowing wellbore.
% This shall be based on thermal conductivity and flow
    rates, at the
% intersection point between the blowing well and the
    relief well, the
% temperature will be mixed based on heat capacities of
    each of the fluid
% and the mass rate of the different fluids.

%Input
% Depth - Reservoir depth [ft RKB]
% D_sb  - Seabed depth [ft RKB]
% Top_OH - Depth of the last casing shoe/top of open hole [
    ft RKB]
% Depth_IP - Depth of intersection point between well and
    relief well
% gamma_k - kill fluid specific gravity [s.g.]
% q_kill - rate of kill fluid [STB/D]
% X - depth vector for the wellbore [ft RKB]

%Output
%T - a temperature vector for the entire wellbore [F]


global  gamma_k T_bh T_s RW RW_t D_sb plot_this
global  Materials  D Fig_temp_RW

N = size(RW_t,1);
```

```
X=RW_t(:,3);  %measured depth vector of RW [m MD RKB]

q_k = q_kill*0.159/86400; %Sm3/s

cp_k = Materials(5);
 m_rate_k = q_k*gamma_k*1000; %kill fluid mass rate [kg/s]

T_st = Materials(8); %seawater surface temperature [celsius
    ]
T_inj = Materials(6); %C
T_sw=(T_s-32)*5/9; % Temperatur i havet C
T_res=(T_bh-32)*5/9; % Temperatur, fluidstr m fra br nnen


U_csg = Materials(2); % W/mK
U_k_c = Materials(3); % W/mk

Depth_sb = D_sb / 3.28084; %m
%Depth_TVD = RW_t(end,2); %m TVD RKB



T = zeros(N,1);
Diam = zeros(N,1);
T_around = zeros(N,1);
Kill_rate = zeros(N,1);
G = (T_res - T_sw)/(D/3.28084-Depth_sb); %Geothermal
    gradient C/m
G_s = (T_st-T_sw)/(Depth_sb); %Water-geothermal gradient C/
    m



A = 2*pi/4*RW(2,2)^2;       %Area of two choke lines with
    the same area
ID_k_c_con = sqrt(4*A/pi) ; % The ID of one pipe which
    gives the same area as 2

T_around(1) = T_st;
T(1) = T_inj;

for i=2:length(X)
    D_TVD = RW_t(i,2); %meter


```

```
65  if D_TVD > D_sb/3.28084
66  Ta = T_sw + G*(D_TVD - Depth_sb); %Celsius
67  else
68  Ta = T_st - G_s*(D_TVD-0);
69  end
70
71
72  if D_TVD <= RW(2,4)/3.28084 %kill n choke lines
73  d_h = ID_k_c_con *0.0254; %The converted kill and choke
        diameter to one diameter [m]
74  U = U_k_c;
75  else
76  d_h = RW(3,2)*0.0254; %inside diameter of casing [m]
77  U = U_csg;
78  end
79
80
81      T(i) = T(i-1) - U*pi*d_h/(cp_k*m_rate_k)*(T(i-1)-Ta)*(X
            (i)-X(i-1));
82
83  Diam(i) = d_h;
84  T_around(i) = Ta;
85  Kill_rate(i) = q_k;
86
87  end %end for i
88
89  T_IP = T(end); %celsius
90
91
92  if strcmp(plot_this,"Yes")
93  %
94  Fig_temp_RW=figure('Name','Fig_temp_RW');
95  figure(Fig_temp_RW)
96  plot(T,X,'Color','#D95319','LineWidth',2)
97
98  grid
99  ylabel('\bf Depth (m RKB MD)')
100 xlabel('\bf Temperatur (C)')
101 set(gca,'Ydir','reverse','Fontsize',12,'fontweight','bold')
102 legend('Temperature inside relief well')
103 title(['Kill rate = ',num2str(round(q_kill/1.44*0.159)),'
        LPM,'])
104 Matrix= [X,T,Diam,T_around,Kill_rate];
105
106 set(gca,'Ydir','reverse','Fontsize',12,'fontweight','bold')
```

```
grid on

else
end


end
```

Listing C.11: retrieve_diameter

```
function [ID_csg, OD_DS,rel_rough] = retrieve_diameter(
    well_sorted,DS,D_avg,Drill_pipe)

%Gaining well inner diameter, e.g. casing ID and open hole
    ID
% if D_avg > well_sorted(end,3) %Open hole
%     ID_csg = well_sorted(end,2);
%     % rel_rough = well(end,5)  m   legge til rel_rough
% elseif D_avg <= well_sorted(end,3) %surface casing
%       ID_csg = well_sorted(end-1,2);
%     % rel_rough = well(end,5)  m   legge til rel_rough
% %elseif legge til mulighet for liner
% end

D_avg = round(D_avg,0);
I=well_sorted(:,3)<=(D_avg);
L=well_sorted(:,4)>= (D_avg );
row=find(I+L==2);
row=row(end);
ID_csg=well_sorted(row,2);
rel_rough=well_sorted(row,5);


%Retrieving Drill String Outer diameter
if Drill_pipe == "Yes"
if D_avg > DS(end,4)
   OD_DS = DS(end,1); % OD of BHA
elseif D_avg <= DS(end,4)
    OD_DS = DS(1,1); % OD DP
end
else
    OD_DS = 0;
end


end
```

Listing C.12: Orkiszewski_correlation

```
function [dp, Flow, rho_avg, rho_l,dp_f,dp_grav,yl, yk,
    Gamma_phase, B_o, R_s,mu_l,f,p_b,Gamma] =
    Orkiszewski_correlation(D_avg, T_avg, p_old, dp,dL, d_h,
    A_p,rel_rough,q_kill,gamma_k)
global gamma_o gamma_API gamma_g R_t q_os q_ws g_c PVT_sim;
     % variables that are constant
%% This plot is based on the Orkiszewski correlation and
    calculates
%  the pressure drop for multiphase flow in a wellbore.
%  Calculate the pressure change with an defined maximum
    error for a fixed
%  length interval
%  Note: This correlation should only be used for vertical
    wells!

%% Input section
% D           - Total depth [ft]
% D_wh        - Depth of well head [ft]
% d_t         - Tubing diameter [in]
% gamma_o     - Specific gravity of oil
% gamma_API   - API gravity of oil
% gamma_g     - Specific gravity of gas
% R_t         - Total gas-oil-ratio [SCF/STB]
% p_wh        - Wellhead backpressure [psig]
% q_os        - Surface flow rate of oil [STB/D]
% q_ws        - Surface flow rate of water [STB/D]
% T_s         - Flowing surface temperature [F]
% T_bh        - Flowing bottom hole temperature [F]



if q_os == 1
    q_os = 0.0001;
end

%% Calculations starting at WH

%Step 2
residual_pressure=100;
%A_p = pi / 4 *d_h^2 ; % ft^2
A_p = A_p/144; %ft
Flow_regime=string("");
Overwrite = 'No';
Orkis_accel="No";
```

```
dp_initial=dp;
%%
% Pressure=zeros(N,1); Pressure(1) = p_wh;
% Depth = zeros(N,1); Depth(1)=D_wh;
% Temperature =zeros(N,1); Temperature(1) = T_s;
% FVF = zeros(N,1); FVF(1)=1;
% GOR = zeros(N,1); GOR(1) = 0;
% Flow_regime = strings(N,1); Flow_regime(1) = 'surface';
% sigma =zeros(N,1); sigma(1)=0;


%%
%Going from bottom to the top of the well
%fprintf('\n Loading %.0f / 100 \n', i)
k=0;
g=32.2;

while residual_pressure > 0.5
k=k+1;

p_avg = p_old + dp/2;
%p_avg = p_old;
%Step 3 - fluid properties at p_avg, T_avg

 z=zfak(p_avg,T_avg,gamma_g,0.9);
% [p_b, B_o,R_s, mu_o] = Glaso(R_t, T_avg, gamma_g, gamma_o
    ,p_avg);


%  p_avg_si = p_avg/14.5*10^5;
%  T_si = 273+(T_avg -32)*5/9;
% %
%   [Bg,B_o,R_s,rho_g,rho_l,~,~,~] =Olgjenka_PVT(p_avg_si,
    T_si,0);
%    [p_b, B_o,R_s, mu_o, mu_g] = Glaso_3(p_avg_si,T_si,
    rho_g);
% %
%  sigma_L=Interfacial_Tension(T_avg,gamma_API,R_s); %lb/s2


%[p_b, R_s, B_o, ~, mu_o,~,~, ~, sigma_L ]=Glaso_PVT(p_avg,
    T_avg,"OFU");
%[p_b, R_s, B_o, Bg, mu_o,mu_g,rho_o, rho_g, sigma_L ]=
    Glaso_PVT(p_avg,T_avg,"Semi-SI");
%[p_b, R_s, B_o, Bg, mu_o,mu_g,rho_o, rho_g, sigma_L ]=
```

```
    Standing_PVT(p_old,T_avg,"Semi-SI");
78  if strcmp(PVT_sim,"Standing")
79  [p_b, R_s, B_o, Bg, mu_o,mu_g,rho_o, rho_g, sigma_L ]=
        Standing_PVT(p_old,T_avg,"OFU");
80  elseif strcmp(PVT_sim,"Glaso")
81  [p_b, R_s, B_o, Bg, mu_o,mu_g,rho_o, rho_g, sigma_L ]=
        Glaso_PVT(p_old,T_avg,"OFU");
82  end
83  % rho_l = (rho_o*q_os*Bo + gamma_k*1000*q_k*Bw)/(q_os*Bo +
        q_k*Bw);
84
85
86  %Step 3.b - corrected flow rates
87  q_o=6.49*10^(-5)*q_os*B_o; %ft^3/sec  - Current oil rate
        down hole
88  q_w = 6.49*10^(-5)*q_ws;   %ft^3/sec  - Current water rate
        down hole
89  q_k = + 6.49*10^(-5)*q_kill;
90  q_l = q_o + q_w + q_k;           %ft^3/sec  - Current total
         liquid rate down hole
91
92  q_g = 3.27*10^(-7)*z*q_os * (R_t-R_s)* (T_avg+460)/p_avg; %
         ft^3/sec - Current gas rate down hole
93  q_t = q_l + q_g;           %ft^3/sec - Current total flow
        rate down hole
94
95
96
97
98  mu_l=mu_o*q_o/q_l + 1*q_w/q_l + 1*q_k/q_l;  % Liquid
        viscosity [cp]
99
100 %Step 3.c - corrected mass flow rates
101 q_mo = q_os*(4.05*10^(-3)*gamma_o + 8.85*10^(-7)*gamma_g*
        R_s); %lb/sec 4.05*10^-3 = STB/D*s.g. --> ft3/s * lb
102 q_mg = 8.85*10^(-7)*q_os*gamma_g*(R_t-R_s);
                          %lb/sec
103 q_mk = q_k* gamma_k *62.4279 ;
                                        %lb/sec kill mass flow
104 q_mt = q_mo + q_mg + q_mk;
                                                %lb/sec
105
106
107 %Step 3.d - corrected densities
108 rho_l = q_mo/q_l + q_mk/q_l; %lb/ft^3
```

```
109 if q_g > 0
110 rho_g = q_mg/q_g;  %lb/ft^3
111 else
112     rho_g=0;
113 end
114 %% Step 4 - Flow regime determination
115
116 v_gD = q_g*(rho_l/(sigma_L*32.2))^0.25 / A_p; % dimension
    less
117 v_t = q_t/ A_p; %ft/sec
118 v_sl = q_l/A_p; %ft/sec
119
120 % Calculating boundary conditions
121 L_B = 1.071 - 0.2218*v_t^2 / (d_h) ;     %Bubble flow
122 L_S = 50 + 36*v_gD * q_l/q_g;            %Slug flow
123 L_M = 75 + 84*(v_gD * q_l/q_g)^0.75;     %Mist flow
124
125 if L_B < 0.13
126     L_B = 0.13;        %L_B has a lower limit of 0.13
127 end
128
129
130
131 if q_g==0
132     Flow = 'Single phase';
133 elseif q_g/q_t < L_B
134    Flow = 'Bubble';
135 elseif q_g/q_t > L_B && v_gD <= L_S
136    Flow = 'Slug';
137 elseif L_M > v_gD && v_gD > L_S
138    Flow = 'Transition';
139 elseif v_gD >= L_M
140    Flow = 'Mist';
141 end
142
143
144 % Overwrite alternating flow regimes
145
146 if strcmp(Overwrite,'Yes')
147     Flow = Flow_OV;
148 end
149
150 %% Calculate some common values
151  N_Re = 1488 * q_t* rho_l * d_h/(A_p*mu_l);
152
```

```
 %% Bubble Flow calculations or single flow for q_g = 0
if strcmp(Flow,'Bubble') || strcmp(Flow,'Single phase')
v_s=0.8; %ft/sec
F_g = 0.5 * (1 + q_t / (v_s*A_p) - sqrt((1+q_t/(v_s*A_p))^2
    - 4*q_g/(v_s*A_p)) );
%F_g = q_g/q_t;
rho_avg = (1-F_g)*rho_l + F_g*rho_g;

if abs(rho_avg - rho_l) < 0.005
    a=0;
end

v_l = q_l/A_p/(1-F_g);
N_Re = 1488 * v_l* rho_l * d_h/mu_l;

if N_Re >= 2300
f=colebrook(N_Re,rel_rough);  %Colebrook equation to find
   friction factor instead of chart
elseif q_l < 50
%f= 0;
f = 64/N_Re ;
else
f = 64/N_Re ;
end
tau_f = f * rho_l * v_l^2 /(2*g_c*d_h);

end

%% Slug Flow calculation
if strcmp(Flow,'Slug') || strcmp(Flow,'Transition')
    v_ba = 1.0 ;
    v_b=0.2;
V = 0;
while abs(v_ba-v_b)>0.005 %Iterative process to deterine
   bubble rise velocity
    V= V+1;
    N_b = 1488 * rho_l *d_h *v_ba / mu_o ;


% Find the C2 coefficient
if N_b <= 3000
 v_b = (0.546 + 8.74 * 10^(-6)*N_Re) * sqrt(g_c * d_h); %ft
    /sec
elseif N_b >= 8000
 v_b = (0.35 + 8.74 * 10^(-6)*N_Re) * sqrt(g_c * d_h); %ft/
```

```
    sec
elseif 8000>N_b && N_b >3000
v_bi = (0.251 + 8.74 * 10^(-6)*N_Re) * sqrt(g_c * d_h); %ft
    /sec
v_b = 0.5*v_bi + sqrt(v_bi^2 + 13.59*mu_l/rho_l/d_h^0.5); %
    ft/sec
end

v_ba= v_ba +0.5*(v_b-v_ba);

v_bv(V)=v_b;  % to avoid everlasting loop
if V>20
v_b = mean(v_bv);
v_ba=v_b; % to stop the loop
end
end


%Correct that the C2 factor will go towards 1.0  for large
    N_b values
if N_b > 20000  %Based on the figures provided by
    orkiszewski
    C1 = 0.35;
    C2 = 1.0;
    v_b = C1*C2*sqrt(g*d_h);
    v_ba = v_b;
end

%Calculating the continuous liquid phase
liq_phase = q_o/(q_o+q_w);

if liq_phase >= 0.5
  cont_phase = 'Oil' ;
else
  cont_phase = 'Water'  ;
end


if v_t < 10 && strcmp(cont_phase,'Water')
Gamma = 0.013/(d_h)^1.38 * log10(mu_l) - 0.681 + 0.232*
    log10(v_t) - 0.428*log10(d_h);
Gamma_min = 0.013/(d_h)^1.38 * log10(mu_l) - 0.681 + 0.232*
    log10(50) - 0.428*log10(d_h);
Gamma_phase = 'water 1';
elseif v_t >= 10 && strcmp(cont_phase,'Water')
```

```
232 Gamma = 0.045/(d_h)^0.799 * log10(mu_l) - 0.709 - 0.162*
        log10(v_t) - 0.888*log10(d_h);
233 Gamma_min = 0.045/(d_h)^0.799 * log10(mu_l) - 0.709 -
        0.162*log10(50) - 0.888*log10(d_h);
234 Gamma_phase = 'water 2';
235 elseif v_t < 10 && strcmp(cont_phase,'Oil')
236 Gamma = 0.0127/(d_h)^1.415 * log10(mu_l + 1) - 0.284 +
        0.167*log10(v_t) + 0.113*log10(d_h);
237 Gamma_min = 0.0127/(d_h)^1.415 * log10(mu_l + 1) - 0.284 +
        0.167*log10(50) + 0.113*log10(d_h);
238 Gamma_phase = 'Oil 1';
239 elseif v_t >= 10 && strcmp(cont_phase,'Oil')
240 Gamma = 0.0274/(d_h)^1.371 * log10(mu_l + 1) + 0.161 +
        0.569*log10(d_h) - log10(v_t)*( 0.01*log10(mu_l + 1)/d_h
        ^1.571 +  0.397 + 0.63*log10(d_h));
241 Gamma_min = 0.0274/(d_h)^1.371 * log10(mu_l + 1) + 0.161 +
        0.569*log10(d_h) - log10(50)*( 0.01*log10(mu_l + 1)/d_h
        ^1.571 +  0.397 + 0.63*log10(d_h));
242 Gamma_phase = 'Oil 2';
243 end
244
245 if Gamma < -0.065 *v_t
246     Gamma = -0.065 *v_t;
247 end
248
249 % if Gamma < Gamma_min
250 %     Gamma=Gamma_min;
251 % end
252
253 % if Gamma < -0.3
254 %     Gamma=-0.3;
255 % end
256
257 %rho_avg = (q_mt + rho_l * v_b *A_p)/(q_t +v_b*A_p) + Gamma
        *rho_l; %lb/ft^3
258
259 rho_avg = rho_l*((q_l+v_b*A_p)/(q_l + q_g + v_b*A_p)) +
        rho_g*q_g/((q_l + q_g + v_b*A_p));
260
261
262 Gamma_bound = - v_b*A_p/(q_t+v_b*A_p)*(1 - rho_avg/rho_l);
263 if v_t > 10 || Gamma < Gamma_bound
264 Gamma  =  Gamma_bound ;
265 end
266
```

```
%
%rho_avg = (q_mt + rho_l * v_b *A_p)/(q_t +v_b*A_p) + Gamma
    *rho_l; %lb/ft^3
rho_avg = rho_l*((q_l+v_b*A_p)/(q_l + q_g + v_b*A_p)) +
    rho_g*q_g/((q_l + q_g + v_b*A_p));

if rho_avg < rho_g
    a=0;
end


if N_Re >= 2300
f=colebrook(N_Re,rel_rough);  %Colebrook equation to find
    friction factor instead of chart
else
f = 64/N_Re ;
end

tau_f = f *rho_l * v_t^2 /(2*g_c *d_h)*((q_l +v_b*A_p)/(q_t
    + v_b*A_p)+Gamma); %psi/ft

if tau_f < 0
    a=0;
end
rho_avg_slug = rho_avg;
tau_f_slug=tau_f;
end

%% Calculate the mistflow
if strcmp(Flow,'Mist')|| strcmp(Flow,'Transition')
v_sg=q_g/A_p;
F_g = 1/(1+q_l/q_g);
rho_avg = (1-F_g)*rho_l + F_g*rho_g;

N_mist = 4.52*10^(-7)*(v_sg*mu_l/sigma_L)^2*rho_g/rho_l;

if N_mist <= 0.005
rel_rough_mist = 34*sigma_L/(rho_g*v_sg^2*d_h);
elseif N_mist > 0.005
rel_rough_mist = 174.7*sigma_L*N_mist^(0.302)/(rho_g*v_sg
    ^2*d_h);
end

f = 1/(4*log10(0.27*rel_rough_mist))^2 + 0.067*
    rel_rough_mist^1.173;
```

```
306
307 % if N_Re >= 2300
308 % f=colebrook(N_Re,rel_rough_mist);  %Colebrook equation to
        find friction factor instead of chart
309 % else
310 % f = 64/N_Re ;
311 % end
312
313 tau_f = f * rho_g*v_sg^2/(2*g_c*d_h);
314
315 rho_avg_mist=rho_avg;
316 tau_f_mist=tau_f;
317 end
318 %% Calculate Transiton flow
319 if strcmp(Flow,'Transition')
320
321 rho_avg=(L_M-v_gD)/(L_M - L_S)*rho_avg_slug + (v_gD-L_S)/(
        L_M-L_S)*rho_avg_mist;
322 tau_f = (L_M-v_gD)/(L_M - L_S)*tau_f_slug + (v_gD-L_S)/(L_M
        -L_S)*tau_f_mist;
323
324 end
325
326
327 %% Calculate pressure drop and length increment
328
329
330 delta_D = 144/(rho_avg+tau_f)*(1 - q_mt*q_g/(4637*A_p^2*
        p_avg))*dp; %ft
331 delta_p = (144/(rho_avg+tau_f)*(1 - q_mt*q_g/(4637*A_p^2*
        p_avg)))^(-1)*dL; % psi
332
333 residual_pressure = abs(dp - delta_p);
334
335
336
337 dp=delta_p;
338
339 if delta_p<0
340     dp=dp_initial+1;
341     dp_initial=dp;
342 end
343 %p_avg = Pressure(i-1) + dp;
344
345 % To adjust for alternating flow regimes each step
```

```
346 if k > 10 && Flow_regime(k-2) == Flow && Flow ==
        Flow_regime(k-4) && Flow_regime(k-3) == Flow_regime(k-3)
347 Overwrite = 'Yes';
348 Flow_OV = Flow;
349 else
350 Overwrite = 'No';
351 end
352
353 if k>1000
354     residual_pressure=0.05;
355   %fprintf('Problems when calculating pressure at step %.0f
          \n', i)
356 end
357
358
359
360
361 dp_grav = rho_avg*0.052*dL / 7.48 ;
362 dp_f = dp - dp_grav;
363 yl = q_l / q_t ;
364 yk = q_k / q_t ;
365 %% Values to be plotted later
366 Pressure(k)=p_avg;
367 Depth(k) = D_avg;
368 Tauf(k) = tau_f;
369 Density(k) = rho_avg;
370 Temperature(k) = T_avg;
371 FVF(k) = B_o;
372 Flow_regime(k)= Flow;
373 GOR(k) = R_s;
374 sigma(k)=sigma_L*2.205*10^-3;
375 Reynold(k) = N_Re;
376
377
378 Matrix = [Pressure', Depth', Flow_regime',Reynold',Density
        ', Tauf'];
379 Header2 = [{'Pressure'}, {'Depth'}, {'Flow Regime'}, {'
        Reynolds'}, {'Density'}, {'Tau_f'}];
380
381 Matrix = [Header2; Matrix];
382 end
383
384 if strcmp(Flow,'Slug')
385 else
386 Gamma_phase = 'Not slug flow' ;
```

```
Gamma=0;

%pressure=p_old - dp ; % psia
end
```

Listing C.13: Standing_PVT

```
function [p_b, R_s, B_o, B_g, mu_o,mu_g,rho_o, rho_g,
    sigma_l ]=Standing_PVT(p_avg,T_avg,Output_units)

% Input
% p - Pressure [psia]
% T - Temperature [F]
% Output_units - "OFU" or "Semi-SI" --> calculates the
    output units

% Global input
% R_t - Total GOR [SCF/STB]
% gamma_o - oil specific gravity
% gamma_g - gas specific gravity


                                    %%%%%%%Units
                                       %%%%%%%%%%%%
%Output                              OFU             Semi-SI
%P_b - Saturation pressure           [psia]      or [Bar]
%R_s - Solution GOR                  [SCF/STB]   or [Sm3/Sm3
    ]
%B_o - Oil formation volume factor   [RB/STB]    or [m3/Sm3]
%B_g - Gas formation volume factor   [ft^3/SCF]  or [m3/Sm3]
%mu_o - Oil viscosity                [cp]        or [cp]
%mu_g - Gas viscosity                [cp]        or [cp]
%rho_o - Oil density                 [lb/ft3]    or [kg/m3]
%rho_g - Gas density                 [lb/ft3]    or [kg/m3]
%sigma_l - Interfacial tension gas-oil [lb/s2]  or [Dyne/cm
    ]


global R_t gamma_o gamma_g

% gamma_o = 0.838;
% gamma_g = 1.2;
% R_t = 615;
% T_avg=260;

gamma_API = 141.5/gamma_o - 131.5; % API degree
```

```
35
36 %% Saturation pressure - Standing correlation
37 p_b = 18.2*((R_t/gamma_g)^(0.83)*10^(0.00091*T_avg)
       /(10^(0.0125*gamma_API))-1.4);
38
39
40 %% Solution gas oil ratio - Standing correlation
41 if p_avg < p_b
42 R_s = ((p_avg/18.2 + 1.4)*(10^(0.0125*gamma_API))
       /10^(0.00091*T_avg))^(1/0.83)*gamma_g;
43 else
44 R_s = R_t;
45 end
46
47 if R_s > R_t
48 R_s =R_t;
49 elseif R_s < 0
50 R_s = 0;
51 end
52
53 %% Oil formation volume factor - Standing correlation
54 if p_avg<=p_b % Checking if below bubble point pressure
55 B_o = 0.972 + 1.47*10^(-4)*(R_s*(gamma_g/gamma_o)^0.5 +
       1.25*T_avg)^1.175;
56 else %pressure must be greater than bubble point pressure
57 % Using Vasquez and Beggs correlation
58 B_ob = 0.972 + 1.47*10^(-4)*(R_t*(gamma_g/gamma_o)^0.5 +
       1.25*T_avg)^1.175;
59 c_o = (-1433 + 5*R_t + 17.2*T_avg - 1180*gamma_g + 12.61*
       gamma_API)/10^5/p_avg; %compressibility factor
60 B_o = B_ob*exp(c_o*(p_b-p_avg)); %[RB/STB]
61 end
62
63 %% Oil viscosity
64
65 %Dead oil viscosity calculated with Glas -correlation
66 c = 3.141*(10^10) * T_avg^(-3.444);
67 d = 10.313*log10(T_avg) - 36.447 ;
68
69 mu_od = c*(log10(gamma_API)^d); %cp
70
71 % Viscosity below bubble point - Standing correlation
72 % and viscosity above bubble point - Vasquez and Beggs
73
74 if p_avg<=p_b % Standing correlation
```

```
A_1 = 10^-(7.4*10^(-4)*R_s + 2.2*10^(-7)*R_s^2);
A_2 = 0.68/(10^(8.62*10^(-5)*R_s)) + 0.25/(10^(1.1*10^(-3)*
    R_s)) + 0.062/(10^(3.74*10^(-3)*R_s));
mu_o = A_1*mu_od^A_2 ; % cp
else % Vasquez and Beggs correlation
A_1 = 10^-(7.4*10^(-4)*R_t + 2.2*10^(-7)*R_t^2);
A_2 = 0.68/(10^(8.62*10^(-5)*R_t)) + 0.25/(10^(1.1*10^(-3)*
    R_t)) + 0.062/(10^(3.74*10^(-3)*R_t));
mu_ob = A_1*mu_od^A_2 ; % cp

A = 2.6*p_avg^1.187*exp(-11.513 -8.98*10^(-5)*p_avg);
mu_o = mu_ob*(p_avg/p_b)^A;
end
%% Oil density

rho_o = (62.42796*gamma_o + 0.0136*gamma_g*R_s)/B_o;
%% Gas FVF and density

z=zfak(p_avg,T_avg,gamma_g,0.9);

T_rank = T_avg + 459.67 ; %Temperature in rankine
B_g = 0.0282793*z*T_rank/p_avg; %rcf/SCF

rho_g_s = 0.076474*gamma_g;
rho_g = rho_g_s / B_g;



%% Lee-Gonzales gas viscosity

% mu_g - [cp], rho_g - [g/cm3] T - [Rankine]

rho_g_mu = rho_g/1000; %g/cm3
M_g = 28.97 *gamma_g; %Molar mass of the gas

A1 = (9.379 + 0.01607*M_g)*T_rank^1.5 /(209.2 + 19.26*M_g +
     T_rank);
A2 = 3.448 + (986.4/T_rank) + 0.01009*M_g;
A3 = 2.447 - 0.2224*A2;

mu_g = A1*10^-4*exp(A2*rho_g_mu^A3); %gas visocisty cP

%% (Abdul-Majeed and Abu Al-Soof, 2000) - Interfacial
   tension

```

```
T_cels = (T_avg-32)*5/9;
%sigma_od=(1.17013 - 1.694*10^(-3)*T_avg)*(38.085-0.259*
    gamma_API); %T =F
sigma_od=(1.11591 - 0.00305*T_cels)*(38.085-0.259*gamma_API
    );
Rs=R_s/5.614; % Convert from scf/STB to m3/m3


if Rs < 50
fraction = 1 / (1+0.02549*Rs^1.0157);
elseif Rs >= 50
fraction = 32.0436*Rs^(-1.1367);
end
%fraction = 0.056379 + 0.94362*exp(-3.849*10^(-3)*R_s);
sigma_l=sigma_od*fraction; %Dyne/cm

sigma_l=sigma_l*(2.20462*10^-3); %lb/s2



%% Change the output units based on unit wish

if strcmp(Output_units,"Semi-SI")
p_b = p_b/14.504; %Bar
R_s = R_s/5.6145833; %Sm3/Sm3
rho_o = rho_o*16.0185; %kg/m3
rho_g = rho_g*16.0185; %kg/m3
sigma_l =sigma_l/(2.20462*10^-3); %dyne/cm
end

end
```

Listing C.14: Glaso_PVT

```
function [p_b, R_s, B_o, B_g, mu_o,mu_g,rho_o, rho_g,
    sigma_l ]=Glaso_PVT(p_avg,T_avg,Output_units)

% Input
% p - Pressure [psia]
% T - Temperature [F]
% Output_units - "OFU" or "Semi-SI" --> calculates the
    output units

% Global input
% R_t - Total GOR [SCF/STB]
% gamma_o - oil specific gravity
```

```
% gamma_g - gas specific gravity


                                    %%%%%%%Units
                                       %%%%%%%%%%%%
%Output                             OFU             Semi-SI
%P_b - Saturation pressure          [psia]      or [Bar]
%R_s - Solution GOR                 [SCF/STB]   or [Sm3/Sm3
    ]
%B_o - Oil formation volume factor  [RB/STB]    or [m3/Sm3]
%B_g - Gas formation volume factor  [ft^3/SCF]  or [m3/Sm3]
%mu_o - Oil viscosity               [cp]        or [cp]
%mu_g - Gas viscosity               [cp]        or [cp]
%rho_o - Oil density                [lb/ft3]    or [kg/m3]
%rho_g - Gas density                [lb/ft3]    or [kg/m3]
%sigma_l - Interfacial tension gas-oil [lb/s2]  or [Dyne/cm
    ]


global R_t gamma_o gamma_g

%  gamma_o = 0.838;
%  gamma_g = 1.2;
% % R_t = 615;
% T_avg=260;

gamma_API = 141.5/gamma_o - 131.5; % API degree

%% Saturation pressure - Glas  correlation
if R_t> 900
    volatile ='Yes';
else
    volatile = 'No';
end

if strcmp(volatile,'No')
p_bc = (R_t/gamma_g)^0.816 * T_avg^0.172/gamma_API^0.989; %
    [psig]
p_b = 10^ (1.7669 + 1.7447*log10(p_bc) - 0.30218*(log10(
    p_bc))^2); %[psig]
elseif strcmp(volatile,'Yes')
p_bc = (R_t/gamma_g)^0.816 * T_avg^0.130/gamma_API^0.989; %
    [psig]      %changed T^0.172 --> T^0.130
p_b = 10^ (1.7669 + 1.7447*log10(p_bc) - 0.30218*(log10(
    p_bc))^2); %[psig]                        )
```

```
end



%% Solution gas oil ratio - Glas  correlation
if p_avg < p_b
x = 10^((-1.7447 + sqrt(1.7447^2-4*(-0.30218)*(1.7669-log10
    (p_avg))))/(2*(-0.30218)));
R_s = (x*gamma_g^0.816 * gamma_API^0.989 / T_avg^0.172)
    ^(1/0.816);
else
R_s = R_t;
end

if R_s > R_t
R_s =R_t;
elseif R_s < 0
R_s = 0;
end

%% Oil formation volume factor - Glas  correlation

% Formation volume factor above or below bubble point

if p_avg <=p_b % Checkin if below bubble point pressure
B_oc = R_s*(gamma_g/gamma_o)^0.526 + 0.968*T_avg ;
B_o = 10^(-6.58511 + 2.91329*log10(B_oc) - 0.27683*(log10(
    B_oc))^2)  + 1; %[RB/STB]
else %pressure must be greater than bubble point pressure
% Using Vasquez and Beggs correlation
B_obc = R_t*(gamma_g/gamma_o)^0.526 + 0.968*T_avg ;
B_ob = 10^(-6.58511 + 2.91329*log10(B_obc) - 0.27683*(log10
    (B_obc))^2)  + 1; %[RB/STB]
c_o = (-1433 + 5*R_t + 17.2*T_avg - 1180*gamma_g + 12.61*
    gamma_API)/10^5/p_avg; %compressibility factor
B_o = B_ob*exp(c_o*(p_b-p_avg)); %[RB/STB]
end
%% Oil viscosity

%Dead oil viscosity calculated with Glas -correlation
c = 3.141*(10^10) * T_avg^(-3.444);
d = 10.313*log10(T_avg) - 36.447 ;

mu_od = c*(log10(gamma_API)^d); %cp
```

```
89
90  % Viscosity below bubble point - Standing correlation
91  % and viscosity above bubble point - Vasquez and Beggs
92
93  if p_avg<=p_b % Standing correlation
94  A_1 = 10^-(7.4*10^(-4)*R_s + 2.2*10^(-7)*R_s^2);
95  A_2 = 0.68/(10^(8.62*10^(-5)*R_s)) + 0.25/(10^(1.1*10^(-3)*
        R_s)) + 0.062/(10^(3.74*10^(-3)*R_s));
96  mu_o = A_1*mu_od^A_2 ; % cp
97  else % Vasquez and Beggs correlation
98  A_1 = 10^-(7.4*10^(-4)*R_t + 2.2*10^(-7)*R_t^2);
99  A_2 = 0.68/(10^(8.62*10^(-5)*R_t)) + 0.25/(10^(1.1*10^(-3)*
        R_t)) + 0.062/(10^(3.74*10^(-3)*R_t));
100 mu_ob = A_1*mu_od^A_2 ; % cp
101
102 A = 2.6*p_avg^1.187*exp(-11.513 -8.98*10^(-5)*p_avg);
103 mu_o = mu_ob*(p_avg/p_b)^A;
104 end
105 %% Oil density
106
107 rho_o = (62.42796*gamma_o + 0.0136*gamma_g*R_s)/B_o;
108 %% Gas density
109
110 z=zfak(p_avg,T_avg,gamma_g,0.9);
111
112 T_rank = T_avg + 459.67 ; %Temperature in rankine
113 B_g = 0.0282793*z*T_rank/p_avg; %rcf/SCF
114
115 rho_g_s = 0.076474*gamma_g;
116 rho_g = rho_g_s / B_g;
117
118
119
120 %% Lee-Gonzales gas viscosity
121
122 % mu_g - [cp], rho_g - [g/cm3] T - [Rankine]
123
124 rho_g_mu = rho_g/1000; %g/cm3
125 M_g = 28.97 *gamma_g; %Molar mass of the gas
126
127 A1 = (9.379 + 0.01607*M_g)*T_rank^1.5 /(209.2 + 19.26*M_g +
        T_rank);
128 A2 = 3.448 + (986.4/T_rank) + 0.01009*M_g;
129 A3 = 2.447 - 0.2224*A2;
130
```

```
mu_g = A1*10^-4*exp(A2*rho_g_mu^A3); %gas visocisty cP

%% (Abdul-Majeed and Abu Al-Soof, 2000) - Interfacial
   tension

T_cels = (T_avg-32)*5/9;
%sigma_od=(1.17013 - 1.694*10^(-3)*T_avg)*(38.085-0.259*
   gamma_API); %T =F
sigma_od=(1.11591 - 0.00305*T_cels)*(38.085-0.259*gamma_API
   );
Rs=R_s/5.614; % Convert from scf/STB to m3/m3


if Rs < 50
fraction = 1 / (1+0.02549*Rs^1.0157);
elseif Rs >= 50
fraction = 32.0436*Rs^(-1.1367);
end
%fraction = 0.056379 + 0.94362*exp(-3.849*10^(-3)*R_s);
sigma_l=sigma_od*fraction; %Dyne/cm

sigma_l=sigma_l/(2.205*10^-3); %lb/s2


%% Change the output units based on unit wish

if strcmp(Output_units,"Semi-SI")
p_b = p_b/14.504; %Bar
R_s = R_s/5.6145833; %Sm3/Sm3
rho_o = rho_o*16.0185; %kg/m3
rho_g = rho_g*16.0185; %kg/m3
sigma_l =sigma_l*(2.205*10^-3); %dyne/cm
end

end
```

Listing C.15: zfak

```
function [ Z ] = zfak( p,T,gg ,zin)
% Output: gas z-factor
% Input:
% p : pressure (psi)
% T : temperature (F)
% gg : gas gravity (specific density)
% zin : initial guess of z-factor (e.g.: 0.9)
%
```

```
p = p*6894.76; % [Pa]Converting Psi to Pa
T = (T+459.67)*5/9; % [K] Converting from Fahrenheit to
    Kelvin


% Sutton correlations for REDUCED PRESSURE AND TEMPERATURE
 TR=T/(94+194.2*gg-41.1*gg^2);
 PR=p/(58.18-9.032*gg-0.248*gg^2)/1e5;
% Hall&Yarborough extended eq. of state. REF O&G JUNE
    18,1973 P82 AND FEB.
%18 1974 P86
% Programmed in FORTRAN by Roy Knapp UT, converted to
    MatLab and included Suttons
%correlation by H. Asheim NTNU
 if TR>1.01
 t = 1.0/TR;
 else
 t=1.0;
 end
 A = 0.06125*t*exp(-1.2*(1.-t)^2);
% B = t*(14.76-9.76*t + 4.58*t*t);
 B = t*(14.76-9.76*t + 4.58*t*t);
 C = t*(90.7 -242.2*t + 42.4*t*t);
 D = 2.18 +2.82*t;
% REDUCED DENSITY CALCULATION BY NEWTON-RAPHSON METHOD
Y=A/zin;
 J=1;
 F=1;
 while (J<50) && (abs(F)>1e-4)
 J=J+1;
 if Y>1
 Y=0.6;
 end
 F=-A*PR + (Y + Y^2 + Y^3 -Y^4)/(1.-Y)^3 -B*Y*Y +C*Y^D;
% CALCULATE DERIVATIVE
 DFDY =(1. +4.*Y +4.*Y*Y -4.*Y^3 +Y^4)/(1.-Y)^4 ...
 -2.*B*Y + D*C*Y^(D-1.);
 Y = Y -0.5*F/DFDY;
 end
 YUT=Y;
% NO Convergence
if (abs(F)<1e-4)
% CONVERGENCE OBTAINED
 Z = A*PR/Y;
else
```

```
 Z =1.0;
end
```

Listing C.16: colebrook

```
function F = colebrook(R,K)
% F = COLEBROOK(R,K) fast, accurate and robust computation of the
%     Darcy-Weisbach friction factor F according to the Colebrook equation:
%                                 -                           -
%       1                        |    K        2.51          |
%  ---------  =  -2 * Log_10 |  ----- + -------------  |
%   sqrt(F)                     |   3.7     R * sqrt(F)   |
%                                 -                           -
% INPUT:
%   R : Reynolds' number (should be >= 2300).
%   K : Equivalent sand roughness height divided by the hydraulic
%       diameter (default K=0).
%
% OUTPUT:
%   F : Friction factor.
%
% FORMAT:
%   R, K and F are either scalars or compatible arrays.
%
% ACCURACY:
%   Around machine precision forall R > 3 and forall 0 <= K,
%   i.e. forall values of physical interest.
%
% EXAMPLE: F = colebrook([3e3,7e5,1e100],0.01)
%
% Edit the m-file for more details.
% Method: Quartic iterations.
% Reference: http://arxiv.org/abs/0810.5564
% Read this reference to understand the method and to modify the code.
% Author: D. Clamond, 2008-09-16.
% Check for errors.
if any(R(:)<2300) == 1,
   warning('The Colebrook equation is valid for Reynolds'' numbers >= 2300.');
end,
if nargin == 1 || isempty(K) == 1,
```

```
    K = 0;
end,
if any(K(:)<0) == 1,
    warning('The relative sand roughness must be non-
        negative.');
end,
% Initialization.
X1 = K .* R * 0.123968186335417556;              % X1 <- K
    * R * log(10) / 18.574.
X2 = log(R) - 0.779397488455682028;              % X2 <-
    log( R * log(10) / 5.02 );
% Initial guess.
F = X2 - 0.2;
% First iteration.
E = ( log(X1+F) - 0.2 ) ./ ( 1 + X1 + F );
F = F - (1+X1+F+0.5*E) .* E .*(X1+F) ./ (1+X1+F+E.*(1+E/3))
    ;
% Second iteration (remove the next two lines for moderate
    accuracy).
E = ( log(X1+F) + F - X2 ) ./ ( 1 + X1 + F );
F = F - (1+X1+F+0.5*E) .* E .*(X1+F) ./ (1+X1+F+E.*(1+E/3))
    ;
% Finalized solution.
F = 1.151292546497022842 ./ F;                   % F <- 0.5
     * log(10) / F;
F = F .* F;                                      % F <-
    Friction factor.
```

Listing C.17: Olgjenka_correlation

```
function [dp,f,rho_l,mu_l,rho_tp,y_l,vm,q_o_dh, q_g_dh,
    q_k_dh,q_t_dh,Bo,N_Re] = Olgjenka_correlation(D_avg,
    T_avg, p_old,dL, d_h,rel_rough,q_kill,A)

global q_os R_t p_s_true gamma_k Depth_IP PVT_sim

gw=gamma_k;            %          vann
Bw=1;            % formasjonsfaktor vann
Co=1.2;          % fordelingsfaktor (til driftfluksmodell)
vo=0.2;          % oppdriftsfart (til driftfluksmodell)
gx=9.81;         % m/s
Rt = R_t/5.6145833;
p_avg = p_old/14.5*10^5;         %Pa
d = d_h/3.28084; %ft to m - diameter

A = A*0.0254^2; %m2
```

```
15
16 if D_avg < Depth_IP
17     q_k = q_kill;
18 else
19     q_k = 0;
20 end
21
22 T=273+(T_avg -32)*5/9; %kelvin
23 Rw=q_k/q_os;           % kill_mudd/oljeforhold
24
25 if strcmp(PVT_sim,"Standing")
26 [p_b, Rs, Bo, Bg, mu_o,mu_g,rho_o, rho_g, sigma_l ]=
       Standing_PVT(p_old,T_avg,"Semi-SI");
27 elseif strcmp(PVT_sim,"Glaso")
28 [p_b, Rs, Bo, Bg, mu_o,mu_g,rho_o, rho_g, sigma_l ]=
       Glaso_PVT(p_old,T_avg,"Semi-SI");
29 end
30 %
31  rho_l = (rho_o*q_os*Bo + gamma_k*1000*q_k*Bw)/(q_os*Bo +
       q_k*Bw);
32
33
34
35 qo = q_os*0.159/86400; %m3/s
36
37 q_o_dh = qo*(Bo); %m3/s down hole oil rate
38 q_g_dh = qo*(Rt-Rs)*Bg; %m3/s down hole gas rate
39 q_k_dh = q_kill*Bw*0.159/86400; %down hole kill rate, in m3
       /s
40 q_t_dh = q_o_dh + q_g_dh + q_k_dh; %total rate down hole
41
42 vsl = (q_o_dh + q_k_dh)/A;
43 vsg = q_g_dh/A;
44 vm = vsl + vsg;
45
46
47 %Flux fractions
48 lambda_l = vsl/vm; %liquid flux fraction
49 lambda_g = vsg/vm; %gas flux fraction
50
51
52 if rho_l > rho_g
53 vo = 1.54 * (gx*sigma_l*10^-3*(rho_l - rho_g)/rho_l^2)
       ^0.25;
54 else
```

```
vo=0.001;
end


% mixture density, liquid fraction and two phase density
    rho_m= rho_g*lambda_g + rho_l*lambda_l;  %mixture
        density
    y_l=0.5*(((vsg/vo +Co*vsl/vo-1)^2 +4*Co*vsl/vo)^0.5 -(
        vsg/vo + Co*vsl/vo-1));
    y_g = 1 - y_l;
    rho_tp=rho_g*(1-y_l)+rho_l*y_l;

%Calculate friction factor


mu_l = mu_o*q_os/(q_os+q_k) + 10*q_k/(q_os+q_k);
N_Re = rho_m*vm*d/(mu_g*lambda_g + mu_l*lambda_l)  ;
%
%
 if N_Re >= 2300
 f=colebrook(N_Re,rel_rough);  %0.015*10^-3/d);  %Colebrook
     equation to find friction factor instead of chart
 else
 f = 0.16/N_Re^0.172 ;
 end

if vsg > 0
C_tp = rho_g/rho_m*lambda_g^2/y_g + rho_l/rho_m*lambda_l^2/
    y_l;
else
 C_tp = rho_l/rho_m*lambda_l^2/y_l;
end
f=f*C_tp;%/f_adjust; %adjusted two phase friction factor
%f = 0.22;

dp = (rho_tp*gx+0.5*f*rho_m/d*vm^2)*dL/3.28084; % Pa

dp_grav = rho_tp*gx*dL/3.28084;
dp_f =(0.5*f*rho_m/d*vm^2)*dL/3.28084;

dp = dp/10^5*14.5;  %psi

rho_l=rho_l/16.0184; %kg/m3 to lb/ft3

end
```

Listing C.18: getBlowoutRate

```
function q_os_bo = getBlowoutRate(p_bh, p_r, p_s, q_max,q_s
    ,J)
% input
% p_bh [psi]
% p_r [bar]
% p_s [bar]
% q_max [SM3/D]
% q_s [SM3/D]
% J [SM3/D/Bar]

p_bh=p_bh/14.5; %From Psi to Bar
%q_max = q_max/0.159;

if p_bh >= p_r
q_os_bo=0;
elseif p_bh > p_s
q_os_bo = J*(p_r-p_bh);
elseif p_bh <= p_s
q_os_bo = q_s +(1-0.2*p_bh/p_s - 0.8*(p_bh/p_s)^2)*q_max;
end

q_os_bo=q_os_bo/0.159;
end
```

Listing C.19: Find_next_blowout_rate

```
%% This script will give the next blowout rate to be used
    in the while-
%  loop used for matching blowout rate with calculated
    blowout rate from
%  the Inflow Performance relation ship and the bottom hole
     pressure

%Under different circumstances the blowout rate will go
    into an
%everlasting alternation and this script should be able to
    break that
%alternation and find the blowout rate with the least error

Blowout_W(W) = q_os_bo ;
Blowout_W_used(W) = q_os;
Pressure_W(W) = Pressure_kill(end);
Difference_W_UC(W) = Blowout_W_used(W) - Blowout_W(W);
Difference_W_CU(W) = Blowout_W(W)- Blowout_W_used(W) ;
diff = Blowout_W_used(W) - Blowout_W(W);
```

```
if Difference_W_UC(W)< 0
   Difference_W_UC(W) = ""; % max(Difference_W_UC);
elseif Difference_W_CU(W)< 0
Difference_W_CU(W) = ""; %min(Difference_W_CU);
end


Matrix_W = string(round([Blowout_W', Blowout_W_used',
    Pressure_W',Difference_W_UC',Difference_W_CU'],2));
Header = [{'Calculated blowout rate'}, {'BO rate used'},{'
    Pressure'},{'Difference Used - Calc'},{'Difference Calc
    - Used'}];
Matrix_W = [Header; Matrix_W];


delta_q =q_os_bo - q_os;


Hard_kill=Blowout_W(find(Blowout_W(W)==Blowout_W==1));

if W > 10 && length(Hard_kill)>2 && all(Hard_kill==
    Hard_kill(1)) && strcmp(Simple_kill,'Yes') || W > 500
%Initiate Hard kill procedure and restart the Blowout loop
Simple_kill = "No";
W=0;
if Q==1
q_os=Blowout_W_used(1);
else
 q_os = double(Rate_matrix(3,3))/0.159; %STB/day
end
delta_q=500;
clear Matrix_W Blowout_W Blowout_W_used Pressure_W
    Difference_W_CU Difference_W_UC Pressure_W_used
    Pressure_W_Perc

p_bh = 0.99*p_r *14.5; %FBHP
FBHP_use=p_bh;
FBHP_perc=99;
q_os = getBlowoutRate(p_bh, p_r, p_s_true/14.5, q_max,q_s,J
    ); %STB/D
Overwrite = 'No';
New_if='No';
WL = 0;
Higher = 'Yes';
end
```

```
53
54 if strcmp(Simple_kill,'Yes')
55
56 q_os=q_os_bo;
57
58
59  if W > 3 && Blowout_W(W) == 0 && Blowout_W(W-1) ==0 &&
        Blowout_W_used(W) == 1
60     q_os=0;
61      delta_q = 0;
62 elseif  Blowout_W(W) == 0
63     q_os=1;
64  end
65 end
66
67 Matrix_W(W+2,2)=string(round(q_os,2));
```

Listing C.20: Find_next_blowout_rate_hard

```
1  %% This script will give the next blowout rate to be used
       in the while-
2  %  loop used for matching blowout rate with calculated
       blowout rate from
3  %  the Inflow Performance relation ship and the bottom hole
        pressure
4
5  %Under different circumstances the blowout rate will go
       into an
6  %everlasting alternation and this script should be able to
       break that
7  %alternation and find the blowout rate with the least error
8
9  Blowout_W(W) = q_os_bo ;
10 Blowout_W_used(W) = q_os;
11 Pressure_W(W) = Pressure_kill(end);
12 Difference_W_UC(W) = Blowout_W_used(W) - Blowout_W(W);
13 Difference_W_CU(W) = Blowout_W(W)- Blowout_W_used(W) ;
14 diff = Blowout_W_used(W) - Blowout_W(W);
15 if Difference_W_UC(W)< 0
16    Difference_W_UC(W) = ""; % max(Difference_W_UC);
17 elseif Difference_W_CU(W)< 0
18 Difference_W_CU(W) = ""; %min(Difference_W_CU);
19 end
20
21
22 Matrix_W = string(round([Blowout_W', Blowout_W_used',
```

```
    Pressure_W',Difference_W_UC',Difference_W_CU'],2));
Header = [{'Calculated blowout rate'}, {'BO rate used'},{'
    Pressure'},{'Difference Used - Calc'},{'Difference Calc
    - Used'}];
Matrix_W = [Header; Matrix_W];


delta_q =q_os_bo - q_os;


if W > 10
C_a = round(Blowout_W(W)/100,0);
C_b = round(Blowout_W(W-2)/100,0);
end


% If the calculated IPR blowout rate goes into an
    everlasting alternating
% process the if statements below shall solve this
if W > 10 && C_a == C_b  && strcmp(Overwrite,'No') &&
    strcmp(New_if,'No')
     q_os = min(Blowout_W_used((W-5):end));
     Overwrite = 'Yes';
elseif strcmp(Overwrite,'Yes')
     if Blowout_W_used(W) > Blowout_W(W) && strcmp(Higher,'
        Yes')
      New_if='Yes';
     q_os= q_os + 0.5*delta_q;
     elseif Blowout_W_used(W) < Blowout_W(W) %&& strcmp(
        Higher,'No')
     q_os = q_os + 300;
     elseif strcmp(Higher,'Yes')
     q_os= q_os + 0.5*delta_q;
     else
     q_os= q_os + 0.5*delta_q;
     Higher = 'Yes';
     end
elseif strcmp(Overwrite,'No')
q_os= q_os + 0.5*delta_q;
end

% When the used blowout rate surpasses the calculated
    blowout rate from
% The IPR curve, the if statement below kicks inn and shoot
     for the
```

```
% Correct value
if strcmp(New_if,'Yes') && WL == 0
WL = WL +1;
min_q = Blowout_W_used(W-1);
max_q = Blowout_W_used(W);
q_os = 0.5*( min_q + max_q);
elseif strcmp(New_if,'Yes')&& WL > 0 &&  Blowout_W_used(W)
    < Blowout_W(W)
min_q = Blowout_W_used(W);
q_os = 0.5*( min_q + max_q);
elseif strcmp(New_if,'Yes')&& WL > 0 &&  Blowout_W_used(W)
    > Blowout_W(W)
max_q = Blowout_W_used(W);
q_os = 0.5*( min_q + max_q);
end


% Under some circumstances the calculated blowout value
    from the IPR curve
% will be unsolveable due to the nature of Orkiszewsi's
    method
% A average of the blowout rates will be provided to stop
    the unsolveable process
if strcmp(New_if,'Yes') && Blowout_W_used(W) ==
    Blowout_W_used(W-1) && Blowout_W_used(W-1) ==
    Blowout_W_used(W-2) && W> 40
     q_os = 1/3*(Blowout_W(W) + Blowout_W(W-1)+
        Blowout_W_used(W));
     delta_q = 0; %To stop the everlassting alternation
end


min_diff_UC = min(Difference_W_UC);
max_rate=Blowout_W_used(find(Difference_W_UC == min_diff_UC
    ,1));
max_calc=Blowout_W(find(Difference_W_UC == min_diff_UC,1));
max_FBHP = Pressure_W(find(Difference_W_UC == min_diff_UC
    ,1));
min_diff_CU = min(Difference_W_CU);
min_rate=Blowout_W_used(find(Difference_W_CU == min_diff_CU
    ,1));
min_calc = Blowout_W(find(Difference_W_CU == min_diff_CU,1)
    );
min_FBHP = Pressure_W(find(Difference_W_CU == min_diff_CU
    ,1));
```

```
91
92
93
94  if W > 9 && diff>0
95  q_os = 0.5*(max_rate+max_calc);
96  if q_os == Blowout_W_used(W)
97      q_os = max_calc;
98  end
99  elseif W > 9 && diff<0
100  q_os = 0.5*(min_rate+min_calc);
101 if q_os == Blowout_W_used(W)
102     q_os = min_calc;
103 end
104 end
105
106
107
108 if isnan(min_diff_UC)==0
109 if  W > 9 && Blowout_W_used(W) < max_rate &&
        Difference_W_UC(W) > min_diff_UC || W>9 && round(
        Blowout_W_used(W),1) == round(Blowout_W_used(W-3),1)
110 % A pressure disontinuity is met
111 delta_q=0;
112 if min_diff_UC <min_diff_CU
113 q_os_bo = 0.5* (max_rate + max_calc);
114 else
115     q_os_bo = 0.5* (min_rate + min_calc);
116 end
117
118 if isempty(min_diff_CU) || isnan(min_diff_CU)
119 q_os_bo = 0.5* (max_rate + max_calc);
120 q_os=max_rate;
121 elseif isempty(min_diff_UC) || isnan(min_diff_UC)
122     q_os_bo = 0.5* (min_rate + min_calc);
123     q_os = min_rate;
124 end
125
126 elseif W>9 && round(Blowout_W_used(W),1) == round(
        Blowout_W_used(W-2),1) && round(Blowout_W_used(W-1),1)
        == round(Blowout_W_used(W-3),1)
127 delta_q=0;
128 if min_diff_UC <min_diff_CU
129 q_os_bo = 0.5* (max_rate + max_calc);
130 q_os = max_rate;
131 else
```

```
    q_os_bo = 0.5* (min_rate + min_calc);
    q_os=min_rate;
end


if isempty(min_diff_CU)
q_os_bo = 0.5* (max_rate + max_calc);
q_os = max_rate;
elseif isempty(min_diff_UC)
    q_os_bo = 0.5* (min_rate + min_calc);
 q_os=min_rate;
end

end

elseif isnan(min_diff_CU)==0

if  W > 9 &&  Difference_W_CU(W) > min_diff_CU || W>9 &&
   round(Blowout_W_used(W),1) == round(Blowout_W_used(W-3)
   ,1)
% A pressure disontinuity is met
delta_q=0;
if min_diff_UC <min_diff_CU
q_os_bo = 0.5* (max_rate + max_calc);
q_os = max_rate;
else
    q_os_bo = 0.5* (min_rate + min_calc);
 q_os=min_rate;
end

if isempty(min_diff_CU) || isnan(min_diff_CU)
q_os_bo = 0.5* (max_rate + max_calc);
q_os = max_rate;
elseif isempty(min_diff_UC) || isnan(min_diff_UC)
    q_os_bo = 0.5* (min_rate + min_calc);
 q_os=min_rate;
end

elseif W>9 && round(Blowout_W_used(W),1) == round(
   Blowout_W_used(W-2),1) && round(Blowout_W_used(W-1),1)
   == round(Blowout_W_used(W-3),1)
delta_q=0;
if min_diff_UC <min_diff_CU
q_os_bo = 0.5* (max_rate + max_calc);
q_os = max_rate;
```

```
else
    q_os_bo = 0.5* (min_rate + min_calc);
 q_os=min_rate;
end


if isempty(min_diff_CU)
q_os_bo = 0.5* (max_rate + max_calc);
q_os = max_rate;
elseif isempty(min_diff_UC)
    q_os_bo = 0.5* (min_rate + min_calc);
 q_os=min_rate;
end

end

end


if W<9
    q_os = getBlowoutRate((100-W*10)/100*p_r*14.5, p_r,
       p_s_true/14.5, q_max,q_s,J); %STB/D
end

if  isempty(q_os)
    a=0;
elseif q_os == 0
a=0;
elseif isempty(q_os_bo)
    a=0;
end
```

Listing C.21: Find_next_blowout_rate_hard_blowout

```
%% This script will give the next blowout rate to be used
   in the while-
%  loop used for matching blowout rate with calculated
   blowout rate from
%  the Inflow Performance relation ship and the bottom hole
    pressure

%Under different circumstances the blowout rate will go
   into an
%everlasting alternation and this script should be able to
   break that
%alternation and find the blowout rate with the least error
```

```
8
9  Blowout_W(W) = q_os_bo ;
10 Blowout_W_used(W) = q_os;
11 Pressure_W(W) = Pressure_kill(end);
12 Difference_W_UC(W) = Blowout_W_used(W) - Blowout_W(W);
13 Difference_W_CU(W) = Blowout_W(W)- Blowout_W_used(W) ;
14 diff = Blowout_W_used(W) - Blowout_W(W);
15 if Difference_W_UC(W)< 0
16    Difference_W_UC(W) = ""; % max(Difference_W_UC);
17 elseif Difference_W_CU(W)< 0
18 Difference_W_CU(W) = ""; %min(Difference_W_CU);
19 end
20
21
22 Matrix_W = string(round([Blowout_W', Blowout_W_used',
       Pressure_W',Difference_W_UC',Difference_W_CU'],2));
23 Header = [{'Calculated blowout rate'}, {'BO rate used'},{'
       Pressure'},{'Difference Used - Calc'},{'Difference Calc
       - Used'}];
24 Matrix_W = [Header; Matrix_W];
25
26
27 delta_q =q_os_bo - q_os;
28
29 if W > 10
30 C_a = round(Blowout_W(W)/100,0);
31 C_b = round(Blowout_W(W-2)/100,0);
32 end
33
34
35 % If the calculated IPR blowout rate goes into an
       everlasting alternating
36 % process the if statements below shall solve this
37 if W > 10 && C_a == C_b  && strcmp(Overwrite,'No') &&
       strcmp(New_if,'No')
38     q_os = min(Blowout_W_used((W-5):end));
39     Overwrite = 'Yes';
40 elseif strcmp(Overwrite,'Yes')
41     if Blowout_W_used(W) > Blowout_W(W) && strcmp(Higher,'
           Yes')
42      New_if='Yes';
43     q_os= q_os + 0.5*delta_q;
44     elseif Blowout_W_used(W) < Blowout_W(W) %&& strcmp(
           Higher,'No')
45     q_os = q_os + 300;
```

```
    elseif strcmp(Higher,'Yes')
    q_os= q_os + 0.5*delta_q;
    else
    q_os= q_os + 0.5*delta_q;
    Higher = 'Yes';
    end
elseif strcmp(Overwrite,'No')
q_os= q_os + 0.5*delta_q;
end

% When the used blowout rate surpasses the calculated blowout rate from
% The IPR curve, the if statement below kicks inn and shoot for the
% Correct value
if strcmp(New_if,'Yes') && WL == 0
WL = WL +1;
min_q = Blowout_W_used(W-1);
max_q = Blowout_W_used(W);
q_os = 0.5*( min_q + max_q);
elseif strcmp(New_if,'Yes')&& WL > 0 &&  Blowout_W_used(W) < Blowout_W(W)
min_q = Blowout_W_used(W);
q_os = 0.5*( min_q + max_q);
elseif strcmp(New_if,'Yes')&& WL > 0 &&  Blowout_W_used(W) > Blowout_W(W)
max_q = Blowout_W_used(W);
q_os = 0.5*( min_q + max_q);
end


% Under some circumstances the calculated blowout value from the IPR curve
% will be unsolveable due to the nature of Orkiszewsi's method
% A average of the blowout rates will be provided to stop the unsolveable process
if strcmp(New_if,'Yes') && Blowout_W_used(W) == Blowout_W_used(W-1) && Blowout_W_used(W-1) == Blowout_W_used(W-2) && W> 40
    q_os = 1/3*(Blowout_W(W) + Blowout_W(W-1)+ Blowout_W_used(W));
    delta_q = 0; %To stop the everlassting alternation
end
```

Listing C.22: Report_preparator

```
%This script will prepare some data for the report
    generator

%% Input values


% Well design
Header1 = [{'Well section'},{'OD'}, {'ID'}, {'Top'}, {'
    Bottom'}];
Header2 = [{'Unit'},{'[in]'}, {'[in]'}, {'[m RKB]'}, {'[m
    RKB]'}];
Type = string(raw(36:(36+size(Well,1)-1)));
input_well = Well(:,1:4);
input_well(1:end,3:4)=round(input_well(1:end,3:4)
    /3.28084,0);
input_well =[Header1; Header2; [Type', string(input_well)
    ]];

% Drill pipe

Header1 = [{'Drill string part'},{'OD'}, {'ID'}, {'Top'}, {
    'Bottom'}];
Header2 = [{'Unit'},{'[in]'}, {'[in]'}, {'[m RKB]'}, {'[m
    RKB]'}];
input_DS = [DS(2,1), DS(2,2), DS(2,4)/3.28084, DS(2,5)
    /3.28084];
input_DS = string(round([input_DS;DS(1,1), DS(1,2), DS(1,4)
    /3.28084, DS(1,5)/3.28084],0));
input_DS =[[{'BHA'}; {'Drill pipe'}], input_DS];
input_DS=[Header1; Header2; input_DS];

% Relief well design
Type = [{'Surface lines'}, {'Kill and choke lines'}, {'
    Casing'}, {'Drill pipe'}, {'BHA'}];
input_RW = RW(:,1:4);
input_RW(1:end,3:4)=round(input_RW(1:end,3:4)/3.28084,0);
input_RW =[Header1; Header2; [Type', string(input_RW)]];

% Relief well trajectory
Header1 = [{'IP'},{'KOP'}, {'Northing'}, {'Easting'}, {'BU
    rate'}, {'Build angle'}, {'Drop rate'}, {'Drop angle'}];
Header2 = [{'m RKB'},{'m RKB'}, {'m'}, {'m'}, {'deg/30m'},
    {'deg'}, {'deg/30m'}, {'deg'}];
input_RW_value = RW_value;
```

```
input_RW_value(1) = round(RW_value(1)/3.28084,0);
input_RW_value =[Header1; Header2; string(input_RW_value)];



Header1 = [{'Total depth'},{'Wellhead depth'}, {'Seabed
    depth'}, {'Rig floor elevation'}, {'Pressure at wellhead
    '}];
Header2 = [{'m RKB TVD'},{'m RKB TVD'}, {'m MSL'}, {'m RKB'
    }, {'Bar'}];
general_values=round([D/3.28084,D_wh/3.28084,(D_sb-
    Rig_elevation)/3.28084,Rig_elevation,p_wh/14.5],0);
general_values = [Header1;Header2;string(general_values)];



Header1 = [{'Oil gravity'}, {'Gas gravity'}, {'GOR'}, {'
    Saturation pressure'},{'Reservoir pressure'},{'PI'},{'
    AOF'}];
Header2 = [{'s.g.'}, {'s.g.'}, {'Sm3/Sm3'}, {'Bar'},{'Bar'
    },{'Sm3/d/bar'},{'Sm3/d'}];
res_fluid_values = [gamma_o, gamma_g, round(R_t
    /5.6145833,0), round(p_s_true/14.504,0),round(p_r,0),
    round(J,0),round(AOF*0.159,0)];
res_fluid_values = [Header1; Header2; string(
    res_fluid_values)];


Header1 = [{'Intersection Point'}, {'Kill fluid viscosity'
    }, {'Kill fluid density range min'}, {'Kill fluid
    density max'}, {'Number of kill fluid density steps'}];
Header2 = [{'m RKB'}, {'cp'}, {'s.g.'}, {'s.g.'}, {'-'}];
Kill_values = [round(Depth_IP/3.28084,0), kill_viscosity,(
    gamma_k-gamma_k_step*Kill_steps), (gamma_k),Kill_steps];
Kill_values = [Header1; Header2; string(Kill_values)];

%Materials
input_Materials = num(5:13,17);
Header1 = string(raw(6:14,15));
Header2 = string(raw(6:14,17));
input_Materials = [Header1, Header2, input_Materials];
Header0= [{'Parameter'},{'Unit'}, {'Value'} ];
input_Materials = [Header0; input_Materials];


```

```
% Answer from user
Header1 = [{'Correlation type'}, {'Chosen correlation'}];
input_answers =[{'Multiphase pressure drop correlation'},
    Multiphase ];
Header0 = [{'PVT correlation set'},PVT_sim];
input_answers=[Header1;input_answers;Header0]


%% Blowout Results

Header1 = [{'Blowout type'},{'Oil rate'}, {'Gas rate'}, {'
    FBHP'}, {'Risked oil rate'}, {'Risked gas rate'}];
Header2 = [{'Unit'},{'Sm3/D'}, {'MSm3/D'}, {'Bar'}, {'Sm3/D
    '}, {'MSm3/D'}];
MB = double(Matrix_blowout);
input_blowout = [MB(3,1:2:8);MB(3,1:2:8)*R_t
    *10^-6/5.6145833;MB(3,2:2:8)]';

risk_blow = [1.92;1.92;1.44;1.44]/100;

input_blowout = string(round([input_blowout, input_blowout
    (:,1:2).*risk_blow],1)) ;
Header0=[{'Open hole to seabed'}, {'Open hole to surface'},
     {'Annulus to seabed'}, {'Annulus to surface'}]';
input_blowout = [Header1; Header2; [Header0,input_blowout
    ]];


%% Kill results and pump capacity

Header1= [{'Kill fluid density'},{'Kill rate'},{'IP
    Pressure'},{'FBHP'}, {'Max pump pressure - annulus'}, {'
    Energy input - annulus'},{'Max pump pressure - drill
    string'}, {'Mud volume - static'}];
Header2= [{'s.g.'},{'LPM'}, {'Bar'},{' Bar'}, {'Bar'}, {'HP
    '}, {'Bar'}, {'m3'}];

[V_OH_t, V_DP] = Wellbore_volume (well_sorted,DS);

for i=1:(Kill_steps+1)
col = 3+2*(i-1);
kill_dens = double(Matrix_kill_surface(3,col));
kill_rate = double(Matrix_kill_surface(3,col+1));
BH_pres = Pressure_BH_surface(i);
IP_pres = Pressure_IP_surface(i);
```

```
[~,dp_tot, HP]= RW_pump_annulus(kill_rate,dp_IP_surface(i),
    kill_dens);
[~,dp_tot_dp, HP_dp]= RW_pump_dp(kill_rate,dp_IP_surface(i)
    ,kill_dens);

Kill_pump_best_sur(i,:) = string(round([kill_dens,
    kill_rate,IP_pres,BH_pres,dp_tot,HP,dp_tot_dp,2*V_OH_t
    ],1)) ;


if dp_tot < 30
Kill_pump_best_sur(i,5) = "< 30" ;
end
if HP < 500
Kill_pump_best_sur(i,6) = "< 500" ;
end
if dp_tot_dp < 30
Kill_pump_best_sur(i,7) = "< 30";
end

end


Kill_pump_best_sur = [Header1; Header2; Kill_pump_best_sur
    ];

for i=1:(Kill_steps+1)
col = 3+2*(i-1);
kill_dens = double(Matrix_kill_seabed(3,col));
kill_rate = double(Matrix_kill_seabed(3,col+1));

BH_pres = Pressure_BH_surface(i);
IP_pres = Pressure_IP_surface(i);

[~,dp_tot, HP]= RW_pump_annulus(kill_rate,dp_IP_seabed(i),
    kill_dens);
[~,dp_tot_dp, HP_dp]= RW_pump_dp(kill_rate,dp_IP_seabed(i),
    kill_dens);

Kill_pump_best_sea(i,:) = string(round([kill_dens,
    kill_rate,IP_pres,BH_pres,dp_tot,HP,dp_tot_dp,2*V_OH_t
    ],1)) ;

if dp_tot < 30
dp_tot = "< 30";
```

```
Kill_pump_best_sea(i,5) = dp_tot ;
end
if HP < 500
HP = "< 500";
Kill_pump_best_sea(i,6) = HP ;
end
if dp_tot_dp < 30
dp_tot_dp = "<30";
Kill_pump_best_sea(i,7) = dp_tot_dp;
end

end
Kill_pump_best_sea = [Header1; Header2; Kill_pump_best_sea];
%% Plots
global plot_this

Well_name=raw(10,6);
plot_this="Yes";
%
% Plot_well
% IPR
% [RW_t] = Build_Relief_well(B_max,B_rate,D_max,D_rate,KOP,Depth_IP/3.28084,Coord);
% T = get_Temperature2(Depth,D_sb, Top_OH,Depth_IP,q_kill_i,X);
[Fig_temp,Fig_temp_sur, Fig_temp_RW, Fig_well,IPR_fig, Fig_Bo, Fig_Bg, Fig_Rs, Fig_rhol, Fig_rhog]= Report_plotter();

global RW_fig
```

Listing C.23: Report_plotter

```
function [Fig_temp,Fig_temp_sur, Fig_temp_RW, Fig_well, IPR_fig, Fig_Bo, Fig_Bg, Fig_Rs, Fig_rhol, Fig_rhog]= Report_plotter()

clear
global R_t gamma_g gamma_o p_r PVT_sim T_bh D D_sb Top_OH Depth_IP X plot_this

global Fig_temp Fig_temp_sur Fig_temp_RW Fig_well IPR_fig Drill_pipe

set(0,'DefaultFigureVisible','off');
```

```
plot_this="Yes";

Depth=D;
N = fix(Depth/10) +1;
X = linspace(0,Depth,N);

T = get_Temperature2(Depth,D_sb, Top_OH,Depth_IP, 0,X);
q_kill=250*1.44/0.159; %STB/D

T_IP = get_IP_Temperature2(q_kill);

Simulate='Blowout and Kill';
Drill_pipe="Yes";

Get_input_values

Plot_actual_well(Well,Unit)

IPR
[RW_t] = Build_Relief_well(B_max,B_rate,D_max,D_rate,KOP,
    Depth_IP/3.28084,Coord);

i=0;
for p_avg =1:round(p_r) %Bar
i=i+1;
Pres(i)=p_avg;
if strcmp(PVT_sim,"Standing")
[p_b(i), Rs(i), Bo(i), Bg(i), mu_o(i),mu_g(i),rho_o(i),
    rho_g(i), sigma_l(i) ]=Standing_PVT(p_avg*14.5,T_bh,"
    Semi-SI");
elseif strcmp(PVT_sim,"Glaso")
[p_b(i), Rs(i), Bo(i), Bg(i), mu_o(i),mu_g(i),rho_o(i),
    rho_g(i), sigma_l(i) ]=Glaso_PVT(p_old,T_bh,"Semi-SI");
end
end

i=0;
T_IP_F = T_IP*9/5 + 32;
for p_avg =1:round(p_r) %Bar
i=i+1;

Pres(i)=p_avg;
if strcmp(PVT_sim,"Standing")
[p_b_IP(i), Rs_IP(i), Bo_IP(i), Bg_IP(i), mu_o_IP(i),
    mu_g_IP(i),rho_o_IP(i), rho_g_IP(i), sigma_l_IP(i) ]=
```

```
    Standing_PVT(p_avg*14.5,T_IP_F,"Semi-SI");
elseif strcmp(PVT_sim,"Glaso")
[p_b_IP(i), Rs_IP(i), Bo_IP(i), Bg_IP(i), mu_o_IP(i),
    mu_g_IP(i),rho_o_IP(i), rho_g_IP(i), sigma_l_IP(i) ]=
    Glaso_PVT(p_old,T_IP_F,"Semi-SI");
end
end

T_mix = (T_bh + T_IP_F)/2;

i=0;
for p_avg =1:round(p_r) %Bar
i=i+1;

Pres(i)=p_avg;
if strcmp(PVT_sim,"Standing")
[p_b_mix(i), Rs_mix(i), Bo_mix(i), Bg_mix(i), mu_o_mix(i),
    mu_g_mix(i),rho_o_mix(i), rho_g_mix(i), sigma_l_mix(i)
    ]=Standing_PVT(p_avg*14.5,T_mix,"Semi-SI");
elseif strcmp(PVT_sim,"Glaso")
[p_b_mix(i), Rs_mix(i), Bo_mix(i), Bg_mix(i), mu_o_mix(i),
    mu_g_mix(i),rho_o_mix(i), rho_g_mix(i), sigma_l_mix(i)
    ]=Glaso_PVT(p_old,T_mix,"Semi-SI");
end
end


T_m_cels = (T_mix-32)*5/9;
T_cels = (T_bh-32)*5/9;
Rt=R_t/5.614;

%matrix=[p',p_b', R_s', B_o', B_g', mu_o',mu_g',rho_o',
    rho_g', sigma_l' ];


Fig_Bo = figure('Name','Fig_Bo');
figure(Fig_Bo);
plot(Pres,Bo,'LineWidth',2)
hold on
plot(Pres,Bo_mix,'LineWidth',2)
hold on
plot(Pres,Bo_IP,'LineWidth',2)
ylabel('\bf Oil FVF - Bo [m3/Sm3]')
xlabel('\bf Pressure [Bar]')
grid on
```

```
legend(['T = ', num2str(T_cels),'C'],['T = ', num2str(round
    (T_m_cels,1)),'C'],['T = ', num2str(round(T_IP,1)),'C'],
    'Location','Best')
title(['R_t=' num2str(round(Rt,0)),'Sm3/Sm3,', '    gamma_o
    =', num2str(gamma_o),',    gamma_g=', num2str(gamma_g)])
set(gca,'Fontsize',12,'fontweight','bold')


Fig_Rs = figure('Name','Fig_Rs');
figure(Fig_Rs);
plot(Pres,Rs,'LineWidth',2)
hold on
plot(Pres,Rs_mix,'LineWidth',2)
hold on
plot(Pres,Rs_IP,'LineWidth',2)
ylabel('\bf Solution Gas-Oil-Ratio - Rs [Sm3/Sm3]')
xlabel('\bf Pressure [Bar]')
grid on
legend(['T = ', num2str(T_cels),'C'],['T = ', num2str(round
    (T_m_cels,1)),'C'],['T = ', num2str(round(T_IP,1)),'C'],
    'Location','Best')
title(['R_t=' num2str(round(Rt,0)),'Sm3/Sm3,', '    gamma_o
    =', num2str(gamma_o),',    gamma_g=', num2str(gamma_g)])
set(gca,'Fontsize',12,'fontweight','bold')

Fig_Bg = figure('Name','Fig_Bg');
figure(Fig_Bg);
plot(Pres,log10(Bg),'LineWidth',2)
hold on
plot(Pres,log10(Bg_mix),'LineWidth',2)
hold on
plot(Pres,log10(Bg_IP),'LineWidth',2)
ylabel('\bf Log10 Gas FVF - Lo10(Bg) [m3/Sm3]')
xlabel('\bf Pressure [Bar]')
grid on
legend(['T = ', num2str(T_cels),'C'],['T = ', num2str(round
    (T_m_cels,1)),'C'],['T = ', num2str(round(T_IP,1)),'C'],
    'Location','Best')
title(['R_t=' num2str(round(Rt,0)),'Sm3/Sm3,', '    gamma_o
    =', num2str(gamma_o),',    gamma_g=', num2str(gamma_g)])
set(gca,'Fontsize',12,'fontweight','bold')

Fig_rhol = figure('Name','Fig_rhol');
figure(Fig_rhol);
plot(Pres,rho_o,'LineWidth',2)
```

```
hold on
plot(Pres,rho_o_mix,'LineWidth',2)
hold on
plot(Pres,rho_o_IP,'LineWidth',2)
ylabel('\bf Oil density - rho_o [kg/m3] ')
xlabel('\bf Pressure [Bar]')
grid on
legend(['T = ', num2str(T_cels),'C'],['T = ', num2str(round
    (T_m_cels,1)),'C'],['T = ', num2str(round(T_IP,1)),'C'],
    'Location','Best')
title(['R_t=' num2str(round(Rt,0)),'Sm3/Sm3,', '    gamma_o
    =', num2str(gamma_o),',    gamma_g=', num2str(gamma_g)])
set(gca,'Fontsize',12,'fontweight','bold')


Fig_rhog = figure('Name','Fig_rhog');
figure(Fig_rhog);
plot(Pres,rho_g,'LineWidth',2)
hold on
plot(Pres,rho_g_mix,'LineWidth',2)
hold on
plot(Pres,rho_g_IP,'LineWidth',2)
ylabel('\bf Gas density - rho_g [kg/m3] ')
xlabel('\bf Pressure [Bar]')
grid on
legend(['T = ', num2str(T_cels),'C'],['T = ', num2str(round
    (T_m_cels,1)),'C'],['T = ', num2str(round(T_IP,1)),'C'],
    'Location','Best')
title(['R_t=' num2str(round(Rt,0)),'Sm3/Sm3,', '    gamma_o
    =', num2str(gamma_o),',    gamma_g=', num2str(gamma_g)])
set(gca,'Fontsize',12,'fontweight','bold')

figure('name','p_b_fig')
plot(Pres,p_b,'LineWidth',2)
hold on
plot(Pres,p_b_mix,'LineWidth',2)
hold on
plot(Pres,p_b_IP,'LineWidth',2)
ylabel('\bf Saturation pressure [Bar] ')
xlabel('\bf Pressure [Bar]')
grid on
legend(['T = ', num2str(T_cels),'C'],['T = ', num2str(round
    (T_m_cels,1)),'C'],['T = ', num2str(round(T_IP,1)),'C'],
    'Location','Best')
title(['R_t=' num2str(round(Rt,0)),'Sm3/Sm3,', '    gamma_o
```

```
    =', num2str(gamma_o),',    gamma_g=', num2str(gamma_g)])
set(gca,'Fontsize',12,'fontweight','bold')

end
```

Listing C.24: Plot_actual_well

```
function Plot_actual_well(Well,Unit)

%global Well Unit
global Depth_IP D_sb Drill_pipe DS Fig_well
W = Well;
DP = DS;

if strcmp(Unit,"Semi-SI units")
W(:,3:4) =  W(:,3:4)/3.28084;
D_IP = Depth_IP/3.28084;
D_s = D_sb/3.28084;
DP(:,3:5) = DP(:,3:5)/3.28084;
end

Fig_well = figure('Name','Fig_well');
figure(Fig_well);

color = [{'g'},{'k'},{'m'},{'b'},{'r'},{'y'}];
for i=1:length(color)
hold on
plot(1,1,char(color(i)),'LineWidth',0.0001)

end

color = repmat({'k'},size(Well,1)-2,1);
color = [{'g'};color;{'m'};{'b'};{'r'}];

for i =1:size(Well,1)
hold on
x=[W(i,1), W(i,1)]; %left side
y = [W(i,3), W(i,4)];
plot(x,y,char(color(i)),'LineWidth',2)

hold on
x=-x;
plot(x,y,char(color(i)),'LineWidth',2)

if i==size(Well,1)

```

```
plot([-W(i,1),W(i,1)],[W(i,4),W(i,4)],char(color(i)),'
    LineWidth',2,'LineStyle','--')

end


end

hold on
plot([-40,40],[D_s,D_s],'blue','LineWidth',2)
hold on
plot([-40,-W(end,1)],[D_IP,D_IP],'red','LineWidth',2)

if strcmp(Drill_pipe, "Yes")
hold on

for i =1:2
x=[DP(i,1), DP(i,1)]; %left side
y = [DP(i,4), DP(i,5)];

hold on
plot(x,y,'y','LineWidth',2)

hold on
x=-x;
plot(x,y,'y','LineWidth',2)

hold on
plot([-DP(2,1),DP(2,1)],[DP(2,5),DP(2,5)],'y','LineWidth'
    ,2)



end

grid on
legend('Riser','Casing','Open hole','Seabed','RW IP','Drill
     string','Location','Best')
xlabel('Diameter [in]')
ylabel('Depth [m RKB TVD]')
set(gca, 'YDir','reverse','Fontsize',12,'fontweight','bold'
    )
end
```

Listing C.25: RW_pump_annulus

```
function [Matrix_RW_p,dp_tot, HP]= RW_pump_annulus(Q,dp_IP,
    gamma_k)
% This function calculates the friction drop along the
    relief well through
% annulus.

%Input
% Flow rate [LPM], RW - relief well design,
% RW_t - relief well trajectory, %gamma_k - kill fluid
    density [s.g]
% Kill_viscosity [cp]

%Output
% Matrix_RW_p - friction drop matrix
% HP - Required pump energy [HP]

global RW RW_t kill_viscosity

rho=gamma_k;
mu= kill_viscosity;
for i = 1:5

if i == 1 || i ==2
%Surface lines and choke/kill
OD_dp=0;
ID_csg = RW(i,2);
L_ft=RW(i,4); %ft
elseif i == 3
%casing-drillpipe
ID_csg=RW(3,2);
OD_dp=RW(4,1);
L_ft=RW(4,4)-RW(2,4) + (RW_t(end,3)-RW_t(end,2))*3.28084;
elseif i ==4
%Casing - BHA
ID_csg=RW(3,2);
OD_dp=RW(5,1);
L_ft=RW(5,4)-RW(4,4);
elseif i ==5
%only casing
ID_csg=RW(3,2);
OD_dp=0;
L_ft= RW(3,4)-RW(5,4);
end


```

```
A=pi/4*(ID_csg^2-OD_dp^2)*0.0254^2; %m2
v=Q*(10^-3/60)/A; %m/s

if i ==2
%choke/kill lines - flow through both lines
v=v/2;
end

d_h = (ID_csg-OD_dp)*0.0254; %m

N_Re = rho*1000*v*d_h/(mu*10^-3);

rel_rough = 0.00177/(d_h/0.0254);

 if N_Re >= 2300
 f=colebrook(N_Re,rel_rough);  %0.015*10^-3/d);  %Colebrook
     equation to find friction factor instead of chart
 else
 f = 0.16/N_Re^0.172 ;
 end

dp(i) = f*rho*1000/2*v^2/d_h*L_ft/3.28084;

if i==2
dp(i)=dp(i)*2; % flow in both choke and kill line
end

Matrix_RW_p(i,:) = [ID_csg, OD_dp, L_ft/3.28084, dp(i)
    *10^-5 ];

end
dp=dp*10^-5;
dp_tot=sum(dp)+dp_IP;
Matrix_RW_p(i+1,:) = [0,0,0,dp_IP ];
Matrix_RW_p(i+2,:) = [0,0,sum(Matrix_RW_p(2:end,3)),dp_tot
    ];


HP = dp_tot*Q/600/0.85*1.34102; % [hp - horse power] 85%
    efficiency

Matrix_RW_p(:,3:4)=round(Matrix_RW_p(:,3:4),1);
header1 = [{'OD'}, {'ID'}, {'Length'}, {'Pressure'} ];
header2 = [{'in'}, {'in'}, {'m MD'}, {'Bar'} ];
header3 = [{'parameter'}, {'unit'}, {'surface'}, {'kill/
```

```
    choke'},{'Casing - DP'},{'Casing - BHA'}, {'Casing - OH'
    },{'dp - interception point'}, {'Sum'} ];
84
85
86  Matrix_RW_p=[header1; header2; string(Matrix_RW_p)];
87  Matrix_RW_p = [header3',Matrix_RW_p];
88
89  Matrix_RW_p((end-1):end,2:3)="";
90  end
```

Listing C.26: RW_pump_dp

```
1   function [Matrix_RW_p,dp_tot, HP]= RW_pump_dp(Q,dp_IP,
        gamma_k)
2   % This function calculates the friction drop along the
        relief well through
3   % annulus.
4
5   %Input
6   % Flow rate [LPM], RW - relief well design,
7   % RW_t - relief well trajectory, %gamma_k - kill fluid
        density [s.g]
8   % Kill_viscosity [cp] dp_IP - differential pressure over
        interception point
9
10  %Output
11  % Matrix_RW_p - friction drop matrix
12  % HP - Required pump energy [HP]
13
14  global RW RW_t kill_viscosity
15
16  rho=gamma_k;
17  mu= kill_viscosity;
18  for i = 1:4
19
20  if i == 1
21  %Surface lines
22  OD_dp=0;
23  ID_csg = RW(1,2);
24  L_ft=RW(i,4); %ft
25  elseif i == 2
26  %drillpipe
27  ID_csg=RW(4,2);
28  OD_dp=0;
29  L_ft=RW(4,4) + (RW_t(end,3)-RW_t(end,2))*3.28084;
30  elseif i ==3
```

```
%BHA
ID_csg=RW(5,2);
OD_dp=0;
L_ft=RW(5,4)-RW(4,4);
elseif i ==4
%only casing
ID_csg=RW(3,2);
OD_dp=0;
L_ft= RW(3,4)-RW(5,4);
end


A=pi/4*(ID_csg^2-OD_dp^2)*0.0254^2; %m2
v=Q*(10^-3/60)/A; %m/s

if i ==2
%choke/kill lines - flow through both lines
v=v/2;
end

d_h = (ID_csg-OD_dp)*0.0254; %m

N_Re = rho*1000*v*d_h/(mu*10^-3);

rel_rough = 0.00177/(d_h/0.0254);

 if N_Re >= 2300
 f=colebrook(N_Re,rel_rough);  %0.015*10^-3/d);  %Colebrook
     equation to find friction factor instead of chart
 else
 f = 0.16/N_Re^0.172 ;
 end

dp(i) = f*rho*1000/2*v^2/d_h*L_ft/3.28084;

if i==2
dp(i)=dp(i)*2; % flow in both choke and kill line
end

Matrix_RW_p(i,:) = [ID_csg, OD_dp, L_ft/3.28084, dp(i)
    *10^-5 ];

end
dp=dp*10^-5;
dp_tot=sum(dp)+dp_IP;
```

```
Matrix_RW_p(i+1,:) = [0,0,0,dp_IP ];
Matrix_RW_p(i+2,:) = [0,0,sum(Matrix_RW_p(2:end,3)),dp_tot
    ];

HP = dp_tot*Q/600/0.85*1.34102; % [hp - horse power] 85%
    efficiency

Matrix_RW_p(:,3:4)=round(Matrix_RW_p(:,3:4),1);
header1 = [{'OD'}, {'ID'}, {'Length'}, {'Pressure'} ];
header2 = [{'in'}, {'in'}, {'m MD'}, {'Bar'} ];
header3 = [{'parameter'}, {'unit'}, {'surface'}, {'Drill
    pipe'},{'BHA'},{'Casing - OH'},{'dp - interception point
    '} {'Sum'} ];


Matrix_RW_p=[header1; header2; string(Matrix_RW_p)];
Matrix_RW_p = [header3',Matrix_RW_p];

Matrix_RW_p((end-1):end,2:3)="";

end
```

Listing C.27: report_gen

```
%% Import packages

import mlreportgen.report.*
import mlreportgen.dom.*

doctype = "pdf";
rpt = Report(['Blowout and Kill report - ',char(Well_name)
    ], 'pdf')

%% Create title page

tp = TitlePage("Title", "Blowout and kill report", "
    Subtitle", char(Well_name), "Image","Front_page.PNG", "
    Author", ....
            "Vetle Arild Mathisen", "PubDate", date);


% pb=mlreportgen.dom.PageBreak
% add(tp,pb)
add(rpt,tp);
%%
% *Preface*
```

```
20
21  ch0=Chapter;
22  ch0.Title = "Preface";
23
24  para_preface1 = Paragraph(['This report is a product of a
        master thesis written by Vetle Arild Mathisen at ' ...
25      ' NTNU during the spring of 2020. The master thesis
            describes the theory behind the simulator and how
            the ' ...
26      ' simulator works. This automatically generated report
            is based on the structure of the blowout and kill
            reports provided by Ranold.'])
27
28
29  add(ch0,para_preface1)
30  add(rpt,ch0)
31
32
33  %%
34  %
35  %
36  %
37  %
38  % *Table of contents*
39
40  add(rpt, TableOfContents);
41  %add(rpt, ListOfFigures);
42  %%
43  % *Chapter - Input values*
44
45  ch1=Chapter;
46  ch1.Title = "Input values";
47
48  para_input = Paragraph(['Most of the data input given from
        the user are shown' ...
49      ' in Table 2.1 to Table 2.8. The entire simulation is
            based upon the provided information. ' ...
50      ' The input data covers rig elevation, well design,
            relief well design, reservoir fluid and ' ...
51      ' reservoir productivity parameters.'])
52
53  add(ch1,para_input)
54
55  Table_general_values = BaseTable(general_values);
56  Table_general_values.Title = "General rig/seabed values";
```

```
Table_general_values.TableWidth = "100%"
add(ch1,Table_general_values)


para_ds = Paragraph(['The well design used in the
    simulation is shown in Table 2.2, when the fluid ' ...
    ' flow through the annulus the drill string design
        shown in Table 2.3 is used together with the inner '
         ...
    ' diameter of the surrounding casing at each depth.
        Figure 2.1 shows the well schematic for the ' ...
    ' used well.'])

add(ch1,para_ds)

Table_input_well = BaseTable(input_well);
Table_input_well.Title = "Well design";
Table_input_well.TableWidth = "14cm"
add(ch1,Table_input_well)

Table_input_DS = BaseTable(input_DS);
Table_input_DS.Title = "Drill string components";
Table_input_DS.TableWidth = "14cm"
add(ch1,Table_input_DS)

fig_well=Figure(Fig_well);
fig_well.Snapshot.Caption = "Well schematic of the
    simulated well";
add(ch1,fig_well);


para_RW = Paragraph(['A relief well is used to kill the
    well and a simplified relief well' ...
    ' trajectory is used for the simulated kill process.
        The relief well trajectory is used ' ...
    ' to calculate the maximum required mud pump pressure
        and the heat change of the kill fluid. ' ...
    ' Table 2.4 presents the different parts of the relief
        well where the kill fluid flows through. ' ...
    ' The relief well trajectory is a simple build, hold
        and drop trajectory and is based on the ' ...
    ' parameters shown in Table 2.5. The calculated relief
        well trajectory is presented in Figure 2.2.'])

add(ch1,para_RW)
```

```
91
92  Table_input_RW = BaseTable(input_RW);
93  Table_input_RW.Title = "Rellief well design";
94  Table_input_RW.TableWidth = "14cm"
95  add(ch1,Table_input_RW)
96
97  Table_input_RW_value = BaseTable(input_RW_value);
98  Table_input_RW_value.Title = "Rellief well trajectory
        parameters";
99  Table_input_RW_value.TableWidth = "100%"
100 add(ch1,Table_input_RW_value)
101
102
103 fig3=Figure(RW_fig);
104 fig3.Snapshot.Caption = "Relief well trajectory used in the
        simulations";
105 add(ch1,fig3);
106
107 para_fluid = Paragraph(['The reservoir fluid is important
        in the calculation of the flowing bottom hole pressure'
        ...
108     ' and the resulting blowout rate. Table 2.6 shows the
            used reservoir fluid and reservoir productivity '
            ...
109     ' parameters. The saturation pressure of the of the
            fluid is only used for the inflow performance
            relationship,' ...
110     ' a calculated saturation pressure is used for the
            multiphase pressure calculations. More on how the
            different ' ...
111     ' reservoir fluids behave for the given temperature and
             pressure is presented in Chapter 2.'])
112
113 add(ch1,para_fluid)
114
115 Table_res_fluid_values = BaseTable(res_fluid_values);
116 Table_res_fluid_values.Title = "Reservoir fluid and
        reservoir productivity parameters";
117 Table_res_fluid_values.TableWidth = "100%"
118 add(ch1,Table_res_fluid_values)
119
120
121 para_kill = Paragraph(['The interception point between the
        relief well and the blowing well' ...
122     ' is shown in Table 2.7 together with the viscosity and
```

```
        density of the kill fluid. The ' ...
123     ' number of kill fluid density steps gives the number
          of different kill densities simulated. ' ...
124     ' The density increase is linear going from the minimum
          to maximum density.'])
125
126 add(ch1,para_kill)
127
128 Table_Kill_values = BaseTable(Kill_values);
129 Table_Kill_values.Title = "Parameters for kill simulation";
130 Table_Kill_values.TableWidth = "100%"
131 %Table_Kill_values.Style = {Hyphenation(" ")};
132 add(ch1,Table_Kill_values)
133
134 para_mat = Paragraph(['Several material properties used in
      the simulation are ' ...
135     ' shown in Table 2.8. These material properties are not
          an input from the user, ' ...
136     ' but assumed in the simulator.'])
137
138 add(ch1,para_mat)
139
140 Table_materials = BaseTable(input_Materials);
141 Table_materials.Title = "Properties of different materials
      used in the simulation";
142 Table_materials.TableWidth = "12 cm"
143 %Table_Kill_values.Style = {Hyphenation(" ")};
144 add(ch1,Table_materials)
145
146 para_ans = Paragraph(['The created simulator gives the user
       the opportunity to choose between two multiphase
      pressure drop correlations and two PVT correlations '
      ...
147     ' sets. The chosen correlations are presented in Table
          2.9.'])
148 add(ch1,para_ans)
149
150 Table_ans = BaseTable(input_answers);
151 Table_ans.Title = "Chosen correlations used in this
      simulation";
152 Table_ans.TableWidth = "12 cm"
153 %Table_Kill_values.Style = {Hyphenation(" ")};
154 add(ch1,Table_ans)
155
156
```

```
157
158
159 %add(ch1,img1);
160 add(rpt,ch1)
161 %%
162 %
163 %
164 % *Chapter - IPR*
165 %
166 %
167
168 Ch2 = Chapter;
169 Ch2.Title = "Temperature, inflow performance relationship
        and reservoir fluid";
170 %%
171 %
172
173
174
175 sec_temp = Section;
176 sec_temp.Title = 'Temperature';
177
178 para_temp = Paragraph(['The temperature in the surrounding
        formation is an important factor' ...
179     ' when calculating the heat loss of the flowing fluid.
            The temperature of the surrounding formation is
            presented in figure 3.1.' ...
180     ' The calculated temperature inside the blowing
            wellbore for a surface blowout is presented in
            figure 3.2.' ...
181     ' During a kill process the temperature of the kill
            fluid and the blowing fluid will mix, thus knowing
            the temperature' ...
182     ' of the kill fluid is important. The calculated
            temperature profile of the kill fluid is shown in
            figure 3.3 for the ' ...
183     ' relief well with a kill rate as shown on the top of
            the figure.'])
184
185
186 add(sec_temp,para_temp)
187 Fig_T_sur=Figure(Fig_temp_sur);
188 Fig_T_sur.Snapshot.Caption = "Calculated temperature inside
        the wellbore during openhole blowout";
189 Fig_T_sur.Snapshot.Height  = '5cm';
```

```
add(sec_temp,Fig_T_sur);

Fig_T=Figure(Fig_temp);
Fig_T.Snapshot.Caption = "Calculated temperature inside the
    wellbore during openhole blowout";
Fig_T.Snapshot.Height  = '5cm';
add(sec_temp,Fig_T);

Fig_T_RW=Figure(Fig_temp_RW);
Fig_T_RW.Snapshot.Caption = "Calculated temperature inside
   the relief well with the kill rate as shown";
Fig_T_RW.Snapshot.Height  = '5cm';
add(sec_temp,Fig_T_RW);


add(Ch2,sec_temp)

pb=mlreportgen.dom.PageBreak

add(Ch2,pb)

sec_IPR = Section;
sec_IPR.Title = 'Inflow performance relationship';

para_IPR = Paragraph(['The inflow performance relationship
   is based on the simple Darcy equation' ...
    ' when the flowing bottom hole pressure is above the
       saturation ' ...
    ' pressure and the Vogel equation when the flowing
       bottom hole pressure' ...
    ' is below the saturation pressure. The inflow
       performance relationship  is used together with '
       ...
    ' the flowing bottom hole pressure to determine the
       blowout rate. The figure below' ...
    ' shows the inflow performance relationship for the
       simulation and is based on the input values.' ...
    ' The productivity index (J), which is a quantification
        of how much the reservoir is able to ' ...
    ' produce for a given drawdown (reservoir pressure -
       bottom hole pressure), the absolute open flow
       potential (AOF) which is an theoretical value ' ...
    ' for the maximum blowout rate is also presented in the
       figure. The AOF will never happen since the flowing
       bottom hole pressure always will be ' ...
```

```
221     ' greater than zero due to the hydrostatic pressure and
            the friction of the flowing fluid.']);
222 add(sec_IPR,para_IPR)
223
224 fig2=Figure(IPR_fig);
225 fig2.Snapshot.Caption = "Inflow performance relationship";
226 add(sec_IPR,fig2);
227
228 add(Ch2,sec_IPR)
229
230
231 add(Ch2,pb)
232
233 sec_PVT = Section;
234 sec_PVT.Title = 'Reservoir fluid - PVT';
235
236 para_PVT = Paragraph(['Some of the most important pressure-
        volume-temperature (PVT) ' ...
237     ' properties used in the simulator is presented below.
            The pressure ranges from ' ...
238     ' reservoir pressure to surface pressure. The
            parameters are shown with three different
            temperatures: ' ...
239     ' the reservoir temperature, ' ...
240     ' the interception point temperature of the kill fluid
            and an average of the two temperature. ' ...
241     ' In the simulator the actual temperature profile at
            each depth is used to calculate the PVT properties.
            '])
242
243 para_pvt_sim = Paragraph([' The PVT properties are
        calculated with the ', char(PVT_sim), '-correlation as
        chosen by the user.'])
244
245
246
247 add(sec_PVT,para_PVT)
248 add(sec_PVT,para_pvt_sim)
249
250 Fig_B=Figure(Fig_Bo);
251 Fig_B.Snapshot.Caption = "Calculated oil formation volume
        factor (Bo), from reservoir pressure to atmospheric
        pressure";
252 Fig_B.Snapshot.Height  = '5cm';
253 add(sec_PVT,Fig_B);
```

```
254
255 Fig_Bgg=Figure(Fig_Bg);
256 Fig_Bgg.Snapshot.Caption = "Calculated gas formation volume
        factor (Bg), from reservoir pressure to atmospheric
       pressure";
257 Fig_Bgg.Snapshot.Height  = '5cm';
258 add(sec_PVT,Fig_Bgg);
259
260 Fig_Rss=Figure(Fig_Rs);
261 Fig_Rss.Snapshot.Caption = "Calculated solution Gas-Oil-
       Ratio (Rs), from reservoir pressure to atmospheric
       pressure";
262 Fig_Rss.Snapshot.Height  = '5cm';
263 add(sec_PVT,Fig_Rss);
264
265 Fig_Rhooil=Figure(Fig_rhol);
266 Fig_Rhooil.Snapshot.Caption = "Calculated oil density, from
        reservoir pressure to atmospheric pressure";
267 Fig_Rhooil.Snapshot.Height  = '5 cm';
268 Fig_Rhooil.Width  = '5 cm';
269 add(sec_PVT,Fig_Rhooil);
270
271 Fig_Rhogas=Figure(Fig_rhog);
272 Fig_Rhogas.Snapshot.Caption = "Calculated gas density, from
        reservoir pressure to atmospheric pressure";
273 Fig_Rhogas.Snapshot.Height  = '5cm';
274 add(sec_PVT,Fig_Rhogas);
275
276 add(Ch2,sec_PVT)
277 add(rpt,Ch2)
278 %%
279 %
280 %
281 % *Chapter - blowout rates*
282
283 Ch3 = Chapter;
284 Ch3.Title = "Blowout rates";
285
286 para_BO = Paragraph(['A blowout release point may be
       located either on the surface, seabed or underground. '
       ...
287     ' The underground blowout is neglected in this
           simulator. The reservoir fluid may flow through
           three different channels:' ...
288     ' through an open/cased hole, through the inside of the
```

```
        drill string or in the annulus. The flow path
        through drill pipe is ' ...
289     ' not calculated in this simulator. The three different
        blowout flow paths are shown in figure 4.1. The
        reservoir may either be fully penetrated or partly
        penetrated,' ...
290     ' the partly penetration is not used in this simulation
        . The blowout preventor (BOP) may be open or partly
        closed, since an open BOP status is more
        conservative' ...
291     ' the restricted BOP is not included. Based on more
        than 30 ' ...
292     ' years of blowout statistics figure 4.2 is created
        which present the risk of each blowout combination.'
        ])
293
294 %Fig_flow_path = mlreportgen.report.FormalImage();
295 Fig_flow_path=Image('Flow_paths.JPG');
296 %Fig_flow_path.Caption = 'Possible blowout paths, courtecy
    of Ranold';
297 Fig_flow_path.Style= {ScaleToFit}
298 para_bo1 = Paragraph('Figure 4.1: possible blowout flow
    paths, courtecy of Ranold.')
299 %Fig_flow_path.Width= '10cm';
300
301 Fig_risk=Image('Blowout_risk_2.JPG');
302 %Fig_flow_path.Caption = 'Possible blowout paths, courtecy
    of Ranold';
303 Fig_risk.Style= {ScaleToFit}
304 para_bo2 = Paragraph('Figure 4.2: Blowout risk statistics
    for appraisal wells from the last 30 years.')
305
306 add(Ch3,para_BO)
307 add(Ch3,Fig_flow_path)
308 add(Ch3,para_bo1)
309
310 add(Ch3,Fig_risk)
311 add(Ch3,para_bo2)
312
313 para_bo4 = Paragraph(['The calculated blowout rates for
    this simulation is presented in Table 3.1 for the
    different blowout scenarios listed.' ...
314     ' These blowout rates are based upon the concept of IPR
        -VLP-matching. The inflow performance relationship (
        IPR) quantify how much ' ...
```

```
315     ' the reservoir is able to produce for a given bottom
          hole pressure. The vertical lift performance (VLP)
          quantify the required pressure ' ...
316     ' the well need to be able to produce/lift a given
          fluid rate. Figure 4.3 illustrate the process of IPR
          -VLP-matching for a general well. ' ...
317     ' The interception between the IPR and the VLP gives
          the highest rate the reservoir can produce that the
          well is able to lift out, ' ...
318     ' the resulting rate is called the blowout rate'])
319
320 add(Ch3,para_bo4)
321
322 Table_Blowout = BaseTable(input_blowout);
323 Table_Blowout.Title = "Blowout rates";
324 Table_Table_Blowout.TableWidth = "100%"
325
326 para_bo5 = Paragraph(['The multiphase pressure drop
      correlation ', char(Multiphase),' is used together with
      the ', char(PVT_sim), ' ' ...
327     ' - PVT correlation the calculate the flowing bottom
          hole pressure. The user can choose between two
          multiphase pressure correlations:' ...
328     ' Olgjenka and Orkiszewski and two PVT correlation sets
          : Standing or Glas . The combination of
          correlations will affect the calculated results
          slightly.'])
329
330
331 add(Ch3,para_bo5)
332 add(Ch3,pb)
333 add(Ch3,Table_Blowout)
334
335 Fig_VLP=Image('IPR-VLP-All.PNG');
336 %Fig_flow_path.Caption = 'Possible blowout paths, courtecy
      of Ranold';
337 Fig_VLP.Style= {ScaleToFit}
338 para_bo3 = Paragraph('Figure 4.3: The IPR-VLP-matching
      process for the different blowout scenarios.')
339
340 add(Ch3,Fig_VLP)
341 add(Ch3,para_bo3)
342
343
344 add(rpt,Ch3)
```

```
%%
%
%
% *Chapter - Calculate kill rates*

Ch4 = Chapter;
Ch4.Title = "Kill rates";


para_kill1=Paragraph(['The kill rate is calculated in the same way as the blowout rate, but kill fluid is present above the interception point. ' ...
    ' The increased flow rate due to the kill fluid increases the friction loss, and the higher weight of the kill fluid increase the hydrostatic pressure. ' ...
    ' The calculated kill rates for the simulated well is shown in Table 5.1 for an open/cased hole to seabed and in Table 5.2 for a open/cased hole to surface. ' ...
    ' The required kill rate to stop an annulus blowout or a drillpipe blowout was neglected since the open hole is the most conservative scenario.'])

para_kill2 = Paragraph(['During the development of the simulator a calibration factor formula was created. This formula is used to calibrate the kill rates ' ...
    ' based on several simulations conducted by the industry standard blowout and kill simulators. The "best prediction" gives the best predicted kill rate ' ...
    ' based on the calibration formula, "Not adjusted" gives the calculated kill rate based on the multiphase pressure drop calculations without any calibrations. ' ...
    ' The higher and lower rate gives the P10 and P90 distributed kill rates'])
add(Ch4,para_kill1)
add(Ch4,para_kill2)
Table_seabed = BaseTable(Matrix_kill_seabed);
Table_seabed.Title = "Kill rates - Open/cased hole to seabed";
Table_surface = BaseTable(Matrix_kill_surface);
Table_surface.Title = "Kill rates - Open/cased hole to surface";
```

```
add(Ch4,Table_seabed)

add(Ch4,Table_surface)

add(rpt,Ch4)
%%
%

Ch5 = Chapter;
Ch5.Title = "Kill rates and pumping capacities - best
   prediction";

para_pump=Paragraph(['The required maximum mud pump
   discharge pressure for the different kill rates ' ...
    ' and kill fluid density are shown for the best
       predicted value. The pressure at the interception
       point and the flowing bottom hole pressure are also
       shown. ' ...
    ' Table 6.1 shows the values for a seabed ' ...
    ' blowout and Table 6.2 shows the value for a surface
       blowout. The required maximum mud pump discharge
       pressure is calculated for two flow paths. ' ...
    ' The first flow path goes through surface lines, down
       choke and kill line and through the annulus. The
       other flow path goes through ' ...
    ' the surface lines and through the inside of the drill
        string.'])

para_pump2=Paragraph(['One limitation to the simulator is
   that the simulator does not use a transient model, ' ...
    ' making the required time to kill the well impossible
       to obtain. The rig must be able to store enough kill
        fluid ' ...
    ' to be able to kill the well, but the required amount
       to reach dynamic kill is not calculated. When the
       well is dynamically ' ...
    ' killed a new mud is injected to ensure no
       hydrocarbons are left in the wellbore and the
       hydrostatic pressure exceeds the reservoir pressure.
        ' ...
    ' Two times the wellbore volume is used for this static
        circulation and the volume is presented the two
       tables below.'])

Table_kill_sea = BaseTable(Kill_pump_best_sea);
```

```
Table_kill_sea.Title = "Kill rates and pumping capacity -
    Open hole to seabed - Best prediction";

Table_kill_surf = BaseTable(Kill_pump_best_sur);
Table_kill_surf.Title = "Kill rates and pumping capacity -
    Open hole to surface - Best prediction";



add(Ch5,para_pump)
add(Ch5,para_pump2)

add(Ch5,Table_kill_sea)
add(Ch5,Table_kill_surf)
add(rpt,Ch5)


%%
% *References*

Ch6 = Chapter;
Ch6.Title = "References";

para_ref1 = Paragraph(['Front page picture - relief-well|
    Coastal Care. URL:https://coastalcare.org/2010/08/feds-
    no-timeline-for-completing-gulf-relief-well/relief-well
    -2. [Online; accessed 19. May 2020].- '])

para_ref2 = Paragraph(['Master Thesis - Mathisen, V. 2020.
    Blowout and kill simulator for vertical wells, NTNU.'])

para_ref3 = Paragraph(['Ranold - Ranold, 2018. Technical
    report - blowout and dynamic wellkill simulations.'])


add(Ch6,para_ref1)
add(Ch6,para_ref2)
add(Ch6,para_ref3)
add(rpt,Ch6)
close(rpt)
rptview(rpt)
```

Listing C.28: AOF_to_PI

```
function J = AOF_to_PI(AOF,p_r,p_s)
% input AOF [STB/D], p_r [bar], p_s[psi]
```

```
3
4  AOF = AOF*0.159; %STB/D to SM3/D
5  p_s = p_s / 14.5; % psi to bar
6  if p_r < p_s
7  J = AOF / p_s*1.8; %SM3/D/Bar
8  else
9    J = AOF / ((p_r - p_s) + p_s/1.8); %SM3/D/Bar
10 end
11
12
13 %AOF_calc = q_s +(1-0.2*p_w/p_s - 0.8*(p_w/p_s)^2)*q_max;
14
15 J = J * 0.433667; %STB/D/psi
16
17 end
```

Listing C.29: API2Gravity

```
1 function gamma_o = API2gravity(API)
2 gamma_o=141.5/(API+131.5)
3 end
```

Listing C.30: gravity2API

```
1 function API = gravity2API(gamma_o)
2 % Converts specific gravity to API density
3 % Input - specific gravity [-]
4 % Output - API density [API]
5 API=141.5/gamma_o - 131.5;
6 end
```

Listing C.31: PI_to_AOF

```
1  function AOF = PI_to_AOF(J,p_r,p_s)
2  % input J [STB/D/Psi], p_r [bar], p_s[psi]
3
4  J = J / 0.433667; %Sm3/D/bar
5
6
7  p_s = p_s / 14.5; % psi to bar
8  if p_r < p_s
9  AOF = J*p_s/1.8; %SM3/D/Bar
10 else
11 AOF = J*((p_r-p_s)+p_s/1.8);
12 end
13
```

```

AOF = AOF/0.159; %STB/D

end
```

Listing C.32: Wellbore_volume

```
function [V_OH_t, V_DP] = Wellbore_volume (well_sorted,DS)


for i = 1:size(well_sorted,1)

 ID = well_sorted(i,2); %in
 L = well_sorted(i,4) - well_sorted(i,3);%ft
 V_OH(i) = pi/4*ID^2*0.0254^2*L/3.28084; %m3
end


V_OH_t = sum(V_OH);

V_DP = pi/4*0.0254^2/3.28084*(DS(1,1)^2*DS(1,3)+DS(2,1)^2*
    DS(2,3));

end
```

Vetle Arild Mathisen

Oppgavens tittel

NTNU

Kunnskap for en bedre verden